universität wien

DISSERTATION

Titel der Dissertation

In vivo Characterization of Natural Product $GABA_A$ Modulators and their Derivatives

Verfasserin

Mag. pharm. Juliane Hintersteiner

angestrebter akademischer Grad

Doktorin der Naturwissenschaften (Dr. rer. nat.)

Wien, 2015

Studienkennzahl lt. Studienblatt:	A 791 449
Dissertationsgebiet lt. Studienblatt:	Pharmazie
Betreuer:	Univ.-Prof. Dr. Steffen Hering

Abstract

Valerenic acid (VA) and piperine positively modulate $GABA_A$ receptors comprising β2- or β3-subunits. The therapeutic potential of these natural products and their derivatives is largely unknown. The aim of this study was to analyze anxiolytic, sedative, and anticonvulsive effects of VA, piperine and selected derivatives.

Effects on anxiety-related behavior of C57BL/6N mice were studied by means of the elevated plus maze (EPM) and the light dark choice test (LDT). Effects on locomotor activity (sedation) were analyzed by means of the open field test. Effects on seizure threshold were assessed making use of the Pentylenetetrazole (PTZ)-tail vein infusion test. Plasma levels of VA and selected piperine derivatives were estimated at different time points after intraperitoneal administration.

Out of the studied VA ester derivatives, the methylester and propylester derivatives induced more pronounced anxiolytic effects with a faster onset than VA. The anticonvulsive effect of the methylester occurred with a faster onset than VA. In contrast, the ethylester of VA induced longer lasting anxiolytic and anticonvulsive effects, occurring with a delayed onset. After intraperitoneal application of VA esters to the animals free VA was detected in plasma, suggesting release of VA. I conclude, that VA esters may serve as prodrugs of VA. VA amide derivatives (VA-amide, VA-methylamide, and VA-tetrazole) displaying stronger positive modulation of β2/3-containing $GABA_A$ receptors over β1-containing receptors compared to VA also induced more pronounced elevation of seizure threshold. In line with this stronger anticonvulsive effect, VA-amide and VA-tetrazole displayed more pronounced anxiolytic effects in the EPM and the LDT than VA. In contrast, unselective compounds were found to be inactive *in vivo* (e.g. VA-dimethylamide) or induced anticonvulsive effects only at higher doses (VA-ethylamide, VA-diethylamide). From the studied piperine derivatives, SCT-66 and compound 23 induced significantly more pronounced anxiolytic effects than piperine. At higher doses ($\geq$ 30 mg/kg) bodyweight both compounds reduced locomotor activity. In addition, SCT-66 also significantly elevated PTZ-induced seizure threshold. Most notably, SCT-66 did -unlike piperine- not reduce body temperature, suggesting no activation of TRPV1 channels *in vivo*.

Taken together, the studied VA derivatives may serve as scaffolds for the development of novel anxiolytics and/or anticonvulsants with faster onset, longer duration and/or stronger action compared to VA. Piperine derivatives SCT-66 and compound 23 induce more pronounced anxiolysis in mice than piperine and thus may be an interesting starting point for the development of novel anxiolytics.

Kurzfassung

Valerensäure (VA) und Piperin modulieren bevorzugt $GABA_A$ Rezeptoren, die aus β2- oder β3-Untereinheiten bestehen. Das therapeutische Potential dieser Naturstoffe und deren Derivate ist noch weitgehend unbekannt. Ziel dieser Arbeit war es, anxiolytische, sedierende und antikonvulsive Effekte der Valerensäure, von Piperin und deren ausgewählten Derivaten zu bestimmen.
Das Angstverhalten von C57BL/6N Mäusen wurde im Elevated Plus Maze (EPM) und im Light/-Dark Choice Test (LDT) untersucht. Die lokomotorische Aktivität (Sedierung) der Tiere wurde im Open Field Test ermittelt. Effekte auf die Krampfschwelle wurden mittels Infusion von Pentylenetetrazole (PTZ)-Tail Vein Infusion Tests festgestellt. Die Plasmaspiegel der VA und ausgewählter Piperin Derivate wurde zu unterschiedlichen Zeitpunkten nach intraperitonealer Applikation bestimmt.
Von den untersuchten VA Ester Derivaten bewirkten der Methylester und der Propylester der VA stärker ausgeprägte anxiolytische Effekte mit schnellerem Wirkungseintritt als die VA. Ebenso trat der antikonvulsive Effekt des Methylesters schneller ein als der der VA. Dagegen bewirkte der Ethylester eine länger andauernde anxiolytische und antikonvulsive Wirkung mit einem verspäteten Wirkungseintritt. Die nach intraperitonealer Applikation im Plasma der Tiere gemessene VA wurde wahrscheinlich *in vivo* aus den Prodrugs freigesetzt. Ich schließe daraus, dass die VA Ester wahrscheinlich als Prodrugs der VA fungieren. Die VA Amid Derivate (VA-Amid, VA-Methylamid und VA-Tetrazol), welche β2/3-haltige $GABA_A$ Rezeptoren stärker gegenüber β1-haltigen Rezeptoren modulieren, erhöhten auch stärker die Krampfschwelle. Diese stärkeren antikonvulsiven Wirkungen sind im Einklang mit den stärker im Vergleich zur VA ausgeprägten anxiolytischen Effekten von VA-Amid und VA-Tetrazol im EPM und LDT. Hingegen waren unselektive Derivate *in vivo* inaktiv (z.B. VA-Dimethylamid) oder wirkten erst in höheren Dosierungen antikonvulsiv (VA-Ethylamid, VA-Diethylamid). Von den untersuchten Piperin Derivaten induzierten SCT-66 und Compound 23 signifikant stärker ausgeprägte anxiolytische Effekte als Piperin. In höheren Dosierungen ($\geq$30 mg/kg Körpergewicht) reduzierten beide Derivate die lokomotorische Aktivität. Zusätzlich erhöhte SCT-66 auch signifikant die PTZ-induzierte Krampfschwelle. Insbesondere reduzierte SCT-66 –im Unterschied zu Piperin- die Körpertemperatur nicht, was auf keine Aktivierung der TRPV1 Kanäle *in vivo* schließen lässt.
Zusammenfassend dienen die untersuchten VA Derivate als mögliche Ausgangsstoffe für die Entwicklung neuer Anxiolytika und/oder Antikonvulsiva mit schnellerem Wirkungseintritt, längerer Wirkdauer und/oder einer stärkeren Wirkung im Vergleich zur VA. Die Piperin Derivate SCT-66 und Compound 23 bewirken eine signifikant stärker ausgeprägte Anxiolyse bei Mäusen als Piperin, und stellen somit interessante Ausgangsverbindungen für die Entwicklung neuer Anxiolytika dar.

Acknowledgements

This project has been supported by the University of Vienna and the FWF Vienna doctoral program of molecular pharmacy "Ion channels and transporters as molecular drug targets". First of all, I want to thank my supervisor Prof. Dr. Steffen Hering, head of the Department of Pharmacology, for giving me the opportunity to work in his group and providing me this fascinating topic for my thesis. A very special thank goes to Prof. Dr. Christoph Schwarzer, who gave me the possibility to work in his lab at the Medical University of Innsbruck, providing me with his knowledge and answering all my questions. Christoph, thank you for your advice and the support with my animal studies! I would like to extend my warmest thanks to Mag. Dr. Sophia Khom for being my colleague, supervisor, and friend. You supported me with your enthusiasm at any time, even in complicated situations. Without you, this work has never been created like it is now, and my gratitude cannot be described in only a few words. I wish you the best for your future career. Thank you for everything, Sophia!! Furthermore, I would like to give my special thanks to my colleagues at the Department of Pharmacology, Mag. Barbara Strommer, Mag. Dr. Katrin Depil, Mag. Angela Schöffmann, Mag. Dr. Tobias Linder, Mag. Denise Luger, Mag. Pryanka Saxena, Mag. Dr. Igor Baburin, Dr. Dipl. Ing. Anette Hohaus, and Mag. Dr. Anna Weinzinger. Thank you for the great time! I also want to thank my Moltaggies from the Moltag doctoral program for the great time, the many exciting discussions and the nice social events we had together! I don't want to miss this special time with you all! My very special thank goes to Peter Höflich, the caregiver of the animals at the Department of Pharmacology. He assisted me at every time I needed help and made my experiments much funnier. Thank you Peter for your help and your joyfulness! I want to thank Prof. Dr. Christian Studenik, who also helped me with my animal studies. Thank you Christian! I want to thank Prof. Dr. Gottfried Reznicek and Prof. Dr. Walter Jäger for supporting me with my first author paper about the valerenic acid prodrugs. In this case, I also want to thank the diploma students Mag. Irmhild Gräbner and Mag. Bernhard Wittig for their help with the plasma samples. I want to thank the group of Prof. Hamburger, especially Dr. Mousshin Oufir for providing the analysis of many plasma samples. I want to give my special thanks to the girls from our secretary Doris Stenitzer, Yvonne Kosch, and Beata Gaisbauer, who are the best in organizing. Last but not least I want to thank my family and friends. Thank you, mum and dad, Roman and Sigrun for believing in me. Thank you Marlene, Lisi, Tina, and Selina for being my best friends and for stimulating me finishing my thesis. Thanks to Manuela for English improvement. My special thanks go to my love Mario, who motivated me in the last year. You were always there for me and induced me to never give up. Thank you, baby!

Table of Contents

Abbreviations

5HT3Rs serotonins type 3 receptors

ACC anterior cingulate cortex

ALLOP allopregnanolone

AP2 clathrin adaptor protein

ARF ADP-ribosylation factor

BGT-1 betaine-GABA transporter 1

BIG2 brefeldin A-inhibited GDP/GTP exchange factor 2

BiP binding immunoglobulin protein

BLA basolateral nucleus

BNST bed nucleus of the stria terminalis

BZ benzodiazepines

CAE childhood absence epilepsy

CeA central amygdala

CeA_L lateral CeA

CeA_M medial CeA

CIE chronic intermittent ethanol

CNS central nervous system

DMSO dimethyl sulfoxide

EDTA ethylenediaminetetraaceticacid

EPM elevated plus maze test

ER endoplasmatic reticulum

FS febrile seizures

GABA gamma-aminobutyric acid

GABARAP $GABA_A$ receptor associated protein

GABAT GABA transaminase

GAD glutamic acid decarboxylase

GAT GABA transporter

GEF guanine exchange factor

GEFS+ general epilepsy with febrile seizures plus

GluClα glutamate-gated chloride channel α homopentamer

GlyRs glycine receptors

GODZ golgi-specific DHHC zinc finger protein

i.p. intraperitoneal

IGEs idiopathic generalized epilepsies

IS internal standard

ITC intercalated

JME juvenile myoclonic epilepsy

LC locus coeruleus

LDT light dark choice test

lITCs lateral intercalated neurons

mPFC medial prefrontal cortex

nAchRs nicotinic acetylcholine receptors

NSF N-ethylmaleimide-sensitive factor

OF open field test

PE phosphatidyl ethanolamine

PFC prefrontal cortex

pLGICs pentameric ligand gated ion channels

PLIC-1 protein-linking integrin-associated protein and cytoskeleton 1

PTZ pentylenetetrazole

TBPS t-butyl bicyclophosphorothionate

TGN trans Golgi network

THDOC tetrahydrodeoxycorticosterone

TM transmembrane

TMN tuberomammillary nucleus

UPS ubiquitin-proteasome system

VA valerenic acid

VGAT vesicular neurotransmitter transporter

VLPO ventrolateral preoptic nucleus

1 Introduction

1.1 $GABA_A$ Receptor

$GABA_A$ receptors mediate fast inhibitory neurotransmission in the mammalian brain (Olsen and Sieghart, 2009). $GABA_A$ receptors are also found outside the central nervous system, in the liver (Minuk et al., 2007), airway smooth muscle cells of the lung (Mizuta et al., 2008) and immune cells (Alam et al., 2006; Bjurstöm et al., 2008).

$GABA_A$ receptors are anion-selective ion channels and belong to the Cys-loop pentameric ligand gated ion channels superfamily (pLGICs), which also includes cation-selective nicotinic acetylcholine receptors (nAchRs), serotonin type 3 receptors (5HT3Rs), Zn2+ activated ion channels, and anion-selective glycine receptors (GlyRs) (Sigel and Steinmann, 2012; Grenningloh et al., 1987). $GABA_A$ receptors are activated by the selective agonists gamma-aminobutyric acid (GABA) and muscimol. $GABA_A$ receptors are blocked by the competitive antagonist bicuculline and the non-competitive antagonists picrotoxin, t-butyl bicyclophosphorothionate (TBPS), and pentylenetetrazole (PTZ) (Macdonald and Olsen, 1994).

GABA is the main inhibitory neurotransmitter in the mammalian brain (Olsen and Sieghart, 2008), and is synthesized in inhibitory neurons from glutamate catalyzed by the enzyme glutamic acid decarboxylase (GAD) (Owens and Kriegstein, 2002). Two GAD isoforms, GAD65 and GAD67, are known in mammals; they are encoded by different genes and show different regional distribution patterns in the the brain. GAD65 is membrane-bound and produces vesicular GABA, whereas GAD67 catalyzes cytoplasmatic GABA production (Erlander et al., 1991).

GABA is transported into vesicles by the vesicular neurotransmitter transporter (VGAT). It can be released vesicularly via $Ca_2{}^+$ dependent exocytosis or non-vesicularly by reverse transport. GABA acts via pre- or postsynaptic receptors, which can be either ionotropic ($GABA_A$) or metabotropic ($GABA_B$) receptors (Owens and Kriegstein, 2002). GABA mediates phasic in-

hibition via synaptic transmission and tonic inhibition via extrasynaptic receptors (Farrant and Nusser, 2005).

After release, GABA is transported from the synaptic cleft into nerve endings and/or glia cells by GABA transporters (GAT). Four GAT proteins have been cloned: GAT-1, GAT-2, GAT-3, and betaine-GABA transporter 1 (BGT-1) (Cherubini and Conti, 2001). GAT-1 is the most abundant GAT isoform in the central nervous system (CNS), whereas the other transporters are expressed to a minor extent. Subsequently, GABA is metabolized by transamination by the catabolic enzyme GABA transaminase (GABAT) (Cherubini and Conti, 2001).

1.1.1 $GABA_A$ Receptor Assembly and Degradation

The efficacy of the GABAergic synaptic transmission is directly related to the number of postsynaptic $GABA_A$ receptors (Luscher et al., 2011). In the endoplasmatic reticulum (ER) $GABA_A$ receptor subunits are assembled to form pentameric receptor complexes (Jacob et al., 2008). Assembly of the receptors is strictly regulated by the interactions with the ER-associated chaperones calnexin and binding immunoglobulin protein (BiP) (Bradley et al., 2008; Connolly et al., 1996; Luscher et al., 2011). Incorrectly folded or fragmented subunits, and most homomeric receptors cannot exit the ER and are degraded by the ubiquitin-proteasome system (UPS) (Jacob et al., 2008). Ubiquitination of $GABA_A$ receptors can be controlled by neural activity. A chronic blockade of neural activity decreases the expression of receptors at the cell surface; enhanced neural activity augments their quantity. This is one possible regulatory mechanism for the homoeostasis of synaptic inhibition (Jacob et al., 2008). The ubiquitin-like protein-linking integrin-associated protein and cytoskeleton 1 (PLIC-1) inhibits UPS thus facilitating movement of $GABA_A$ receptors from the ER to the Golgi apparatus by interacting with the intracellular domain of α and β subunits (Luscher et al., 2011).

The entry into the Golgi network and ensuing trafficking to the plasma membrane are regulated by a multitude of $GABA_A$ receptor associated proteins (Jacob et al., 2008). The Golgi-specific DHHC zinc finger protein (GODZ) facilitates translocation of $GABA_A$ receptors through the Golgi apparatus and to the plasma membrane by palmitoylation of the $\gamma 2$ subunits (Luscher et al., 2011).

The exit from the Golgi apparatus is suggested to be mediated by Brefeldin A-inhibited GDP/GTP exchange factor 2 (BIG2) that interacts with β subunits of $GABA_A$ receptors . BIG2 is a Sec7 domain-containing guanine exchange factor (GEF), which catalyzes the exchange of GDP-GTP of class I ADP-ribosylation factor (ARF) 1 and 3 (Luscher et al., 2011).

The activation of these proteins is crucial for membrane budding of vesicles from the Golgi apparatus and therefore for passage of proteins through the trans Golgi network (TGN) toward

the plasma membrane (Luscher et al., 2011). BIG2 is also involved in endocytic recycling of $GABA_A$ receptors (Shin et al., 2004).

The $GABA_A$ receptor associated protein (GABARAP) interacts with the γ subunits, with microtubules, and the N-ethylmaleimide-sensitive factor (NSF) (Wang et al., 1999). It is enriched in the Golgi apparatus, but not at GABAergic synapses (Kittler et al., 2001) and facilitates the translocation of $GABA_A$ receptors to the cell surface (Leil et al., 2004).

Trafficking of $GABA_A$ receptors by GABARAP involves a lipid conjugation and delipidation cycle (Tanida et al., 2004). Supplementation of phosphatidyl ethanolamine (PE) to the C-terminus of GABARAP involves activating conjugating and deconjugating enzymes and is required for dendritic accumulation of GABARAP and cell surface expression of $GABA_A$ receptors mediated by GABARAP (Olsen et al., 2007; Luscher et al., 2011).

Gephyrin is the main protein that stabilizes $GABA_A$ receptors at inhibitory synapses (Fritschy, 2008). The endocytosis is mainly mediated via clathrin- and dynamin-dependent mechanisms involving interactions of the $GABA_A$ receptor β and γ subunits with the clathrin adaptor protein (AP2) (Kittler et al., 2008, 2005, 2000).

1.1.2 $GABA_A$ Receptor Subtypes

The functional properties of $GABA_A$ receptors are dependent on their subunit composition (Olsen and Sieghart, 2008; Sigel et al., 1990). $GABA_A$ receptors are composed of five protein subunits of which 19 have been cloned from mammalian species (α1-6, β1-3, γ1-3, δ, ϵ, θ, π, ρ1-3) (Olsen and Sieghart, 2009; Simon et al., 2004). Within each family of subunits, there is approximately 70 % sequence identity and between families, there is about 20 % sequence identity or 50 % sequence similarity (Olsen and Tobin, 1990). Each subunit has a length of almost 450 amino acid residues and they all possess a common topological organization: a large extracellular N-terminal domain, a short extracellular C–terminal domain, and four transmembrane (TM) segments. The ion channel is formed by the TM2 segments from all five subunits and there is a large intracellular loop between TM3 and TM4 (Sigel and Steinmann, 2012).

In principle, a wide range of different $GABA_A$ receptor types can be formed, but there is evidence that only a limited number of subunit combinations actually reaches the neuronal cell surface (Jacob et al., 2008). Most $GABA_A$ receptors expressed on the surface of neurons have two α and two β subunits and one other subunit (γ, δ or ϵ) (Jacob et al., 2008; Möhler, 2006).

$GABA_A$ receptor heterogeneity is determined mainly by the existence of six different α subunit isoforms (Olsen and Sieghart, 2008). The α1 subunit is part of the major type of $GABA_A$ receptors, which consists of $\alpha 1 \beta 2 \gamma 2$ subunits that are highly expressed in both synaptic and extrasynaptic neurons (Möhler, 2006). The brain regions where this receptor subtype is most

prominent are the cerebral cortex, hippocampus, olfactory bulb, thalamic relay nuclei, pallidum striatum, basal forebrain, cerebellum, deep cerebellar nuclei, amygdala, brainstem, substantia nigra pars reticulate, and inferior colliculus (Möhler, 2006).

$\alpha 2$ subunits are coexpressed with $\beta 3$ and $\gamma 2$. $\alpha 2\beta 3\gamma 2$ receptors are found mainly in the cerebral cortex, hippocampal pyramidal neurons, inferior olivary neurons, striatum, olfactory bulb, hypothalamus, amygdala, motor neurons, and superior colliculus (Möhler, 2006).

$\alpha 3$ subunits – mainly coexpressed with β and $\gamma 2$ subunits- are located in the cerebral cortex, hippocampus, cerebellum, olfactory bulb, medullary reticular formation, thalamic reticular neurons, inferior olivary neurons, amygdala, superior colliculus, spinal cord, brainstem, medial septum, basal forebrain cholinergic neurons, raphe and locus coeruleus (Möhler, 2006).

The $\alpha 4/\alpha 6$ subunits are insensitive to classical benzodiazepines (BZ) and zolpidem (Möhler, 2006). $\alpha 4$ subunits are located in the dendate gyrus and thalamus, and receptors containing $\alpha 6$ subunits are expressed in the cerebellum and granule cell layer (Möhler, 2006).

Like $\alpha 4/\alpha 6$ subunits, $\alpha 5$ subunits show limited distribution in the brain. Higher densities are found in the hippocampus, olfactory bulb, cerebral cortex, amygdala, hypothalamus, superior colliculus, superior olivary neurons, spinal trigeminal neurons, and spinal cord (Möhler, 2006).

$\beta 1$ subunits are expressed in the cerebral cortex, olfactory bulb mitral cells, hippocampus, the substantia nigra, superior colliculus, and cerebellum (Uusi-Oukari and Korpi, 2010). $\beta 2$ subunits are the most abundant and wide spread. Their expression correlates with the expression of the $\alpha 1$ subunit. Consequently, $\alpha 1$ and $\beta 2$ subunits have a high probability of assembling into the same receptor (Uusi-Oukari and Korpi, 2010).

The distribution of $\beta 3$ containing $GABA_A$ receptors is higher in the perinatal than in the adult brains (Laurie et al., 1992; Olsen and Sieghart, 2008; Zhang et al., 1991). The expression patterns of $\beta 3$ subunits strongly correlate with those of the $\alpha 2$ subunits, suggesting that they assemble into a single receptor subtype (Uusi-Oukari and Korpi, 2010).

$GABA_A$ receptors containing $\gamma 1$ subunits occur in the amygdala, hypothalamus and septum (Wisden et al., 1992), mainly coexpressed with $\alpha 2$ subunits (Uusi-Oukari and Korpi, 2010). In the human, bovine, and rat brain, two splice variations of $\gamma 2$ subunits exist ($\gamma 2$S and $\gamma 2$L). In contrast to the short $\gamma 2_S$, the long $\gamma 2_L$ isoform has additional 8 amino acids in the putative cytoplasmatic loop domain, which contains a proteinkinase C consensus phosphorylation site (Whiting et al., 1990). Only a minority of $GABA_A$ receptors in the CNS contains $\gamma 3$ subunits (Wisden et al., 1992).

The δ subunits are mainly coassembled with $\alpha 1$, $\alpha 4$, and $\alpha 6$ subunits at peri- and extrasynaptic sites, thus mediating tonic inhibition (Glykys et al., 2007). $GABA_A$ receptors containing δ subunits in combination with $\alpha 4$ or $\alpha 6$ subunits occur in the dentate gyrus and cerebellum

(Möhler, 2006). $GABA_A$ receptors containing $\alpha 1/\delta$ complexes are abundant in hippocampal interneurons (Glykys et al., 2007). ϵ and θ subunits are localized in monoaminergic nuclei of the brainstem (Moragues et al., 2002; Sinkkonen et al., 2000). ρ subunits are expressed in the retina superficial gray layer of the superior colliculus, and in the cerebellar purkinje cells (Boue-Grabot et al., 1998; Wegelius et al., 1998). The π subunit occurs in hippocampus and peripheral cortex, and also in digestive tissue like the gall bladder, and in female peripheral organs (uterus and ovaries) (Hedblom and Kirkness, 1997; Neelands and Macdonald, 1999).

1.1.3 $GABA_A$ Receptor Binding Sites

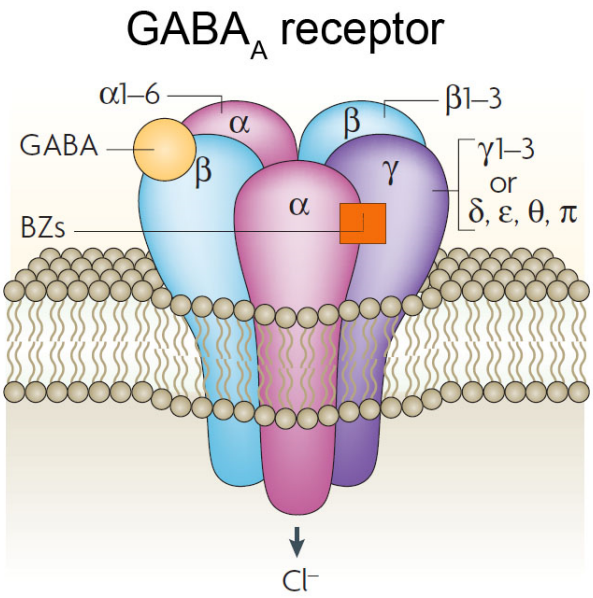

Figure 1.1: Structure of the $GABA_A$ receptor and its binding sites (Jacob et al., 2008).

The arrangement of subunits in $GABA_A$ receptors has been predicted by homology modelling of the extracellular domains based on the crystal structure of ACh binding protein as template (Sieghart, 2015). Some crystal structures of bacterial homologues (ELIC, GLIC) (Bocquet et al., 2009; Hilf and Dutzler, 2008) and the crystal structure of the first anion-selective Cys-loop receptor, a glutamate-gated chloride channel α homopentamer (GluClα) (Hibbs and Gouaux, 2011) provide additional support for the models, although these proteins have a limited level of sequence identity with $GABA_A$ receptor subunits. Also, the crystal structure of a human $GABA_A$ receptor $\beta 3$ homopentamer has been solved (Miller and Aricescu, 2014).

1.1.3.1 GABA Binding Site

Each subunit of the $GABA_A$ receptor has a plus (+) and a minus (-) side. GABA activates $GABA_A$ receptors via two GABA-binding sites, which are located at the extracellular β+α-interfaces. The ligand binding site is located at subunit interfaces formed of amino acid residues that are arranged in 6 loops A-F (Boileau et al., 2002).

In the loop A region (β2W92-D101), amino acid residues β2Y97 and β2L99 line the GABA binding site (Boileau et al., 2002).

Amino acid residues β2T160 and β2D163 in the loop B region (β2I154-D163) are believed to be located in or near the GABA binding site. In addition, this region experiences structural rearrangements during channel gating (Newell et al., 2004). Salt bridges between the side chains of β2R207, β2E153, and β2E155 stabilize the closure of the channel (Newell et al., 2004; Venkatachalan and Czajkowski, 2008; Wagner et al., 2004). The residue β2E155 in the loop B region can form hydrogen bonds and salt bridges with the primary amine of GABA (Cromer et al., 2002) and involved in ligand binding and channel gating (Newell et al., 2004).

In the loop C region (β2V199-S209) 4 amino acid residues were identified that face into the GABA binding pocket: β2S204, β2Y205, β2R207, and β2S209. Amino acid residues β2F200, β2S201, β2T202, and β2G203 are not part of the GABA pocket, but influence GABA affinity (Wagner and Czajkowski, 2001). The conformation of loop C has an extended conformation that is suggested to traverse the GABA binding pocket from the rim to the bottom (Wagner and Czajkowski, 2001). Furthermore, this region of the binding pocket is constricted during pentobarbital-mediated gating of the receptor (Wagner and Czajkowski, 2001). The salt bridge between βE153 and βK196, located on β7 and β9, is involved in regulating loop C and plays a critical role for activation of the $GABA_A$ receptor via GABA (Venkatachalan and Czajkowski, 2008). Amino acid residue β2R207 is suggested to have also a direct interaction with the GABA molecule within the binding mechanism and may therefore be crucial for the stabilization of the agonist-receptor complex (Wagner et al., 2004). The residue β2N149 on the β7 strand, part of one N-glycosylation site, extends along the agonist-binding loop C, providing further contacts between these units and the β7 strand, which may facilitate the ECD - TMD signal transduction Miller and Aricescu (2014).

The loop D region (α1Y59-K70) is a β-strand with amino acid residues α1F64, α1R66, and α1S68 that line a part of the GABA binding pocket (Boileau et al., 2002).

Loop E of the GABA binding pocket (α1M113-L132) is physically linked to the BZ binding site (loop A α1H101) by a short stretch of 11 amino acid residues. In this region, α1N115, α1L117, α1T129, and α1Arg131 are thought to line the GABA binding pocket. In addition, amino acid

residues α1E122, α1L127, and α1R131 are in and near the GABA binding site and move in response to modulation of BZ (Kloda and Czajkowski, 2007).

Loop F (α1Pro174-Asp191) consists of amino acid residues α1V178, α1V180, and α1D183 lining the GABA binding site. This region is also suggested to act as a dynamic element during channel gating transitions (Newell and Czajkowski, 2003).

1.1.4 Modulation of $GABA_A$ Receptors

$GABA_A$ receptors are targets of endogenous modulatory systems, mainly the neurosteroid (Belelli and Lambert, 2005) and endocannabinoid system (Sigel and Lüscher, 2011). Besides endogenous modulation, $GABA_A$ receptors are modulated by a number of exogenous molecules (Sigel and Steinmann, 2012). Selected modulators are described in more detail in this chapter.

1.1.4.1 Benzodiazepines

BZ have been clinically used over the last decades and are the most commonly prescribed class of drugs for the treatment of anxiety, insomnia, epilepsy, and status epilepticus. They have anxiolytic, sedative, muscle relaxant and anticonvulsive effect (Berezhnoy et al., 2004; Engin et al., 2012; Sigel and Buhr, 1997).

BZ are allosteric modulators of $GABA_A$ receptors, i.e. they bind to a separate binding site from GABA itself and increase the open probability of the $GABA_A$ channel (Olsen, 1981; Study and Barker, 1981). The γ2 subunit is crucial for the action of BZ, as substitution by γ1 or γ3 significantly alters sensitivity for BZ (Hevers and Lüddens, 1998).

The high-affinity "classical" BZ binding site is located on the extracellular site of the $GABA_A$ receptor, between the α+γ- interface (Sigel and Buhr, 1997). BZ interact with $GABA_A$ receptors containing the α1, α2, α3 or α5 subunits and thus potentiate GABAergic inhibition, and are insensitive to α4/α6 containing receptors (Bateson, 2004). Photoaffinity labeling and mutagenesis studies identified amino acid residues in α and γ subunits that are crucial for BZ action (Sieghart, 2015; Sigel and Buhr, 1997). Amino acid residues H101, Y159, G200, T206, and Y209 on the α1 subunit and F77, A79, T81, and M130 on the γ2 subunit are suggested to be a part of the binding pocket for ligands on the BZ binding site (Berezhnoy et al., 2004). H101 in α1, α2, α3, and α5 subunits controls the allosteric response to ligands of the BZ binding site (Berezhnoy et al., 2004; Wieland et al., 1992).

The region around γ2F77 (γ2T73-γ2T81) has β-sheet structure and undergoes conformational changes upon channel gating (Teissére and Czajkowski, 2001). Amino acid residues γ2T73, γ2D75, γ2A79, and γ2T81 line the BZ binding pocket (Teissére and Czajkowski, 2001).

In addition to the high-affinity BZ binding site at the α+γ- interface, a low affinity binding site for classical BZ has been developed at the α1+β2- interface, located pseudosymmetrically to the α1+γ2- interface (Baur et al., 2008). This site prevents potentiation of BZ induced $GABA_A$ activation through the classical BZ binding site at the α1+γ2- interface. The limitation of the action of BZ site ligands may contribute to the safety of these drugs (Baur et al., 2008). In addition, Ramerstorfer et al. demonstrated BZ-like modulatory effects via this α+β- interface by CGS 9895 (2-p-methoxyphenylpyrazolo[4,3-c]quinolin-3(5H)-one). This high-affinity antagonist at the α1+γ2- binding site positively modulates with low potency α1β3 receptors that have no classical BZ binding site (Ramerstorfer et al., 2011; Sieghart, 2015). The results of this study also showed that the inhibitory effect of flurazepam is mediated via α1+β2-, but not via α1+β3- , indicating a possible β-subunit specific action of this compound (Ramerstorfer et al., 2011; Sieghart, 2015).

In α1β2γ2 receptors, an additional phase of potentiation was observed for diazepam at higher concentrations. Mutations in this receptor subtype abolished the micromolar but not the nanomolar component of potentiation. In addition, diazepam at high concentrations also potentiated α1β2 receptors without the classical BZ binding site, suggesting another low-affinity binding site for diazepam (Walters et al., 2000). This binding site is suggested in the TM domain, but its exact location has not yet been established. Middendorp et al. described novel compounds acting via the classical BZ binding site that have affinity to this low-affinity binding site (Middendorp et al., 2015).

A point mutation that substitutes arginine for histidine in the α1/α2/α3/α5 subunits (like in α4 and α6), makes the $GABA_A$ receptor insensitive to allosteric modulation by BZ (Wieland et al., 1992). The comparison of drug-induced behavioral responses in mutant and wild type mice allows a characterization of subunit-dependent BZ effects *in vivo* (Olsen and Sieghart, 2008; Rudolph and Möhler, 2014).

Mediation of Sedative and Hypnotic Effects

The sedative effect of diazepam is predominantly mediated via the α1 subunit, and can be eliminated by point mutation (α1H101R) in mice (Bateson, 2004; McKernan et al., 2000; Rudolph et al., 1999).

The hypnotic activity of zolpidem is also mediated via the α1 subunit (Kopp et al., 2004). The sedative effect of etomidate is mediated via the β2 subunit (Reynolds et al., 2003).

Mediation of Anxiolytic Effects

Both α2 and α3 subunits are suggested to mediate anxiolytic effects of BZ (Morris et al., 2006). Löw et al. described that anxiolytic effects of diazepam are mediated via α2 subunits, but not

via α3 subunits (Löw et al., 2000). Other studies describe an α3 selective agonist TP003 that has anxiolytic effects in both rodents and non-human behavioral models of anxiety (Dias et al., 2005). The involvement of α3 subunits in mediating anxiolytic effects of BZ still remains controversial (Rudolph and Möhler, 2014).

Mediation of Anticonvulsive Effects

The subunit(s) mediating anticonvulsive effects of BZ are not yet identified. In α1H101R mice, the anticonvulsive effect of diazepam is attenuated, suggesting an involvement of α1 subunits in mediating anticonvulsive effects (Rudolph et al., 1999). Other studies suggest that anticonvulsive effects are not mediated by any single subunit, but rather different subunits act synergistically (Fradley et al., 2007).

In contrast, the anticonvulsive effect of zolpidem seems to be mediated exclusively via α1 subunit-containing receptors (Bateson, 2004; Crestani et al., 2000).

Mediation of Myorelaxation

The muscle relaxant effect of diazepam is mainly mediated via α2 subunits. In higher doses, α3 subunits are also involved (Crestani et al., 2001).

Mediation of Dependence and Addictive Properties

Abuse of BZ is a significant clinical phenomenon, but the subunit(s) involved in the mechanism of BZ dependence is still unclear (Reynolds et al., 2012). The involvement of the α1 subunit was suggested (Tan et al., 2010). Other studies elicited also α2 and α3 subunits as key mediators of reward-related effects of BZ (Reynolds et al., 2012).

1.1.4.2 Non-classical BZ

Zolpidem, zopiclone, and zaleplone ("z-drugs") are structurally different from BZ, but also bind to the BZ pocket (Bateson, 2004). They possess a similar clinical profile of high efficacy and low toxicity like BZ (Goa and Heel, 1986).

Zolpidem acts as a short duration hypnotic with fast onset and does not alter the pattern of physiological sleep (Depoortere et al., 1986). It has sedative, myorelaxant, and anticonvulsive effects with a strong preference to the sedative effect due to its preferential binding to α1 subunit containing $GABA_A$ receptors (Bateson, 2004). Zolpidem has a 10- to 20-fold lower affinity for α2 and α3 subunit-containing $GABA_A$ receptors, and relatively little affinity for α5-containing

receptors (Fitzgerald et al., 2014; Langer et al., 1990; Pritchett and Seeburg, 1991). Zolpidem only acts on $GABA_A$ receptors containing $\gamma 2$ subunits (Khom et al., 2006; Lüddens et al., 1994).

While development of tolerance after prolonged use of BZ has been reported (File, 1981; Galpern et al., 1991), tolerance after zolpidem treatment is still unclear (Fitzgerald et al., 2014). Comparing the effects of midazolam and zolpidem in mice, a tolerance to anticonvulsive and locomotor-impairing effects were observed for midazolam, but not for zolpidem (Ebert et al., 2008; Perrault et al., 1992). Tolerance to rate-decreasing and sedative effects were observed after repeated administration of classical BZ, but not zolpidem (Cohen and Sanger, 1994; Elliot and White, 2000; Sanger and Zivkovic, 1992). In contrast, other studies observed decreased thresholds for PTZ-induced seizures after zolpidem administration (Vlainić and Pericić, 2009), also EEG sleep recordings have shown sleep impairments after repeated daily administration of zolpidem in rats (Ebert et al., 2008). Tolerance for the ataxic-like effects after treatment with zolpidem was also seen in both rats and non-human primates (Elliot and White, 2000; Griffiths et al., 1992; Voss et al., 2003).

Taken together, zolpidem induces development of tolerance, but the incidence is lower than for classical BZ (Fitzgerald et al., 2014). Prolonged activation of $\alpha 1$ containing $GABA_A$ receptors alone may thus cause less severe neuroadapative changes that underlie tolerance effects than non-specific activation of $GABA_A$ receptors by BZ (Fitzgerald et al., 2014).

1.1.4.3 Ethanol

Ethanol potentiates extrasynaptic $GABA_A$ receptors containing $\alpha 4/6$ and δ subunits at pharmacologically relevant concentrations (Olsen et al., 2007; Sundstrom-Poromaa et al., 2002; Wallner et al., 2003). At higher concentrations, which are usually not reached by normal alcohol consumption, ethanol also potentiates synaptic $GABA_A$ receptors containing γ subunits (Wallner et al., 2003).

In addition, ethanol is ten times less sensitive to $\beta 2$ containing than to $\beta 3$ containing $GABA_A$ receptors (Wallner et al., 2003). $\beta 3$ containing receptors are also suggested to mediate anesthetic actions of etomidate and propofol (see Section 1.1.4.4). The higher preference of ethanol for $\beta 3$ containing $GABA_A$ receptors is determined by differences in amino acid residues in the N-terminus between β subunits (Wallner et al., 2014). The position $\beta 3$Y66 is homologous to $\gamma 2$T81 that determines sensitivity for imidobenzodiazepines at the classical $\alpha+/\gamma$- interface (Kucken et al., 2003; Teissére and Czajkowski, 2001; Wallner et al., 2014).

The binding site for ethanol in $GABA_A$ receptors containing $\beta 3$ and δ subunits is believed to be at the $\alpha 4/6+\beta 3$- interface (Wallner et al., 2014). This site is homologous to the classical BZ binding site. Selected BZ site ligands including alcohol agonistic imidazobenzodiazepines (e.g.

RO15-4513) with a large moiety at the C7 position of the benzodiazepine ring may compete with alcohol for its binding pocket at this site. This may explain the competitive relationship between ethanol and imidobenzodiazepine alcohol antagonists (Wallner et al., 2014).

Regarding alcohol withdrawal effects, chronic application of ethanol leads to an impairment in GABAergic neurotransmission with concomitant changes in subunit compositions of $GABA_A$ receptors in the cerebral cortex, hippocampus, and amygdala (Devaud et al., 1997; Diaz et al., 2011; Kumar et al., 2009; Liang et al., 2007). In the basolateral amygdala (BLA), surface expression of $\alpha 1$, $\alpha 2$, and δ subunits was shown to be decreased after chronic intermittent ethanol (CIE) administration over forty days (Lindemeyer et al., 2014). In contrast, the expression of $\alpha 4$ and $\gamma 2$ subunits is increased after CIE treatment in the BLA (Lindemeyer et al., 2014), hippocampal CA1, and dentate gyrus neurons (Liang et al., 2007).

$GABA_A$ receptors containing $\alpha 2$ subunits in the BLA play a crucial role in mediating anxiety behavior (see Section 1.2.1 and Section 1.1.4.1), suggesting that down-regulation of surface $\alpha 2$ subunits in the BLA might explain development of withdrawal-anxiety after ethanol intoxication (Lindemeyer et al., 2014). Sedative and – to some extent – anticonvulsive actions of BZ are mediated by $\alpha 1$ subunits (see chapter Section 1.1.4.1), suggesting that decreases in the $\alpha 1$ subunit might be associated with disruption of sleep patterns, hyperexcitability, and decreased seizure threshold during ethanol withdrawal (Ehlers and Slawecki, 2000; Kokka et al., 1993; Lindemeyer et al., 2014).

1.1.4.4 Anesthetics

General anesthesia became a regular procedure for surgery around 1850, based on ether, nitrous oxide, and chloroform. In the meantime, the medication used for anesthesia has evolved greatly and now involves sophisticated combinations of anesthetics, sedatives, and muscle relaxants instead of single drugs (Rudolph and Antkowiak, 2004).

General anesthetics were initially believed to interact with the lipid bilayer of neuronal cells (Siegwart et al., 2002). Today, it is clear that general anesthetics modulate ligand gated ion channels, including $GABA_A$ receptors (Rudolph and Antkowiak, 2004). At low concentrations anesthetics potentiate GABA induced currents, at high concentrations they activate $GABA_A$ receptors directly in the absence of GABA (Sieghart, 2015).

General anesthetics can be applied either intravenously (like barbiturates, etomidate, and propofol) or by inhalation (volatile agents like desfluran, isofluran, enfluran, and halothane). Li et al. identified amino acid residues α1M236 and β3M286 that contribute to the binding site for general anesthetics on $GABA_A$ receptors by use of the radiolabeled photoreactive etomidate analog 3|H|azietomidate. This binding site is located in the TM domain at the interface between the α and β subunits (Li et al., 2006).

Barbiturates

Barbiturates like pentobarbitone and phenobarbitone have anticonvulsive, anxiolytic, sedative, anesthetic, hypnotic, and – in overdose – respiratory depressive effects (Löscher and Rogawski, 2012). They modulate $GABA_A$ receptors allosterically by increasing the open time of the $GABA_A$ receptor (Leeb-Lundberg et al., 1980; MacDonald et al., 1989). At higher concentrations, barbiturates are able to activate $GABA_A$ receptors directly in the absence of GABA (ffrench Mullen et al., 1993; Macdonald and Olsen, 1994; Mathers and Barker, 1980). At higher millimolar concentrations, barbiturates even block $GABA_A$ receptors (Drafts and Fisher, 2006).

Modulatory activity and direct activation are two distinct mechanisms that depend on the subunit composition of the $GABA_A$ receptor (Chang et al., 2003; Serafini et al., 2000; Thompson et al., 1996). The amino residue β2G219 is suggested to mediate potentiation (Chang et al., 2003), whereas α6T69 was identified as a key residue for mediating direct activation of $GABA_A$ receptors by pentobarbital (Drafts and Fisher, 2006).

The strength of the effects of barbiturates depends on isoforms of both the α and β subunits (Thompson et al., 1996). Barbiturates have strong preference for $GABA_A$ receptors containing α6 subunits over those containing α1 subunits (Chang et al., 2003).

Etomidate

Etomidate is a subunit selective modulator of $GABA_A$ receptors with a strong preference for receptors containing β2 and β3 subunits over β1 subunits (Belelli et al., 1997). The amino acid residue N265 in the TM2 domain of β2 and β3 subunits plays a key role in mediating selectivity of etomidate (Belelli et al., 1997; Reynolds et al., 2003).

Anesthetic actions of etomidate are mediated via $GABA_A$ receptors containing β3 subunits, whereas sedation is mediated exclusively via β2 containing $GABA_A$ receptors (Reynolds et al., 2003).

In receptors containing β2 subunits, the effect of etomidate is also influenced by α subunits. Both potency and efficacy of etomidate is most marked in receptors containing α6 subunits (Hill-Venning et al., 1997).

Besides the described binding site for general anesthetics (Li et al., 2006), other studies provide evidence for an etomidate binding site located at the TM β3+β3- interface of $\alpha1\beta3$ receptors (Chiara et al., 2012; Sieghart, 2015).

Propofol

Propofol is the most important and most frequently used intravenous general anesthetic (Yip et al., 2013).

Amino acid residues αM236 and βM286 in within the $\beta+\alpha+$ site of $\alpha1\beta3$ $GABA_A$ receptors are suggested to be contact residues for propofol (Stewart et al., 2014). The amino acid residue β3N265, which determines the selectivity of etomidate, also might influence the selectivity of propofol (Jurd et al., 2003). Modulation of propofol via β-$\alpha+$ and β-$\gamma+$ is also suggested (Stewart et al., 2014). Additionally, amino acid residues α1F385 at the large intracellular loop of $\alpha1\beta2$ $GABA_A$ receptors (Moraga-Cid et al., 2011) , and β2Y444 in the TM4 were identified to influence the action of propofol (Richardson et al., 2007).

Recently, a new binding site for propofol was identified by photolabeling on both β3 homopentamers and $\alpha1\beta3$ heteropentamers (Yip et al., 2013). This binding site includes β3H267 (Yip et al., 2013), an amino acid residue that coordinates the potentiation of propofol on $GABA_A$ receptors (Miller and Aricescu, 2014) and amino acid residues β3F221, β3N265, and β2G219 (Yip et al., 2013).

1.1.4.5 Neurosteroids

Neurosteroids are endogenous modulators of $GABA_A$ receptors, they play an important role in mediating stress responses by inducing anxiolysis or sedation (Adams et al., 2015). The endogenous neurosteroids that act most potently on both synaptic and extrasynaptic $GABA_A$ receptors are allopregnanolone (ALLOP) and tetrahydrodeoxycorticosterone (THDOC) (Belelli and Lambert, 2005).

Neurosteroids potentiate GABA induced currents at low concentrations, and are able to activate $GABA_A$ receptors directly at higher concentrations. These high concentrations can occur during the ovarian cycle or pregnancy (Belelli and Lambert, 2005).

Amino acid residues in the TM domains of $GABA_A$ receptor α subunits α1Q241 and α1N407 mediate the potentiation of GABA induced currents at low steroid concentrations. The effect of direct activation of $GABA_A$ receptors at high steroid concentrations is thought to be mediated by amino acid residues α1T236 and β2Y284, located at the $\beta+\alpha-$ interface (below the GABA-binding pocket) (Hosie et al., 2006; Sieghart, 2015).

1.2 Involvement of the GABA System in the Pathology of Neurological Disorders

The balance between excitatory and inhibitory synaptic signals in the CNS is a prerequisite for proper brain function (Nuss, 2015). Dysregulation of the balance can lead to neurological disorders. If the balance is shifted to the excitatory side, i.e. reduction of inhibitory GABAergic neurotransmission, insomnia, anxiety, and seizures appear. Enhancement of inhibitory GABAergic transmission leads to sedation and anxiolysis and potentially also amnesia, ataxia, and loss of consciousness (Möhler et al., 2002).

1.2.1 Anxiety Disorders

Anxiety disorders are caused by dysfunctions of brain circuits that regulate emotional responses to potentially threatening stimuli (Farrant and Nusser, 2005) and are characterized by negative emotional feelings. Feelings of worry and apprehension are part of normal behavior and crucial for defense mechanisms. Excessive severe anxiety that becomes frequent or appears in inappropriate situations is considered as pathological. Three main types of anxiety disorders are described in DSM-5 *(Diagnostic and Statistical Manual of Mental Disorders, Fifth Edition)*:

- Anxiety disorders (including generalized anxiety disorders, panic disorders, agoraphobia, phobias, and social anxiety disorders)
- Obsessive-compulsive and related disorders
- Trauma- and stressor-related disorders (includes posttraumatic stress disorder, acute stress disorder, and adjustment disorders)

(Nuss, 2015).

The amygdala, the medial prefrontal cortex (mPFC), and the hippocampus are mainly involved in the circuit of anxiety (Ehrlich et al., 2009). Among other subdivisions, the amygdala encompasses the anatomically and functionally different nuclei, the BLA and the central amygdala (CeA). The BLA receives potential negative emotional signals from the thalamus and sensory association cortex (Nuss, 2015) and activates the CeA through glutamatergic projection neurons and intercalated (ITC) clusters of GABAergic neurons surrounding the BLA (Busti et al., 2011; Ehrlich et al., 2009).

The smaller paracapsular lateral ITCs (lITCs) convey feedforward inhibition to the BLA, whereas medial ITCs (mITCs) facilitate feedforward inhibition from BLA to CeA (Ehrlich et al., 2009).

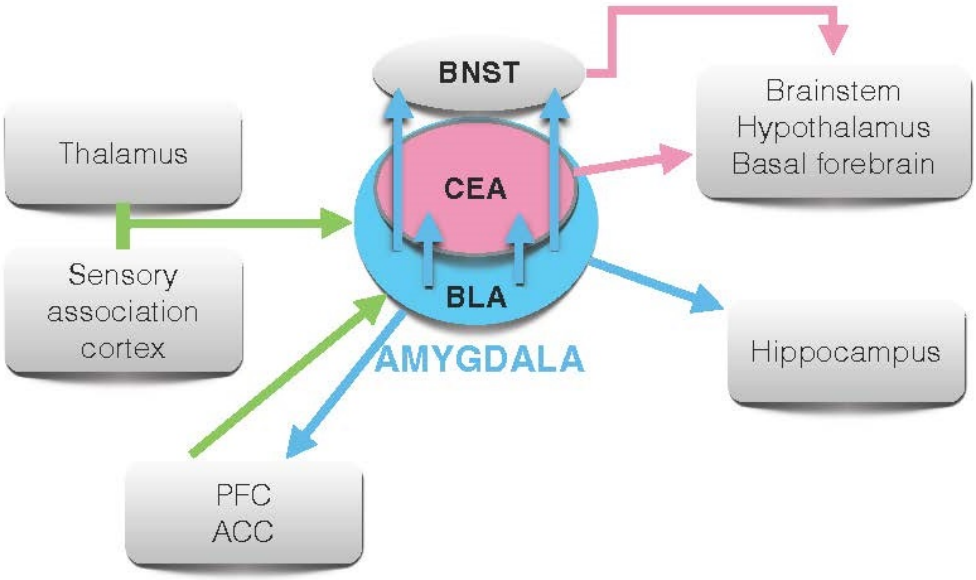

Figure 1.2: Neural circuits in anxiety disorders. Green arrows indicate inputs to BLA; blue arrows indicate outputs of the BLA; pink arrows indicate outputs of the CeA and BNST. Anterior cingulate cortex (ACC); Basolateral amygdala (BLA); Bed nucleus of the stria terminalis (BNST); Central nucleus of the amygdala (CeA); Prefrontal cortex (PFC). Figure adapted from (Nuss, 2015).

Both control input and output inhibitory signals of the amygdala and may therefore play a major role controlling CeA excitability and fear expression (Ehrlich et al., 2009).

Within the CeA, lateral (CeA_L) and a medial (CeA_M) divisions have been identified (Ehrlich et al., 2009). The CeA_M is the principal output area of the amygdala and accounts for the expression of fear responses (Busti et al., 2011; Ehrlich et al., 2009), operating by GABAergic interneurons containing $\alpha 2$ subunits (Rudolph and Möhler, 2014).

The anterior cingulate cortex (ACC) and the mPFC regulate the expression of anxiety by receiving and sending excitatory glutamatergic projection to and from the BLA (Figure 1.2). They are activated simultaneously with the amygdala during the presence of emotional stimuli (Nuss, 2015).

Neuroimaging studies show a deficit of $GABA_A$ receptors in patients with anxiety disorders in areas that are known to be involved in the process of anxiety (amygdala, cerebral cortex, and hippocampus) (Möhler et al., 2002). In mice, reducing the gene dosage of the $\gamma 2$ receptor subunit (which anchors $GABA_A$ receptors in the subsynaptic membrane) leads to a reduced synaptic clustering of $GABA_A$ receptors, enhanced anxiety responses, and a bias for threat cues (Crestani et al., 1999).

Panic disorder, a severe form of anxiety, is characterized by spontaneous paroxysmal fear attacks (Malizia et al., 1998). Patients who suffer from this disease show a reduced binding of the BZ

antagonist flumazenil and lower levels of GABA in their occipital cortex (Goddard et al., 2001; Malizia, 1999; Malizia et al., 1998). Furthermore, they are less sensitive to BZ agonists than healthy people (Malizia et al., 1998; Roy-Byrne et al., 1990). Flumazenil leads to severe fear and panic attacks in patients with anxiety disorders, but not in healthy individuals (Nutt et al., 1990). In this case, flumazenil could act as an inverse agonist or blocks an endogenous agonist which is not able then to operate as a compensatory tool as it does in healthy controls (Malizia et al., 1998).

1.2.2 Sleeping Disorders

Insomnia is the most prevalent form of sleeping disorders and is generally classified into three forms: sleep onset insomnia, sleep maintenance insomnia, and terminal insomnia. The last form describes the inability to fall asleep again after waking up (Nuss, 2015).

The onset and maintenance of sleep are both strongly influenced by GABAergic neurotransmission (Nuss, 2015). GABA-containing neurons in the ventrolateral preoptic nucleus (VLPO) are under tonic inhibition from noradrenergic neurons in the locus coeruleus (LC). Inhibition of the neurons of the LC results in activation of the GABAergic neurons of the VLPO. This leads to a release of GABA into the tuberomammillary nucleus (TMN), where it inhibits histamine release into the cortex (Nelson et al., 2002).

The TMN is located in the hypothalamus and plays an important role in controlling waking and sleeping (Sherin et al., 1998). Inhibition of histaminergic TMN neurons leads to loss of consciousness and sleep (Nelson et al., 2002). TMN neurons are innervated from GABAergic neurons in the VLPO (Sherin et al., 1998). These neurons express nine different $GABA_A$ receptor subunits: $\alpha1$, $\alpha2$, $\alpha5$, $\beta1$, $\beta2$, $\beta3$, $\gamma1$, $\gamma2$ and ϵ (May et al., 2013).

Regarding the α subunits, $\alpha2$ and $\alpha1$ play a dominant role over $\alpha5$ subunits at the BZ site of the TMN neurons of mice, measured by the modulation of zolpidem (May et al., 2013). The endogenous sleep pathway in the hypothalamus operates through $\beta1$-containing $GABA_A$ receptors. In contrast, the inhibition of neuronal firing by low propofol doses relies on $\beta3$-containing receptors, suggesting that sleep and anesthesia depend on different $GABA_A$ receptor types (Yanovsky et al., 2012).

1.2.3 Epilepsy

Patients who suffer from epilepsy show electrical brain abnormalities, which can range from asymptomatic electrographic seizures to generalized convulsions with a loss of consciousness (Yaffe et al., 2014). It is important to distinguish between the terms “seizure” and “epilepsy”. An

epileptic seizure occurs as an abnormal excessive or synchronous activity in the brain, whereas epilepsy is an enduring predisposition to generate epileptic seizures (Fisher et al., 2005).

Epilepsies can be divided into different forms depending on their pathological origin. They can be symptomatic due to other diseases, for example, a tumor, a trauma, or metabolic or cerebral disorders. In contrast, many forms of epilepsy are cryptogenic or idiopathic. Idiopathic partial and generalized epilepsies are the most abundant heritable seizure forms, accounting for 40 % of all epilepsies. They are not associated with trauma or other disorders but are triggered mainly by genetic factors (Steinlein, 2001).

Deficits in GABAergic transmission are associated with the pathogenesis of epilepsy, as abnormalities in GABAergic transmission are observed in acquired and genetic epilepsy in animals (Treiman, 2001). In families with idiopathic generalized epilepsies (IGEs, epilepsy-causing mutations have been identified in four $GABA_A$ receptor genes: GABRG2, GABRA1, GABRD, and GABRB3, encoding $\gamma 2$, $\alpha 1$, δ, and $\beta 3$ subunits (Cossette et al., 2012; Macdonald et al., 2010).

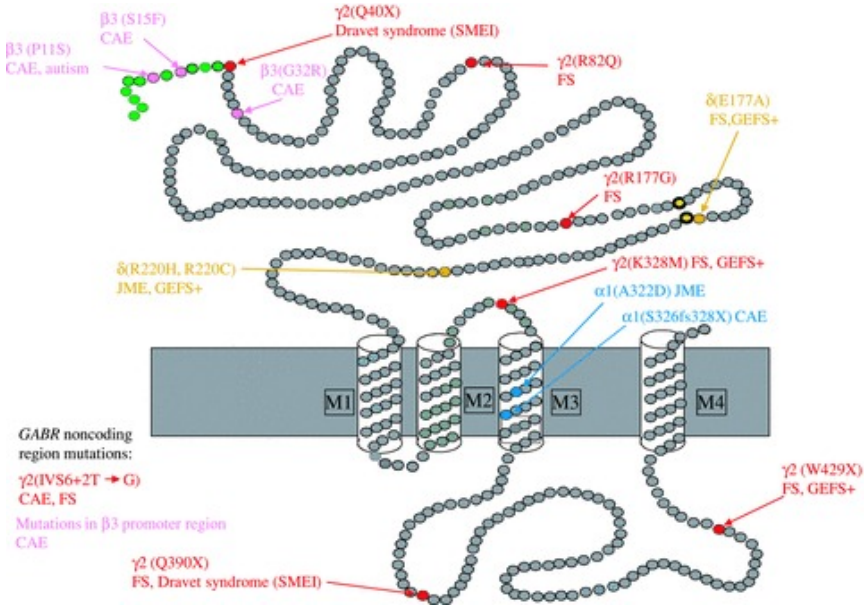

Figure 1.3: $GABA_A$ receptor $\alpha 1$ (blue), $\beta 3$ (pink), $\gamma 2$ (red), and δ (yellow) subunit mutations associated with genetic epilepsy forms. Childhood absence epilepsy (CAE); General epilepsy with febrile seizures plus (GEFS+); Febrile seizures (FS); Juvenile myoclonic epilepsy (JME). Figure from (Macdonald et al., 2010).

Recently, other mutations in $GABA_A$ receptor genes associated with epilepsy have been identified:

- $\alpha 1$ D219N in GABRA1
- $\alpha 1$ K353delins18X in GABRA1
- $\gamma 2$ P83S in GABRG2 (Lachance-Touchette et al., 2011)

- α1 T292I in GABRA1
- β3 N110D in GABRB3
- β3 Y302C in GABRB3
- β3 D120N in GABRB3
- β3 E180G in GABRB3 (Epi4K Consortium et al., 2013)
- γ2 R43Q in GABRG2 (Hancili et al., 2014; Sancar and Czajkowski, 2004)
- β2 M79T in GABRB2

(Srivastava et al., 2014).

2 Methods

2.1 *in vivo*

Animals

All procedures involving animals were approved by the Austrian Federal Ministry of Science and Research in compliance with the European convention for the protection of vertebrate animals used for experimental and other scientific purposes ETS no.: 123. Every effort was taken to minimize the number of animals used in this study. Female Xenopus laevis frogs were purchased from NASCO (Fort Atkinson, USA) and kept in groups in temperature-controlled, continuous-flow water tanks (20 ± 1°C). Male C57BL/6N mice were obtained from Charles River Laboratories (Sulzfeld, Germany). Mice (age 3-6 months) were group-housed (maximum 5 mice per type IIL cage) with free access to food and water. At least 24h before the commencement of experiments, they were transferred to the testing facility, continuing ad libitum access to food and water. The temperature in the holding (for mice and frogs) and testing facilities was fixed to 22±2°C; the humidity ranged between 40-60 %; a 12h light-dark cycle was in operation (lights on from 07.00 to 19.00). Intraperitoneal (i.p.) injection of control or compound-containing solutions was done 15, 30, 60, 90, 120, and 150 min before testing, depending on the respective experiment. Application of the solvent alone did not influence animal behavior. All doses are indicated as mg/kg bodyweight of the animal (Hintersteiner et al., 2014).

2.1.1 Elevated Plus Maze Test

The animals' behavior was tested over 5 min on an elevated plus maze (EPM) 1 m above ground consisting of two closed and two open arms, each 50x5 cm in size. The test instrument was built from gray PVC; the height of closed arm walls was 20 cm. Illumination intensity was set to 180 lux. Animals were placed in the center, facing an open arm. Analysis of open arm time,

open arm distance, open arm entries, closed arm entries and total distance was automatically done with Video-Mot 2 equipment and software (TSE systems, Bad Homburg, Germany) (Lister, 1987; Hintersteiner et al., 2014).

2.1.2 Light Dark Choice Test

The light/dark test (LDT) is described by Crawley and Goodwin (Crawley and Goodwin, 1980). The behavior of the animals was tested over 10 minutes in the light/dark box. Illumination intensity was set to 400 lux in the light box. Animals were placed in the lit area, facing the entrance of the dark area. Analysis of the time in the lit area was automatically done by Acti-Mot2 (Crawley and Goodwin, 1980).

2.1.3 Open Field Test

Exploration of a novel environment was tested by means of the open field test (OF) over 10 min in a 50x50 cm box build from gray PVC equipped with infra-red beams. Illumination intensity was set to 150 lux in the center. The time in the center and total ambulation of mice was analyzed using ActiMot-2 equipment and software (TSE-systems, Bad Homburg, Germany). Arenas were subdivided into 3 fields: border (up to 8 cm from wall), center (20x20 cm, i.e. 16 % of total area), and intermediate area according to the recommendations of EMPRESS (European Mouse Phenotyping Resource of Standardised Screens) (Khom et al., 2013).

2.1.4 PTZ tail-vein Infusion Test

Seizure threshold was determined by PTZ tail-vein infusion on freely moving animals at a rate of 100µl/min (10 mg/ml PTZ in saline, ph = 7.4). Infusion was stopped when animals displayed generalized clonic seizures. Animals were immediately killed by cervical displacement after onset of seizures. PTZ-tail vein infusion tests were performed in assistance with Prof. Schwarzer, Medical University of Innsbruck. The seizure threshold dose was calculated from the infused volume in relation to bodyweight.

2.1.5 Measurement of Body Temperature

A temperature probe (Type 1 Thermocouple probe RET-3 connected to a Type T Thermometer, Physitemp. Instruments Inc., Clifton, USA), lubricated with glycerol, was inserted into the rectum of the mouse for a depth of up to 1 cm. The temperature probe remained in the animal till a stable temperature was reached (maximum 10 min) (Khom et al., 2013).

2.1.6 Sample Preparation for Determining VA and Piperine Derivatives

Blood samples were taken 15, 30, and 60 min after i.p. injection of the compounds. 10 min after i.p injection of thiopental (150 mg/kg bodyweight in 0.9 % sodium chloride solution) blood samples (500–800 ml) were collected and compiled into ethylenediaminetetraaceticacid (EDTA)-coated microtubes (1.6 mg EDTA/sample) and centrifuged at 12.000 rpm for 5 min at 4 °C. Plasma samples were transferred into 1.5 ml tubes and stored at -80 °C until analysis.

Sample Preparation for VA and Derivatives

For sample preparation, a liquid–liquid extraction method together with an internal standard (IS) acetoxyvalerenic acid was applied for the quantification of VA in plasma. To 100 ml of plasma sample 10 ml of IS solution (1 mg/ml 10 % aqueous dimethyl sulfoxide (DMSO)) was added. These solutions were extracted by liquid–liquid partition with 400 ml of dichloromethane/t-butylmethylether (80:20, v/v) and vortexed for 5 min. From the clear lower organic layer the solvent was removed through a constant nitrogen stream at room temperature (25 °C). The residue was dissolved with 100 ml of methanol, sonicated, centrifuged for 5 min (15.000 rpm) and the supernatant was finally transferred to autosampler vials (Macherey-Nagel vial N9, 0.2 ml with integrated insert; Macherey-Nagel, Düren, Germany) (Hintersteiner et al., 2014; Sampath et al., 2012). Sample preparation for piperine derivatives was done by Dr. Mousshin Oufir, University of Basel.

2.2 *in vitro*

2.2.1 Two-microelectrode Voltage Clamp Technique

Expression and Functional Characterization of $GABA_A$ Receptors

Preparation of stage V-VI oocytes from Xenopus laevis (NASCO, Fort Atkinson, USA), synthesis of capped off run-off poly (A^+) rat cRNA transcripts from linearized cDNA templates (pCMV vector) was performed as described (Khom et al., 2006). Briefly, female Xenopus laevis were anaesthetized by exposing them for 15 min to a 0.2 % solution of MS-222 (methane sulfonate salt of 3-aminobenzoic acid ethyl ester) before surgically removing parts of the ovaries. Follicle membranes from isolated oocytes were enzymatically digested with 2 mg/ml collagenase (Type 1A). Oocytes were stored at 18 °C in ND96 solution (Methfessel et al., 1986). After isolation, oocytes were injected with about 10-50 nl of nuclease-free water containing the different rat cRNAs (100-2000ng/μl/subunit).

For expression of $\alpha1\beta3\gamma2$s receptors, cRNAs were mixed in a ratio of 1:1:10 (Boileau et al., 2002); to avoid formation of homooligomeric $\beta1$-receptors in the case of $\alpha1\beta1\gamma2$s a ratio of 3:1:10 was used (Krishek et al., 1996).

Electrophysiological experiments were done using the two-microelectrode voltage clamp technique at a holding potential of -70 mV making use of a TURBO TEC 01C amplifier (npi electronic, Tamm, Germany) and an Axon Digidata 1322A interface (Molecular Devices, Sunnyvale, CA). Data acquisition was carried out using pCLAMP v.9.2 (Molecular Devices, Sunnyvale, CA).

The bath solution contained 90 mM NaCl, 1 mM KCl, 1 mM $MgCl_2.6H_2O$, 1 mM $CaCl_2$ and 5 mM HEPES (pH 7.4).

Microelectrodes were filled with 2 M KCl and had resistances between 1 and 3 MΩ.

Perfusion System

GABA and drugs were applied by means of fast perfusion system; drug or control solutions were applied by means of a TECAN Miniprep 60 permitting automation of the experiments. To elicit I_{GABA} the chamber was perfused with 120 μl of GABA-containing solution at volume rate between 300 and 1000 μl/s. The I_{GABA} rise time ranged between 100 and 250 ms (Khom et al., 2006). To account for possible slow recovery from increasing levels of desensitization in the presence of high compound concentrations, the duration of washout periods was extended stepwise, i.e. 1 min (GABA EC_{3-7}) to 1.5 min (co-application of GABA EC_{3-7} in the presence $\leq 1\mu$M compound) to 2.5 min (co-application of GABA EC_{3-7} in the presence of $\leq$10 μM compound) to 5min (co-application of GABA EC_{3-7} and $\leq 100\mu$M compound) to 15min (GABA EC_{3-7} in the presence of 300-500μM compound). Potential run-down or run-up effects were ruled out by application of GABA control at the end of each experiment. Oocytes with maximal current amplitudes >5 μA were discarded to exclude voltage-clamp errors.

Analyzing Concentration-response Curves

Stimulation of chloride currents by modulators of the $GABA_A$ receptor was measured at a GABA concentration eliciting between 3 and 7 % of the maximal current amplitude (EC_{3-7}). The EC_{3-7} was determined at the beginning of the experiment for each oocyte by application of 1 mM GABA followed by submaximal GABA concentrations. Enhancement of the chloride current was defined as $(I_{(GABA+Comp)}/I_{GABA}) - 1$, where $I_{(GABA+Comp)}$ is the current response in the presence of compound and I_{GABA} is the control GABA current. Concentration-response curves were generated and the data were fitted by non-linear regression analysis using Origin software (OriginLab Corporation, USA).

Data were fitted to the Hill equation:

$$y = A1 + (A2 - A1) * xn/(kn + xnH) \tag{2.1}$$

In Equation (2.1) k corresponds to the EC50 value, x values are logs of concentration, and nH is the Hill coefficient (Khom et al., 2013).

2.3 Statistical Analysis

Statistical significance was calculated by paired students t-test and one-way ANOVA followed by a post-hoc mean comparison with Bonferroni, respectively (OriginLab Corporation, USA or GraphPad, La Jolla, USA). P-values of <0.05 were accepted as statistically significant. All data are given as mean ± SEM (Hintersteiner et al., 2014).

3 Aims

General

$GABA_A$ receptors are targets for anxiolytic and anticonvulsive drugs. $GABA_A$ receptor modulators, such as the widely prescribed BZ have been used to treat anxiety disorders and epilepsy for decades (see Section 1.1.4.1).

However, these drugs have adverse effects such as sedation, daytime drowsiness, and anterograde amnesia. Also, long-term use of classical BZ can lead to tolerance, addiction, and withdrawal reactions (Chouinard, 2004). These unwanted effects are believed to be a result of relatively unselective modulation of $GABA_A$ receptors. Thus, there is a medical need for subunit-selective/subtype-selective modulators (Engin et al., 2012).

Valerenic acid (VA), piperine and their derivatives have been identified as $\beta 2/3$ subunit-selective modulators of $GABA_A$ receptors with a promising pharmacological profile (Khom et al., 2013, 2010). A major aim of these studies is to further investigate the therapeutic potential of these compounds.

Specific

The present study was designed to investigate the following properties of VA, piperine and derivatives, especially:

- Studying effects on anxiety-related behavior in C57BL/6N mice by means of the EPM test and LDT, and using the OF test to characterize effects on locomotor activity (sedation).
- Assessing anticonvulsive activity using the PTZ tail-vein infusion test.
- Insights into the pharmacokinetic properties of VA and piperine derivatives will be obtained by measuring plasma levels at different time points after i.p. administration.

4 Results

The four following subsections provide the results of the work of this thesis. The declaration of the contribution is described at the beginning of each paper or paper draft.

Publications in Peer Reviewed Journals

4.1

Hintersteiner, J., Haider, M., Luger, D., Schwarzer, C., Reznicek, G., Jäger, W., Khom, S., Mihovilovic, M.D., Hering, S., 2014. *Esters of valerenic acid as potential prodrugs.* Eur. J. Pharmacol. 735, 123–131. doi:10.1016/j.ejphar.2014.03.019

4.2

Khom, S., Strommer, B., Schöffmann, A., **Hintersteiner, J.**, Baburin, I., Erker, T., Schwarz, T., Schwarzer, C., Zaugg, J., Hamburger, M., Hering, S., 2013. *GABAA receptor modulation by piperine and a non-TRPV1 activating derivative.* Biochem. Pharmacol. 85, 1827–1836. doi:10.1016/j.bcp.2013.04.017

4.3

Schöffmann, A., Wimmer, L., Goldmann, D., Khom, S., **Hintersteiner, J.**, Baburin, I., Schwarz, T., Hintersteininger, M., Pakfeifer, P., Oufir, M., Hamburger, M., Erker, T., Ecker, G.F., Mihovilovic, M.D., Hering, S., 2014. *Efficient modulation of γ-aminobutyric acid type A receptors by piperine derivatives.* J. Med. Chem. 57, 5602–5619. doi:10.1021/jm5002277

Publication in Preparation

4.4

Khom, S., **Hintersteiner, J.***, Luger, D.*, Haider, M., Pototschnig, G., Schwarzer, C., Mihovilovic, MD., Hering, S. *Probing the Potential of Valerenic Acid and Derivatives as Scaffolds for the Development of Novel Anticonvulsants.*

(*) Both authors contributed equally to the paper
Status: Paper draft in preparation, **version 2015 July 14**

4.1 Paper I
Esters of Valerenic Acid as Potential Prodrugs (Hintersteiner et al., 2014)

Hintersteiner, J., Haider, M., Luger, D., Schwarzer, C., Reznicek, G., Jäger, W., Khom, S., Mihovilovic, M.D., Hering, S., 2014. *Esters of valerenic acid as potential prodrugs.* Eur. J. Pharmacol. 735, 123–131. doi:10.1016/j.ejphar.2014.03.019

Contribution

- Effects on explorative behavior by means of the EPM test
- Effects on seizure threshold by means of PTZ-tail vein infusion (Assistance)
- Sample collection and preparation for detection of VA in plasma samples

European Journal of Pharmacology 735 (2014) 123–131

Results

Contents lists available at ScienceDirect

European Journal of Pharmacology

journal homepage: www.elsevier.com/locate/ejphar

Behavioural pharmacology

Esters of valerenic acid as potential prodrugs

Juliane Hintersteiner [a], Maximilian Haider [b], Denise Luger [a], Christoph Schwarzer [c], Gottfried Reznicek [d], Walter Jäger [e], Sophia Khom [a], Marko D. Mihovilovic [b], Steffen Hering [a,*]

[a] Department of Pharmacology and Toxicology, University of Vienna, Althanstrasse 14, A-1090 Vienna, Austria
[b] Institute of Applied Synthetic Chemistry, Vienna University of Technology, Getreidemarkt 9, A-1060 Vienna, Austria
[c] Department of Pharmacology, Innsbruck Medical University, Peter-Mayr-Straße 1, 1a A-6020 Innsbruck, Austria
[d] Department of Pharmacognosy, University of Vienna, Althanstrasse 14, A-1090 Vienna, Austria
[e] Department of Clinical Pharmacy and Diagnostics, University of Vienna, Althanstrasse 14, A-1090 Vienna, Austria

ARTICLE INFO

Article history:
Received 9 December 2013
Received in revised form
7 March 2014
Accepted 19 March 2014
Available online 27 March 2014

Keywords:
$GABA_A$ receptors
Valerenic acid derivatives
Behavioral analysis
2-Microelectrode-voltage-clamp-technique
LC–MS/MS

ABSTRACT

Valerenic acid (VA) is a $\beta_{2/3}$ subunit-specific modulator of γ-aminobutyric acid (GABA) type A ($GABA_A$) receptors inducing anxiolysis. Here we analyze if VA-esters can serve as prodrugs and if different ester structures have different in vitro/in vivo effects. Modulation of $GABA_A$ receptors expressed in *Xenopus* oocytes was studied with 2-microelectrode-voltage-clamp. Anxiolytic effects of the VA-esters were studied on male C57BL/6N mice by means of the elevated plus maze-test; anticonvulsant properties were deduced from changes in seizure threshold upon pentylenetetrazole infusion. VA was detected in plasma confirming hydrolysis of the esters and release of VA in vivo. Esterification significantly reduced the positive allosteric modulation of $GABA_A$ ($\alpha_1\beta_3\gamma_{2S}$) receptors in vitro. in vivo, the studied VA-ester derivatives induced similar or even stronger anxiolytic and anticonvulsant action than VA. While methylation and propylation of VA resulted in faster onset of anxiolysis, the action of VA-ethylester was longer lasting, but occurred with a significant delay. The later finding is in line with the longer lasting anticonvulsant effects of this compound. The estimated VA plasma concentrations provided first insight into the release kinetics from different VA-esters. This might be an important step for its future clinical application as a potential non-sedative anxiolytic and anticonvulsant.

1. Introduction

γ-Aminobutyric acid (GABA) type A receptors ($GABA_A$) are the major inhibitory neurotransmitter receptors in the mammalian brain. $GABA_A$ receptors belong to the superfamily of Cys-loop-type ligand-gated ion channels (Olsen and Sieghart, 2008). Nineteen $GABA_A$ receptor subunits have been identified in the human genome, comprising α_{1-6}, β_{1-3}, γ_{1-3}, δ, ε, θ, π and ρ_{1-3} (Simon et al., 2004). Five receptor subunits form a chloride-selective ion channel. Receptor activation opens the channel and induces transmembrane chloride currents (I_{GABA}) modulating neuronal excitability and transmitter release (Sieghart, 2006; Sigel and Steinmann, 2012). There is consensus that the major adult receptor isoform consists of $2\alpha_1$, $2\beta_2$ and one γ_2 subunit (Olsen and Sieghart, 2008).

$GABA_A$ receptors play a major role in the treatment of central nervous system (CNS) diseases such as generalized anxiety and panic disorders, epilepsy, and sleep disturbances (Möhler, 2006). They are the molecular target of the classical benzodiazepines (e.g. diazepam) and subtype-selective benzodiazepine site ligands such as zolpidem or zopiclone, barbiturates, anaesthetics, and anticonvulsants (Sigel and Steinmann, 2012). Beside these drugs, $GABA_A$ receptors are modulated by multiple natural products (Johnston et al., 2006).

We and others have shown that valerenic acid (VA), a constituent of *Valeriana officinalis*, enhances I_{GABA} through $GABA_A$ receptors. VA binds with nanomolar affinity (Benke et al., 2009) and modulates $GABA_A$ receptors in an allosteric manner. VA selectively interacts with receptors comprising $\beta_{2/3}$-subunits (Benke et al., 2009; Khom et al., 2007). A point mutation in the β_2-subunit (N265S) of recombinant receptors prevents I_{GABA}

* Corresponding author. Tel.: +43 1 4277 55301/55310; fax: +43 1 4277 9553.
E-mail addresses: juliane.hintersteiner@univie.ac.at (J. Hintersteiner), maximilian.haider@univie.ac.at (M. Haider), denise.luger@univie.ac.at (D. Luger), schwarzer.christoph@i-med.ac.at (C. Schwarzer), gottfried.reznicek@univie.ac.at (G. Reznicek), walter.jaeger@univie.ac.at (W. Jäger), sophia.khom@univie.ac.at (S. Khom), marko.mihovilovic@tuwien.ac.at (M.D. Mihovilovic), steffen.hering@univie.ac.at (S. Hering).

http://dx.doi.org/10.1016/j.ejphar.2014.03.019

enhancement while the "reversed mutation" in β_1 (S266N) enhances current stimulation to extents observed on $\beta_{2/3}$-subunit containing receptors (Khom et al., 2007). Valerenic acid induces anxiolysis in the elevated plus maze and the light/dark choice test in mice (Benke et al., 2009; Khom et al., 2010). Anxiolysis was absent in β_3(N265M) point-mutated mice supporting the hypothesis that the anxiolytic effects of VA are caused by interaction with β_3-containing $GABA_A$ receptors (Benke et al., 2009).

A recently published pharmacokinetic study on rats revealed that approximately 34% of VA are absorbed after oral administration with a half-life between 2.7 and 5 h (Sampath et al., 2012). This good bioavailability is in line with the reported anxiolysis of VA after oral administration in mice (Benke et al., 2009).

Together these findings make VA or one of its derivatives (Khom et al., 2010; Kopp et al., 2010) interesting drug candidates. Little is known, however, how this molecule penetrates the blood-brain barrier (Neuhaus et al., 2008). Ester prodrugs can enhance the lipophilicity (by masking charged groups such as carboxylic acids) and thereby affect the time course of drug action (Beaumont et al., 2003). Therefore four VA-esters (VA-methylester (VA-ME), VA-ethylester (VA-EE), VA-propylester (VA-PE) and VA-pivaloyloxymethylester (VA-POM)) have been synthesized in order to address the following questions about the biological activity of these potential prodrugs: (i) Does esterification affect modulation of I_{GABA} through $GABA_A$ receptors? (ii) Do VA-esters represent prodrugs (i.e. are esters hydrolyzed in vivo and is VA detectable in the plasma? (iii) Are VA-esters active in vivo and – if so – does esterification affect the anxiolytic and anticonvulsant properties of VA?

2. Materials and methods

All experiments on animals were carried out in accordance to the Austrian Animal Experimental Law, which is in line with the EU directive 2010/63/EU.

2.1. Chemicals

Valerenic acid (VA) was purchased from HWI Pharma Solutions (Rülzheim, Germany) and converted into the aforementioned derivatives as described below (for structural formulae see Fig. 1). Chemicals used in this study were obtained from Sigma-Aldrich (Vienna, Austria) except where otherwise stated. Dichloromethane (DCM), dimethylsulfoxide (DMSO), formic acid, methanol and *t*-butylmethylether were of p.a. quality and purchased from ROTH (Karlsruhe, Germany). For HPLC analysis double distilled water and acetonitrile, HPLC quality (VWR Int., Vienna, Austria) were used.

LogP values for the aimed compounds were calculated using ACD/ChemSketch freeware.

All reactions were carried out in oven dried 4 ml-reaction vials under an argon atmosphere. DCM was predistilled and then desiccated on Al_2O_3 columns (PURESOLV, Innovative Technology; Amesbury, USA). Reaction mixtures were magnetically stirred and monitored by thin layer chromatography using Merck Silica $60F_{254}$ plates (Merck, Vienna, Austria). Flash chromatography was performed on a Sepacore Flash System (2 × Büchi Pump Module C-605, Büchi Pump Manager C-615, Büchi UV Photometer C-635, Büchi Fraction Collector C-660; Büchi Labortechnik, Flawil, Switzerland) using Merck silica gel (0.040–0.063 mm, 230–400 mesh). Yields refer to chromatographically and spectroscopically pure compounds. ^{1}H-NMR (200 MHz) and ^{13}C-NMR (50 MHz) were recorded on Bruker AC 200 (200 MHz; Bruker, Karlsruhe, Germany). The chemical shifts δ are reported relative to the residual solvent peaks. All ^{1}H and ^{13}C shifts are given in ppm (s=singulet, d=doublet, t=triplet, q=quadruplet, m=multiplet). Specific rotation was measured on an Anton Paar MCP500 polarimeter (Anton Paar GmbH; Graz, Austria) at 20 °C in DCM.

LC–MS/MS analyses were carried out on an Ultimate 3000 RSLC-series system (Thermo Fisher Scientific Austria, Vienna, Austria) coupled to a triple quadrupol mass spectrometer API 4000 (AB Sciex Instruments, Framingham, USA).

2.2. Synthesis of valerenic acid esters

2.2.1. Valerenic acid methylester (VA-ME)

Valerenic acid (30.0 mg, 1 Eq., 0.13 mmol) and 4-dimethylaminopyridine (DMAP, 1.6 mg, 0.1 Eq, 0.01 mmol) were dissolved in 1.3 ml dry DCM under an Argon atmosphere and cooled to 0 °C, then 1-ethyl-3-(3-dimethylaminopropyl)carbodiimide (EDCI; 36.8 mg, 1.5 Eq, 0.19 mmol) was added in one portion. After stirring the mixture for five min methanol (23.7 µl, 4.5 Eq, 0.59 mmol) was added dropwise and the mixture was left warming to room temperature overnight. The solution was taken up in 50 ml ethylacetate (EtOAc) and was subsequently washed with saturated NH_4Cl solution (three times), saturated $NaHCO_3$ solution (three times) and once with brine; it was then dried and concentrated under reduced pressure. Purification of the crude material via column chromatography (LP:EtOAc=30:1) provided 30.2 mg (94%) of Valerenic acid methylester as a colorless oil.

- **^{1}H-NMR (200 MHz, $CDCl_3$):** δ=0.77 (d, J_1=7.0, 3*H*), 1.37–1.98 (m, 14*H*), 2.19 (t, J_1=7.5 Hz, 1*H*), 2.90–2.99 (m, 1*H*), 3.49–3.56 (m, 1*H*), 3.72 (s, 3*H*), 7.01 (dq, J_1=1.4 Hz, J_2=9.8 Hz, 1*H*)
- **^{13}C-NMR (50 MHz, $CDCl_3$)** δ=12.0 (s), 12.4 (s), 13.5 (s), 24.5 (d), 25.4 (d), 28.7(d), 33.0 (t), 34.3 (t), 37.4 (d), 47.4 (t), 51.7 (s), 125.7 (q), 130.9 (q), 133.4 (t), 169.0 (q)

Analytical data is consistent with the reported data for Valerenic acid methylester (Kopp et al., 2010).

2.2.2. Valerenic acid ethylester (VA-EE)

Using the analogous procedure as for the preparation of VA-ME, treatment of valerenic acid (20.0 mg, 1 Eq, 0.09 mmol) with 4-dimethylaminopyridine (1.0 mg, 0.1 Eq, 0.009 mmol), EDCI (24.4 mg, 1.5 Eq, 0.13 mmol) and ethanol (22.3 µl, 4.5 Eq, 0.38 mmol) yielded 20.2 mg (95%) of VA-EE as colorless oil.

- **^{1}H-NMR (200 MHz, $CDCl_3$, ppm):** δ=0.78 (d, J=7.0, 3*H*), 1.29 (t, J=7.1 Hz, 3*H*), 1.37–2.02 (m, 14*H*), 2.19 (t, J=7.6 Hz, 2*H*), 2.92–2.98 (m, 1*H*), 3.46–3.56 (m, 1*H*), 4.17 (q, J=7.1 Hz, 2*H*), 7.01 (dq, J_1=9.8 Hz, J_2=1.4 Hz, 1*H*)
- **^{13}C-NMR (50 MHz, $CDCl_3$, ppm):** δ=12.0 (s), 12.4 (s), 13.5 (s), 14.3 (s), 24.5 (d), 25.5 (d), 28.7(d), 33.1 (t), 34.3 (t), 37.4 (d), 47.4 (t), 60.4 (d), 125.7 (q), 130.9 (q), 133.4 (t), 169.0 (q)

Analytical data is consistent with the reported data for Valerenic acid ethylester (Kopp et al., 2010).

2.2.3. Valerenic acid propylester (VA-PE)

Using the analogous procedure as for the preparation of VA-ME, treatment of valerenic acid (30.0 mg, 1 Eq, 0.13 mmol) with 4-DMAP (1.6 mg, 0.1 Eq, 0.01 mmol), EDCI (36.8 mg, 1.5 Eq, 0.19 mmol) and propanol (28.5 µl, 4.5 Eq, 0.38 mmol) yielded 35.1 mg (99%) of VA-PE as colorless oil.

- **^{1}H-NMR (200 MHz, $CDCl_3$, ppm):** δ=0.77 (d, J=7.0, 3*H*), 0.95 (t, J=7.4 Hz, 3*H*), 1.37–2.01 (m, 16*H*), 2.19 (t, J=7.7 Hz, 2*H*), 2.91–2.97 (m, 1*H*), 3.48–3.55 (m, 1*H*), 4.07 (t, J=6.7 Hz, 2*H*), 7.02 (dq, J_1=9.8 Hz, J_2=1.3 Hz, 1*H*)

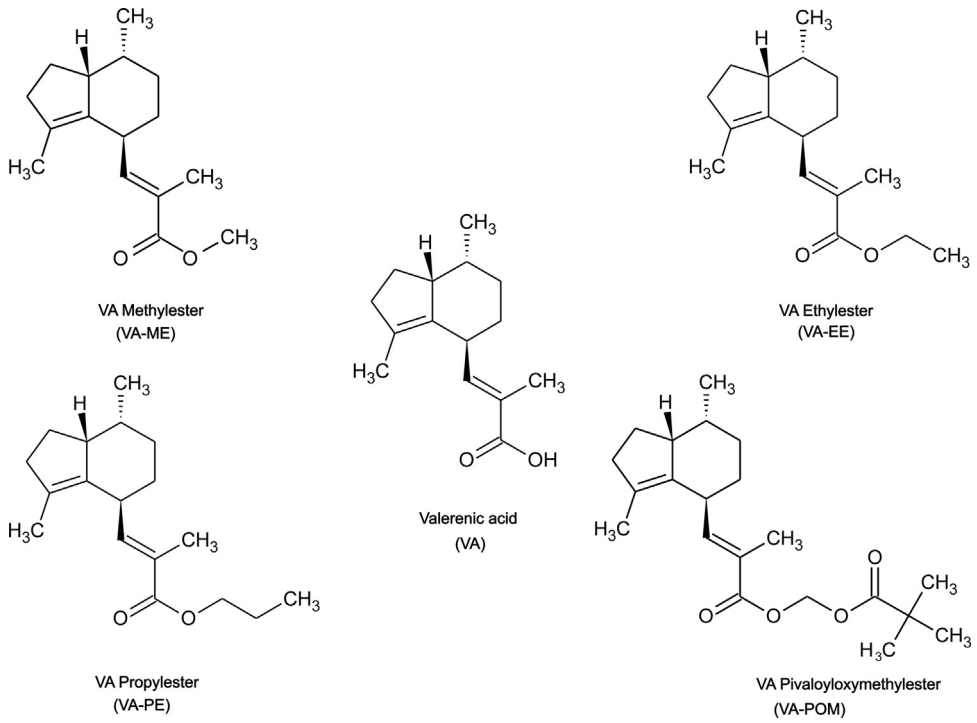

Fig. 1. Structural formulae of VA and synthesized ester derivatives.

- **^{13}C-NMR (50 MHz, $CDCl_3$, ppm)** δ=10.5 (s), 12.0 (s), 12.4 (s), 13.5 (s), 24.5 (d), 25.5 (d), 28.7(d), 33.1 (t), 34.3 (t), 37.4 (d), 47.4 (t), 66.0 (d), 126.0 (q), 130.7 (q), 133.5 (q), 143.3 (d) 168.7 (q)

$[\alpha]_D^{20} = -77.0$ (c=0.2, DCM);

2.2.4. Valerenic acid pivaloyloxymethylester (VA-POM)

Valerenic acid (20 mg, 1 Eq, 0.13 mmol) and 1,8-diazabicycloundec-7-ene (21.4 µL, 1.1 Eq, 0.14 mmol) were dissolved in dry DCM (1.3 ml) under an argon atmosphere; pivaloyloxymethyl chloride (20.2 µl, 1.1 Eq, 0.14 mmol) was added dropwise (Urban et al., 2005). The mixture was stirred overnight until full conversion before it was taken up in 50 ml EtOAc and subsequently washed three times with saturated NH_4Cl and $NaHCO_3$ solution and one time with brine. The organic phase was dried and concentrated in vacuo. Purification by column chromatography (LP:EtOAc=4:1) furnished 19.1 mg (85%) of VA-POM as a slightly yellow oil.

- **^{1}H-NMR (200 MHz, $CDCl_3$, ppm):** δ=0.78 (d, J=6.9, 3H), 1.21 (s, 9H), 1.38–1.98 (m, 15H), 2.20 (t, J=7.4 Hz, 2H), 2.91–2.95 (m, 1H), 3.50–3.55 (m, 1H), 5.81 (s, 2H), 7.09 (dq, J_1=9.8 Hz, J_2=1.1 Hz, 1H)
- **^{13}C-NMR (50 MHz, $CDCl_3$, ppm)** δ=12.0 (s), 12.2 (s), 13.5 (s), 24.5 (d), 25.3 (d), 26.8 (s), 28.7(d), 33.0 (t), 34.3 (t), 37.4 (d), 38.8 (q), 47.4 (t), 79.9 (d), 125.0 (q), 131.2 (q), 133.1 (q), 145.6 (d) 167.0 (q), 177.2(q)

$[\alpha]_D^{20} = -70.4$ (c=0.6, DCM);

2.3. Expression and functional characterization of $GABA_A$ receptors

Preparation of stage V–VI oocytes from *Xenopus laevis* (Nasco, Ft. Atkinson, WI), synthesis of capped off run-off poly(A^+) cRNA transcripts from linearized cDNA templates (pCMV vector) was performed as described (Khom et al., 2006). Briefly, female *Xenopus laevis* were anaesthetized by exposing them for 15 min to a 0.2% solution of MS-222 (methane sulfonate salt of 3-aminobenzoic acid ethyl ester), before surgically removing parts of the ovaries. Follicle membranes from isolated oocytes were enzymatically digested with 2 mg/ml collagenase (Type 1 A). One day after isolation, the oocytes were injected with about 10–50 nl of diethylpyrocarbonate—treated water containing the different cRNAs at a concentration of approximately 150–3000 ng/µl/subunit. The amount of cRNA was determined by means of a NanoDrop ND-1000 (Kisker-biotech, Steinfurt, Germany). To ensure expression of the γ-subunit in the case of $\alpha_1\beta_3\gamma_{2S}$ receptors, cRNAs were mixed in a ratio of 1:1:10 (Boileau et al., 2002). Oocytes were stored at 18 °C in ND96 solution (Methfessel et al., 1986). Electrophysiological experiments were conducted using the two-microelectrode voltage-clamp method at a holding potential of −70 mV using a TURBO TEC 01C amplifier (npi electronic, Tamm, Germany) and an Axon Digidata 1322 A interface (Molecular Devices, Sunnyvale, CA) applying pCLAMP v. 9.2 data acquisition. The bath solution consisted of 90 mM NaCl, 1 mM KCl, 1 mM $MgCl_2 \cdot 6H_2O$, 1 mM $CaCl_2$ and 5 mM 2-(4-(2-hydroxyethyl)-1-piperazinyl)-ethanesulfonic acid (HEPES; pH 7.4). Microelectrodes were filled with 2 M KCl and had resistances between 1 and 3 M Ω (Khom et al., 2006).

2.4. Perfusion system

GABA and the tested compounds were applied by means of fast perfusion system (Baburin et al., 2006). Drug or control solutions were applied by means of a TECAN Miniprep 60 (npi electronic, Tamm, Germany) permitting automation of the experiments. To elicit I_{GABA} the chamber was perfused with 120 µl of GABA-containing solution at volume rate between 300 and 1000 µl/s. The I_{GABA} rise time ranged between 100 and 250 ms. To account for possible slow recovery from increasing levels of desensitization in the presence of high compound concentrations, the duration of washout periods was extended from 1.5 min (GABA EC_{3-7}) to 3 min (co-application of GABA EC_{3-7} and 1 µM compound) to 5–10 min (co-application of GABA EC_{3-7} and 10 µM compound) to 15–20 min (co-application of GABA EC_{3-7} and

30 μM compound) to 30 min (GABA EC_{3-7} and 100 μM compound). Oocytes with maximal current amplitudes >3 μA were discarded to exclude voltage-clamp errors (Khom et al., 2006).

2.5. Analyzing concentration–response curves

Stimulation of chloride currents by modulators of the $GABA_A$ receptor was measured at a GABA concentration eliciting between 3 and 7% of the maximal current amplitude (EC_{3-7}). The EC_{3-7} was determined at the beginning of each experiment.

Enhancement of the chloride current was defined as $(I_{(GABA+Compound)}/I_{GABA})-1$, where $I_{(GABA+Compound)}$ is the current response in the presence of the compound and I_{GABA} is the control GABA current. Each data point represents the mean ± S.E.M from at least 5 oocytes and ≥ 2 oocyte batches.

2.6. Behavioral analysis

2.6.1. Animals

Male mice (C57BL/6N) were obtained from Charles River Laboratories (Sulzfeld, Germany). For maintenance, mice were group-housed (maximum 5 mice per type IIL cage) with free access to food and water. At least 24 h before the commencement of experiments, mice were transferred to the testing facility, where they were given free access to food and water. The temperature in the maintenance and testing facilities was 22 ± 2 °C; the humidity was 40–60%; a 12 h light-dark cycle was in operation (lights on from 07.00 to 19.00). Only male mice – aged 3–6 months – were tested. Compounds at a dose of 3 mg/kg bodyweight or solvent alone were applied by intraperitoneal (i.p.) injection. The dose was chosen according to a previously published dose–response curve (Khom et al., 2010). Testing solutions were prepared in a solvent composed of saline (0.9% NaCl solution with 10% DMSO and 3% Polysorbat 80). The final DMSO concentration was fixed to 10% (Broadwell et al., 1982). Application of the solvent alone did not influence animal behavior.

2.6.2. Elevated plus maze (EPM) test

The animals' behavior was tested over 5 min on an elevated plus maze 1 m above ground consisting of two closed and two open arms, each 50 × 5 cm in size. The test instrument was built from grey PVC; the height of closed arm walls was 20 cm. Illumination intensity was set to 180 lx. Animals were placed in the center, facing an open arm. Analysis of open and closed arm entries, distance and time on open arm was automatically done with Video-Mot 2 equipment and software (TSE systems, Bad Homburg, Germany). Drugs or solvent were applied 15, 30 or 60 min before testing.

2.6.3. Seizure threshold

Seizure threshold was determined by pentylenetetrazole (PTZ) tail-vein infusion on freely moving animals at a rate of 100 μl/min (10 mg/ml PTZ in saline). Infusion was stopped when animals displayed generalized clonic seizures. Animals were killed by cervical displacement immediately after the first generalized seizure. The seizure threshold dose was calculated from the infused volume in relation to body weight. The compounds were injected 15, 30, 60, 90, 120 or 150 min before PTZ infusion. At the infusion rate of 100 μl/min, generalized seizures are induced within 90 s.

2.7. Detection of free VA in the plasma

2.7.1. Sampling

Blood samples were taken 15, 30, 60 and 120 min after i.p. injection of the compounds. 10 min after i.p injection of thiopental (150 mg/kg bodyweight in 0.9% sodium chloride solution) blood samples (500–800 μl) were collected and compiled into ethylenediamine tetra-acetic acid (EDTA)-coated micro tubes (1.6 mg EDTA/sample) and centrifuged at 12,000 rpm for 5 min at 4 °C. Plasma samples were transferred into 1.5 ml tubes and stored at −80 °C until analysis.

2.7.2. Sample preparation

A liquid–liquid extraction method together with an internal standard (IS) acetoxyvalerenic acid (ACVA; PhytoLab GmbH&Co KG, Vestenbergsgreuth, Germany) was applied for the quantification of VA in plasma. To 100 μl of plasma sample 10 μl of IS solution (1 μg/ml 10% aqueous DMSO) was added. These solutions were extracted by liquid–liquid partition with 400 μl of dichloromethane/*t*-butylmethylether (80:20, v/v) and vortexed for 5 min. From the clear lower organic layer the solvent was removed through a constant nitrogen stream at room temperature (25 °C). The residue was dissolved with 100 μl of methanol, sonicated, centrifuged for 5 min (15,000 rpm) and the supernatant was finally transferred to autosampler vials (Macherey-Nagel vial N9, 0.2 ml with integrated insert; Macherey-Nagel, Düren, Germany).

2.7.3. Quantification of valerenic acid by LC–MS/MS

The samples (10 μl) were analyzed by liquid chromatography/mass spectrometry (LC–MS/MS) on an Ultimate 3000 RSLC-series system (Thermo Fisher Scientific Austria, Vienna, Austria) coupled to a triple quadrupol mass spectrometer (AB Sciex Instruments API 4000) equipped with an orthogonal APCI source operated in negative mode and displayed with Analyst 1.5 software.

LC separation was performed on an Acclaim RSLC 120C18 column (3 μm, 150 × 2.1 mm I.D., Thermo Fisher Scientific Austria, Vienna, Austria), preceded by an Acclaim 120C18 guard cartridge (5 μm, 10 × 2 mm I.D., Thermo Fisher Scientific Austria, Vienna, Austria), at a flow rate of 0.500 ml/min and a column temperature of 30 °C. The mobile phase consisted of a continuous linear gradient, mixed from aqueous formic acid, pH 3.5 (mobile phase A), and acetonitril (mobile phase B), to elute VA. The gradient ranged from 50% B (0 min) to 80% at 8 min, kept constant at 80% until 10 min, and finally decreased linearly to 50% again at 11 min. Between sampling, the column was purged with 98% B (acetonitrile) for 4 min before equilibrating for 6 min resulting in a total analysis time of 18 min. Within this setup valerenic acid eluted at 4.06 min., acetoxyvalerenic acid (IS) at 7.02 min. Selective and sensitive detection and quantification was carried out using MS/MS fragmentation of VA resp. acetoxyvalerenic acid (ACVA) giving a quasimolecular ion at *m/z* 233 $[M-H]^-$ (VA) and *m/z* 291 $[M-H]^-$ (ACVA). MRM *m/z* 233/84 (VA) as well as *m/z* 291/249 (ACVA) were used for calibration curves to give a linear concentration range from 0.1 ng/ml (LLOD, $S/N=4$) to 500 ng/ml (correlation coefficient 0.9996). Extraction efficiencies (average 84%) were determined by comparison of peak areas between quality control (QC) and analysis samples. For validation, quality control (QC) samples were prepared in the same way as the calibration standards.

The triple quadrupol mass spectrometer operated with the following parameters: APCI neg., NC-5, CUR 10, GS1 30, GS2 18, TEM 400 °C, CAD 12, EP-11, DP-65, CXP-5, CEM 2100, DF 200. MRM *m/z* 233/84 (VA): CE-29, dwell time 300 ms. MRM *m/z* 291/249 (ACVA): CE-24, dwell time 300 ms.

2.8. Statistical analysis

Statistical significance of electrophysiological data was calculated using a paired Student *t*-test; for in vivo experiments, one-way

ANOVA (followed by posthoc Bonferroni analysis) was used. Statistical analysis was done with Origin software (OriginLab Corporation; USA). *P*-values of <0.05 were accepted as statistically significant. All data are given as mean ± S.E.M.

3. Results

3.1. I_{GABA} modulation by VA-esters

Fig. 1 displays the structures of the studied VA-derivatives (see Section 2 for synthesis). As expected, I_{GABA} modulation by VA-esters was less pronounced than by VA. This is shown in Fig. 2 illustrating modulation of I_{GABA} through $\alpha_1\beta_3\gamma_{2S}$ $GABA_A$ receptors during co-application of GABA (EC_{3-7}) and either VA, VA-ME, VA-EE, VA-PE or VA-POM.

VA-ME and VA-EE induced significantly stronger I_{GABA} enhancement than VA-PE and VA-POM (max. I_{GABA} potentiation $_{(VA\text{-}ME\ 30\ \mu M)}$: 70 ± 13% ($n=5$) and max. I_{GABA} potentiation $_{(VA\text{-}EE\ 30\ \mu M)}$: 52 ± 15% ($n=6$) vs. max. I_{GABA} potentiation $_{(VA\text{-}PE\ 30\ \mu M)}$: 27 ± 6% ($n=5$) and max. I_{GABA} potentiation $_{(VA\text{-}POM\ 30\ \mu M)}$: 21 ± 6% ($n=6$). Compared to VA the modulation of I_{GABA} at 30 μM was drastically reduced (from 6.2-fold (VA-ME) to 20.6-fold reduction (VA-POM)). At 1 μM none of the studied ester derivatives induced significant I_{GABA} enhancement (Fig. 2 A).

3.2. Anxiolytic action of VA-esters

For investigation of the time course of in vivo activity of the different derivatives, effects on anxiety-related behavior were tested 15, 30 and 60 min after i.p. application of either solvent (=control) or drug containing solutions at a dose of 3 mg/kg bodyweight.

As illustrated in Fig. 3A, 15 min after injection, control mice spent 29.7 ± 2.7% of the total time ($n=33$) in the open arms (OA) of the EPM. An increase of time spent in the OA was observed upon application of VA-ME and VA-PE (VA-ME: 50.0 ± 7.3%; $n=16$, $P<0.01$; VA-PE: 45.1 ± 3.9%; $n=19$; $P<0.01$) Animals treated with VA-esters also covered significantly longer distances on the OA (Control: 327.8 ± 30.8 cm; $n=33$ vs. VA-ME: 451.1 ± 53.4 cm; $n=16$, $P<0.05$ vs. VA-PE: 546.7 ± 37.1 cm; $n=19$, $P<0.01$, see Fig. 3D) suggesting anxiolytic activity. No significant effects on time spent in the OA, covered distance on the OA, OA and CA entries were observed for VA-EE (Figs. 3 and 4A and D). Animals treated with VA-POM covered a significantly shorter distance on the OA (Fig. 3D) and displayed fewer OA entries (Fig. 4A) compared to control littermates, while no significant effect on time spent on the OA and CA entries was observed (Fig. 3A and Fig. 4D).

30 min after injection mice treated with VA, VA-ME, VA-PE and VA-EE spent significantly more time in the OA compared to control mice (control: 32.8 ± 3.1%; $n=19$ vs. VA: 45.5 ± 4.6%; $n=14$; $P<0.05$ vs. VA-ME: 51.9 ± 5.5%; $n=13$; $P<0.01$; VA-EE:

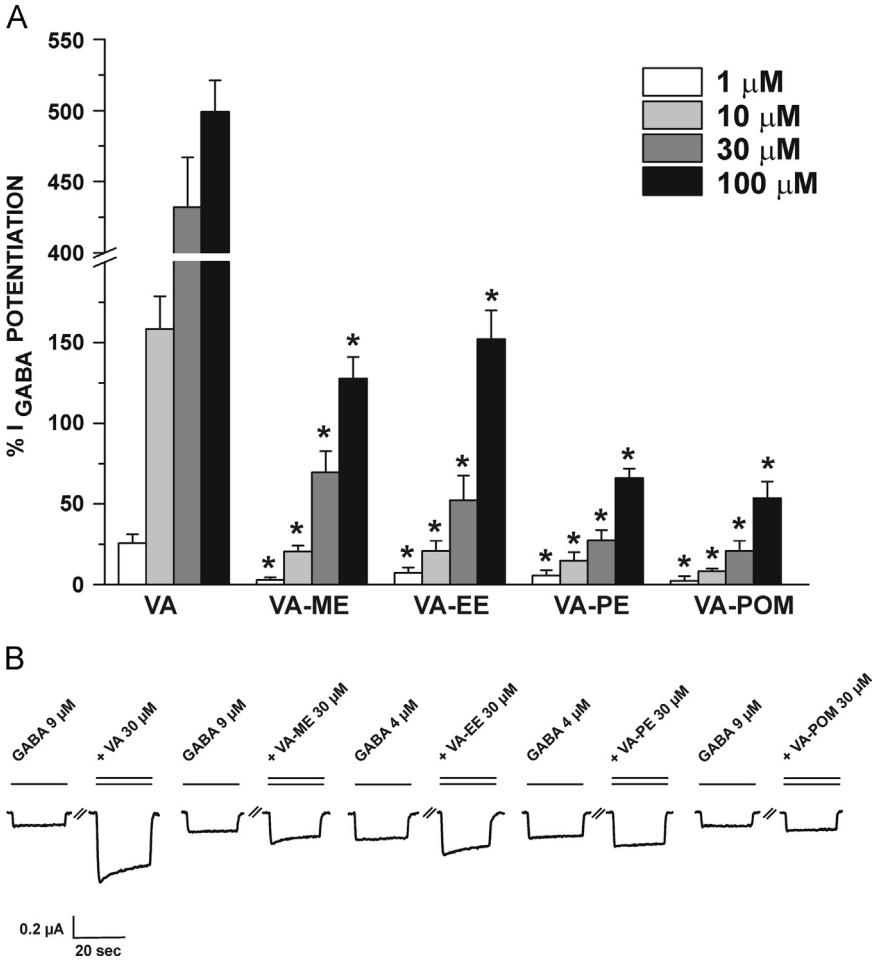

Fig. 2. I_{GABA} modulation by VA-ester derivatives **(A)** Enhancement of I_{GABA} through $GABA_A$ receptors composed of $\alpha_1\beta_3\gamma_{2S}$ subunits by 1 μM (white bars), 10 μM (light grey bars), 30 μM (dark grey bars) and 100 μM (black bars) of the indicated compounds. Each value represents the mean ± S.E.M from at least 5 oocytes and ≥2 oocyte batches. (*) indicates significantly different from I_{GABA} enhancement by VA at the same concentration ($P<0.05$, Student's *t*-test) **(B)** Typical traces for the potentiation of chloride currents through $\alpha_1\beta_3\gamma_{2S}$ channels by VA-derivatives at a GABA EC_{3-7}. Control currents (GABA, single bar) and corresponding currents elicited by co-application of GABA and the indicated compound (double bar) are shown.

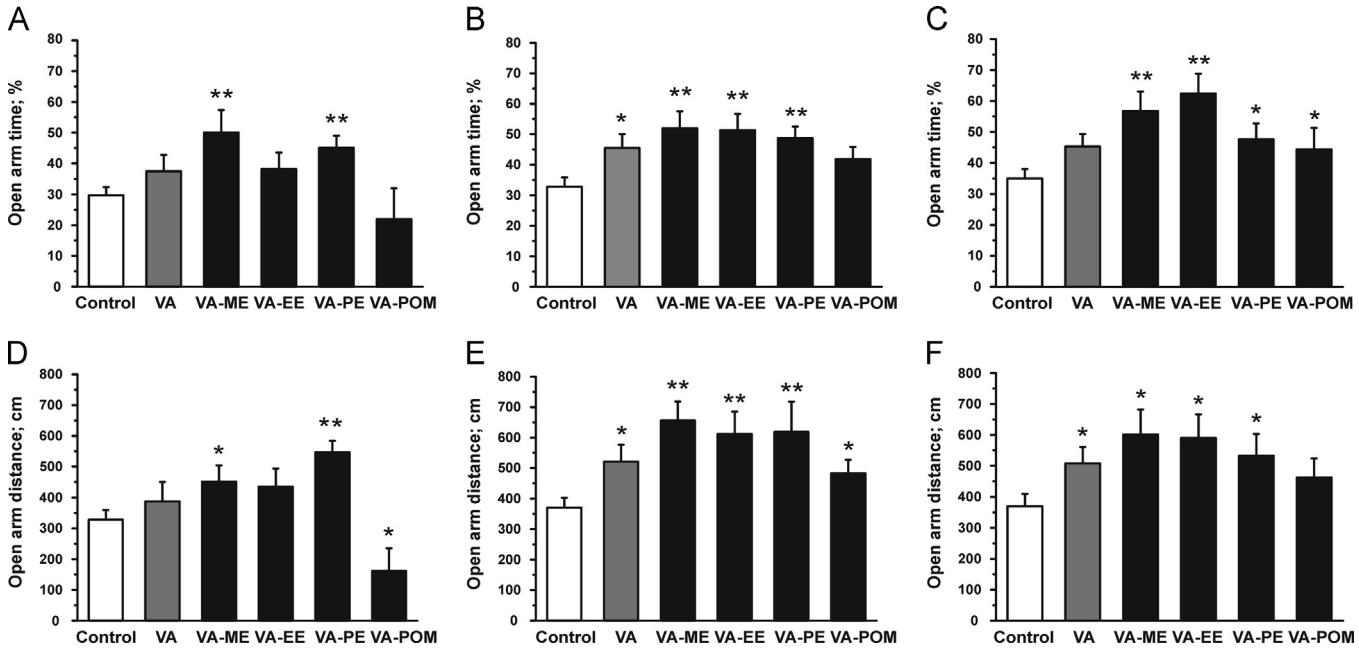

Fig. 3. Effects on explorative behavior of VA-esters in the elevated plus maze test are compared to saline-treated control (white bars) mice at a dose of 3 mg/kg bodyweight. Bars display the time spent (in % of the total time) on the open arms (**(A)**–**(C)**) and the open arm distance (**(D)**–**(F)**) 15 (left column), 30 (mid column) and 60 (right column) min after i.p. application of the indicated compounds. Each bar represents a mean ± S.E.M from at least 8 different mice. (*) indicates statistically significant differences with $P < 0.05$, (**) with $P < 0.01$ to control.

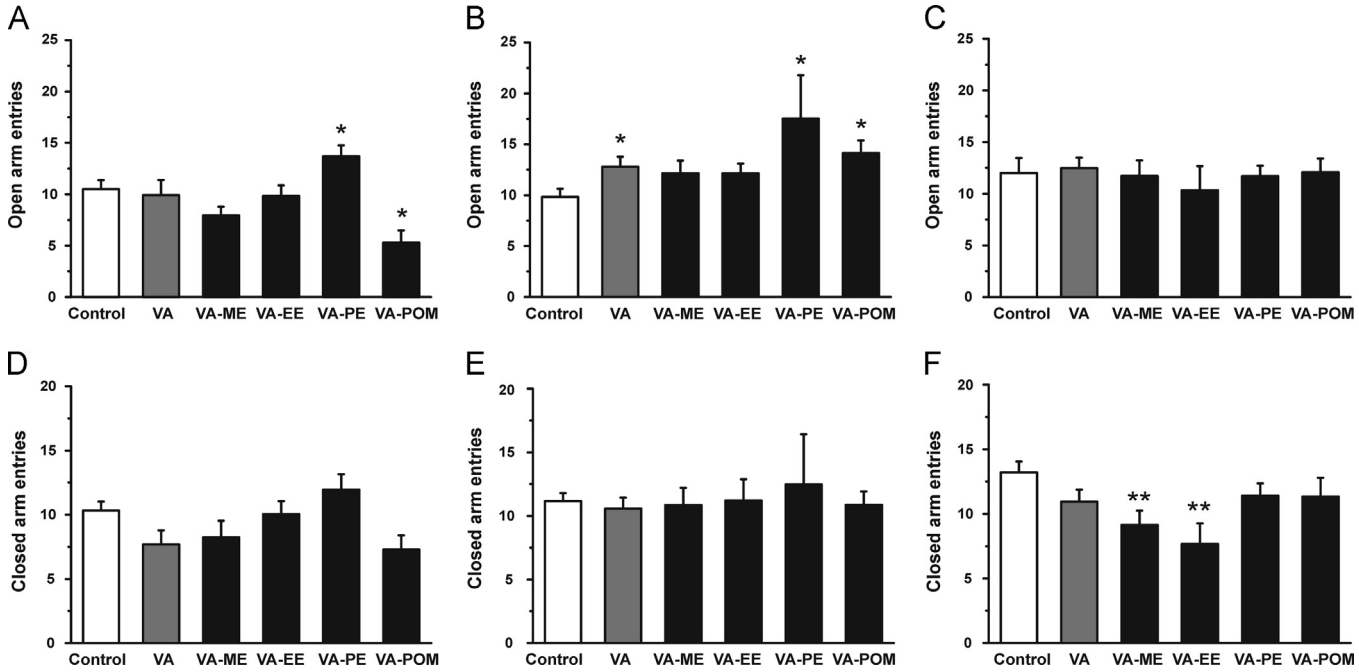

Fig. 4. Number of entries to the open (OA; **(A)**–**(C)**) and closed arms (CA; **(D)**–**(F)**) of the elevated plus maze 15 (left column), 30 (mid column) and 60 (right column) min after i.p. application of the indicated compound are compared to control (white bars) at a dose of 3 mg/kg bodyweight. Each bar represents a mean ± S.E.M from at least 8 different mice. (*) indicates statistically significant differences with $P < 0.05$, (**) with $P < 0.01$ to control.

51.3 ± 5.4%; $n = 15$; $P < 0.01$; VA-PE: 48.7 ± 3.7%; $n = 17$; $P < 0.01$; see Fig. 3B). These increase in time spent in the OA was accompanied by longer distances covered on the OA compared to control animals (Control: 370.4 ± 32.4 cm; $n = 19$ vs. VA: 521.2 ± 55.1 cm; $n = 14$, $P < 0.05$ vs. VA-ME: 655.9 ± 62.6 cm; $n = 13$, $P < 0.01$; VA-EE: 611.8 ± 73.7 cm; $n = 15$, $P < 0.01$; VA-PE: 618.3 ± 100.0 cm; $n = 17$, $P < 0.05$; Fig. 3E). Mice treated with VA and VA-PE also visited the OA more frequently, while no effect on OA visits upon VA-ME and VA-EE application was observed (Fig. 4B). Interestingly, significantly increased ambulation on the OA (482.6 ± 44.9 cm; $n = 15$, $P < 0.05$; Fig. 3E) and a higher number of OA visits (Fig. 4B) were also observed for mice treated with VA-POM compared to control littermates. However, time spent on the OA did apparently not differ significantly from control (Fig. 3B). No differences in the number of CA entries between control and compound treated mice were observed 30 min after application (Fig. 4E).

As illustrated in Figs. 3 and 4C, 60 min after injection, the exploratory drive (time spent in OA and OA entries) in mice

treated with VA was not significantly different from control animals, although mice covered a longer distance on the OA (Control: 369.6 ± 40.3 cm; $n=15$ vs. VA: 508.2 ± 52.5 cm; $n=17$, $P<0.05$; Fig. 3F). In contrast, application of VA-ME, VA-EE and VA-PE induced increased ambulation of open arms also 60 min after treatment (VA-ME: 56.7 ± 6.3%; $n=14$; $P<0.01$; VA-EE: 62.9 ± 7.2%; $n=8$; $P<0.05$; and VA-PE: 47.6 ± 5.1%; $n=10$; $P<0.05$; Fig. 3C) accompanied by longer distances on the OA (VA-ME: 601.0 ± 81 cm.2; $n=14$, $P<0.05$ vs. VA-EE: 589.8 ± 76.1 cm; $n=8$, $P<0.05$ vs. VA-PE: 532.7 ± 70.5 cm; $n=10$, $P<0.05$; Fig. 3F). Furthermore, while the number of OA entries did not differ from control, the number of CA entries significantly dropped upon treatment with VA-ME and VA-EE compared to control mice (Fig. 4C and F). Weaker, yet significant effects on time spent in the OA were also observed for mice treated with VA-POM (44.4 ± 7.0%; $n=12$; $P<0.05$), while the other parameters did significantly not differ from control (Figs. 3 and 4C and F).

No significant changes in total distance were observed for any drug at any time point, suggesting no sedative effects at this dose.

3.3. Anticonvulsant action of VA-esters

Loreclezole, a $GABA_A$ receptor modulator selective for $\beta_{2/3}$ subunits, displays in vivo anticonvulsant activity (Greenfield, 2013; Groves et al., 2006; Sanna et al., 1996; Wingrove et al., 1994). It was therefore interesting to study if VA and the ester derivatives would induce comparable effects.

Application of VA induced an increased threshold against pentylenetetrazole (PTZ)-induced seizures 30 min after application of VA (control: 39.5 ± 2.8 mg/kg; $n=7$ vs. VA: 49.0 ± 1.8 mg/kg; $n=4$; $P<0.05$). No anticonvulsant effect was observed either at 15 or 60 min after VA application (see Fig. 5A). In contrast to VA, VA-ME significantly increased seizure threshold already 15 min after application (48.8 ± 0.5 mg/kg; $n=4$; $P<0.01$). The anticonvulsant effect persisted 30 min after treatment (50.0 ± 0.5 mg/kg; $n=3$; $P<0.05$), however, VA-ME did not induce any significant effects on seizure threshold 60 min after application.

In contrast to VA, VA-EE did not induce anticonvulsant effects until 60 min after drug treatment (control: 39.5 ± 2.8 mg/kg; $n=7$ vs. 47.5 ± 2.4 mg/kg; $n=3$; $P<0.05$). Seizure threshold was further significantly increased 90 min after application (52.0 ± 2.3 mg/kg; $n=4$; $P<0.05$) and remained at the same level even 120 min after application (51.7 ± 2.6 mg/kg; $n=4$; $P<0.05$). 150 min after application the seizure threshold of VA-EE-treated mice did not differ from the control (see Fig. 5B).

As illustrated in Fig. 5C, VA-PE's anticonvulsant activity was comparable to VA: Seizure threshold was significantly elevated 30 min after compound application (control: 39.5 ± 2.8 mg/kg; $n=7$ vs. VA-PE: 54.7 ± 1.3 mg/kg; $n=4$; $P<0.05$). The seizure threshold elevation at this time point was even more pronounced than that of VA or the other derivatives ($P<0.05$). However, no statistically significant anticonvulsant effects could be detected at a later time point.

No significant changes in seizure threshold were observed upon application of VA-POM until 60 min. At this time point VA-POM significantly increased seizure threshold (control: 39.5 ± 2.8 mg/kg; $n=7$ vs. VA-POM: 48.4 ± 2.1 mg/kg; $n=4$; $P<0.05$). No anticonvulsant activity, however, was observed 90 min after application (Fig. 5D).

As shown in Table 1 high concentrations of free VA could be detected in plasma samples already after 15 min indicating rapid hydrolysis of the VA-esters.

4. Discussion

Valerenic acid, from *V. officinalis*, is an efficient modulator of $GABA_A$ receptors. VA binds with nanomolar affinity, modulates

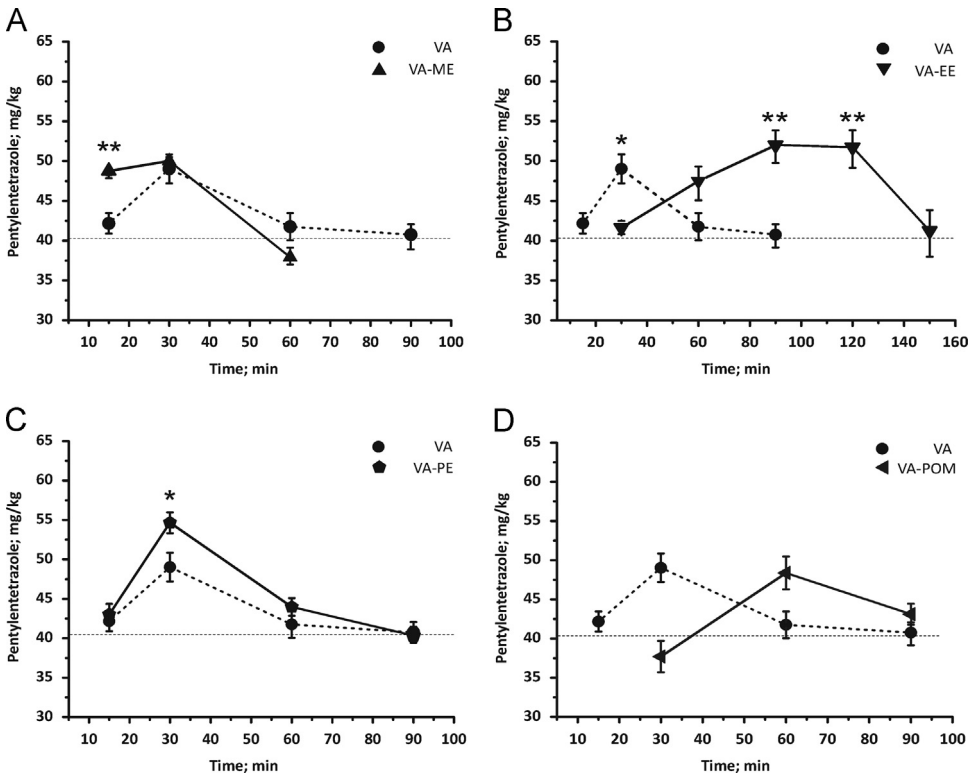

Fig. 5. Changes in seizure threshold upon PTZ-infusion are compared at a dose of 3 mg/kg bodyweight of VA (dotted line) and **(A)** VA-ME, **(B)** VA-EE, **(C)** VA-PE and **(D)** VA-POM. Each data point represents the mean ± S.E.M from at least 3 mice; (*) indicates statistically significant differences with $P<0.05$; (**) indicates statistically significant differences with $P<0.01$ to VA.

Table 1
Plasma concentrations of free VA; 15, 30 and 60 min after application of VA and VA-esters (3 mg/kg bodyweight) are indicated in ng/ml. Each data point represents the mean ± S.E.M of 4 animals per group.

Compound	15 min	30 min	60 min
VA	640.7 ± 131.8	105.2 ± 18.6	61.3 ± 21.8
VA-ME	164.2 ± 47.2	76.7 ± 19.7	24.2 ± 4.3
VA-EE	117.4 ± 19.3	84.1 ± 11.3	20.2 ± 4.1
VA-PE	274.5 ± 51.8	174.6 ± 52.3	43.7 ± 6.7
VA-POM	166.5 ± 9.1	80.4 ± 27.1	11 ± 1.5

I_{GABA} at low micromolar concentrations and causes anxiolysis in rodents with little sedation (Benke et al., 2009; Khom et al., 2010, 2007). VA specifically interacts with receptors containing β_2 and β_3 subunits (Benke et al., 2009; Khom et al., 2007). A point mutation in the β_3 subunit (N265M) prevents anxiolytic activity of VA in mice. It was therefore concluded that anxiolysis occurs via neurons expressing β_3 comprising $GABA_A$ receptors (Benke et al., 2009). Subunit-selective ligands like VA would be expected to exhibit a selective therapeutic profile with fewer side effects and may thus represent an interesting lead structure for the development of novel $GABA_A$ receptor modulators (Atack, 2011a, 2011b, 2010; Möhler, 2012).

Little is known, however, if different VA-esters with higher lipophilicity would have different anxiolytic and anticonvulsant action. Neuhaus et al. (2008) hypothesized that VA does not permeate the blood-brain barrier by passive diffusion through the lipid bilayer but rather *via* a paracellular transport route.

Therefore, we have now performed a proof-of-concept study to test if masking the carboxylic acid of VA by esterification (Fig. 1) would affect the in vivo activity of VA. Four VA-esters with different lipophilicity (LogP: VA (5.13 ± 0.31) < VA-ME (5.64 ± 0.28) < VA-EE (6.17 ± 0.28) < VA-PE (6.70 ± 0.28) < VA-POM (6.97 ± 0.40), Fig. 1; calculated using ACD/ChemSketch freeware) were designed and their anxiolytic and anticonvulsant activity subsequently analyzed.

As expected, esterification of VA significantly reduced I_{GABA} modulation (Fig. 2), which was evident for all 4 tested derivatives. None of the VA-esters increased I_{GABA} at 1 μM, while significant stimulation was induced by VA (Fig. 2).

It is expected that the esters are transformed into the highly active VA by esterases ubiquitously found in the blood, liver, brain and other organs and tissues (Liederer and Borchardt, 2006). This assumption is in line with the observed in vivo action of the VA-esters (VA-ME, VA-EE and VA-PE, Figs. 3–5) and was directly confirmed by estimation of the plasma concentrations of VA (Table 1).

In order to obtain information about potential differences in the time courses of anxiolytic activity of esters, behavior was analyzed 15, 30, 60 min after treatment. As shown in Figs. 3 and 4, methylation and propylation of VA resulted in a faster onset of anxiolysis, while VA-EE and VA-POM displayed no activity after 15 min. All esters were almost equally active after 30 min with the exception of the VA-POM that did not cause significant anxiolysis (Fig. 3B). A longer lasting anxiolytic action of VA-ME and VA-EE is evident from Fig. 3C where both compounds were at 60 min significantly more active than VA. These alterations may depend on different factors including distinct distribution of the prodrug into organs dependent on its lipophilicity. This may also include alterations of binding to plasma proteins or fatty tissue. A second important factor is the conversion of the non-active prodrug into the active VA by esterases.

The anticonvulsant activity of VA and the ester derivatives was observed for the first time. Significant differences in onset and length of the anticonvulsant action of the VA-esters are evident from Fig. 5. VA (dotted line in Fig. 5A–D) displayed little activity after 15 min, reached maximal anticonvulsant activity after 30 min that decayed until 90 min. A comparable transient time course of action was observed for the propylester (VA-PE) displaying, however, significantly stronger effects at 30 min. An exceptional result was obtained with the ethylester of VA: remarkably, VA-EE displayed no significant anticonvulsant activity at early time points (15 and 30 min, Fig. 5B). However, a long-lasting anticonvulsant action of this compound until 120 min is evident from Fig. 5B. The anticonvulsant action of VA-POM was similarly delayed but not so long lasting as VA-EE (compare Fig. 5B and D). The late anticonvulsant effects of VA-EE (Fig. 5B) are in line with its pronounced anxiolytic effect after 60 min (Fig. 3C). In contrast, VA-ME displayed highest anxiolytic and anticonvulsant activities at the earliest time-point (15 min). The most lipophilic VA-POM displayed the least anxiolytic or anticonvulsant activity compared to the most polar VA. This might relate to two possible explanations: either the ethylester is stronger bond to proteins or lipophilic surfaces, leading to a slower but longer distribution, or the ethylester is less accessible for esterases, leading to an increased stability of this potential prodrug. The first reason appears unlikely, because the lipophilicity of the ethylester is comparable to those of the methyl- and propylesters, which both display faster onset of effects. Of note is the fact, that the most lipophilic ester (VA-POM) displayed comparatively little in vivo activity, suggesting that this compound might be trapped in lipophilic structures.

Hydrolysis of VA-esters in plasma was confirmed employing an LC–MS/MS assay as already described (Sampath et al., 2012). Plasma levels after i.p. application of any of the VA-esters after 15 min were lower than after application of VA despite the stronger in vivo activity (Figs. 3–5). Tissue binding and delayed hydrolysis of VA-esters by esterases might contribute to the lower plasma levels of VA.

However, in vivo VA-esters were similarly or even more active than VA (VA-ME, VA-EE, VA-PE) (see Figs. 3–5) which may indicate a rapid penetration of these potential prodrugs into brain. Based on their lipophilicity it cannot be excluded that parent VA-esters may reach significant brain concentration. Although esterification of VA strongly reduces I_{GABA} modulation in vitro (Fig. 2) their potentially better penetration of the blood–brain barrier may contribute to the overall anxiolytic and anticonvulsant activity. The much slower onset and longer lasting anticonvulsant activity of VA-EE and VA-POM may reflect a slower hydrolysis in the brain (see Fig. 5B and D). Ongoing animal studies shall therefore verify time- and dose-dependent penetration of VA-esters into brain.

Taken together, several VA-esters display similar or stronger in vivo activity than VA. The different time courses of anticonvulsant activity (e.g. fast onset of the VA-ME and long lasting effects of the VA-EE) may be beneficial for potential therapeutic use of this molecule. Future studies will show whether the increased lipophilicity of the esters will affect the oral bioavailability of VA.

Acknowledgments

The research was funded by the Austrian Science Fund (FWF) grants TRP 107-B11, P21241 and P22395. Juliane Hintersteiner and Denise Luger are fellows of the graduate school program MolTag (Austrian Science Fund FWF-W1232), Maximilian Haider is supported by the Initiativkolleg Functional Molecules IK 1041-N. The authors thank Hugo Kubinyi for valuable comments on the manuscript.

References

Atack, J.R., 2010. GABAA receptor alpha2/alpha3 subtype-selective modulators as potential nonsedating anxiolytics. Curr. Top. Behav. Neurosci. 2, 331–360.

Atack, J.R., 2011a. GABAA receptor subtype-selective modulators. I. α2/α3-selective agonists as non-sedating anxiolytics. Curr. Top. Med. Chem. 11, 1176–1202.

Atack, J.R., 2011b. GABAA receptor subtype-selective modulators. II. α5-selective inverse agonists for cognition enhancement. Curr. Top. Med. Chem. 11, 1203–1214.

Baburin, I., Beyl, S., Hering, S., 2006. Automated fast perfusion of *Xenopus* oocytes for drug screening. Pflüg. Arch. Eur. J. Physiol 453, 117–123.

Beaumont, K., Webster, R., Gardner, I., Dack, K., 2003. Design of ester prodrugs to enhance oral absorption of poorly permeable compounds: challenges to the discovery scientist. Curr. Drug Metab. 4, 461–485.

Benke, D., Barberis, A., Kopp, S., Altmann, K.-H., Schubiger, M., Vogt, K.E., Rudolph, U., Möhler, H., 2009. GABA A receptors as in vivo substrate for the anxiolytic action of valerenic acid, a major constituent of valerian root extracts. Neuropharmacology 56, 174–181.

Boileau, A.J., Baur, R., Sharkey, L.M., Sigel, E., Czajkowski, C., 2002. The relative amount of cRNA coding for gamma2 subunits affects stimulation by benzodiazepines in GABA(A) receptors expressed in *Xenopus* oocytes. Neuropharmacology 43, 695–700.

Broadwell, R.D., Salcman, M., Kaplan, R.S., 1982. Morphologic effect of dimethyl sulfoxide on the blood–brain barrier. Science 217, 164–166.

Greenfield Jr, L.J., 2013. Molecular mechanisms of antiseizure drug activity at GABAA receptors. Seizure J. Br. Epilepsy Assoc.

Groves, J.O., Guscott, M.R., Hallett, D.J., Rosahl, T.W., Pike, A., Davies, A., Wafford, K. A., Reynolds, D.S., 2006. The role of GABAbeta2 subunit-containing receptors in mediating the anticonvulsant and sedative effects of loreclezole. Eur. J. Neurosci. 24, 167–174.

Johnston, G.A.R., Hanrahan, J.R., Chebib, M., Duke, R.K., Mewett, K.N., 2006. Modulation of ionotropic GABA receptors by natural products of plant origin. Adv. Pharmacol. San Diego Calif. 54, 285–316.

Khom, S., Baburin, I., Timin, E., Hohaus, A., Trauner, G., Kopp, B., Hering, S., 2007. Valerenic acid potentiates and inhibits GABA(A) receptors: molecular mechanism and subunit specificity. Neuropharmacology 53, 178–187.

Khom, S., Baburin, I., Timin, E.N., Hohaus, A., Sieghart, W., Hering, S., 2006. Pharmacological properties of GABAA receptors containing gamma1 subunits. Mol. Pharmacol. 69, 640–649.

Khom, S., Strommer, B., Ramharter, J., Schwarz, T., Schwarzer, C., Erker, T., Ecker, G. F., Mulzer, J., Hering, S., 2010. Valerenic acid derivatives as novel subunit-selective GABAA receptor ligands—in vitro and in vivo characterization. Br. J. Pharmacol. 161, 65–78.

Kopp, S., Baur, R., Sigel, E., Möhler, H., Altmann, K.-H., 2010. Highly potent modulation of GABA(A) receptors by valerenic acid derivatives. ChemMedChem 5, 678–681.

Liederer, B.M., Borchardt, R.T., 2006. Enzymes involved in the bioconversion of ester-based prodrugs. J. Pharm. Sci. 95, 1177–1195.

Methfessel, C., Witzemann, V., Takahashi, T., Mishina, M., Numa, S., Sakmann, B., 1986. Patch clamp measurements on *Xenopus laevis* oocytes: currents through endogenous channels and implanted acetylcholine receptor and sodium channels. Pflüg. Arch. Eur. J. Physiol 407, 577–588.

Möhler, H., 2006. GABAA receptors in central nervous system disease: anxiety, epilepsy, and insomnia. J. Recept. Signal Transduction Res. 26, 731–740.

Möhler, H., 2012. The GABA system in anxiety and depression and its therapeutic potential. Neuropharmacology 62, 42–53.

Neuhaus, W., Trauner, G., Gruber, D., Oelzant, S., Klepal, W., Kopp, B., Noe, C.R., 2008. Transport of a GABAA receptor modulator and its derivatives from *Valeriana officinalis* L. s. l. across an in vitro cell culture model of the blood–brain barrier. Planta Med. 74, 1338–1344.

Olsen, R.W., Sieghart, W., 2008. International Union of Pharmacology. LXX. Subtypes of gamma-aminobutyric acid(A) receptors: classification on the basis of subunit composition, pharmacology, and function. Update. Pharmacol. Rev. 60, 243–260.

Sampath, C., Haug, K., Thanei, S., Hamburger, M., Derendorf, H., Frye, R., Butterweck, V., 2012. Pharmacokinetics of valerenic acid in rats after intravenous and oral administrations. Planta Med. 78, 575–581.

Sanna, E., Murgia, A., Casula, A., Usala, M., Maciocco, E., Tuligi, G., Biggio, G., 1996. Direct activation of GABAA receptors by loreclezole, an anticonvulsant drug with selectivity for the beta-subunit. Neuropharmacology 35, 1753–1760.

Sieghart, W., 2006. Structure, pharmacology, and function of GABAA receptor subtypes. Adv. Pharmacol. San Diego Calif. 54, 231–263.

Sigel, E., Steinmann, M.E., 2012. Structure, function, and modulation of GABA (A) receptors. J. Biol. Chem. 287, 40224–40231.

Simon, J., Wakimoto, H., Fujita, N., Lalande, M., Barnard, E.A., 2004. Analysis of the set of GABA(A) receptor genes in the human genome. J. Biol. Chem. 279, 41422–41435.

Urban, M., Sarek, J., Tislerova, I., Dzubak, P., Hajduch, M., 2005. Influence of esterification and modification of A-ring in a group of lupane acids on their cytotoxicity. Bioorg. Med. Chem. 13, 5527–5535.

Wingrove, P.B., Wafford, K.A., Bain, C., Whiting, P.J., 1994. The modulatory action of loreclezole at the gamma-aminobutyric acid type A receptor is determined by a single amino acid in the beta 2 and beta 3 subunit. Proc. Nat. Acad. Sci. U.S.A. 91, 4569–4573.

4.2 Paper II
$GABA_A$ Receptor Modulation by Piperine and a non-TRPV1 Activating Derivative
(Khom et al., 2013)

Khom, S., Strommer, B., Schöffmann, A., **Hintersteiner, J.**, Baburin, I., Erker, T., Schwarz, T., Schwarzer, C., Zaugg, J., Hamburger, M., Hering, S., 2013. *GABAA receptor modulation by piperine and a non-TRPV1 activating derivative.* Biochem. Pharmacol. 85, 1827–1836. doi:10.1016/j.bcp.2013.04.017

Contribution

- Measurement of body temperature after i.p. application of compounds

Biochemical Pharmacology 85 (2013) 1827–1836

Contents lists available at SciVerse ScienceDirect

Biochemical Pharmacology

journal homepage: www.elsevier.com/locate/biochempharm

$GABA_A$ receptor modulation by piperine and a non-TRPV1 activating derivative

Sophia Khom [a,1], Barbara Strommer [a,1], Angela Schöffmann [a], Juliane Hintersteiner [a], Igor Baburin [a], Thomas Erker [b], Thomas Schwarz [b], Christoph Schwarzer [c], Janine Zaugg [d], Matthias Hamburger [d], Steffen Hering [a,*]

[a] Department of Pharmacology and Toxicology, University of Vienna, Althanstraße 14, A-1090 Wien, Austria
[b] Department of Medicinal Chemistry, University of Vienna, Althanstraße 14, A-1090 Wien, Austria
[c] Institute of Pharmacology, Innsbruck Medical University, Peter-Mayr-Str., A-6020 Innsbruck, Austria
[d] Institute of Pharmaceutical Biology, University of Basel, Klingelbergstrasse 50, CH-4056 Basel, Switzerland

ARTICLE INFO

Article history:
Received 28 January 2013
Accepted 17 April 2013
Available online 25 April 2013

Keywords:
$GABA_A$ receptors
TRPV1 channels
2-Microelectrode voltage clamp technique
Behavioural pharmacology
Piperine

ABSTRACT

The action of piperine (the pungent component of pepper) and its derivative SCT-66 ((2E,4E)-5-(1,3-benzodioxol-5-yl))-*N*,*N*-diisobutyl-2,4-pentadienamide) on different gamma-aminobutyric acid (GABA) type A ($GABA_A$) receptors, transient-receptor-potential-vanilloid-1 (TRPV1) receptors and behavioural effects were investigated.

$GABA_A$ receptor subtypes and TRPV1 receptors were expressed in *Xenopus laevis* oocytes. Modulation of GABA-induced chloride currents (I_{GABA}) by piperine and SCT-66 and activation of TRPV1 was studied using the two-microelectrode-voltage-clamp technique and fast perfusion. Their effects on explorative behaviour, thermoregulation and seizure threshold were analysed in mice. Piperine acted with similar potency on all $GABA_A$ receptor subtypes (EC_{50} range: 42.8 ± 7.6 μM ($\alpha_2\beta_2$)–59.6 ± 12.3 μM ($\alpha_3\beta_2$)). I_{GABA} modulation by piperine did not require the presence of a γ_{2S}-subunit, suggesting a binding site involving only α and β subunits. I_{GABA} activation was slightly more efficacious on receptors formed from $\beta_{2/3}$ subunits (maximal I_{GABA} stimulation through $\alpha_1\beta_3$ receptors: 332 ± 64% and $\alpha_1\beta_2$: 271 ± 36% vs. $\alpha_1\beta_1$: 171 ± 22%, $p < 0.05$) and α_3-subunits ($\alpha_3\beta_2$: 375 ± 51% vs. $\alpha_5\beta_2$:136 ± 22%, $p < 0.05$). Replacing the piperidine ring by a *N*,*N*-diisobutyl residue (SCT-66) prevents interactions with TRPV1 and simultaneously increases the potency and efficiency of $GABA_A$ receptor modulation. SCT-66 displayed greater efficacy on $GABA_A$ receptors than piperine, with different subunit-dependence. Both compounds induced anxiolytic, anticonvulsant effects and reduced locomotor activity; however, SCT-66 induced stronger anxiolysis without decreasing body temperature and without the proconvulsive effects of TRPV1 activation and thus may serve as a scaffold for the development of novel $GABA_A$ receptor modulators.

1. Introduction

Piperine (1-piperoylpiperidine) is the pungent component of several pepper species and activates transient receptor potential of the subfamily V member 1 (TRPV1) receptors [1,2]. We have recently shown that piperine modulates γ-aminobutyric acid (GABA) type A ($GABA_A$) receptors [3]. Via TRPV1-activation, piperine affects pain signalling and regulation of the body temperature [4,5], while $GABA_A$ receptor modulation is expected to induce fast inhibitory synaptic neurotransmission in the mammalian brain, resulting in, for example, anxiolysis, sedation, hypnosis, muscle relaxation, analgesia and anticonvulsant effects [6–11].

Piperine complies in all respects with Lipinski's "rule of five" and could therefore be a scaffold for the development of novel $GABA_A$ receptor modulators [3,12]. However, it is currently unknown whether piperine interacts preferentially with specific $GABA_A$ receptor subtypes. Moreover, simultaneous activation of TRPV1 receptors may cause unwanted side effects including changes in pain sensation and body temperature that would be an obstacle to its therapeutic use [5]. Here we analyse the action of piperine and its derivative SCT-66 ((2E,4E)-5-(1,3-benzodioxol-5-yl))-*N*,*N*-diisobutyl-2,4-pentadienamide) on nine $GABA_A$ receptor subtypes and on TRPV1 receptors. Unlike piperine, SCT-66 did not activate TRPV1 receptors. This compound increased I_{GABA} more potently and more efficaciously than piperine, although with altered subunit dependence. In vivo studies in mice revealed that

* Corresponding author. Tel.: +43 1 4277 55301/10; fax: +43 1 4277 9553.
E-mail address: steffen.hering@univie.ac.at (S. Hering).
[1] Both authors contributed equally to this work.

0006-2952
http://dx.doi.org/10.1016/j.bcp.2013.04.017

only piperine affects thermoregulation; that both piperine and SCT-66 have anticonvulsant and anxiolytic effects and reduce locomotor activity; and that SCT-66 has a stronger anxiolytic effect than piperine.

2. Materials and methods

All procedures involving animals were approved by the Austrian Animal Experimentation Ethics Board in compliance with the European Convention for the Protection of Vertebrate Animals used for Experimental and Other Scientific Purposes (ETS No. 123). Every effort was made to minimize the number of animals used.

2.1. Reagents

Piperine was obtained from Sigma™ (Vienna, Austria) and the piperine derivative SCT-66 (2E,4E)-5-(1,3-benzodioxol-5-yl))-*N*,*N*-diisobutyl-2,4-pentadienamide) was synthesized as described below (for structural formulae see Fig. 1): To a solution of piperic acid chloride (3 mmol, 0.71 g) in 10 mL dry THF, diisobutylamine (10.5 mmol; 1.357 g) was added and stirred overnight. The reaction mixture was evaporated and purified by column chromatography (toluene/ethyl acetate 20:3) to give the compound SCT-66 (0.661 g, 67%) as oil.

^{1}H NMR (200 MHz, $CDCl_3$): δ 7.,54–7.34 (m, 1H), 7,00 (d, J = 1.4 Hz, 1H), 6.90 (dd, J = 8.0, 1.6 Hz, 1H), 6.84–6.71 (m, 3H), 6.39 (d, J = 14.6 Hz, 1H), 5.97 (s, 2H), 3.28 (d, J = 7.5 Hz, 2H), 3.19 (d, J = 7.5 Hz, 2H), 2.12–1.88 (m, 2H), 0.98–0.82 (m, 12H). ^{13}C NMR (50 MHz, $CDCl_3$): δ 167.0, 148.4, 148.3, 142.5, 138.5, 131.2, 125.6, 122.7, 120.8, 108.7, 105.9, 101.5, 56.2, 54.9, 29.2, 27.2, 20.5, 20.3. MS m/z: 329 (12%, M^+), 201 (100%), 115 (39%), 57 (17%), 43 (23%). CHN for $C_{20}H_{27}NO_3$: calc.: C 72.92, H 8.26, N 4.25; found: C 72.78, H 8.13, N 4.16.

Stock solutions of piperine and SCT-66 were prepared in 100% DMSO (100 mM for oocyte experiments, 10 mg/μl for animal experiments; Dimethyl Sulfoxide). All chemicals were purchased from Sigma™, Vienna, Austria except where stated otherwise.

2.2. Expression and functional characterization of $GABA_A$ receptors and TRPV1 channels

Preparation of stage V-VI oocytes from *Xenopus laevis* and synthesis of capped off run-off poly(A^+) cRNA transcripts from linearized cDNA templates (pCMV vector) were performed as previously described [13]. Briefly, female *X. laevis* (NASCO™, Fort Atkinson, WI, USA) were anaesthetized by exposing them for 15 min to a 0.2% solution of MS-222 (methane sulfonate salt of 3-aminobenzoic acid ethyl ester) before surgically removing parts of the ovaries. Follicle membranes from isolated oocytes were digested with 2 mg/ml collagenase (Type 1A). Selected stage V-VI oocytes were injected with about 10–50 nl of DEPC- treated water (diethyl pyrocarbonate) containing the different cRNAs at a concentration of approximately 300–3000 pg/nl. The amount of cRNA was determined by means of a NanoDrop ND-1000 (Kisker-biotech™, Steinfurt, Germany).

$GABA_A$ receptors: To ensure expression of the gamma-subunit in rat $GABA_A$ receptors, cRNAs for expression of $\alpha_1\beta_2\gamma_{2S}$, $\alpha_2\beta_2\gamma_{2S}$, $\alpha_3\beta_2\gamma_{2S}$ and $\alpha_5\beta_2\gamma_{2S}$ receptors were mixed in a ratio of 1:1:10. For receptors comprising only α and β subunits ($\alpha_1\beta_2$, $\alpha_2\beta_2$, $\alpha_1\beta_3$, $\alpha_2\beta_2$, $\alpha_3\beta_2$, $\alpha_5\beta_2$), the cRNAs were mixed in a ratio 1:1. cRNAs for

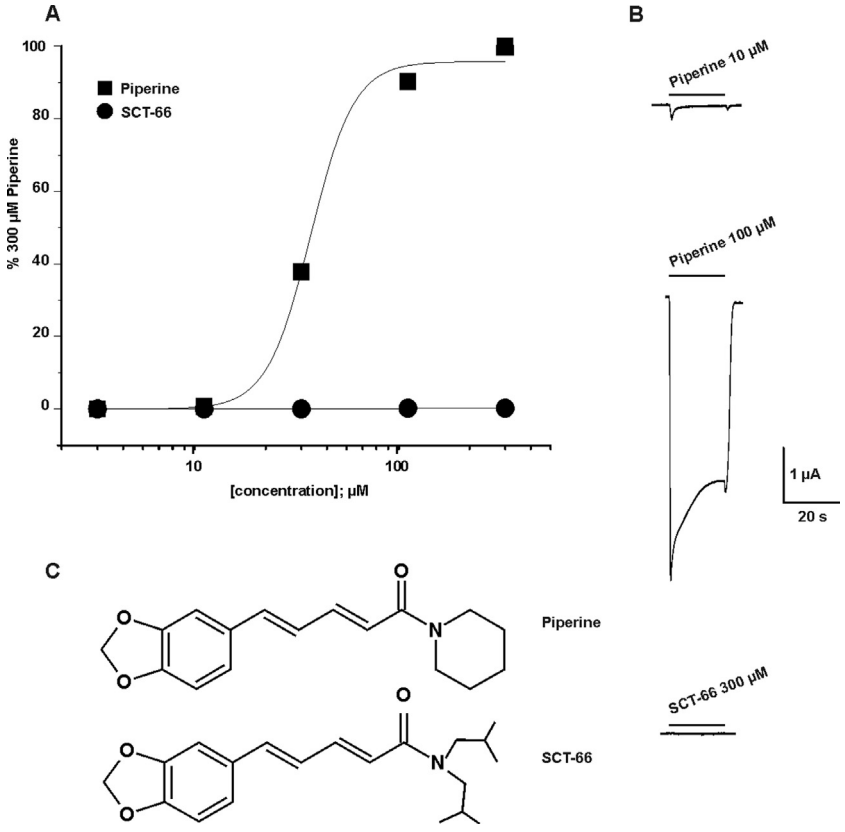

Fig. 1. Comparison of TRPV1 activation by piperine and SCT-66. (A) The concentration–response relationship for piperine (■; 3–300 μM) and SCT-66 (●, 3–300 μM) are shown. These normalized data were generated by measuring the net currents evoked in response to a test concentration of agonist and are expressed as a percentage of a preceding 300 μM piperine control response recorded in the same cell. Data are expressed as the mean ± S.E.M with n = 3–10 individual cells. The EC_{50} for piperine was 33.3 ± 0.1 μM (Hill coefficient of 4.1 ± 0.1; n = 3–10 per concentration). The EC_{50} value of piperine agrees with [2]. (B) Typical traces showing activation of TRPV1 channels by piperine and the lack of TRPV1 activation by SCT-66 at the indicated concentrations. (C) Structural formulae of piperine and its derivative SCT-66.

$\alpha_1\beta_1$ channels were injected in a ratio 3:1 to avoid formation of β_1 homomeric $GABA_A$ receptors [14,15].

TRPV1 channels: The rat TRPV1 clone was a gift from Prof. David Julius (Department of Cellular and Molecular Pharmacology, University of California, San Francisco).

After injection, oocytes were stored at 18 °C for 24–48 h in ND96 solution containing penicillin G (10 000 IU/100 ml) and streptomycin (10 mg/100 ml) [16]. Electrophysiological experiments on $GABA_A$ receptors and TRPV1 channels were performed using the two-microelectrode-voltage-clamp method at a holding potential of −70 mV ($GABA_A$ receptors) and −60 mV (TRPV1), respectively, making use of a TURBO TEC 01 C amplifier (npi electronic™, Tamm, Germany) and an Axon Digidata 1322A interface (Molecular Devices™, Sunnyvale, CA). Data acquisition was done using pCLAMP v.9.2. The bath solution contained 90 mM NaCl, 1 mM KCl, 1 mM $MgCl_2 \cdot 6H_2O$, 1 mM $CaCl_2$ and 5 mM HEPES (pH 7,4). Microelectrodes were filled with 2 M KCl.

2.3. Perfusion system

GABA, piperine and SCT-66 were applied by means of a fast perfusion system [17, ScreeningTool, npi electronic™, Tamm, Germany] to study I_{GABA} modulation and TRPV1 activation. To elicit I_{GABA}, the chamber was perfused with 120 μl of GABA-containing solution at a volume rate between 300 and 1000 μl/s. The I_{GABA} rise time ranged from 100 to 250 ms [13].

To account for possible slow recovery from increasing levels of desensitization in the presence of high GABA or piperine/SCT-66 concentrations, the duration of washout periods was extended from 1.5 min (for 1–10 μM GABA, <10 μM piperine/SCT-66) to 30 min (for ≥30 μM GABA, ≥10 μM piperine/SCT-66). To exclude voltage-clamp errors, oocytes with maximal current amplitudes >3 μA were discarded.

Because of low solubility in the bath solution, piperine and SCT-66 were used up to a concentration of 300 μM. Equal amounts of DMSO were present in all testing solutions. The maximum DMSO concentration in the bath (0.3%) had no observable effects on I_{GABA} or TRPV1.

2.4. Analysing concentration–response curves

Stimulation of chloride currents by modulators of the $GABA_A$ receptor was measured at a GABA concentration eliciting between 3 and 7% of the maximal current amplitude (EC_{3-7}). The EC_{3-7} was determined at the beginning of each experiment.

Enhancement of the chloride current was defined as $(I_{(GABA+Comp)}/I_{GABA}) - 1$, where $I_{(GABA+Comp)}$ is the current response in the presence of a given compound and I_{GABA} is the control GABA current. Concentration–response curves for activation of TRPV1 channels were generated by comparing the peak response evoked by a test concentration of the compounds at the different concentrations to that evoked by a previous control current recorded in response to 300 μM piperine.

Data were fitted by non-linear regression analysis using Origin software (OriginLab Corporation, USA). Data were fitted to the equation: $1/(1 + (EC_{50}/[Comp])^{n_H})$, where n_H is the Hill coefficient. Each data point represents the mean ± S.E.M. from at least 3 oocytes and ≥2 oocyte batches.

2.5. Behavioural analysis

2.5.1. Animals

Male mice (C57BL/6N) were obtained from Charles River Laboratories™ (Sulzfeld, Germany). For maintenance, mice were group-housed (maximum 5 mice per type IIL cage) with free access to food and water. At least 24 h before the commencement of experiments, mice were transferred to the testing facility, where they were given free access to food and water. The temperature in the maintenance and testing facilities was 23 ± 1 °C; the humidity was 40–60%; a 12 h light–dark cycle was in operation (lights on from 07:00 to 19:00). Only male mice aged 3–6 months were tested. Compounds were applied by intraperitoneal (i.p.) injection of aqueous solutions (either control or compound) 30 min before each test, except for body temperature, which was measured 3 h after injection. Testing solutions were prepared in a solvent composed of saline 0.9% NaCl solution with 10% DMSO and 3% Tween 80. The final DMSO concentration did not exceed 10% (see [18] for effects of DMSO on blood-brain barrier penetration). 1 M NaOH was used to adjust the pH to 7.4. All solutions were prepared freshly on the day of the experiment. Application of the solvent alone did not influence animal behaviour.

2.5.2. Measurement of body temperature

A temperature probe (Type T Thermocouple probe RET-3 connected to a Type T Thermometer, Physitemp Instruments Inc™; Clifton, USA), lubricated with glycerol, was inserted into the rectum of the mouse for a depth of up to 1 cm. The temperature probe remained in the animal till a stable temperature was reached (maximum 10 s).

2.5.3. Open Field Test (OF)

Ambulation was tested over 10 min in a 50 cm × 50 cm × 50 cm field box equipped with infrared rearing detection. Illumination was set to 150 lx. The explorative behaviour of C57BL/6N mice was analysed using the Actimot2 equipment and software (TSE-systems™, Bad Homburg, Germany). Areas were subdivided into border (up to 8 cm from wall), centre (20 cm × 20 cm, i.e. 16% of total area), and intermediate areas according to the recommendations of EMPRESS (European Mouse Phenotyping Resource of Standardized Screens; http://empress.har.mrc.ac.uk). The test was automatically started when the mouse was placed in the centre area.

2.5.4. Elevated Plus Maze Test (EPM)

The animal's behaviour was tested over 5 min on an elevated plus maze 1 m above ground consisting of two closed and two open arms, each 30 cm × 5 cm in size. The height of the closed arm walls was 20 cm. Illumination was set to 180 lx. Animals were placed in the centre, facing an open arm. Analysis was done automatically with Video-Mot2 equipment and software (TSE-systems™, Bad Homburg, Germany) [19].

2.5.5. Seizure threshold

Seizure threshold was determined by pentylentetrazole (PTZ)-tail-vein infusion on freely moving animals at a rate of 100 μl/min (100 mg/ml PTZ in saline). Infusion was stopped when animals displayed generalized clonic seizures. Animals were killed by cervical displacement immediately after the first generalized seizure. The seizure threshold dose was calculated from the infused volume in relation to body weight [20]. Piperine and SCT-66 were applied 30 min before PTZ infusion. Control animals were pre-treated with 10% DMSO in saline containing 3% Tween 80. At the infusion rate of 100 μl/min, generalized seizures are induced within 2 min after beginning infusion of PTZ.

2.5.6. Statistical analysis

Statistical significance of electrophysiological data was calculated using a paired Student *t*-test with a confidence interval of $p < 0.05$; for in vivo experiments, one-way ANOVA (Bonferroni Adjustment) was used. Statistical analysis was done with Origin software (OriginLab Corporation; USA). *p*-values of <0.05 were accepted as statistically significant. All data are given as mean ± S.E.M. (*n*).

3. Results

3.1. Replacing the piperidine ring by a N,N-diisobutyl-residue prevents activation of TRPV1 receptors

In line with previous studies piperine induced marked inward currents when applied to oocytes expressing TRPV1 receptors (Fig. 1A and B, [2]). A simple structural modification (replacing the piperidine ring by a *N,N*-diisobutyl residue; Fig. 1C) completely eliminated activation of TRPV1 receptors by SCT-66 (300 μM, Fig. 1A and B).

3.2. Different γ_2 subunit dependence of piperine and SCT-66

In order to analyse the interaction of piperine and SCT-66 with different $GABA_A$ receptor subtypes, receptors composed of different subunits were heterologously expressed in *Xenopus* oocytes and I_{GABA} modulation by both compounds was studied by means of the 2-microelectrode voltage-clamp technique and a fast-perfusion system (see Section 2).

First the enhancement of I_{GABA} by piperine and SCT-66 through $\alpha_1\beta_2$ and $\alpha_1\beta_2\gamma_{2S}$ receptors was compared. As illustrated in Fig. 2A, omitting the γ_{2S} subunit had no significant effect on I_{GABA} enhancement ($I_{GABA,max}$) or on the potency (EC_{50}) of piperine ($\alpha_1\beta_2$: $EC_{50} = 50.0 \pm 7.9$ μM, $I_{GABA,max} = 271 \pm 36\%$, $n = 13$ vs. $\alpha_1\beta_2\gamma_{2S}$: $EC_{50} = 52.4 \pm 9.4$ μM, $I_{GABA,max} = 302 \pm 27\%$; $n = 6$; $p > 0.05$; data for modulation of I_{GABA} through $\alpha_1\beta_2\gamma_{2S}$ receptors by piperine taken from [3]). This finding suggests that piperine interacts with a binding site located on α and/or β subunits or the α/β interface. In contrast, co-expression of a γ_{2S} subunit resulted in significant reduction of I_{GABA} enhancement by SCT-66 ($\alpha_1\beta_2$: $1256 \pm 292\%$; $n = 4$; $p < 0.05$; $\alpha_1\beta_2\gamma_{2S}$: $378 \pm 15\%$, $n = 6$; $\alpha_2\beta_2\gamma_{2S}$: $572 \pm 51\%$, $n = 5$; $\alpha_3\beta_2\gamma_{2S}$: 584 ± 20, $n = 5$ and $\alpha_5\beta_2\gamma_{2S}$: $398 \pm 26\%$, see Fig. 2D, Tables 1 and 2) suggesting a role of γ_2 in receptor modulation. Co-expression of a γ_{2S}-subunit did, however, not significantly affect the potency of SCT-66 (see Tables 1 and 2).

3.3. Piperine potentiates $GABA_A$ receptors composed of $\alpha_{1/2/3/5}$ and $\beta_{1/2/3}$ subunits

In order to investigate a potential subunit dependent action of piperine and SCT-66, we studied their interaction with 8 different receptor subtypes ($\alpha_1\beta_1$, $\alpha_1\beta_2$, $\alpha_1\beta_3$, $\alpha_2\beta_2$, $\alpha_3\beta_2$ and $\alpha_5\beta_2$) (Fig. 2A, B, D and E, Table 1). The highest efficacy of piperine was observed for receptors containing α_3 subunits, with maximal I_{GABA} potentiation (EC_{3-7}) of $375 \pm 51\%$ ($n = 6$), followed by $GABA_A$ receptors composed of α_1 and β_2 subunits ($271 \pm 36\%$, $n = 13$) and α_2 and β_2 subunits, respectively (248 ± 48; $n = 6$) (see also Table 1). Piperine was significantly less efficacious on $\alpha_5\beta_2$ receptors ($I_{GABA,max} = 136 \pm 22\%$, $n = 6$, Fig. 2A, Tables 1 and 2). The potencies of I_{GABA} modulation, however, did not significantly differ with EC_{50} values ranging from 42.8 ± 17.6 μM ($\alpha_2\beta_2$) to 59.6 ± 12.3 μM ($\alpha_3\beta_2$), Fig. 2B illustrates the effect of piperine on $GABA_A$ receptors with three different β-subunits. $\alpha_1\beta_2$ and $\alpha_1\beta_3$ receptors were more efficaciously modulated by piperine than $\alpha_1\beta_1$ receptors (maximal I_{GABA} modulation of $\alpha_1\beta_2$ receptors: $271 \pm 36\%$, $\alpha_1\beta_3$ $332 \pm 64\%$ vs. $\alpha_1\beta_1$ receptors: $171 \pm 22\%$; (see Fig. 2 C for representative I_{GABA} through $GABA_A$ receptors composed of α_3 and β_2 subunits in the absence and presence of 30 μM piperine).

3.4. Higher potency and different subunit dependence of SCT-66

SCT-66 displayed a higher potency on all subunit compositions tested (Fig. 2E and F, Tables 1 and 2 e.g. on $\alpha_1\beta_2\gamma_{2S}$ receptors: EC_{50}(SCT-66): 21.5 ± 1.7 μM, $n = 6$ compared to EC_{50}(piperine):57.6 ± 4.2 μM, $n = 6$, $p < 0.01$ and I_{GABA} was more efficaciously modulated by SCT-66 than by piperine. Stronger maximal I_{GABA} enhancement by SCT-66 ranged from 1.2-fold ($\alpha_1\beta_2\gamma_{2S}$ receptors) to 6.5-fold ($\alpha_1\beta_{1)}$ (Tables 1–2). Taken together, the stronger I_{GABA} enhancement by SCT-66 was accompanied by an apparent change in receptor subtype dependence (SCT-66 was e.g. equally efficacious on receptors comprising different β-subunits compared to piperine that was more efficacious on $\beta_{2/3}$ incorporating receptors, compare Fig. 2B to Fig. 2E).

3.5. Piperine and SCT-66 shift the GABA concentration–response curve

GABA concentration–response curves in the presence of piperine and SCT-66 for $\alpha_3\beta_2$ receptors are compared in Fig. 3. Almost-saturating concentrations of piperine and SCT-66 (100 μM, Fig. 2A, B, D and E) shifted the curves to the left (5.7 ± 1.9 μM and $n_H = 1.1 \pm 0.1$ (control); 2.7 ± 0.8 μM and $n_H = 1.1 \pm 0.2$ (piperine), and 1.9 ± 0.4 μM and $n_H = 1.1 \pm 0.1$ (SCT-66). Enhancement of $I_{GABA,max}$ by piperine and SCT-66 was statistically not significant ($I_{GABA;\ max\text{-}piperine} = 123 \pm 3$; $n = 4$ and $I_{GABA;\ max\text{-}SCT\text{-}66} = 129 \pm 6\%$, $n = 3$; $p > 0.05$). Neither piperine nor SCT-66 (up to 300 μM) activated $GABA_A$ receptors when applied in the absence of GABA.

3.6. Effects of piperine and SCT-66 on thermoregulation

Changes in body temperature might indicate activation of TRPV1 channels in vivo [21]. Core body temperature of male C57BL/6N mice was measured rectally shortly before application of saline, piperine or SCT-66. Basal values did not differ between the groups, averaging 36.80 ± 0.04 °C ($n = 184$). This temperature measurement was repeated 3 hours after injection of compound (to avoid interference from stress-induced hyperthermia early after injection). As illustrated in Fig. 4, a dramatic drop of body temperature was observed after injection of piperine at doses higher than 3 mg/kg bodyweight: application of 10 mg/kg bodyweight piperine significantly ($p < 0.01$) reduced body temperature of mice (Control: 36.10 ± 0.10 °C; $n = 38$ vs. 10 mg/kg bodyweight piperine 34.86 ± 0.29 °C; $n = 16$). An even more pronounced effect was observed upon application of 30 mg/kg bodyweight: body temperature was lowered to 30.37 ± 0.84 °C ($n = 9$; $p < 0.01$). In contrast, no significant changes in body temperature were observed after application of SCT-66 at all tested doses (see Fig. 4), thereby resulting in a statistically significant difference between the two drugs as analysed by one-way ANOVA ($p < 0.01$).

3.7. Piperine and SCT-66 reduce locomotor activity

In the Open-Field-Test (OF, see Section 2), control mice covered a distance of 39.3 ± 1.9 m, ($n = 20$; Fig. 5; white bar). Injection of piperine resulted in a dose-dependent reduction of ambulation: significant reductions were apparent from doses ≥3 mg/kg bodyweight, and the highest dose of 30 mg/kg reduced ambulation by approximately 50% compared to control littermates (control: 39.3 ± 1.9 m; $n = 20$ vs. 30 mg/kg bodyweight piperine 21.0 ± 3.7 m; $n = 13$; $p < 0.01$; see Fig. 5A; black bars for piperine). Unlike piperine, SCT-66 did not affect ambulation over a broad range (0.3–10 mg/kg bodyweight; see Fig. 5A, SCT-66 shaded bars). Only at a dose of 30 mg/kg bodyweight SCT-66 significantly reduced locomotor activity (Control: 39.3 ± 1.9 m; $n = 20$ vs. 30 mg/kg bodyweight SCT-66: 28.6 ± 2.5 m, $n = 10$, $p < 0.01$), however, this effect was still weaker than with piperine at the same dose.

3.8. Piperine and SCT-66 influence anxiety-related behaviour in the OF test

The marked influence of even low doses of piperine (≥3 mg/kg) on the locomotor activity of mice makes it difficult to analyse

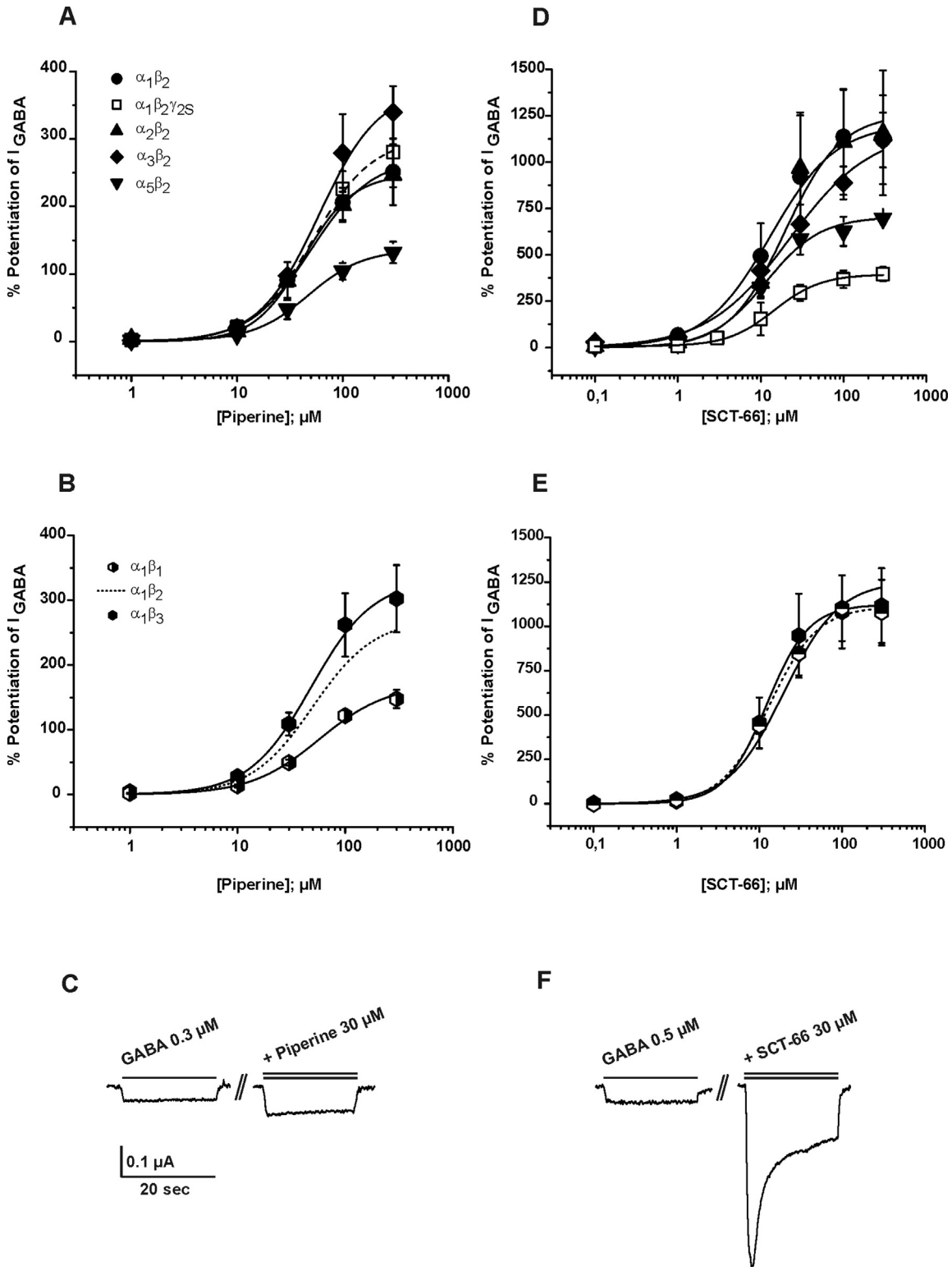

Fig. 2. I_{GABA} modulation by piperine and SCT-66 concentration–response curves for I_{GABA} modulation through $GABA_A$ receptors of the indicated subunit combinations by piperine (A and B) and SCT-66 (D and E) at a GABA concentration eliciting 3–7% of the maximal GABA response (EC_{3-7}). The enhancement of I_{GABA} by piperine trough $\alpha_1\beta_2\gamma_{2S}$ receptors (dashed line) receptors is taken from [3]. Each data point represents the mean ± S.E.M. from at least five oocytes and at least two oocyte batches. (C and F) Typical traces illustrating I_{GABA} enhancement by 30 μM compound. Control currents (GABA, single bar) and corresponding currents elicited by co-application of GABA and 30 μM piperine/SCT-66 (double bar) are shown.

anxiolytic properties in activity-based testing conditions. At lower doses, the only difference observed was an increase in distances travelled in the centre area (control: 8.8 ± 0.6%, $n = 20$ vs. SCT-66 0.3 mg/kg bodyweight: 10.7 ± 1.1%, $n = 12$; $p < 0.05$) in mice treated with SCT-66 at a dose of 0.3 mg/kg bodyweight.

3.9. Piperine and SCT-66 reduce anxiety-related behaviour in the EPM test

In order to analyse the impact of piperine and SCT-66 on anxiety-related behaviour, male C57BL/6N mice were tested

Table 1
Potency and efficiency of piperine/SCT-66 enhancement of $GABA_A$ receptors with different subunit compositions.

Subunit combination	EC_{50} (μM)	Maximum stimulation of-I_{GABA} at EC_{3-7}	Hill coefficient (n_H)	Number of experiments (n)
Piperine				
$\alpha_1\beta_1$	57.6 ± 4.2	171 ± 22	1.4 ± 0.2	10
$\alpha_1\beta_2$	50.0 ± 7.9	271 ± 36	1.5 ± 0.3	13
$\alpha_1\beta_3$	48.3 ± 7.3	332 ± 64	1.5 ± 0.3	7
$\alpha_2\beta_2$	42.8 ± 17.6	248 ± 48	1.9 ± 0.5	6
$\alpha_3\beta_2$	59.6 ± 12.3	375 ± 51	1.4 ± 0.2	6
$\alpha_5\beta_2$	47.5 ± 17.9	136 ± 22	1.7 ± 0.4	6
SCT-66				
$\alpha_1\beta_1$	13.3 ± 2.9	1112 ± 136	1.5 ± 0.2	4
$\alpha_1\beta_2$	19.8 ± 9.7	1256 ± 292	1.3 ± 0.4	4
$\alpha_1\beta_3$	12.3 ± 4.5	1128 ± 155	1.5 ± 0.3	3
$\alpha_1\beta_2\gamma_{2S}$	21.5 ± 1.7	378 ± 15	1.8 ± 0.2	6
$\alpha_2\beta_2$	13.1 ± 9.0	1204 ± 233	1.1 ± 0.3	4
$\alpha_2\beta_2\gamma_{2S}$	24.1 ± 7.5	572 ± 51	1.3 ± 0.3	5
$\alpha_3\beta_2$	22.2 ± 12.1	1169 ± 195	0.9 ± 0.2	3
$\alpha_3\beta_2\gamma_{2S}$	15.1 ± 1.8	584 ± 20	1.6 ± 0.2	5
$\alpha_5\beta_2$	11.5 ± 2.7	705 ± 24	1.3 ± 0.2	3
$\alpha_5\beta_2\gamma_{2S}$	14.2 ± 1.4	398 ± 26	2.0 ± 0.3	5

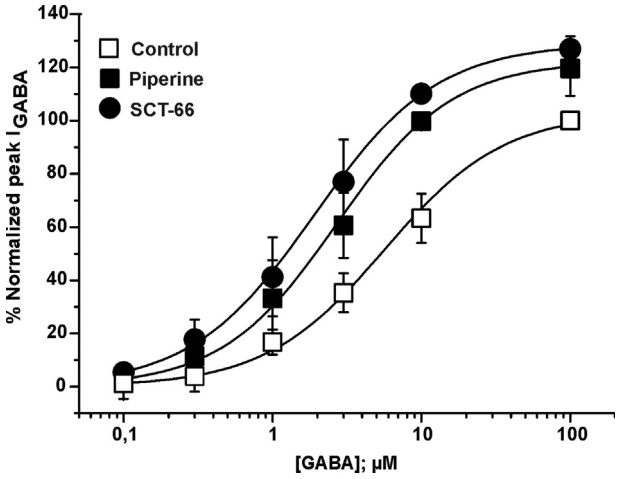

Fig. 3. Piperine and SCT-66 shift the GABA concentration–response curve towards higher GABA sensitivity GABA concentration–response curves for $\alpha_3\beta_2$ $GABA_A$ receptors in the absence (control, □) and in the presence of 100 μM piperine (■), and 100 μM SCT-66 (●) are compared. The corresponding EC_{50} values and Hill-coefficients were 5.7 ± 1.9 μM and n_H = 1.1 ± 0.1 (control) and 2.7 ± 0.8 μM and n_H = 1.1 ± 0.2 (piperine), and 1.9 ± 0.4 μM and n_H = 1.1 ± 0.1 (SCT-66), respectively. Each data point represents the mean ± S.E.M. from at least four oocytes and at least two oocyte batches.

30 min after i.p. injection in the Elevated-Plus-Maze-test (EPM, see Materials and Methods section). As illustrated in Fig. 6A, control mice (treated with saline; white bar) spent 28.6 ± 2.1% of the total test time in the open arms (OA) of the EPM (n = 27). While the behaviour of mice treated with 0.1 mg/kg bodyweight of piperine did not significantly differ from saline-treated control littermates, upon application of higher doses (i.e. 0.3 and 1 mg/kg bodyweight) mice spent significantly ($p < 0.01$) more time in the OA (0.3 mg/kg bodyweight: 43.0 ± 4.2%, n = 22 and 1 mg/kg bodyweight: 45.7 ± 6.3%, n = 16, black bars). At a dose of 1 mg/kg bodyweight piperine significantly reduced ambulation (see Fig. 6D), thus, higher doses were not investigated. Unlike piperine, SCT-66 did not significantly influence overall ambulation at the tested doses (0.3–10 mg/kg bodyweight; see Fig. 6D shaded bars). As shown in Fig. 6A, a significant increase in the time spent in the OA was observed with increasing doses of SCT-66, reaching a maximum at a dose of 1 mg/kg bodyweight (control: 28.6 ± 2.1, n = 27 vs. 1 mg/kg bodyweight SCT-66: 45.1 ± 5.7%, n = 14, $p < 0.01$). This effect remained stable and did not change even when applying higher doses (3–10 mg/kg bodyweight). Moreover, mice treated with 0.3 mg/kg bodyweight SCT-66 visited the OA more frequently than control mice (control: 12.4 ± 0.9, n = 27 vs. 0.3 mg/kg bodyweight SCT-66: 13.7 ± 1.1, n = 22, $p < 0.05$), while the number of visits to the OA did not differ at the other doses of piperine and SCT-66, respectively (see Fig. 6B). Accordingly, the number of closed arm (CA) entries also dropped significantly at doses ≥0.3 mg/kg bodyweight piperine and SCT-66, respectively (Fig. 6 C).

3.10. Piperine and SCT-66 modulate seizure threshold

The seizure threshold as assessed using pentylentetrazole (PTZ) tail vein infusions was significantly increased 30 min after i.p. injection of piperine at 3 or 10 mg/kg bodyweight (Control: 39.4 ± 2.8 mg/kg bodyweight PTZ; n = 7; vs. 3 mg/kg bodyweight

Table 2
Comparison of efficiencies for $GABA_A$ receptors of different subunit compositions. (*) indicates statistically significant ($p < 0.05$) differences.

Piperine	$\alpha_1\beta_2$	$\alpha_1\beta_2$	$\alpha_1\beta_3$	$\alpha_1\beta_2\gamma_{2S}$[1]	$\alpha_2\beta_2$	$\alpha_3\beta_2$	$\alpha_5\beta_2$
$\alpha_1\beta_1$		*	*	*			
$\alpha_1\beta_2$	*						*
$\alpha_1\beta_3$	*						*
$\alpha_1\beta_2\gamma_{2S}$[a]	*						*
$\alpha_2\beta_2$							*
$\alpha_3\beta_2$							*
$\alpha_5\beta_2$		*	*	*	*	*	

SCT-66	$\alpha_1\beta_1$	$\alpha_1\beta_2$	$\alpha_1\beta_3$	$\alpha_1\beta_2\gamma_{2S}$	$\alpha_2\beta_2$	$\alpha_2\beta_2\gamma_{2S}$	$\alpha_3\beta_2$	$\alpha_3\beta_2\gamma_{2S}$	$\alpha_5\beta_2$	$\alpha_5\beta_2\gamma_{2S}$
$\alpha_1\beta_1$				*		*		*	*	*
$\alpha_1\beta_2$				*						*
$\alpha_1\beta_3$				*		*		*	*	*
$\alpha_1\beta_2\gamma_{2S}$	*	*	*		*	*	*	*	*	
$\alpha_2\beta_2$				*		*		*		*
$\alpha_2\beta_2\gamma_{2S}$	*		*	*	*		*			*
$\alpha_3\beta_2$				*		*		*		*
$\alpha_3\beta_2\gamma_{2S}$	*		*	*	*		*		*	*
$\alpha_5\beta_2$	*		*	*				*		*
$\alpha_5\beta_2\gamma_{2S}$	*	*	*		*	*	*	*	*	*

[a] E_{max} values for enhancement of I_{GABA} through $\alpha_1\beta_2\gamma_{2S}$ receptors by piperine are taken from [3].

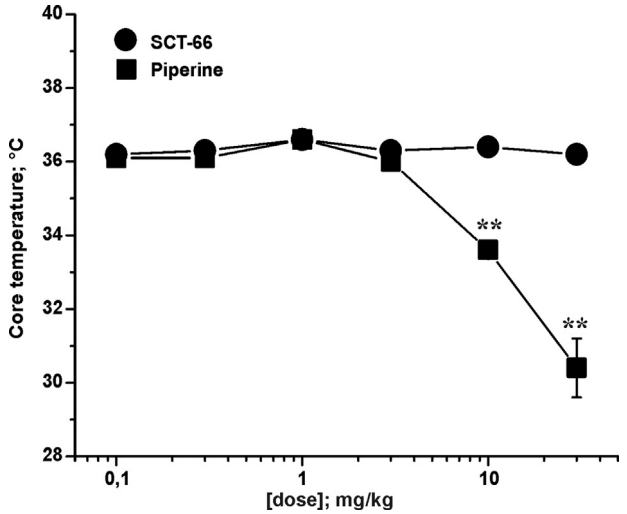

Fig. 4. SCT-66 does not reduce body temperature in mice Effects of piperine and SCT-66 on body temperature 3 h after injection of (■) piperine or (●) SCT-66 at the indicated doses (mg/kg bodyweight) are illustrated. Each data point represents the mean ± S.E.M. of at least 9 mice. (**) indicates statistically significant ($p < 0.01$) differences to control (ANOVA with Bonferroni).

piperine: 46.2 ± 5.4 mg/kg bodyweight PTZ; $n = 4$; $p < 0.05$ and 10 mg/kg bodyweight piperine, respectively: 48,7 ± 2.1 mg/kg bodyweight PTZ; $n = 4$; $p < 0.01$). A dose of 30 mg/kg bodyweight, however, resulted in a significant drop in seizure threshold (30.3 ± 3.4 mg/kg bodyweight PTZ; $n = 4$; $p < 0.01$; Fig. 7A). Doses below 3 mg/kg bodyweight did not affect seizure threshold.

Unlike piperine, SCT-66 did not display any observable effects on the seizure threshold up to 3 mg/kg bodyweight. Only higher doses significantly raised the seizure threshold (10 mg/kg bodyweight SCT-66: 47.6 ± 3.4 mg/kg bodyweight PTZ; $n = 4$; $p < 0.01$ and 30 mg/kg bodyweight SCT-66: 55.8 ± 2.8 mg/kg bodyweight PTZ, $n = 4$, $p < 0.01$; Fig. 7B).

4. Discussion

Natural products from distinct structural classes including flavonoids [22–25], terpenoids [26–28], sesquiterpenes [29–31], diterpenes [32], triterpene glycosides [33], polyacetylenes [34], (neo)lignans [28,35], alkaloids [3] or (furano)coumarins [36,37] have been shown to modulate $GABA_A$ receptors.

We have recently reported that besides activating TRPV1 receptors [2] piperine modulates $GABA_A$ receptors [3]. Here we report that replacing the piperidine ring by a *N,N*-diisobutyl-residue prevents activation of TRPV1 (Fig. 1A and B). In order to get insights into their therapeutic potentials we subsequently characterized the actions of piperine and its derivative SCT-66 in vitro and in vivo.

4.1. Subunit-dependent modulation of $GABA_A$ receptors by piperine

Comparable enhancement of I_{GABA} through $\alpha_1\beta_2$ receptors as through the $\alpha_1\beta_2\gamma_{2S}$ [3] and the similar potencies on the two receptor subtypes suggests that piperine interacts with a binding

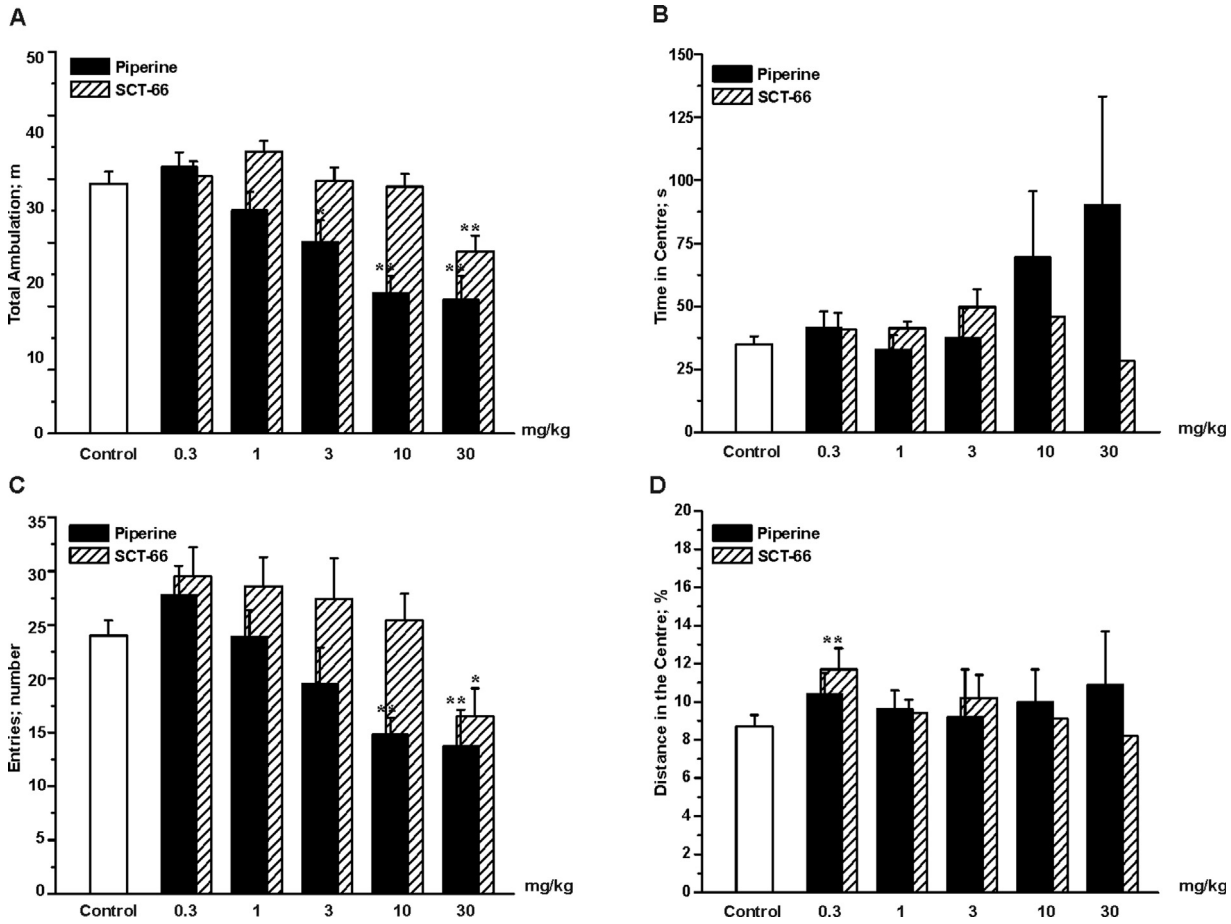

Fig. 5. Piperine and SCT-66 dose-dependently reduce locomotor activity in the OF test. Bars indicate in (A) the total distance travelled, in (B) the time spent in the centre, in (C) the number of entries to the centre and in (D) the distance travelled in the centre as % of the total distance after application of the indicated dose (mg/kg bodyweight) of piperine (black bars), SCT-66 (shaded bars) or control (white bars). Bars always represent means ± S.E.M. from at least 8 different mice. (*) indicates statistically significant differences with $p < 0.05$, (**) $p < 0.01$ to control (ANOVA with Bonferroni).

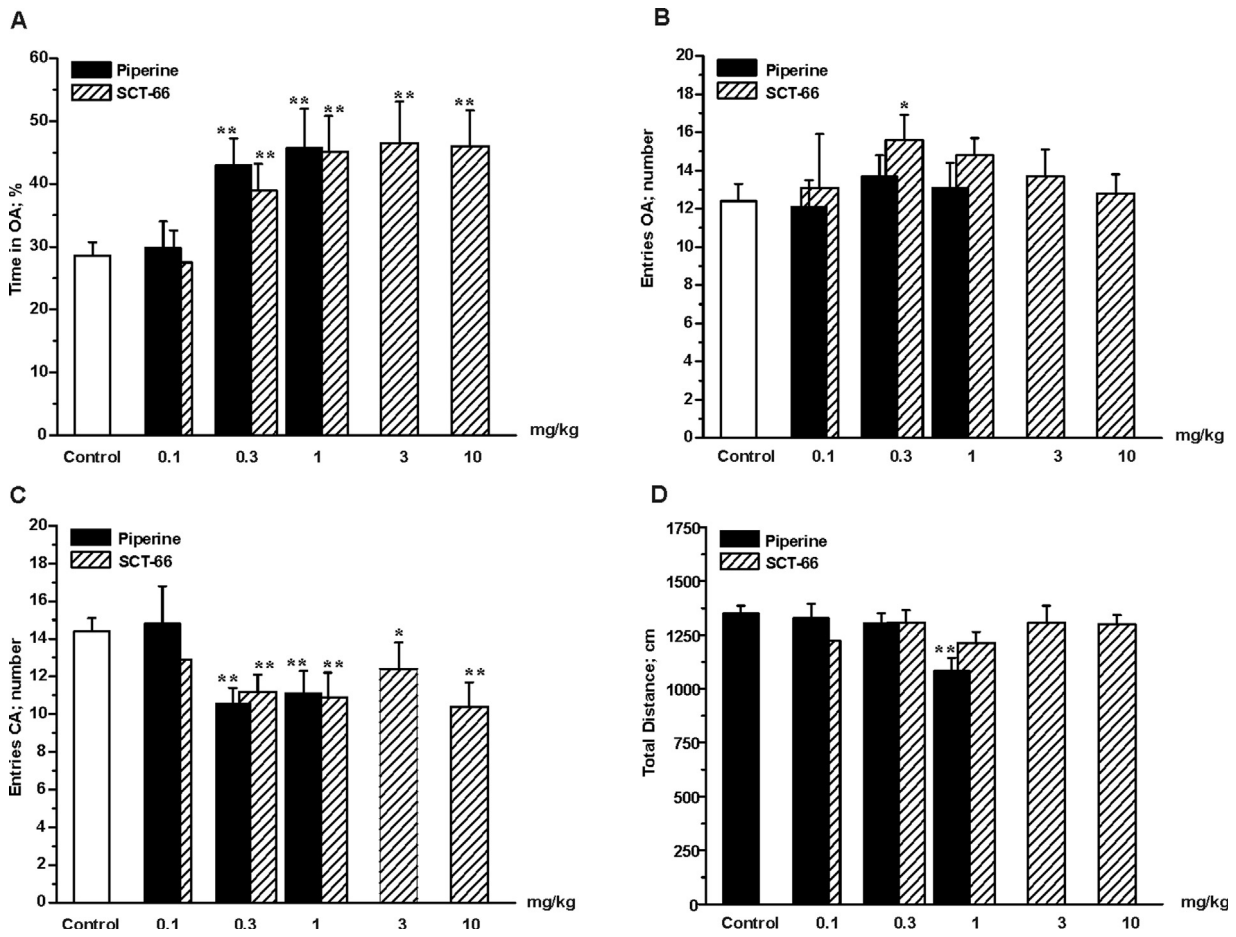

Fig. 6. Piperine and SCT-66 display anxiolytic-like effects in the EPM test. Bars indicate in (A) the time spent in the open arms (OA) in % of the total time, in (B) the number of OA entries, in (C) the number of closed arm (CA) entries and in (D) the total distance after application of the indicated dose in mg/kg bodyweight of either piperine (black bars) or SCT-66 (shaded bars), respectively. White bars illustrate the behaviour of control mice. Bars represent means ± S.E.M. from at least 9 different mice. (*) indicates statistically significant differences with $p < 0.05$, (**) $p < 0.01$ to control (ANOVA with Bonferroni).

site located on α and/or β subunits. This hypothesis is in line with our previous findings that $GABA_A$ receptor modulation by piperine is not blocked by flumazenil [3].

I_{GABA} enhancement by piperine was most efficacious for $GABA_A$ receptors with α_3 subunits, weakest for $GABA_A$ receptors incorporating α_5 subunits (Fig. 2A) and dependent on the β-subunit (Fig. 2B). While there was no significant difference in enhancement of I_{GABA} through $GABA_A$ receptors with either β_2 or β_3 subunits, incorporation of β_1 subunits reduced enhancement of I_{GABA} (see also Fig. 2B).

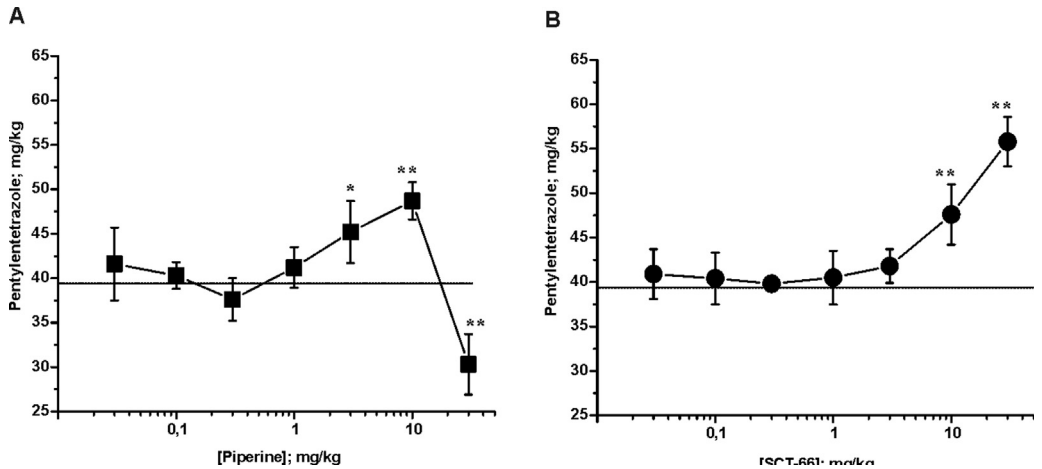

Fig. 7. Piperine and SCT-66 affect seizure threshold differently. Changes in seizure threshold upon PTZ-infusion of the indicated dose (mg/kg bodyweight) of piperine (A) and SCT-66 (B) are depicted. Each data point represents the mean ± S.E.M. of a least 3 mice. (*) indicates statistically significant differences with $p < 0.05$, (**) $p < 0.01$ to control (ANOVA with Bonferroni).

4.2. SCT-66 modulates $GABA_A$ receptors with higher potency and efficiency

A principle finding was that replacing the piperidine ring by a *N,N*-diisobutyl-residue did not only diminish interaction with TRPV1 receptors but additionally increased potency and efficacy of $GABA_A$ receptor modulation and affected subunit dependency (Figs. 2E, D and Table 1). Replacing the piperidine ring by a *N,N*-diisobutyl-residue not only diminished the $\beta_{2/3}$ subunit dependence (Fig. 2F), but also induced γ-subunit dependence. Hence, I_{GABA} stimulation in $\alpha_1\beta_2\gamma_{2S}$ receptors was about four times smaller than in $\alpha_1\beta_2$ receptors. These data suggest differences in the binding pockets of the two molecules and/or the existence of an additional binding site for SCT-66 involving the γ-subunit.

4.3. Consequences of different receptor specificity on anxiety, locomotor activity and seizure threshold

In order to analyse the consequences of the structural changes in the piperine scaffold we compared the in vivo action of piperine and SCT-66. However, before analyzing behavioural effects of piperine and SCT-66, the consequences of different TRPV1 activity were studied: since TRPV1 channels are involved in a variety of physiological processes including thermoregulation [38], measuring changes in body temperature is one way to detect their activation. In agreement with the literature, piperine at doses ≥ 10 mg/kg bodyweight drastically lowered body temperature of mice (compare to similar results in rats in [39]). In contrast, SCT-66 did not affect thermoregulation even at high doses (see Fig. 4). Our data derived on TRPV1 channels expressed on oocytes indicate that SCT-66, unlike piperine, does not interact with TRPV1 channels. While the in vivo effects of piperine are thus likely to include a TRPV1-related component, it seems that the in vivo effects of SCT-66 do not.

First insights into the behavioural effects of piperine and SCT-66 were obtained from the OF and the EPM test. Though both compounds reduced animals' locomotor activity, SCT-66 did so only at higher doses (see Fig. 5A). Considering the higher potency and efficiency of SCT-66 on $GABA_A$ receptors in vitro (Fig. 2D and E and Table 1) we speculate that the reduced locomotor activity induced by piperine at doses ≥10 mg/kg reflects interactions with vanilloid receptors. A plausible explanation would be that the alterations in pain sensation and thermoregulation result in depressed ambulation as discomfort and pain may well interfere with the exploratory drive. In contrast, reduced ambulation upon application of high doses of SCT-66 may indeed reflect sedation resulting from an enhancement of I_{GABA}. This is further supported by our finding of relatively subtype-independent, strong modulation of $GABA_A$ receptors by SCT-66 that did not differ between receptors containing α_1, α_2 or α_3 subunits, which is seen as a prerequisite for sedative actions of drugs [40,41].

As both tests depend on motor activity, potential anxiolytic effects of piperine could be observed only in one parameter of the EPM test, where mice treated with low doses of either piperine spent significantly more time in the open arms of the maze (see Fig. 6A). In contrast, clear anxiolytic effects were observed for SCT-66, which agrees with the stronger enhancement of I_{GABA} (see Fig. 2D and E) and the lack of TRPV1 activation observed in vitro.

Beside influences on emotional behaviour, positive allosteric modulators of $GABA_A$ receptors also influence the seizure threshold. Thus, enhancing GABAergic signalling was shown to significantly increase seizure threshold in mice. Importantly, the seizure threshold is independent of motor activity. Consistent with the data obtained from behavioural testing, the effects of piperine on the PTZ-induced seizure threshold suggest the involvement of more than just one receptor/target in vivo. Thus, piperine revealed a biphasic dose-response curve displaying increased thresholds at doses of 3–10 mg/kg bodyweight, which reverts to decreased thresholds at a dose of 30 mg/kg (Fig 7A). In contrast SCT-66 significantly increased the threshold at a dose of 10–30 mg/kg (Fig. 7B). Little information is available on the effects of TRPV1 activation on seizure threshold. The proposed effects of TRPV1 on epilepsy are controversial: while some groups suggest TRPV1 agonists as potential candidates for antiepileptics [42], others have shown increased glutamate release from hippocampal granule cells as a consequence of TRPV1 activation [43]. We can also not exclude the involvement of receptors other than $GABA_A$ and TRPV1. However, TRPV1 activation has been shown to cause vasodilation [44], and we observed vasodilatory effects during the PTZ tail-vein infusion experiments with piperine at doses of 10–30 mg/kg (data not shown), but not with SCT-66.

4.4. Conclusions and outlook

Replacing the piperidine ring by the *N,N*-diisobutyl residue of piperine diminished interaction with TRPV1 receptors, enhanced potency and efficacy of I_{GABA} modulation, diminished the higher efficacy of piperine on α_3-subunit and/or $\beta_{2/3}$-subunit containing receptors (compare Fig. 2A and B with Fig. 2D and E) and induced a γ_2 subunit dependence (Fig. 2 D). Piperine and SCT-66 induced anxiolytic-like, anticonvulsant action with SCT-66 and less depression of locomotor activity compared to piperine (Figs. 5–7). Its higher receptor specificity (lack of interaction with TRPV1) and higher potency and efficacy of I_{GABA} modulation and its in vivo action suggest that SCT-66 may represent a suitable scaffold for development of novel $GABA_A$ receptor modulators with anxiolytic and anticonvulsant potential. The addition of 2 extra methyl groups in SCT-66 significantly increased flexibility in the side chain and almost doubled the molecular volume of this part of the molecule. The generation of further piperine derivatives and studies on different $GABA_A$ receptor subtypes will help to clarify the structural basis of the receptor selectivity (TRPV1 vs. $GABA_A$) and changes in I_{GABA} modulation.

Conflict of interest

The authors declare no conflict of interests.

Acknowledgments

This work was supported by the Austrian Science Fund (FWF P21241, TRP10, P22395 and the doctoral programme "Molecular drug targets" W1232 to S.H.) and the Swiss National Science Foundation (Project 31600-113109 to M.H.)

References

[1] Szallasi A. Piperine: researchers discover new flavor in an ancient spice. Trends Pharmacol Sci 2005;26:437–9.
[2] McNamara FN, Randall A, Gunthorpe MJ. Effects of piperine, the pungent componentof black pepper, at the human vanilloid receptor (TRPV1). Br J Pharmacol 2005;144:781–90.
[3] Zaugg J, Baburin I, Strommer B, Kim HJ, Hering S, Hamburger M. HPLC based activity profiling: discovery of piperine as a positive GABA(A) receptor modulator targeting a benzodiazepine-independent binding site. J Nat Prod 2010;73:185–91.
[4] Di Marzo V, Gobbi G, Brain Szallasi A. TRPV1: a depressing TR(i)P down memory lane. Trends Pharmacol Sci 2008;29:594–600.
[5] Gunthorpe MJ, Chizh BA. Clinical development of TRPV1 antagonists: targeting a pivotal point in the pain pathway. Drug Discov Today 2009;14:56–67.
[6] Olsen RW, Sieghart W. International Union of Pharmacology. LXX. Subtypes of gamma-aminobutyric acid(A) receptors: classification on the basis of subunit composition, pharmacology, and function. Update. Pharmacol Rev 2008;60:243–60.
[7] Savic MM, Majumder S, Huang S, Edwankar RV, Furtmüller R, Joksimović S, et al. Novel positive allosteric modulators of GABAA receptors: do subtle

differences in activity at alpha1 plus alpha5 versus alpha2 plus alpha3 subunits account for dissimilarities in behavioral effects in rats. Prog Neuropsychopharmacol Biol Psychiatry 2010;34:376–86.
[8] Rudolph U, Knoflach F. Beyond classical benzodiazepines: novel therapeutic potential of GABAA receptor subtypes. Nat Rev Drug Discov 2011;10:685–97.
[9] Möhler H. The GABA system in anxiety and depression and its therapeutic potential. Neuropharmacology 2012;62:42–53.
[10] Trincavelli ML, Da Pozzo E, Daniele S, Martini C. The GABAA-BZR complex as target for the development of anxiolytic drugs. Curr Top Med Chem 2012;12:254–69.
[11] Knabl J, Witschi R, Hosl K, Reinold H, Zeilhofer UB, Ahmadi S, et al. Reversal of pathological pain through specific spinal GABAA receptor subtypes. Nature 2008;451:330–4.
[12] Lipinski CA, Lombardo F, Dominy BW, Feeney PJ. Experimental and computational approaches to estimate solubility and permeability in drug discovery and development settings. Adv Drug Deliv Rev 1997;23:3–25.
[13] Khom S, Baburin I, Timin EN, Hohaus A, Sieghart W, Hering S. Pharmacological properties of GABAA receptors containing gamma1 subunits. Mol Pharmacol 2006;69:640–9.
[14] Boileau AJ, Baur R, Sharkey LM, Sigel E, Czajkowski C. The relative amount of cRNA coding for gamma2 subunits affects stimulation by benzodiazepines in GABA(A) receptors expressed in Xenopus oocytes. Neuropharmacology 2002;43:695–700.
[15] Krishek BJ, Moss SJ, Smart TG. Homomeric beta 1 gamma-aminobutyric acid A receptor-ion channels: evaluation of pharmacological and physiological properties. Mol Pharmacol 1996;49:494–504.
[16] Methfessel C, Witzemann V, Takahashi T, Mishina M, Numa S, Sakmann B. Patch clamp measurements on *Xenopus laevis* oocytes: currents through endogenous channels and implanted acetylcholine receptor and sodium channels. Pflugers Arch 1986;407:577–88.
[17] Baburin I, Beyl S, Hering S. Automated fast perfusion of Xenopus oocytes for drug screening. Pflugers Arch 2006;453:117–23.
[18] Broadwell RD, Salcman M, Kaplan RS. Morphologic effect of dimethyl sulfoxide on the blood-brain barrier. Science 1982;217:164–6.
[19] Khom S, Strommer B, Ramharter J, Schwarz T, Schwarzer C, Erker T, et al. Valerenic acid derivatives as novel subunit-selective GABAA receptor ligands – in vitro and in vivo characterization. Br J Pharmacol 2010;161:65–78.
[20] Loacker S, Sayyah M, Wittmann W, Herzog H, Schwarzer C. Endogenous dynorphin in epileptogenesis and epilepsy: anticonvulsant net effectvia kappa opioid receptors. Brain 2007;130:1017–28.
[21] Rawls SM, Benamar K. Effects of opioids, cannabinoids, and vanilloids on body temperature. Front Biosci (Schol Ed) 2011;3:822–45.
[22] Hui KM, Huen MS, Wang HY, Zheng H, Sigel E, Baur R, et al. Anxiolytic effect of wogonin, a benzodiazepine receptor ligand isolated from *Scutellaria baicalensis* Georgi. Biochem Pharmacol 2002;64:1415–24.
[23] Huen MS, Hui KM, Leung JW, Sigel E, Baur R, Wong JT, et al. Naturally occurring 2′-hydroxyl-substituted flavonoids as high-affinity benzodiazepine site ligands. Biochem Pharmacol 2003;66:2397–407.
[24] Marder M, Viola H, Wasowski C, Fernandez S, Medina JH, Paladini AC. 6-methylapigenin and hesperidin: new valeriana flavonoids with activity on the CNS. Pharmacol Biochem Behav 2003;75:537–45.
[25] Yang X, Baburin I, Plitzko I, Hering S, Hamburger M. HPLC-based activity profiling for GABAA receptor modulators from the traditional Chinese herbal drug Kushen (Sophora flavescens root). Mol Divers 2011;15:361–72.
[26] Granger RE, Campbell EL, Johnston GA. (+)- And (−)-borneol: efficacious positive modulators of GABA action at human recombinant alpha1beta2gamma2L GABA(A) receptors. Biochem Pharmacol 2005;69:1101–11.
[27] Garcia DA, Bujons J, Vale C, Sunol C. Allosteric positive interaction of thymol with the GABAA receptor in primary cultures of mouse cortical neurons. Neuropharmacology 2006;50:25–35.
[28] Zaugg J, Ebrahimi SN, Smiesko M, Baburin I, Hering S, Hamburger M. Identification of GABA A receptor modulators in Kadsura longipedunculata and assignment of absolute configurations by quantum-chemical ECD calculations. Phytochemistry 2011;72:2385–95.
[29] Khom S, Baburin I, Timin E, Hohaus A, Trauner G, Kopp B, et al. Valerenic acid potentiates and inhibits GABA(A) receptors: molecular mechanism and subunit specificity. Neuropharmacology 2007;53:178–87.
[30] Benke D, Barberis A, Kopp S, Altmann KH, Schubiger M, Vogt KE, et al. GABA A receptors as in vivo substrate for the anxiolytic action of valerenic acid, a major constituent of valerian root extracts. Neuropharmacology 2009;56:174–81.
[31] Zaugg J, Eickmeier E, Ebrahimi SN, Baburin I, Hering S, Hamburger M. Positive GABA(A) receptor modulators from Acorus calamus and structural analysis of (+)-dioxosarcoguaiacol by 1D and 2D NMR and molecular modeling. J Nat Prod 2011;74:1437–43.
[32] Zaugg J, Khom S, Eigenmann D, Baburin I, Hamburger M, Hering S. Identification and characterization of GABA(A) receptor modulatory diterpenes from Biota orientalis that decrease locomotor activity in mice. J Nat Prod 2011;74:1764–72.
[33] Cicek SS, Khom S, Taferner B, Hering S, Stuppner H. Bioactivity-guided isolation of GABA(A) receptor modulating constituents from the rhizomes of Actaea racemosa. J Nat Prod 2010;73:2024–8.
[34] Baur R, Simmen U, Senn M, Sequin U, Sigel E. Novel plant substances acting as beta subunit isoform-selective positive allosteric modulators of GABAA receptors. Mol Pharmacol 2005;68:787–92.
[35] Taferner B, Schuehly W, Huefner A, Baburin I, Wiesner K, Ecker GF, et al. Modulation of GABAA-receptors by honokiol and derivatives: subtype selectivity and structure-activity relationship. J Med Chem 2011;54:5349–61.
[36] Zaugg J, Eickmeier E, Rueda DC, Hering S, Hamburger M. HPLC-based activity profiling of Angelica pubescens roots for new positive GABAA receptor modulators in Xenopus oocytes. Fitoterapia 2011;82:434–40.
[37] Singhuber J, Baburin I, Ecker GF, Kopp B, Hering S. Insights into structure-activity relationship of GABAA receptor modulating coumarins and furanocoumarins. Eur J Pharmacol 2011;668:57–64.
[38] Nieto-Posadas A, Jara-Oseguera A, Rosenbaum T. TRP channel gating physiology. Curr Top Med Chem 2011;11:2131–50.
[39] Jancso-Gabor A, Szolcsanyi J, Jancso N. Irreversible impairment of thermoregulation induced by capsaicin and similar pungent substances in rats and guinea-pigs. J Physiol 1970;206:495–507.
[40] Löw K, Crestani F, Keist R, Benke D, Brünig I, Benson JA, et al. Molecular and neuronal substrate for the selective attenuation of anxiety. Science 2000;290(5489):131–4.
[41] Dias R, Sheppard WF, Fradley RL, Garrett EM, Stanley JL, Tye SJ, et al. Evidence for a significant role of alpha 3-containing GABAA receptors in mediating the anxiolytic effects of benzodiazepines. J Neurosci 2005;25:10682–88.
[42] Fu M, Xie Z, Zuo H. TRPV1: a potential target for antiepileptogenesis. Med Hypotheses 2009;73:100–2.
[43] Bhaskaran MD, Smith BN. Effects of TRPV1 activation on synaptic excitation in the dentate gyrus of a mouse model of temporal lobe epilepsy. Exp Neurol 2010;223:529–36.
[44] Baylie RL, Brayden JE. TRPV channels and vascular function. Acta Physiol (Oxf) 2011;203:99–116.

4.3 Paper III
Efficient Modulation of γ-aminobutyric Acid Type A Receptors by Piperine Derivatives (Schöffmann et al., 2014)

Schöffmann, A., Wimmer, L., Goldmann, D., Khom, S., **Hintersteiner, J.**, Baburin, I., Schwarz, T., Hintersteininger, M., Pakfeifer, P., Oufir, M., Hamburger, M., Erker, T., Ecker, G.F., Mihovilovic, M.D., Hering, S., 2014. *Efficient modulation of γ-aminobutyric acid type A receptors by piperine derivatives.* J. Med. Chem. 57, 5602–5619. doi:10.1021/jm5002277

Contribution

- Sample collection and preparation for detection of two derivatives (compound 23, compound 25) in plasma samples
- Effects on explorative behavior by means of the EPM test (Assistance)

Results

Journal of Medicinal Chemistry

Article

pubs.acs.org/jmc

Efficient Modulation of γ-Aminobutyric Acid Type A Receptors by Piperine Derivatives

Angela Schöffmann,[†,⊥] Laurin Wimmer,[‡,⊥] Daria Goldmann,[§,⊥] Sophia Khom,[†] Juliane Hintersteiner,[†] Igor Baburin,[†] Thomas Schwarz,[§,▽] Michael Hintersteininger,[§] Peter Pakfeifer,[†] Mouhssin Oufir,[∥] Matthias Hamburger,[∥] Thomas Erker,[§] Gerhard F. Ecker,[§] Marko D. Mihovilovic,[‡] and Steffen Hering*[,†]

[†]Department of Pharmacology and Toxicology and [§]Division of Drug Design and Medicinal Chemistry, Department of Pharmaceutical Chemistry, University of Vienna, Althanstrasse 14, A-1090 Vienna, Austria

[‡]Institute of Applied Synthetic Chemistry, Vienna University of Technology, Getreidemarkt 9, A-1060 Vienna, Austria

[∥]Pharmaceutical Biology, Department of Pharmaceutical Sciences, University of Basel, Klingelbergstrasse 50, CH-4056 Basel, Switzerland

Supporting Information

ABSTRACT: Piperine activates TRPV1 (transient receptor potential vanilloid type 1 receptor) receptors and modulates γ-aminobutyric acid type A receptors ($GABA_AR$). We have synthesized a library of 76 piperine analogues and analyzed their effects on $GABA_AR$ by means of a two-microelectrode voltage-clamp technique. $GABA_AR$ were expressed in *Xenopus laevis* oocytes. Structure−activity relationships (SARs) were established to identify structural elements essential for efficiency and potency. Efficiency of piperine derivatives was significantly increased by exchanging the piperidine moiety with either *N*,*N*-dipropyl, *N*,*N*-diisopropyl, *N*,*N*-dibutyl, *p*-methylpiperidine, or *N*,*N*-bis(trifluoroethyl) groups. Potency was enhanced by replacing the piperidine moiety by *N*,*N*-dibutyl, *N*,*N*-diisobutyl, or *N*,*N*-bistrifluoroethyl groups. Linker modifications did not substantially enhance the effect on $GABA_AR$. Compound **23** [(2*E*,4*E*)-5-(1,3-benzodioxol-5-yl)-*N*,*N*-dipropyl-2,4-pentadienamide] induced the strongest modulation of $GABA_A$ (maximal GABA-induced chloride current modulation ($I_{GABA\text{-}max}$ = 1673% ± 146%, EC_{50} = 51.7 ± 9.5 μM), while **25** [(2*E*,4*E*)-5-(1,3-benzodioxol-5-yl)-*N*,*N*-dibutyl-2,4-pentadienamide] displayed the highest potency (EC_{50} = 13.8 ± 1.8 μM, $I_{GABA\text{-}max}$ = 760% ± 47%). Compound **23** induced significantly stronger anxiolysis in mice than piperine and thus may serve as a starting point for developing novel $GABA_AR$ modulators.

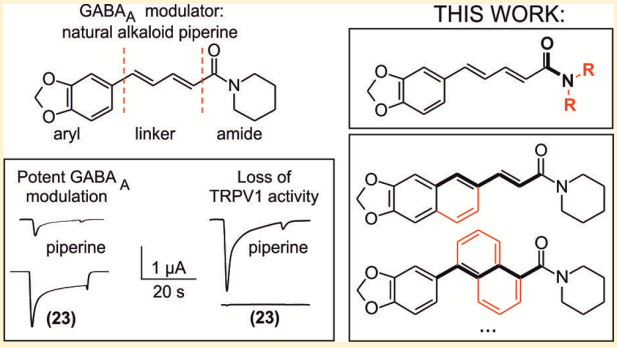

INTRODUCTION

γ-Aminobutyric acid type A ($GABA_A$) receptors are the major inhibitory neurotransmitter receptors in mammalian brain.[1−3] $GABA_A$ receptors belong to the superfamily of Cys loop ligand-gated ion channels. Five receptor subunits form a central chloride-conducting pore.[4−6] Nineteen genes encoding different subunits have been discovered in the human genome, comprising α_{1-6}, β_{1-3}, γ_{1-3}, δ, ε, θ, π, and ρ_{1-3}.[7,8] Different subunit combinations may theoretically form a vast number of receptor subtypes with different pharmacological properties (see ref 9 for review). There is consensus that the most abundantly occurring receptor subtype is formed of two α_1, two β_2, and one γ_2 subunits ($\alpha_1\beta_2\gamma_2$ receptor).[10−12]

Drugs that enhance chloride currents through $GABA_A$ receptors play an important role in the treatment of general anxiety, panic disorders, sleep disturbances, and epilepsy.[13−17] The most widely used benzodiazepines induce, however, a variety of side effects including dependence, unwanted sedation, and amnesia, complicating their long-term use.[18−20] Hence, there is high unmet medical need for $GABA_A$ receptor modulators lacking these unwanted effects.

Besides their modulation by clinically used drugs such as benzodiazepines, barbiturates, neurosteroids, and anesthetics,[3,9,15,21−27] $GABA_A$ receptors are modulated by numerous natural products that may provide lead structures for drug development.[28−30]

In this context, we[31] and others[32] have reported that piperine (1-piperoylpiperidine), the pungent component of several pepper species and activator of transient receptor potential vanilloid type 1 receptor (TRPV1),[33] also modulates $GABA_A$ receptors. We could establish that replacing the piperidine ring of piperine by a *N*,*N*-diisobutyl residue, resulting in (2*E*,4*E*)-5-(1,3-benzodioxol-5-yl))-*N*,*N*-diisobutyl-2,4-pentadienamide (SCT-66;[34] referred to as **24** in this work), diminishes the interaction with TRPV1 receptors. Furthermore, **24** enhanced

Received: February 15, 2014
Published: June 6, 2014

dx.doi.org/10.1021/jm5002277 | J. Med. Chem. 2014, 57, 5602−5619

chloride currents through $GABA_A$ receptors more potently and more efficiently than piperine and displayed, concordantly, a stronger anxiolytic action.[34]

Based on these findings, a library of piperine derivatives was synthesized and investigated with respect to modulation of $\alpha_1\beta_2\gamma_{2S}$ $GABA_A$ receptors expressed in *Xenopus laevis* oocytes. Within this study we emphasized modifications at the amide functionality and on the diene motif within piperine in order to enhance the modulatory potential of analogue structures. Their structure−activity relationship on $GABA_A$ receptors was analyzed by establishing binary classification models.

RESULTS AND DISCUSSION

Modification of Amide Nitrogen. Starting with piperine as lead structure from prior biological assessment, the molecule can be structurally divided into three parts: the 1,3-benzodioxole or aromatic function, the olefinic linker region comprising four carbon atoms, and the amide function natively constituted by a piperidine ring (Figure 1). Within this study, we investigated modifications at the amide group as well as in the linker region.

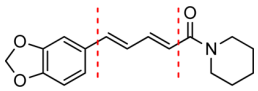

Figure 1. Piperine molecule can be structurally divided into three moieties: the 1,3-benzodioxole or aromatic function, the linker region comprising four carbon atoms, and the amide function natively constituted by a piperidine ring.

Modifications at the amide function were implemented in a straightforward fashion (Scheme 1). Piperic acid amides (**1**−**16**, **20**−**23**, and **25**−**43**) were synthesized by treating piperic acid chloride with the corresponding amine in the presence of triethylamine in tetrahydrofuran (THF). Compounds **17** and **18** were prepared in the same way from benzodioxolyl acryloyl chloride. Treatment of piperine with Lawesson's reagent[35] gave thioamide **44**. Reduction of the carbonyl group of piperine with lithium aluminum hydride afforded unsaturated amine **45** (Scheme 2).

First, we studied the effects of systematic modifications of the amide nitrogen on I_{GABA} modulation through $\alpha_1\beta_2\gamma_{2S}$ receptors. As illustrated in Figure 2A,B, 10 compounds (**22**, **23**, **25**, **28**, **33**, **34**, **35**, **38**, and **43**) at 100 μM induced stronger I_{GABA} modulation than piperine (≥220%)[31] and were classified as highly active. I_{GABA} potentiation of these compounds ranged between 294% ± 66% (**28**) and 1091% ± 257% (**23**, see Table 1). At this concentration, three derivatives (**17**, **30**, and **39**) were less efficient, while the other compounds did not significantly modulate I_{GABA} (see Figure 2A,B and Table 1).

Five derivatives of this first set (**22**, **23**, **25**, **35**, and **43**) with amide modifications enhanced I_{GABA} through $\alpha_1\beta_2\gamma_{2S}$ $GABA_A$ receptors with higher efficiency ($I_{GABA\text{-}max}$: **23** > **22** > **25** > **35**) and/or higher potency (EC_{50}: **25** < **43**) than piperine (Figure 2C,D and Table 2).

***N,N*-Dipropyl-Substituted Compounds 22 And 23 Display the Highest Efficiency.** Compounds **22** (*N*,*N*-dipropyl) and **23** (*N*,*N*-diisopropyl) modulated I_{GABA} most efficiently ($I_{GABA\text{-}max}$ for **22**, 1581% ± 74%; $I_{GABA\text{-}max}$ for **23**, 1673% ± 146%; $I_{GABA\text{-}max}$ for piperine, 302% ± 27%). Compounds **35** ($I_{GABA\text{-}max}$ 733% ± 60%) and **25** ($I_{GABA\text{-}max}$ 760% ± 47%) were less efficient, underscoring the important role of a noncyclic disubstituted amide motif (Figure 2C).

***N,N*-Dibutyl-Substituted Compound 25 Displays the Highest Potency.** Figure 2D illustrates I_{GABA} modulation by the most potent N-substituted piperine derivative (EC_{50} for **25**, 13.8 ± 1.8 μM < EC_{50} for **43**, 23.1 ± 3.3 μM < EC_{50} for piperine, 52.4 ± 9.4 μM[31]). Based on the modifications at the amide group, it can be concluded that installation of noncyclic substituents bearing 3−4 carbons each at the tertiary amide improves both efficacy and potency of the analogue compounds.

Rigidification of the Linker Region Has No Significant Effect on I_{GABA} Modulation. The influence of linker rigidity on I_{GABA} modulation was studied by means of a library comprising 32 linker derivatives. According to Zaugg et al.[31] and Pedersen et al.,[32] a carbon chain containing at least four carbons, a conjugated double bond adjacent to the amide group, and a bulky amine moiety seem to facilitate efficient receptor binding and/or I_{GABA} modulation.

Based on previous reports by Zaugg et al.,[31] we hypothesized that rigidification of the linker part of the structure may beneficially affect biological activity.[31] This assessment was based in particular on a decrease in modulatory capacity when partially saturated linkers were installed or when structural flexibility was increased by extending the linker length.

Three major structural modifications were envisaged (Scheme 1). (i) Replacement of the linker by an aryl ring (phenyl, heteroaryl, naphthyl): in this arrangement, both alkene groups of the diene system of the linker would be integrated into the rigid aromatic core. (ii) Integration of one linker double bond into a naphthyl ring: this compound class was expected to render more flexibility but still adopt a more rigidified system compared to the piperine diene structure; moreover, arrangement should allow for different angles of the aryl core relative to the amide anchoring group depending on the substitution site at the naphthyl system. (iii) "Ring closure" of the diene motif with the aryl part, consequently generating a carboxylate-substituted naphthyl lead structure: in this arrangement the double bond adopts a bent geometry, and again different angles of the aryl and amide parts can be obtained depending on the substitution site.

For the synthesis of aryl-bridged compounds, two different methods were utilized. For a number of products (**46**, **49**, **53**, and **58**−**64**) (Scheme 3), the corresponding bromo-substituted aromatic carboxylic acids were reacted with 3,4-(methylenedioxy)phenylboronic acid under Suzuki−Miyaura cross-coupling conditions.[36] The resulting bis(aryl)carboxylic acids were converted to the final amide products via the corresponding acid chloride intermediates. Alternatively, the corresponding bromobenzoic acid amides were prepared prior to the coupling step. Subsequent Suzuki−Miyaura coupling with 3,4-(methylenedioxy)phenylboronic acid afforded the final products **47**, **48**, **50**−**52**, and **54**−**57** (Scheme 3).

In order to access the 5-position of the naphtho[2,3-*d*]dioxole core, naphtho[2,3-*d*]dioxol-5-ol triflate was chosen as a precursor.[37] Heck coupling[38] employing methyl acrylate afforded **65a**, which gave acrylic acid **65b** after cleavage of the methyl ester (Scheme 4). Amide formation yielded the final products **65**−**67**.

Iridium-catalyzed direct borylation[39] of naphtho[2,3-*d*]-dioxole allowed direct access to the 6-position of the naphtho[2,3-*d*]dioxole core. Boronic acid ester **68a** obtained in this step was converted into the corresponding bromide[40]

Scheme 1. Structural Modifications of the Piperine Scaffold

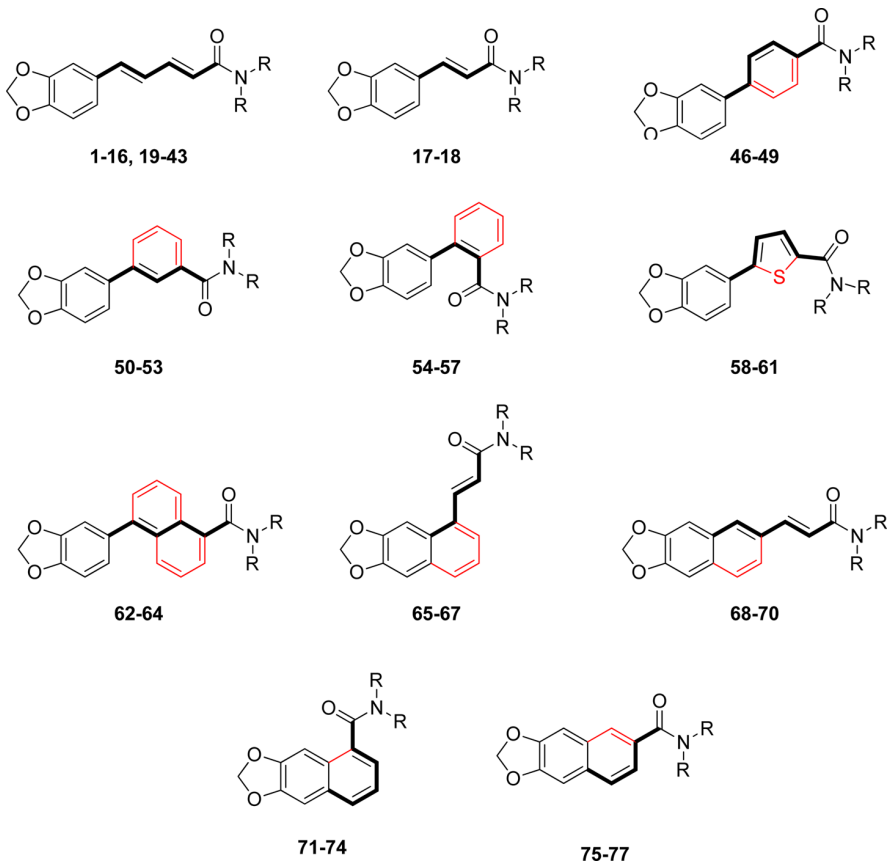

68b and coupled under standard Heck cross-coupling conditions to afford acrylate **68c** (Scheme 4). The methyl ester was hydrolyzed, and acid **68d** was converted into products **68**–**70** (Scheme 4).

Naphthodioxol-5-ol triflate was also used in a palladium-catalyzed hydroxycarbonylation reaction[41] to provide access to carboxylic acid **71a**, which was further converted to products **71**–**74** (Scheme 4). A different route was chosen to synthesize derivatives of naphtodioxole-6-carboxylic acid: By treating bis(bromomethyl)benzodioxole with iodide, a highly reactive diene was generated in situ,[42] which was intercepted with methyl acrylate in a Diels–Alder reaction. The resulting decaline derivative **75a** was oxidized with 2,3-dichloro-5,6-dicyano-1,4-benzoquinone (DDQ) to afford naphthaline **75b**. Saponification of the methyl ester gave carboxylic acid **75c**, which was further converted to final products **75**–**77** (Scheme 4).

At 100 μM, five compounds (**47**, **51**, **53**, **72**, and **73**) modulated I_{GABA} more efficiently than piperine (see Figure 3A,B and Table 2). I_{GABA} potentiation ranged from 280% ± 52% (**51**) to 514% ± 76% (**72**). I_{GABA} enhancement by **46**, **50**, **52**, **69**, **75**, **76**, and 77 was less pronounced compared to piperine [I_{GABA} potentiation range 42% ± 1% (**46**) to 178% ± 30% (**50**)]. None of the other derivatives induced significant I_{GABA} enhancement (see Figure 3A,B and Table 2).

Concentration–response curves of I_{GABA} modulation by linker-modified derivatives **47**, **53**, **56**, **72**, and **73** are illustrated in Figure 3C,D. The combination of *N*,*N*-dipropyl amide from the series **1**–**45** with the two most efficient modifications in the linker region (1,4-phenylene and naphthodioxol-5-yl) resulted in **47** ($I_{GABA\text{-}max}$ = 603% ± 87%, EC_{50} = 70.8 ± 21.1 μM), **72** ($I_{GABA\text{-}max}$ = 706% ± 58%, EC_{50} = 102.0 ± 11.2 μM), and **73** ($I_{GABA\text{-}max}$ = 480% ± 85%, EC_{50} = 31.8 ± 5.3 μM) inducing stronger I_{GABA} enhancement than piperine (Table 3). These findings underscore the general validity of favorable N,N-functionalization also for this series of linker-modified compounds. However, none of the modifications led to compounds with a higher activity than the initial parent compound **23**.

Selectivity Profile. Previously, we have shown that **24**[34] [(2*E*,4*E*)-5-(1,3-benzodioxol-5-yl)-*N*,*N*-diisobutyl-2,4-pentadienamide] similarly modulates $GABA_A$ receptors containing either $\beta_{2/3}$ or β_1 subunits, in contrast to the preferential modulation of $\beta_{2/3}$ receptors by piperine.[34]

In the present study, analysis of the most efficient piperine derivative (**23**) revealed that $GABA_A$ receptors composed of $\alpha_1\beta_2\gamma_{2S}$ ($I_{GABA\text{-}max}$ = 1673% ± 146%) and $\alpha_5\beta_2\gamma_{2S}$ ($I_{GABA\text{-}max}$ = 1624% ± 156%) subunits were more efficiently modulated than receptors containing $\alpha_3\beta_2\gamma_{2S}$ subunits ($I_{GABA\text{-}max}$ = 1284.6% ± 142%; see Table 4). Significantly weaker potentiation was observed for receptors composed of $\alpha_2\beta_2\gamma_{2S}$ ($I_{GABA\text{-}max}$ = 980% ± 129%) and $\alpha_4\beta_2\gamma_{2S}$ subunits ($I_{GABA\text{-}max}$ = 1316% ± 55%). Replacing the β_2 subunits by β_3 subunits did not significantly alter the strength of I_{GABA} potentiation, whereas modulation of $GABA_A$ receptors containing β_1 subunits was significantly less pronounced ($I_{GABA\text{-}max}$ = 1157% ± 69%; $p < 0.05$). In comparison with $\alpha_1\beta_2\gamma_{2S}$ receptors, **23** displayed an increased potency for $\alpha_2\beta_2\gamma_{2S}$ receptors, followed by $\alpha_1\beta_3\gamma_{2S}$, $\alpha_3\beta_2\gamma_{2S}$, and

dx.doi.org/10.1021/jm5002277 | J. Med. Chem. 2014, 57, 5602–5619

Journal of Medicinal Chemistry Article

Scheme 2. Synthesis of Piperine Derivatives with Modification of the Amide Function and Truncated Alkene Spacer[a]

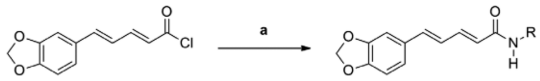

	R = H				
1	(4-methylthio)phenyl	7	2-(5-chloro)pyridyl	13	cyclopentyl
2	(3,4,5-trimethoxy)phenyl	8	(3-phenyl)propyl	14	benzyl
3	(2,4,6-trifluoro)phenyl	9	(2-hydroxy)phenyl	15	decyl
4	(2-dimethylamino)ethyl	10	(2-hydroxy-4-nitro)phenyl	16	adamantyl
5	(2-(3,4-dimethoxy)phenyl)ethyl	11	butyl		
6	3-pyridyl	12	(3,3-diphenyl)propyl		

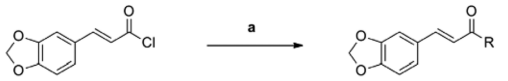

	R =		
17	piperidinyl	18	-N*i*Pr$_2$

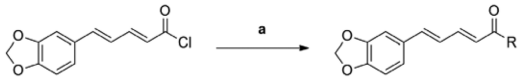

	R =				
19	piperidinyl	30	thiomorpholinyl		
20	-NMe$_2$	31	(4-Me)piperazinyl	40	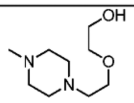
21	-NEt$_2$	32	(4-Et)piperazinyl		
22	-N*i*Pr$_2$	33	(2-Me)piperidinyl		
23	-NPr$_2$	34	(3-Me)piperidinyl	41	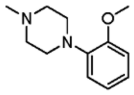
24	-N*i*Bu$_2$	35	(4-Me)piperidinyl		
25	-N*n*Bu$_2$	36	(3-OH)piperidinyl		
26	-N(*n*-hexyl)$_2$	37	(4-OH)piperidinyl		
27	-N(cyclohexyl)$_2$	38	(*cis*-2,6-dimethyl)piperidinyl	42	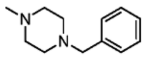
28	-N(CH$_2$)$_6$				
29	morpholinyl	39	(3-CF$_3$)piperidinyl	43	-N(CH$_2$CF$_3$)$_2$

	X =		
44	S	45	H

[a]Conditions: (a) Amine (3.5 equiv), dry THF, rt. (b) Lawesson's reagent, dry THF, rt. (c) LiAlH$_4$, THF, rt.

$\alpha_4\beta_2\gamma_{2S}$ receptors. EC$_{50}$ values for the other receptor subtypes did not differ from those for $\alpha_1\beta_2\gamma_{2S}$ (see Figure 4A,B and Tables 4 and 5).

Like **23**, derivative **25** most efficiently enhanced I_{GABA} through GABA$_A$ receptors composed of $\alpha_1\beta_2\gamma_{2S}$ subunits ($I_{GABA\text{-}max}$ = 760% ± 47%; see Table 4 and Figure 4C,D). Replacing the α_1 subunit by $\alpha_{2/3/4/5}$ subunits significantly reduced I_{GABA} potentiation by **25** (see Table 4 and Figure 4C). Notably, **25** displayed a more pronounced $\beta_{2/3}$ preference compared to piperine or **23** [inducing a 3.9-fold ($\alpha_1\beta_3\gamma_{2S}$) to 5-fold ($\alpha_1\beta_2\gamma_{2S}$) stronger I_{GABA} enhancement compared to $\alpha_1\beta_1\gamma_{2S}$ receptors]. Compound **25** showed comparable potency for most of the tested receptor subtypes ranging from 13.8 ± 1.8 μM to 56.7 ± 21.0 μM; significantly higher EC$_{50}$ values were estimated for $\alpha_1\beta_3\gamma_{2S}$ receptors (see Tables 4 and 6).

These data support the previous observation that when the cyclic piperidine residue is replaced by *N*,*N*-dialkyl moieties such as *N*,*N*-dipropyl (**23**), *N*,*N*-diisopropyl (**24**),[34] or *N*,*N*-dibutyl (**25**), efficiency and potency can be significantly enhanced. However, while **24**[34] lost its ability to distinguish between the β-subunit isoforms, preferential modulation of $\beta_{2/3}$ receptors by **23** was comparable to piperine, and it was even more pronounced for **25** (see Figure 4 B,D and Tables 4−6). Thus, **23** and **25** display—compared to classical GABA$_A$ receptor modulators such as benzodiazepines—a distinct subunit selectivity profile. Unlike benzodiazepines, **23** and **25** also modulate GABA$_A$ receptors containing α_4 subunits with high efficiency and are not dependent on the presence of a γ_{2S} subunit (data not shown). Whether this subunit selectivity profile has any pharmacological relevance has to be clarified in further studies.

dx.doi.org/10.1021/jm5002277 | J. Med. Chem. 2014, 57, 5602−5619

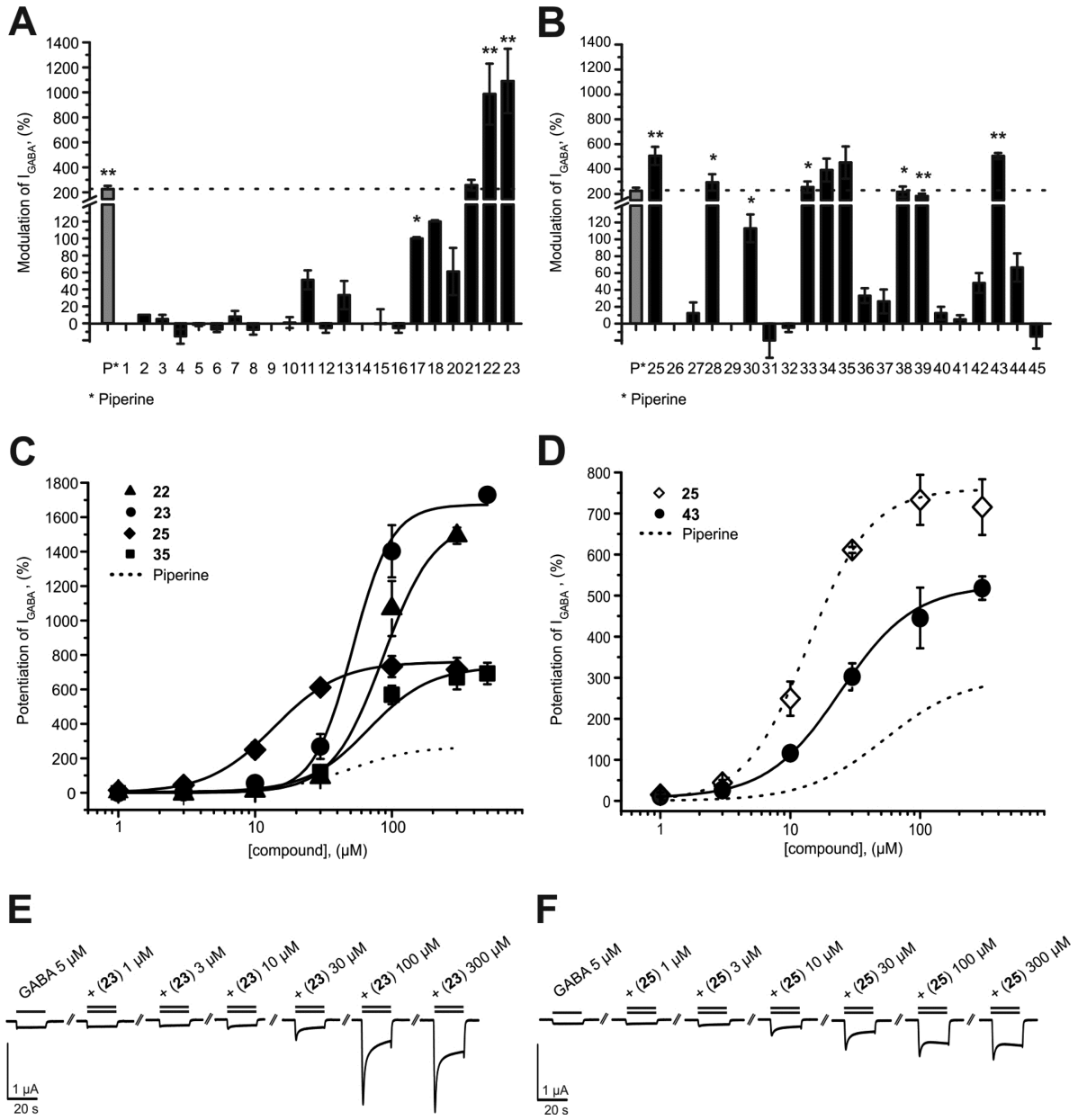

Figure 2. (A, B) Modulation of chloride currents through $GABA_A$ receptors composed of α_1, β_2, and γ_{2S} subunits by 100 μM piperine and the indicated derivatives (dotted line indicates cutoff for highly active compounds). (C, D) Concentration-dependent I_{GABA} (EC_{3-7}) enhancement through $\alpha_1\beta_2\gamma_{2S}$ $GABA_A$ receptors, (C) for **22** (▲), **23** (●), **25** (◆), and **35** (■), ranked by efficiency, and (D) for **25** (○) and **43** (●), ranked by potency, compared to piperine (dotted line). (E, F) Representative I_{GABA} modulated by (E) **23** and (F) **25**. Data represent mean ± SEM from at least three oocytes and two oocyte batches. Asterisks indicate statistically significant differences from zero: $*p < 0.05$, $**p < 0.01$. Data for piperine were taken from ref 31.

Structure–Activity Relationships: General Trends. When the whole data set was analyzed, several distinct SARs could be deduced. They are mostly related to the substitution pattern at the amide nitrogen atom, as this was the main point of variation in the data set. Thus, concerning *N*,*N*-dialkyl-substituted amides, there is evidence that I_{GABA} enhancement is related in a nonlinear (parabolic) function to the number of carbon atoms (Figure 5), with the optimum being dipropyl (**23**). This type of parabolic relationship is quite common, especially when it refers to a parameter that is linked to lipophilicity of the compounds and activity data obtained in a cellular assay. It has, for example, also been observed for a series of capsaicin analogues with respect to their TRPV1 activation.[43] Interestingly, whether the alkyl chains are linear or branched does not reverse the order: **20** (dimethyl) < **21** (diethyl) < **23** (dipropyl)/**22** (diisopropyl) < **25** (dibutyl)/**24**[34] (diisobutyl) < **26** (dihexyl)/**27** (dicyclohexyl). With respect to compounds where the amide nitrogen atom is part of a ring, methylpiperines **33**, **34**, and **35** induced the strongest I_{GABA} potentiation, followed by azepane amide **28** and piperine. Interestingly, the dimethylpiperine **38** was comparably active to the parent compound. Introduction of a second heteroatom

dx.doi.org/10.1021/jm5002277 | J. Med. Chem. 2014, 57, 5602–5619

Table 1. I_{GABA} Modulation through $\alpha_1\beta_2\gamma_{2S}$ $GABA_A$ Receptors by Indicated Compounds (100 μM)[a]

compd	modulation of I_{GABA} (%)	n	compd	modulation of I_{GABA} (%)	n
1	0 ± 0	3	**25**	506 ± 74**	3
2	10 ± 0	3	**26**	0 ± 0	3
3	5 ± 5	3	**27**	13 ± 13	3
4	−15 ± 9	3	**28**	294 ± 66*	3
5	−2 ± 2	3	**29**	0 ± 0	3
6	−7 ± 3	3	**30**	113 ± 17*	3
7	8 ± 7	3	**31**	−20 ± 20	3
8	−8 ± 6	3	**32**	−5 ± 5	3
9	0 ± 0	3	**33**	359 ± 50*	3
10	1 ± 7	3	**34**	439 ± 31*	3
11	51 ± 11	3	**35**	568 ± 54	3
12	−6 ± 6	3	**36**	33 ± 9	3
13	33 ± 17	3	**37**	26 ± 14	3
14	0 ± 0	3	**38**	218 ± 43*	3
15	−1 ± 17	3	**39**	183 ± 20**	3
16	−6 ± 6	3	**40**	12 ± 8	3
17	79 ± 8*	3	**41**	5 ± 5	3
18	66 ± 30	3	**42**	48 ± 12	3
20	61 ± 28	3	**43**	445 ± 74**	3
21	258 ± 28	3	**44**	17 ± 17	3
22	986 ± 244*	3	**45**	−16 ± 14	3
23	1091 ± 257*	3			

[a]All data are given as mean ± SEM. Asterisks indicate statistically significant differences from zero: *p < 0.05, **p < 0.01.

Table 2. I_{GABA} Modulation through $\alpha_1\beta_2\gamma_{2S}$ $GABA_A$ Receptors by Indicated Compounds (100 μM)[a]

compd	modulation of I_{GABA} (%)	n	compd	modulation of I_{GABA} (%)	n
46	42 ± 1**	3	**62**	13 ± 2	3
47	364 ± 55**	3	**63**	12 ± 4	3
48	49 ± 7	3	**64**	4 ± 4	3
49	30 ± 15	3	**65**	105 ± 18	3
50	178 ± 32*	3	**66**	67 ± 23	3
51	280 ± 52**	3	**67**	18 ± 9	3
52	63 ± 12*	3	**68**	−1 ± 12	3
53	298 ± 31**	3	**69**	74 ± 1*	3
54	34 ± 8	3	**70**	32 ± 12	3
55	79 ± 24	3	**71**	32 ± 10	3
56	114 ± 11	3	**72**	334 ± 23**	3
57	15 ± 15	3	**73**	514 ± 76**	3
58	−5 ± 12	3	**74**	60 ± 17	2
59	134 ± 39	3	**75**	58 ± 29*	3
60	51 ± 21	3	**76**	122 ± 26*	3
61	11 ± 2	3	**77**	138 ± 29*	3

[a]All data are given as mean ± SEM. Asterisks indicate significant differences from zero: *p < 0.05, **p < 0.01.

into the ring led to almost complete loss of I_{GABA} enhancement (*N*-alkylpiperazine amides **31**, **32**, **40**, **41**, and **42** and morpholine amide **29**).

Replacement of the tertiary nitrogen atom for a secondary one, irrespective of alkyl or aryl substitution, led to a complete loss of activity (aryl-substituted N, **1**−**3**, **5**−**7**, **9**, and **10**; alkyl-substituted N, **4**, **8**, and **11**−**16**). Reducing the H-bond acceptor strength of the amide by synthesizing the respective thioamide (**44**) abolished the modulatory activity. Reduction of the amide to the analogous amine changed the profile of the compound from potentiation (piperine at 100 μM, 226% ± 26%)[31] to inactive (**45** at 100 μM, −16% ± 14%; Table 1).

With respect to the linker region, shortening the distance by removing one vinylene unit significantly reduced I_{GABA} enhancement (piperine vs **17** and **22** vs **18**). All the other modifications, such as rigidification by inserting benzene, thiophene, or naphthalene moieties, reduced I_{GABA} potentiation by at least a factor of 5 compared to **23**. Interestingly, the modulatory activity did not seem to be related to distance of pharmacophoric substructures, such as the benzodioxole and the amide moiety. For naphthalene analogues **72** and **65**, an increase in distance led to a decrease of activity, whereas in the case of **22** and **18**, a decrease of distance led to a decrease of activity. Comparing **23** and **70**, which show identical distance of these two moieties, **70** completely lacks activity (32% ± 12%, Table 1). In conclusion, the best compounds achieved in terms of efficiency were the piperine analogues **22** and **23**.

Computational Analysis. In order to rationalize the trends observed in the SAR with respect to physicochemical properties and chemical substructures, we explored the possibility to apply quantitative structure−activity relationship (QSAR) methods. As I_{GABA} potentiation does not allow classical QSAR analysis, binary classification models were built from five methods and three descriptor sets. For these studies, all 76 piperine derivatives described above were employed. Sixteen compounds showing ≥200% I_{GABA} potentiation were assigned to an active class, since they were at least as active as the lead compound piperine. The remaining 60 ligands were assigned to an inactive class. Classification methods comprised instance-based classifier (IBk), J48 decision tree (J48), naïve-Bayes classifier (NB), random forest (RF), and support vector machine (SMO) implemented in the software package WEKA.[44] The software package Molecular Operating Environment (MOE) was used for calculation of 2D descriptors and fingerprints. The three descriptor sets used comprised six 2D descriptors obtained after applying a feature selection algorithm on the whole panel of 125 2D MOE descriptors (6D), 11 physical chemical properties (PHYSCHEM), and MACCS fingerprints (MACCS).

The statistical parameters obtained for the 15 best classification models are listed in Table 7. Most of the models possess reliable quality (except models 11 and 13); that is, values of the Matthews correlation coefficient (MCC) are higher than 0.4 and total accuracy varies from 0.7 to 0.9.

Models 3 and 4, although possessing the best statistical performance parameters, are not discussed further, as they are difficult to interpret. Instead, models 7 and 12 are discussed in more detail, because these models (i) show almost equal performance, (ii) were built using descriptors of physical chemical properties and MACCS fingerprints, (iii) provide clear separation between active and inactive instances, and (iv) allow us to trace back the decisive chemical and structural descriptors for the data set.

The decision tree obtained in model 7 with PHYSCHEM descriptors (Figure 6) uses as a first criterion for separation of active and inactive piperine derivatives: the topological polar surface area. By applying a threshold of 39, 25 inactive ligands exhibiting polar substituents at the amide nitrogen were filtered out. These include compounds **1**−**16** with monosubstituted amide function and compounds **29**, **31**, **32**, **36**, **37**, **40**−**42**, and **44** containing several heteroatoms (e.g., OH groups or an additional nitrogen as in piperazines or both). Thus, application of a single filter decreased the number of inactive ligands in the

dx.doi.org/10.1021/jm5002277 | J. Med. Chem. 2014, 57, 5602−5619

Scheme 3. Synthesis of Piperine Analogues Containing an Aryl Spacer[a]

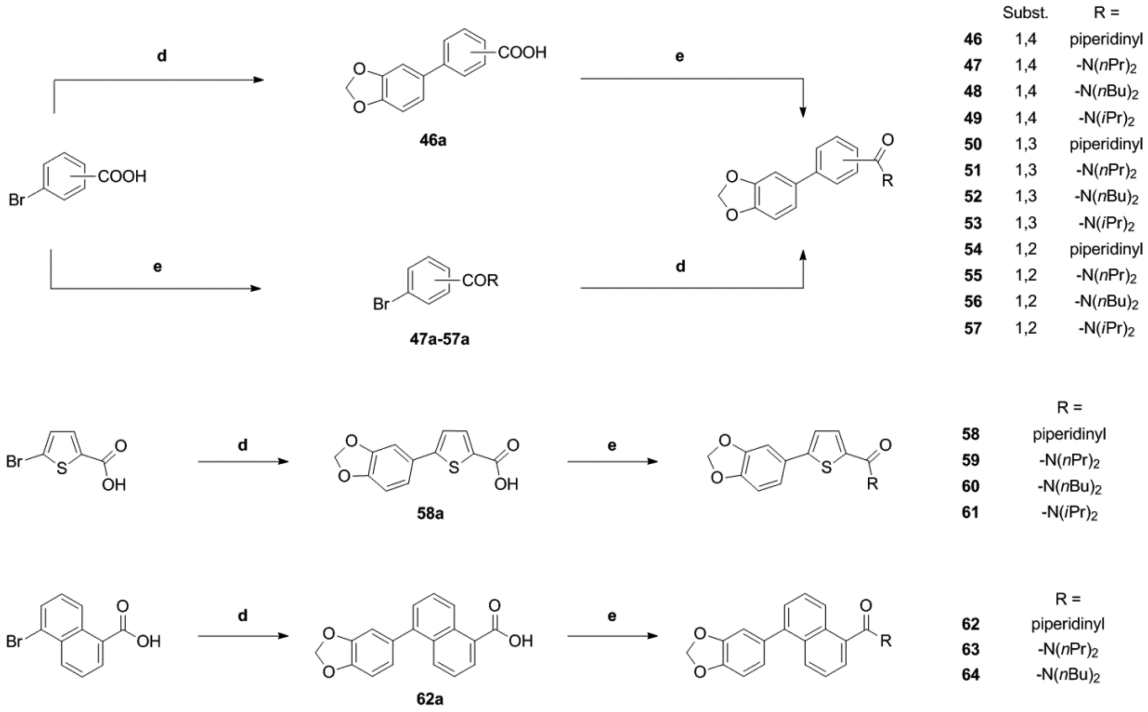

	Subst.	R =
46	1,4	piperidinyl
47	1,4	-N(*n*Pr)$_2$
48	1,4	-N(*n*Bu)$_2$
49	1,4	-N(*i*Pr)$_2$
50	1,3	piperidinyl
51	1,3	-N(*n*Pr)$_2$
52	1,3	-N(*n*Bu)$_2$
53	1,3	-N(*i*Pr)$_2$
54	1,2	piperidinyl
55	1,2	-N(*n*Pr)$_2$
56	1,2	-N(*n*Bu)$_2$
57	1,2	-N(*i*Pr)$_2$

	R =
58	piperidinyl
59	-N(*n*Pr)$_2$
60	-N(*n*Bu)$_2$
61	-N(*i*Pr)$_2$

	R =
62	piperidinyl
63	-N(*n*Pr)$_2$
64	-N(*n*Bu)$_2$

[a]Conditions: (d) Boronic acid, $Pd(PPh_3)_4$ 2 mol %, K_2CO_3, DME/EtOH/water, 140 °C, mw, 1 h. (e) Either $(COCl)_2$, cat. DMF, and DCM or EDCI·HCl, HOBt, and dry DCM, followed by amine.

data set almost by half, from 60 to 35 compounds. In the next branch of the decision tree, 10 compounds with less than four rotatable bonds were excluded from the data set. These included highly rigid piperine derivatives with linker regions modified to either a single double bond (**17**) or to an aromatic system (**46**, **50**, **54**, **58**, **62**, **65**, **68**, **71**, and **75**). Furthermore, 11 compounds with high lipophilicity (log P > 5.2) were filtered out: **26** and **27** with *n*-hexyl and cyclohexyl sustituents at the amide nitrogen, as well as **48**, **52**, **56**, **60**, **64**, **67**, **70**, **77**, and **63**, which have dibutyl and dipropyl substituents in the same region. The fact that the top-ranked compounds are either *N*,*N*-dipropyl-, *N*,*N*-dibutyl-, or *N*,*N*-diisobutyl-substituted is reflected in the next leaf, which assigns five compounds (**23**, **24**,[34] **25**, **43**, and **73**) with more than seven rotatable bonds to the active class. The last two branches of the decision tree filter out compounds on the basis of their molecular weight and refractivity.

The decision tree obtained for model 12 with MACCS fingerprints (Figure 7) is fully in line with the one based on the PHYSCHEM descriptor set. The first filtering criterion was presence or absence of an NH group. It filtered 21 derivatives (**1**−**16**, **31**, **32**, **40**, **42**, and **45**), most of which were those showing high polar surface area (TPSA). The next branching filter was presence of a sulfur atom, which removes six inactive ligands (**30**, **44**, and **58**−**61**) from the data set. The next leaf separates compounds that do not have a six-membered ring as in piperidinyl, cyclohexyl, and morpholinyl, which led to seven correctly classified active ligands (**21**−**23**, **24**,[34] **25**, **28**, and **43**) and three missclassified inactives (**18**, **20**, and **26**). This criterion is in line with the filter "b_rotN > 7" for active compounds in the PHYSCHEM model.

To summarize, active piperine analogues are mainly characterized by a topological polar surface smaller than 39, have at least three rotatable bonds (better more than 7), and show a log P value smaller than 5.2.

Compounds 25 and 23 Induce Anxiolysis in Mice. Activation of TRPV1 by piperine and its derivatives may cause unwanted side effects, including changes in pain sensation and body temperature and induction of fear that would interfere with $GABA_A$-mediated effects[45,46] (for review see ref 47). In order to rule out potential activation of TRPV1, selected compounds were studied in *X. laevis* oocytes for interaction with TRPV1 prior to in vivo characterization. The most potent (**25**) and most efficient (**23**) piperine analogues (Table 3, Figure 2C,D) did not activate TRPV1 expressed in *Xenopus* oocytes (upon application of 100 μM, data not shown). Both compounds were further characterized concerning their anxiolytic activity (see also ref 34).

As illustrated in Figure 8A, male C57BL/6N mice treated with **23** at doses ≥0.3 mg/kg body weight spent significantly more time in the open arms (OA) of the elevated plus maze (EPM) test compared to a saline-treated control group (control, 28.7% ± 2.7% for n = 41; **23** at 0.3 mg/kg, 45.6% ± 3.2% for n = 17; p < 0.01). This effect was dose-dependent and reached its maximum at a dose of 3 mg/kg body weight, indicating strong anxiolytic effects of **23**. Similarly, mice treated with **25** also spent significantly more time in the OA of the EPM test at doses ≥0.3 mg/kg body weight compared to saline-treated control littermates (control, 28.7% ± 2.7% for n = 41; **25** at 0.3 mg/kg, 39.8% ± 4.1% for n = 23; p < 0.05; Figure 8B). The anxiolytic effect of **25** reaching its maximum at a dose of 3 mg/kg body weight (**25** at 3 mg/kg, 43.9% ± 4.3% for n = 12), however, was less pronounced compared to **23**.

Application of doses ≥10 mg/kg of **23** or **25** did not further increase the anxiolytic effect in the EPM, which is presumably due to the concomitant occurring/developing of reduced

dx.doi.org/10.1021/jm5002277 | J. Med. Chem. 2014, 57, 5602−5619

Journal of Medicinal Chemistry Article

Scheme 4. Synthesis of Piperine Analogues with (Partial) Integration of the Spacer Motif into an Aryl Core[a]

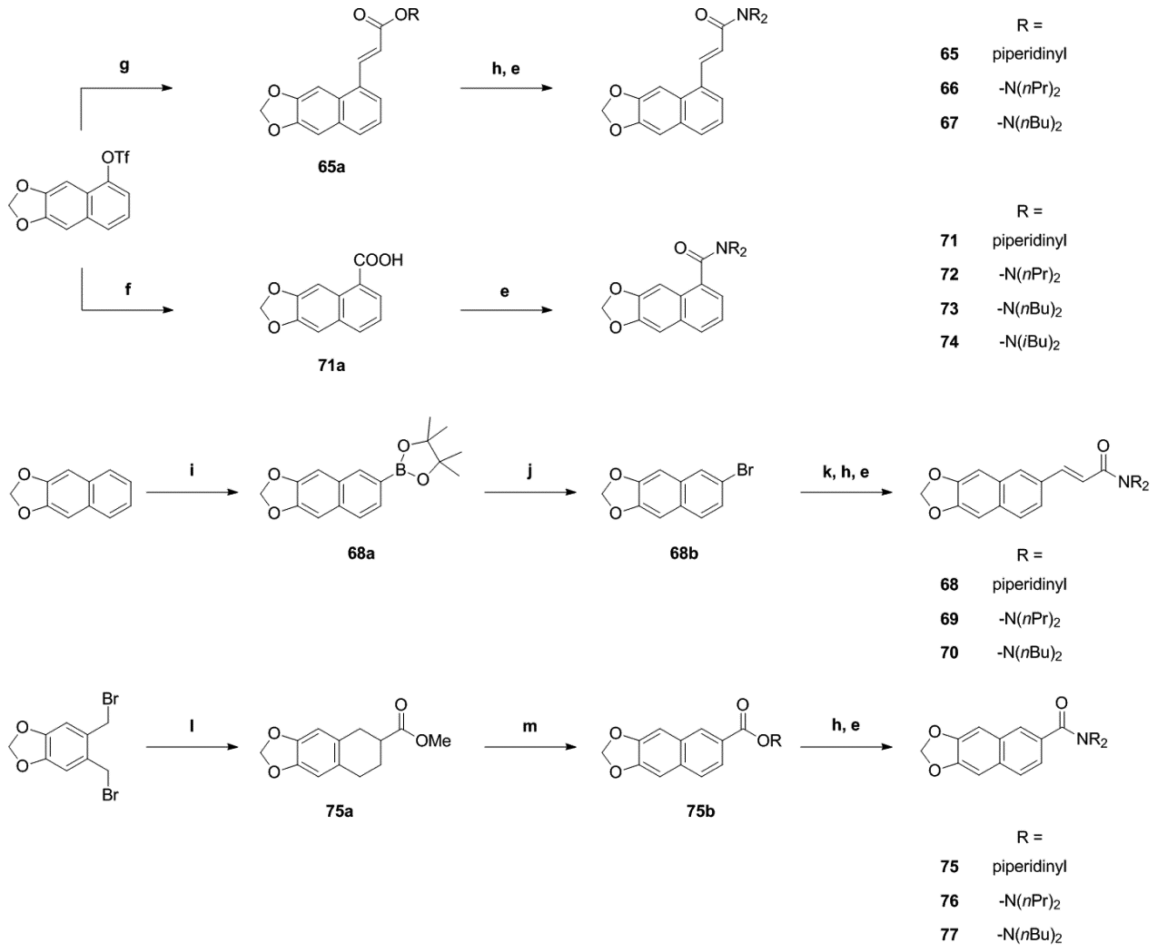

[a]Conditions: (e) Either $(COCl)_2$, cat. DMF, and DCM or EDCI·HCl, HOBt, and dry DCM, followed by amine. (f) CO, $Pd(OAc)_2$, dppp, Hünig's base, DMF/water, 70 °C. (g) Methyl acrylate, $Pd(OAc)_2$ 5 mol %, phenanthroline monohydrate 5.5 mol %, NEt_3, dry DMF. (h) LiOH, THF/water, rt. (i) B_2pin_2, $[Ir(OMe)cod]_2$ 1.5 mol %, 4,4′-di-*tert*-butyl-2,2′-bipyridine 3 mol %, cyclohexane, reflux. (j) $CuBr_2$, MeOH/water. (k) Methyl acrylate, $Pd(OAc)_2$ 3 mol %, (*o*-tolyl)$_3$P 6 mol %, NEt_3, 80 °C. (l) Methyl acrylate, NaI, dry DMF, 90°C. (m) DDQ, benzene, 80 °C.

locomotor activity (see Figure 8C,D for sedative effects in the open field test). Compared to piperine and the previously studied **24**[34] (Figure 8A, shaded bars taken from ref 34), anxiolysis induced by **23** was significantly ($p < 0.05$) more enhanced, which might reflect the stronger I_{GABA} potentiation by **23** and/or the higher potency of **23** on receptors containing $\alpha_{2/3}$ and β_3 subunits. Interestingly, the anxiolytic effect of the most potent and also more efficient derivative **25** did not differ from that of piperine and **24**.[34] It has, thus, to be clarified in further studies to what extent derivatization of the amide moiety affects the anxiolytic properties of piperine derivatives and whether receptors/channels other than $GABA_A$ receptors are targeted in vivo by these compounds.

Significant amounts of **23** and **25** were detected in mouse plasma after intraperitoneal (ip) application (see Table 8). The estimated plasma concentrations were below the micromolar concentrations required for significant I_{GABA} potentiation of $GABA_A$ receptors expressed in *Xenopus* oocytes. However, drugs are commonly less potent on ion channels expressed in *Xenopus* oocytes as compared to channels expressed in either mammalian cells or even native tissues.[48] The metabolite formation of **23** and **25** is currently unknown. At the current stage of our research, we cannot exclude that the observed anxiolytic and sedative effects are induced by more active metabolites. Furthermore, the currently unknown brain-barrier penetration of **23** and **25** and possible tissue accumulation warrants further research.

CONCLUSIONS

Piperine analogues modulating $GABA_A$ receptor with the highest efficiency show a tertiary amide nitrogen, substituted with flexible alkyl chains with a total of 6−8 carbon atoms. Polar substituents as well as rigid substituents give rise to a decrease of activity. Modifications of the linker region that lead to rigidification of the molecules also did not improve efficacy.

Compound **23** [(2*E*,4*E*)-5-(1,3-benzodioxol-5-yl))-*N*,*N*-dipropyl-2,4-pentadienamide] induced the strongest modulation of $GABA_A$ receptors (maximal GABA-induced chloride current enhancement $I_{GABA\text{-}max}$ = 1673.0% ± 146.3% and EC_{50} = 51.7 ± 9.5 μM, vs piperine, $I_{GABA\text{-}max}$ = 302% ± 27% and EC_{50} = 52.4 ± 9.4 μM), while **25** [(2*E*,4*E*)-5-(1,3-benzodioxol-5-yl))-*N*,*N*-dibutyl-2,4-pentadienamide] displayed the highest potency (EC_{50} = 13.8 ± 1.8 μM) but was less efficient than **23** ($I_{GABA\text{-}max}$ = 760% ± 47%). Both piperine analogues did not

dx.doi.org/10.1021/jm5002277 | J. Med. Chem. 2014, 57, 5602−5619

Journal of Medicinal Chemistry Article

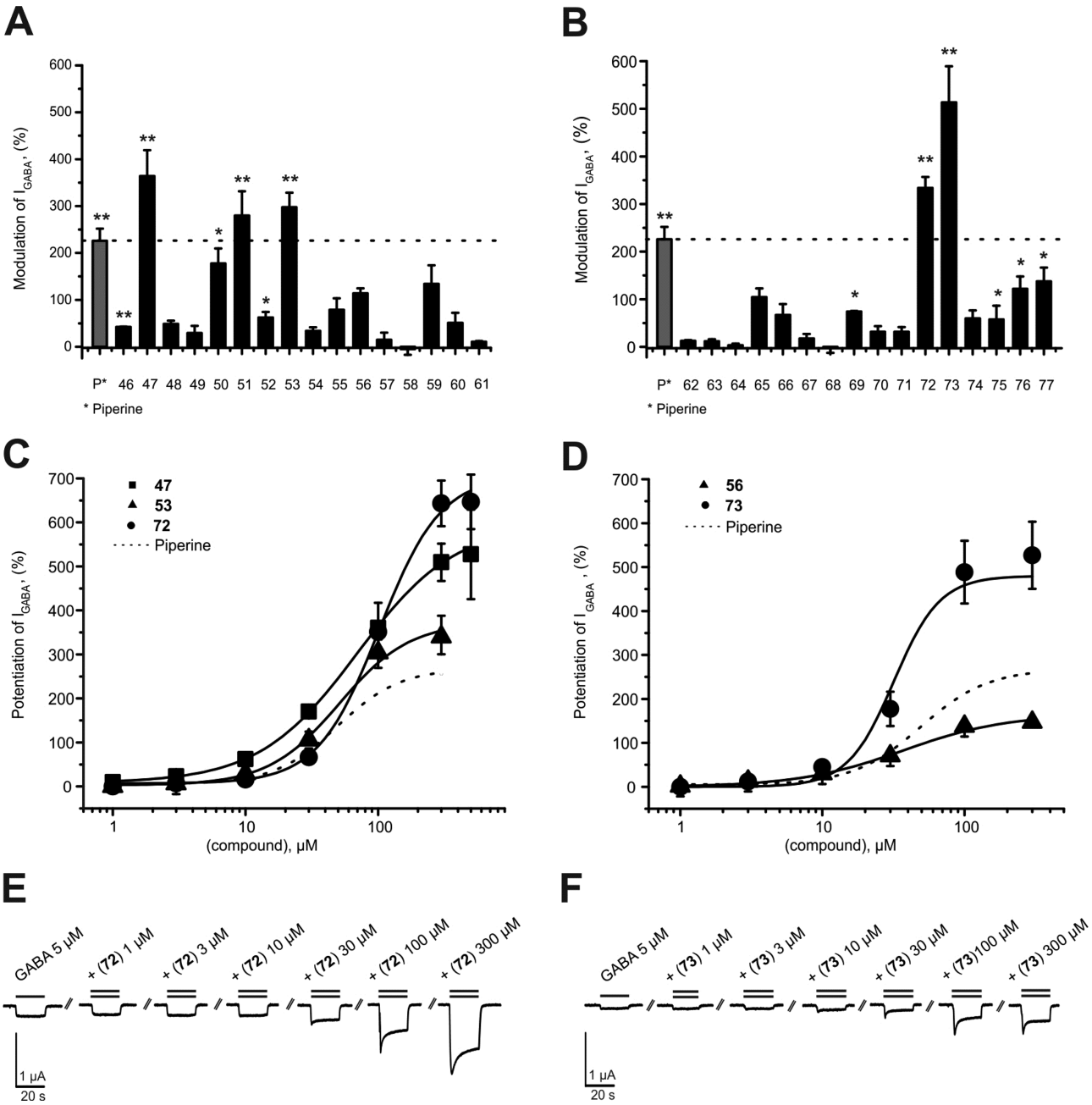

Figure 3. (A, B) Modulation of chloride currents through $GABA_A$ receptors composed of α_1, β_2, and γ_{2S} subunits by 100 μM piperine and the indicated derivatives (dotted line indicates cutoff for highly active compounds). (C, D) Concentration-dependent I_{GABA} (EC_{3-7}) enhancement through $\alpha_1\beta_2\gamma_{2S}$ $GABA_A$ receptors: (C) by **47** (■), **53** (▲), and **72** (●), ranked by efficiency, and (D) by **56** (▲) and **73** (●), ranked by potency, compared to piperine (dotted line). (E, F) Representative I_{GABA} modulated by (E) **72** and (F) **73**. Data represent mean ± SEM from at least three oocytes and two oocyte batches. Asterisks indicate statistically significant differences from zero: *p < 0.05, **p < 0.01. Data for piperine were taken from ref 31.

activate TRPV1 and induced pronounced anxiolytic action with little sedation, suggesting their potential use as scaffolds for drug development. The established determinants of efficacy may be used for future synthesis of improved $GABA_A$ modulators.

■ EXPERIMENTAL SECTION

Biological Activity. All experiments on animals were carried out in accordance with the Austrian Animal Experimental Law, which is in line with EU Directive 2010/63/EU. Every effort was made to minimize the number of animals used.

Expression of $GABA_A$ Receptors in *Xenopus laevis* Oocytes and Two-Microelectrode Voltage-Clamp Experiments. Preparation of stage V–VI oocytes from *X. laevis* and synthesis of capped runoff poly(A) cRNA transcripts from linearized cDNA templates (pCMV vector) was performed as previously described.[49] Female *X. laevis* frogs (Nasco) were anesthetized by 15 min incubation in a 0.2% MS-222 (methanesulfonate salt of 3-aminobenzoic acid ethyl ester; Sigma–Aldrich, Vienna, Austria) solution before removal of parts of

dx.doi.org/10.1021/jm5002277 | J. Med. Chem. 2014, 57, 5602–5619

Table 3. Efficiency and Potency of Further Characterized Piperine Derivatives and Piperine[a]

compd	$I_{GABA\text{-}max}$ (%)	EC_{50} (μM)	n_H	n
piperine	302 ± 27	52.4 ± 9.3	1.5 ± 0.2	3
22	1581 ± 74**	86.7 ± 13.9	2.3 ± 0.2	6
23	1673 ± 146**	51.7 ± 9.5	3.1 ± 0.8	6
25	760 ± 47**	13.8 ± 1.8**	1.8 ± 0.1	6
35	733 ± 60**	67.7 ± 11.0	1.9 ± 0.3	6
43	505 ± 24**	23.1 ± 3.3*	1.6 ± 0.2	6
47	603 ± 87*	70.8 ± 21.1	1.2 ± 0.2	3
53	388 ± 64	55.3 ± 17.6	1.5 ± 0.2	3
56	165 ± 4**	36.8 ± 2.0	1.2 ± 0.0	3
72	706 ± 58**	102.0 ± 11.2	1.9 ± 0.2	5
73	480 ± 85	31.8 ± 5.3	2.7 ± 0.2	6

[a]From ref 31, including number of experiments n. Asterisks indicate significant differences from piperine: *$p < 0.05$; **$p < 0.01$.

Table 4. Efficiency and Potency of 23 and 25 on $GABA_A$ Receptors of Different Subunit Compositions[a]

receptor subtype	$I_{GABA,max}$ (%)	EC_{50} (μM)	n_H	n
Compound **23**				
$\alpha_1\beta_1\gamma_{2S}$	1157 ± 69*	57.5 ± 7.3	1.8 ± 0.1	5
$\alpha_1\beta_2\gamma_{2S}$	**1673 ± 146**	**51.7 ± 9.5**	**3.1 ± 0.8**	**6**
$\alpha_1\beta_3\gamma_{2S}$	1240 ± 128	34.7 ± 5.7	1.9 ± 0.2	5
$\alpha_2\beta_2\gamma_{2S}$	980 ± 129**	26.4 ± 6.6	1.9 ± 0.4	6
$\alpha_3\beta_2\gamma_{2S}$	1285 ± 142	36.6 ± 7.2	1.9 ± 0.3	5
$\alpha_4\beta_2\gamma_{2S}$	1316 ± 55*	34.7 ± 3.8	1.7 ± 0.1	7
$\alpha_5\beta_2\gamma_{2S}$	1624 ± 156	61.9 ± 10.4	1.4 ± 0.1	7
Compound **25**				
$\alpha_1\beta_1\gamma_{2S}$	152 ± 30**	15.9 ± 4.9	1.3 ± 0.6	5
$\alpha_1\beta_2\gamma_{2S}$	**760 ± 47**	**13.8 ± 1.8**	**1.8 ± 0.1**	**8**
$\alpha_1\beta_3\gamma_{2S}$	587 ± 8**	29.5 ± 2.9**	1.5 ± 0.1	4
$\alpha_2\beta_2\gamma_{2S}$	512 ± 26**	14.8 ± 1.9	2.2 ± 0.3	4
$\alpha_3\beta_2\gamma_{2S}$	617 ± 42*	16.0 ± 2.7	1.8 ± 0.1	6
$\alpha_4\beta_2\gamma_{2S}$	419 ± 73**	56.7 ± 21.0	1.3 ± 0.3	4
$\alpha_5\beta_2\gamma_{2S}$	387 ± 20**	17.2 ± 1.4	1.7 ± 0.2	5

[a]Asterisks indicate significant differences from $\alpha_1\beta_2\gamma_{2S}$ receptor subtype as follows: *$p < 0.05$; **$p < 0.01$.

the ovaries. Follicle membranes from isolated oocytes were enzymatically digested with 2 mg/mL collagenase (type 1A, Sigma–Aldrich, Vienna, Austria).

Selected oocytes were injected with 10–50 nL of DEPC-treated water (diethyl pyrocarbonate, Sigma, Vienna, Austria) containing the different $GABA_A$ cRNAs at a concentration of approximately 300–3000 pg·nL^{-1}·$subunit^{-1}$.

To ensure expression of the γ_{2S} subunit in the case of $\alpha_{1/2/3/5}\beta_{2/3}\gamma_{2S}$ receptors, cRNAs were mixed in a ratio of 1:1:10. For expression of receptors composed of $\alpha_4\beta_2\gamma_{2S}$ and $\alpha_1\beta_1\gamma_{2S}$, cRNAS were mixed in a ratio of 3:1:10. The amount of cRNAs was determined by means of a NanoDrop ND-1000 (Kisker-Biotech, Steinfurt, Germany).

Oocytes were stored at +18 °C in modified ND96 solution (90 mM NaCl, 1 mM $CaCl_2$, 1 mM KCl, 1 mM $MgCl_2 \cdot 6H_2O$, and 5 mM HEPES [4-(2-hydroxyethyl)-1-piperazineethanesulfonic acid], pH 7.4, all from Sigma–Aldrich, Vienna, Austria).

Chloride currents through $GABA_A$ receptors (I_{GABA}) were measured at room temperature (+21 ± 1 °C) by means of a two-microelectrode voltage clamp technique making use of a Turbo TEC-05X amplifier (npi electronic, Tamm, Germany). I_{GABA} were elicited at a holding potential of −70 mV. Data acquisition was carried out by means of an Axon Digidata 1322A interface using pCLAMP v.10 (Molecular Devices, Sunnyvale, CA). The modified ND96 solution was used as bath solution. Microelectrodes were filled with 2 M KCl and had resistances between 1 and 3 MΩ.

Fast Perfusion System. GABA and the studied derivatives were applied by means of the ScreeningTool (npi electronic, Tamm, Germany) fast perfusion system as described previously.[50] To elicit I_{GABA}, the chamber was perfused with 120 μL of GABA- or compound-containing solution at a volume rate of 300 μL/s.[34] Care was taken to account for possible slow recovery from increasing levels of desensitization in the presence of high drug concentrations. The duration of washout periods was therefore extended from 1.5 min (<10 μM compounds) to 30 min (≥10 μM compounds). Oocytes with maximal current amplitudes >3 μA were discarded to exclude voltage clamp errors.

Data Analysis: $GABA_A$ Receptors. Stimulation of chloride currents by modulators of the $GABA_A$ receptor was measured at a GABA concentration eliciting between 3% and 7% of the maximal current amplitude (EC_{3-7}). The GABA EC_{3-7} was determined for each oocyte individually. Enhancement of the chloride current was defined as $(I_{GABA+compd}/I_{GABA}) - 1$, where $I_{GABA+compd}$ is the current response in the presence of a given compound and I_{GABA} is the control GABA current. $I_{GABA\text{-}max}$ reflects the maximal I_{GABA} enhancement. Concentration–response curves were generated and the data were fitted by nonlinear regression analysis using Origin Software (OriginLab Corp.). Data were fitted to the equation $1/(1 + (EC_{50}/[\text{compound}])^{nH})$, where n_H is the Hill coefficient. Each data point represents the mean ± SEM from at least three oocytes and ≥2 oocyte batches. Statistical significance was calculated by paired Student t-test with a confidence interval of <0.05.

Molecular Modeling and Quantitative Structure–Activity Relationships. *Data Set.* The 2D structures of 76 piperine derivatives and piperine were drawn in the InstantJChem package for Excel (www.chemaxon.com/products/jchem-for-excel) and exported in sdf format. The LigPrep tool provided by Schrödinger in the Maestro package (Maestro, version 9.2; Schrödinger LLC, New York, 2011) was used to generate low-energy 3D structures and protonated states. All possible stereoisomers per ligand were computed and one low-energy conformation was generated per each stereoisomer in MMFF force field. The protonated states were determined at pH 7.4 (pH used in the experiments). For compounds **33**, **34**, **36**, **38**, and **39**, several stereisomers were determined. Since these structures were not ionizable at this pH, the stereoisomers were considered equal in terms of 2D structure and duplicates were removed. Subsequently, the structures were imported into MOE, where partial atomic charges were calculated in the MMFF94 force field. Piperine (obtained from Sigma–Aldrich, Vienna, Austria) was used as a reference compound to determine the class labels of its derivatives. Potentiation of GABA current by piperine was 226% ± 26%;[31] therefore, compounds with potentiation ≥200% were assigned to the active class, otherwise to the inactive. This led to an unbalanced data set with 17 "active" and 60 "inactive" compounds.

Descriptor Sets. One hundred forty-three 2D descriptors implemented in MOE were calculated. The full list is provided in Supporting Information (Table S1A). Descriptors showing no variance were removed from the data set, and the remaining 125 descriptors (Supporting Information, Table S1B) underwent feature selection by the BestFirst algorithm implemented in the software package WEKA version 3.7.9. Consequently, the six descriptors left (set 6D) were used for further classification studies (Table 9). Additionally, as a reference descriptor set, we used 11 descriptors of physicochemical properties (set PHYSCHEM) from the list of 125 descriptors described above (Table 10). These descriptors allow us to trace molecular features important for biological activity and have previously shown good performance in application to ligand-based studies.[51] As an attempt to trace the structural features relevant to the activity of piperine derivatives, MACCS fingerprints (MACCS Keys; MDL Information Systems, Inc., San Leandro, CA) were computed in MOE. MACCS are a set of structural keys, where each key describes a small substructure consisting of up to 10 non-hydrogen atoms. A Python script (Supporting Information) was applied to divide the fingerprints into bit strings. The latter were further used in the classification studies as descriptor set "MACCS".

Journal of Medicinal Chemistry Article

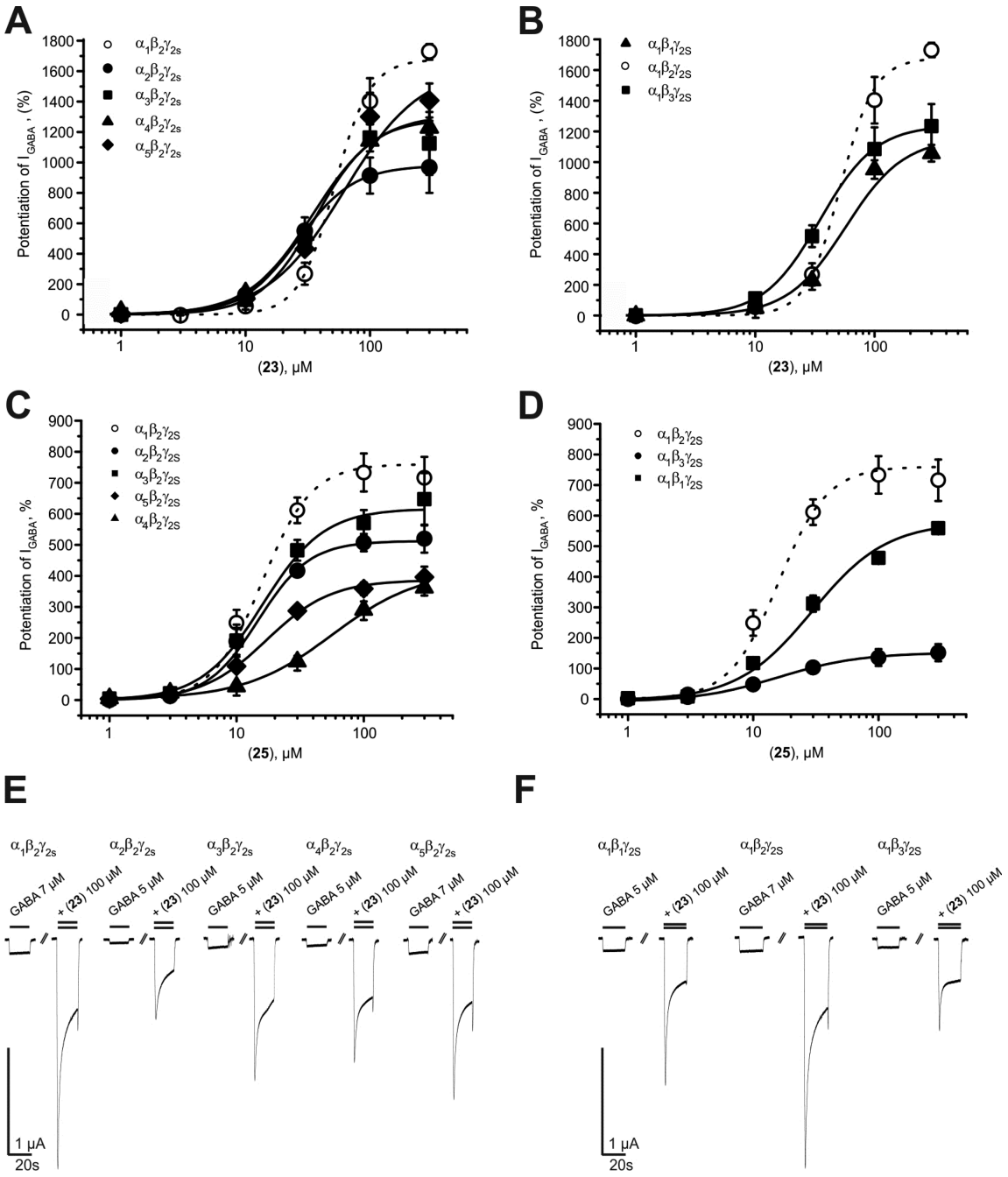

Figure 4. Analysis of subunit preferential I_{GABA} enhancement by (A, B) the most efficient (**23**) and (C, D) the most potent (**25**) piperine derivatives. (E, F) Representative I_{GABA} through seven $GABA_A$ receptor subtypes by **23** at 100 μM. Data represent mean ± SEM from at least three oocytes and two oocyte batches.

Computational Methods. As classification methods, instance-based classifier (IBk), J48 decision tree (J48), naïve-Bayes classifier (NB), random forest (RF), and Support vector machine (SMO) were used as implemented in Weka. All methods were used with the default parameter settings. Nevertheless, different costs were associated with misclassified compounds since the data set was unbalanced. The costs were evaluated by use of an in-house script (Supporting Information), which consequently built models with different costs of the false positive (FP) and false negative (FN) compounds (from 1 to 200 with step of 1 for FN and from 0 to 20 with step of 0.1 for FP). Moreover, inside the script the 10-fold cross-validation was applied and statistical parameters were computed. Subsequently, one model per method and descriptor set was selected on the basis of highest values of MCC, accuracy, sensitivity, and specificity and was taken for visual inspection and possible interpretation. The cost-sensitive parameters obtained for the best 15 models are listed in Table 11.

Statistical Parameters. The statistical parameters of every model were calculated on the basis of values from confusion matrix (for details see ref 52), where TP and TN stand for correctly classified active and inactive compounds and FP and FN for misclassified inactive and active ligands. The true-positive rates of active (sensitivity) and inactive (specificity) classes were calculated by the following formulas:

Journal of Medicinal Chemistry Article

Table 5. Comparison of Potency and Efficiency of 23 for $GABA_A$ Receptors of Different Subunit Compositions[a]

	$\alpha_1\beta_2\gamma_{2S}$		$\alpha_1\beta_1\gamma_{2S}$		$\alpha_1\beta_3\gamma_{2S}$		$\alpha_2\beta_2\gamma_{2S}$		$\alpha_3\beta_2\gamma_{2S}$		$\alpha_4\beta_2\gamma_{2S}$		$\alpha_5\beta_2\gamma_{2S}$	
	P	E	P	E	P	E	P	E	P	E	P	E	P	E
$\alpha_1\beta_2\gamma_{2S}$				*				**				*		
$\alpha_1\beta_1\gamma_{2S}$					**		*				*			*
$\alpha_1\beta_3\gamma_{2S}$													*	
$\alpha_2\beta_2\gamma_{2S}$												**	*	**
$\alpha_3\beta_2\gamma_{2S}$														
$\alpha_4\beta_2\gamma_{2S}$													*	
$\alpha_5\beta_2\gamma_{2S}$														

[a]Potency (P), expressed as EC_{50}, and efficiency (E), expressed as $I_{GABA\text{-}max}$, are compared. Asterisks indicate statistical significance as follows: *p < 0.05, **p < 0.01.

Table 6. Comparison of Potency and Efficiency of 25 for $GABA_A$ Receptors of Different Subunit Compositions[a]

	$\alpha_1\beta_2\gamma_{2S}$		$\alpha_1\beta_1\gamma_{2S}$		$\alpha_1\beta_3\gamma_{2S}$		$\alpha_2\beta_2\gamma_{2S}$		$\alpha_3\beta_2\gamma_{2S}$		$\alpha_4\beta_2\gamma_{2S}$		$\alpha_5\beta_2\gamma_{2S}$	
	P	E	P	E	P	E	P	E	P	E	P	E	P	E
$\alpha_1\beta_2\gamma_{2S}$				**	**	**		**		*		**		**
$\alpha_1\beta_1\gamma_{2S}$					*	**		**		**		*		**
$\alpha_1\beta_3\gamma_{2S}$							**	*	**				**	**
$\alpha_2\beta_2\gamma_{2S}$														**
$\alpha_3\beta_2\gamma_{2S}$												*		**
$\alpha_4\beta_2\gamma_{2S}$														
$\alpha_5\beta_2\gamma_{2S}$														

[a]Potency (P), expressed as EC_{50}, and efficiency (E), expressed as $I_{GABA\text{-}max}$, are compared. Asterisks indicate statistical significance as follows: *p < 0.05, **p < 0.01.

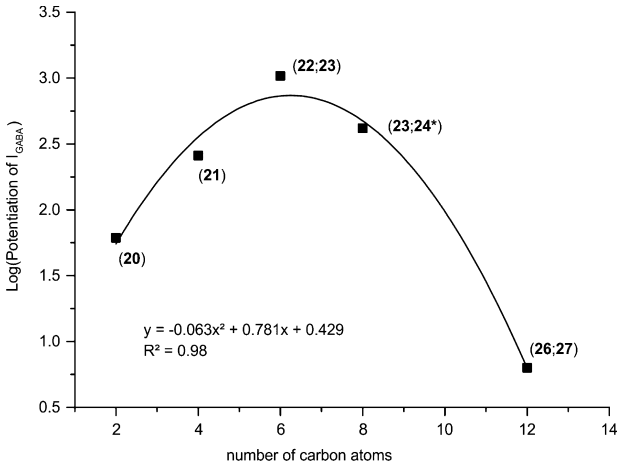

Figure 5. Relation between log(potentiation of I_{GABA}) of dialkyl-substituted piperine derivatives at the amide nitrogen and number of carbon atoms at this region. Data for **24*** were taken from ref 34.

$$\text{sensitivity} = \frac{TP}{TP + FN}$$

$$\text{specificity} = \frac{TN}{TN + FP}$$

The accuracy of the model was defined as the ratio of correctly predicted compounds to the total amount of compounds.

$$\text{accuracy} = \frac{TP + TN}{\text{total}}$$

Additionally, the Matthews correlation coefficient (MCC) was used to assess the quality of the obtained models. It was calculated from the formula

$$MCC = \frac{TP \cdot TN - FP \cdot FN}{\sqrt{(TP + FP)(TP + FN)(TN + FP)(TN + FN)}}$$

MCC is independent of the class sizes and therefore gives a rational evaluation of prediction in our case. It can return values from −1 to +1, where +1 determines perfect prediction, 0 means random classification, and −1 represents a total misclassification. The value of 0.4 was taken as a threshold to filter the best-performing models.

Behavioral Studies. Male mice (C57BL/6N) were obtained from Charles River Laboratories (Sulzfeld, Germany). For maintenance, mice were group-housed (maximum five mice per type IIL cage) with free access to food and water. At least 24 h before the commencement of experiments, mice were transferred to the testing facility, where they were given free access to food and water. The temperature in the maintenance and testing facilities was 23 ± 1 °C; the humidity was 40−60%; a 12 h light−dark cycle was in operation (lights on from 07:00 to 19:00). Only male mice aged 3−6 months were tested.

Compounds were applied by intraperitoneal (ip) injection 30 min before each test. Testing solutions were prepared in a solvent composed of 0.9% NaCl solution with 10% dimethyl sulfoxide (DMSO) and 3% Tween 80. Application of the solvent alone did not influence animal behavior. All doses are indicated as milligrams per kilogram of body weight of the animal.

Elevated Plus Maze Test. The animals' behavior was tested over 5 min on an elevated plus maze 1 m above ground consisting of two closed and two open arms, each 50 × 5 cm in size. The test instrument was built from gray PVC; the height of closed arm walls was 20 cm. Illumination was set to 180 Lux. Animals were placed in the center, facing an open arm. Analysis of open and closed arm entries and time on open arm was automatically done with Video-Mot 2 equipment and software (TSE Systems, Bad Homburg, Germany).[34]

Open Field Test. Ambulation was tested over 10 min in a 50 × 50 cm flexfield box equipped with infrared rearing detection. Illumination was set to 150 Lux. The animals' explorative behavior was analyzed by use of the ActiMot 2 equipment and software (TSE-systems, Bad Homburg, Germany). Arenas were subdivided into border (up to 8 cm from wall), center (20 × 20 cm, 16% of total area), and intermediate area according to the recommendations of EMPRESS (European

dx.doi.org/10.1021/jm5002277 | J. Med. Chem. 2014, 57, 5602−5619

Journal of Medicinal Chemistry Article

Table 7. Statistical Parameters of the 15 Best Models Obtained after 10-Fold Cross-Validation

model	classification method	TP, TN, FP, FN[a]	sensitivity	specificity	accuracy	MCC, ROC
		Descriptor Set 6D				
1	IBk	12, 52, 8, 5	0.706	0.867	0.831	0.542, 0.825
2	J48	15, 46, 14, 2	0.882	0.767	0.792	0.556, 0.818
3	NB	16, 49, 11, 1	0.941	0.817	0.844	0.659, 0.831
4	RF	13, 52, 8, 4	0.765	0.867	0.844	0.588, 0.838
5	SMO	16, 39, 21, 1	0.941	0.650	0.714	0.491, 0.796
		Descriptor Set PHYSCHEM				
6	IBk	10, 52, 8, 7	0.588	0.867	0.805	0.446, 0.749
7	J48	15, 46, 14, 2	0.882	0.767	0.792	0.556, 0.828
8	NB	15, 40, 20, 2	0.882	0.667	0.714	0.457, 0.828
9	RF	15, 46, 14, 2	0.882	0.767	0.792	0.556, 0.811
10	SMO	15, 36, 24, 2	0.882	0.600	0.662	0.400, 0.741
		Descriptor Set MACCS				
11	IBk	9, 45, 15, 8	0.529	0.750	0.701	0.250, 0.619
12	J48	12, 48, 12, 5	0.706	0.800	0.779	0.453, 0.797
13	NB	12, 42, 18, 5	0.706	0.700	0.701	0.345, 0.713
14	RF	13, 43, 17, 4	0.765	0.717	0.727	0.409, 0.730
15	SMO	10, 56, 4, 7	0.588	0.933	0.857	0.561, 0.761

[a]TP = true positive, TN = true negative, FP = false positive, FN = false negative.

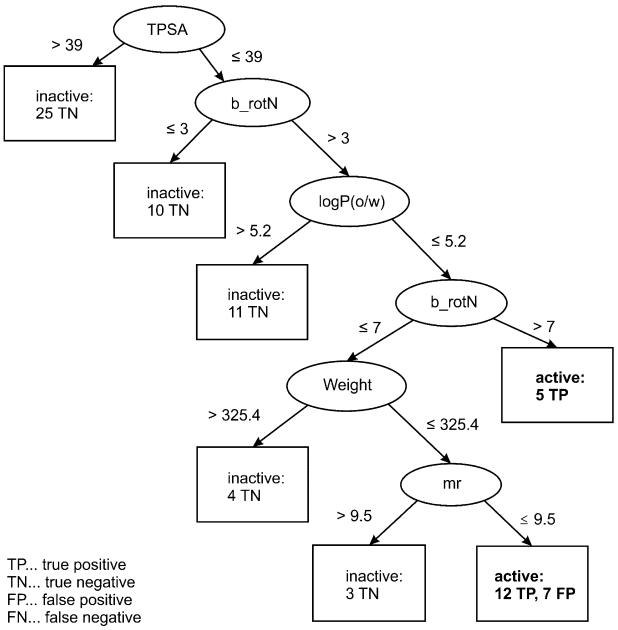

Figure 6. Decision tree obtained for the data set of 76 piperine derivatives with PHYSCHEM descriptor set.

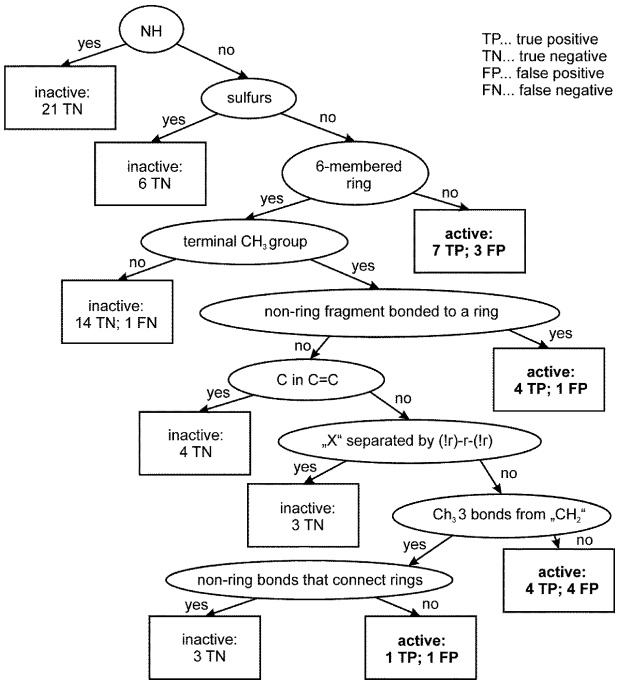

Figure 7. Decision tree obtained for the data set of 76 piperine derivatives with MACCS fingerprints.

Mouse Phenotyping Resource of Standardised Screens; http://empress.har.mrc.ac.uk).

Estimation of Plasma Levels. Trunk blood from male C57BL/6N (6 months) was taken 15, 30, and 60 min after ip application of **23** and **25** (doses 1, 3, and 10 mg/kg body weight; injection solutions were prepared as described for behavioral analysis). At each time point, mice were euthanized and blood samples (500−800 μL) were collected and compiled into ethylenediaminetetraacetic acid (EDTA)-coated microtubes (1.6 mg of EDTA/sample) and centrifuged at 12 000 rpm for 5 min at 4 °C. Plasma samples were transferred into 1.5 mL tubes and stored at −80 °C until analysis.

Materials. All solvents used were of UPLC grade. Acetonitrile and dimethyl sulfoxide (DMSO) were supplied by Scharlau (Barcelona, Spain). Methanol was from Lab-Scan (Gliwice, Poland). Ammonium formate, formic acid and trifluoroacetic acid (TFA) were purchased from BioSolve (Valkenswaard, Netherlands), and HPLC-grade water was obtained from an EASYpure II (Barnstead, Dubuque, IA) water purification system. Blank K_3EDTA C57BL/6N mouse plasma was collected for generating plasma calibrators and quality controls (QC).

Preparations of Calibrators and Quality Control Samples. Two separate sets of **23** and **25** stock solutions were prepared in DMSO for making calibrators and quality control (QC) samples. Plasma calibrators were prepared by spiking corresponding stock solutions into a blank plasma sample. The following **23** and **25** concentrations were added: 20, 50, 100, 250, 500, 1000, and 2000 ng/mL. The same blank plasma and both stock solutions (for QC) were used to generate three level plasma QC samples at 60, 1000, and 1600 ng/mL for both **23** and **25**.

dx.doi.org/10.1021/jm5002277 | J. Med. Chem. 2014, 57, 5602−5619

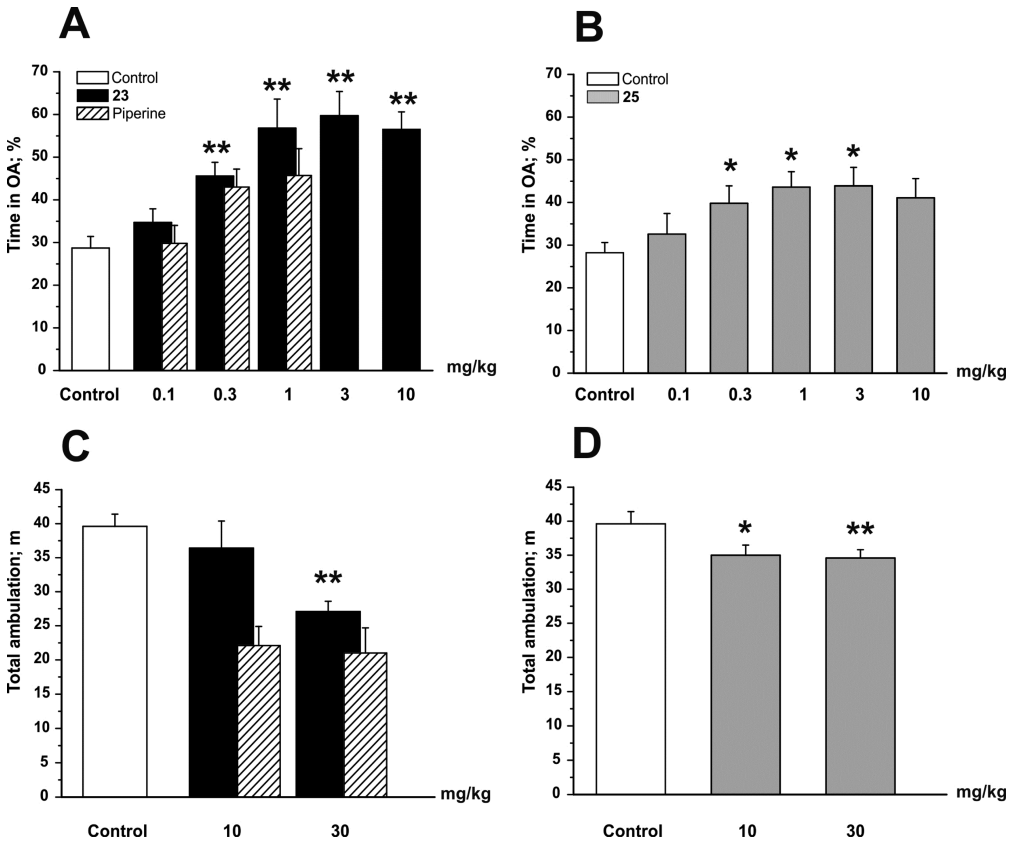

Figure 8. Compounds **23** and **25** display anxiolytic effects in the EPM test and little sedation in the OF test. Bars indicate time spent in open arms (OA) as a percentage of the total time 30 min after ip application of the indicated dose (in milligrams per kilogram of body weight) of (A) **23** and (B) **25** and the total ambulation after application of (C) **23** and (D) **25**. White bars illustrate the behavior of control mice. Bars represent means ± SEM from at least eight different mice. Asterisks indicate statistically significant differences to control $*p < 0.05$, $**p < 0.01$ [analysis of variance (ANOVA) with Bonferroni]. Shaded bars for the behavioral effects of piperine are taken from ref 34. Behavioral experiments comparing the sedative and anxiolytic potential of piperine, **23**, and **25** have been conducted in parallel.

Table 8. Estimated Plasma Levels of Derivatives 23 and 25 after Intraperitoneal Application[a]

applied dose (mg/kg body weight)	mean plasma concn (ng/mL)	*n*
Compound **23**		
1	60.6 ± 14.5	3
3	194.0 ± 50.2	3
10	593.0 ± 92.4	3
Compound **25**		
1	41.5 ± 8.7	3
3	172.0 ± 19.0	3
10	419.0 ± 37.2	3

[a]Data are given as mean ± SEM; *n* indicates the number of animals used.

Table 9. Set of Six 2D Descriptors Selected by BestFirst Algorithm for Classification Studies

name	definition
density	molecular mass density: weight divided by vdw_vol (amu/Å^3)
lip_don	no. of OH and NH atoms
opr_brigid	no. of rigid bonds[53]
PEOE_RPC+ numeric	relative positive partial charge: largest positive q_i divided by the sum of positive q_i
PEOE_VSA+3	sum of v_i where q_i is in the range [0.15, 0.20)
SMR	molecular refractivity (including implicit hydrogens)[a]

[a]This property is an atomic contribution model[54] that assumes the correct protonation state (washed structures). The model was trained on ∼7000 structures and results may vary from the mr descriptor.

Two internal standard (IS) stock solutions of **22** and **24** were prepared in DMSO in order to generate working solutions (WS) at 200 ng/mL in methanol.

Sample Preparation for UHPLC-MS/MS Analysis. Plasma proteins were precipitated by the addition of 50 μL of WS at 200 ng/mL of the corresponding IS: **22** (for **23**) or **24** (for **25**) and 500 μL of ice-cold acetonitrile to 20 μL of K_3EDTA mouse plasma. Samples were vortexed at 1400 rpm for 10 min and then centrifuged at 13200*g* for 20 min at 10 °C. The supernatant was transferred into a 96-deep-well plate for drying under nitrogen gas flow (Evaporex EVX-96, Apricot Designs, Monrovia, CA) and redissolved in 200 μL of injection solvent (65% 10 mM ammonium formate + 0.05% formic acid, 35% acetonitrile + 0.05% formic acid) before MS/MS analysis.

LC-MS/MS Analyses. Quantification was performed on a 1290 Infinity LC system coupled with a 6460 triple quadrupole mass spectrometer with Jet Stream Technology, and data was processed with a MassHunter Workstation Software version B.06.00 (Agilent; Waldbronn, Germany). The 1290 Infinity LC system was equipped with a binary capillary pump, degasser, autosampler, autosampler thermostat, thermostated column compartment, and FlexCube. Separation was performed at 55 °C on a Kinetex XB-C18 column, 100 × 2.1 mm, 1.7 μm particle size (Phenomenex; Torrance, CA); mobile phase of (A) 0.05% formic acid in 10 mM ammonium formate

Table 10. Eleven Descriptors of Physical Chemical Properties Used in the Study

name	definition
a_acc	no. of hydrogen-bond acceptor atoms
a_don	no. of hydrogen-bond donor atoms
b_rotN	no. of rotatable bonds[a]
log_P(o/w)	log of octanol/water partition coefficient[b]
mr	molecular refractivity (including implicit hydrogens)[c]
PEOE_VSA_HYD	total hydrophobic van der Waals surface area
TPSA	polar surface area[d] (Å^2)
vsa_acc	approximate sum of VDW surface areas (Å^2) of pure hydrogen-bond acceptors
vsa_don	approximate sum of VDW surface areas (Å^2) of pure hydrogen-bond donors
vsa_hyd	approximate sum of VDW surface areas (Å^2) of hydrophobic atoms
Weight	molecular weight (including implicit hydrogens) (amu)

[a]A bond is rotatable if it has order 1, is not a ring, and has at least two heavy neighbors. [b]Calculated from a linear atom-type model with r^2 = 0.931. [c]Calculated from an 11-descriptor linear model with r^2 = 0.997. [d]Calculated from group contributions to approximate the polar surface area from connection table.

Table 11. Cost-Sensitive Parameters

method	cost FP	cost FN
Descriptor Set 6D		
IBk	1	1
J48	6	1
NB	5	3
RF	9	5
SMO	52	19.1
Descriptor Set PHYSCHEM		
IBk	1	1
J48	18	11
NB	1	1
RF	21	2
SMO	49	18.1
Descriptor Set MACCS		
IBk	3	2
J48	29	12
NB	1	8
RF	4	1
SMO	3	2.2

and (B) 0.05% formic acid in ACN, gradient 40% B for 1 min, linear gradient to reach 88% B after 5.3 min, shifted to 100% B for 1 min, and back to equilibrium condition of 40% B for 0.7 min; flow rate of 0.5 mL/min; total run time of 7 min. Sample injected volume was 1 μL and autosampler was set at 10 °C. Needle wash solution was MeOH/ACN/IPA/H_2O (1:1:1:1 v/v/v/v). Flexible cube was set at a flow rate of 1 mL/min for 20 s.

MS parameters were manually optimized as follow: drying N_2 gas of 320 °C at a flow rate of 10 L/min, nebulizer pressure of 20 psi, sheath N_2 gas of 400 °C at a flow rate of 11 L/min, nozzle voltage of 0 V, capillary voltage of 2.5 kV, and delta EMV 0 V. Quantification was determined in multiple reaction monitoring (MRM) mode with an ESI-MS/MS system in positive ionization mode. The MRM transitions of both **23** and **25** and corresponding internal standard were as shown in Table S2 (Supporting Information).

Syntheses. Details of synthesis and characterization of selected products **25**, **51**, and **62** and key intermediates **65a**, **68a−c**, **71a**, and **75a,b** are described below. Synthetic procedures and characterization data for all other compounds are included in Supporting Information. Purity was determined either by elemental analysis or by HPLC and was >95%. Unless otherwise noted, chemicals were purchased from commercial suppliers and used without further purification. Microwave reactions were performed on a Biotage Initiator Sixty microwave unit (Biotage AB, Uppsala, Sweden). Flash column chromatography was performed on silica gel 60 from Merck (40−63 mm), whereas most separations were performed by using a Büchi Sepacore medium-pressure liquid chromatography (MPLC) system with a 9g column (Buchi Labortechnik AG, Flawil, Switzerland). For thin-layer chromatography (TLC), aluminum-backed silica gel was used. Melting points were determined by using a Kofler-type Leica Galen III micro hot stage microscope (Aigner-Unilab Laborfachhandel GmbH, Vienna, Austria) and are uncorrected. For compounds unknown in the literature, either high-resolution mass spectrometry (HR-MS) or combustion analysis was performed. HR-MS was performed by E. Rosenberg at the Institute for Chemical Technologies and Analytics, Vienna University of Technology; all samples were analyzed by liquid chromatography/ion trap time-of-flight mass spectrometry (LC/IT-TOF-MS) in positive or negative ion detection mode with the recording of MS and MS/MS spectra. Combustion analysis was carried out in the Microanalytical Laboratory, Institute of Physical Chemistry, University of Vienna. NMR spectra were recorded on a Bruker AC 200 (200 MHz), a Bruker Avance DP160 (200 MHz), or a Bruker Avance 400 (400 MHz) spectrometer (Bruker GmbH, Vienna, Austria) and chemical shifts are reported in parts per million (ppm). For assignment of ^{13}C multiplicities, standard ^{13}C distortionless enhancement by polarization transfer (DEPT) or attached proton test (APT) spectra were recorded. HPLC analyses were performed on a Agilent 1200 HP-LC system with a Kinetex XB-C18, 2.6 μm, 50 × 2.1 mm column (Agilent Technologies GmbH, Vienna, Austria). The mobile phase was composed of ACN/water (gradient 50:50 up to 95:5 v/v) with 0.1% AcOH added. GC−MS runs were performed on a Thermo Finnigan Focus GC/DSQ II with a standard capillary column BGB 5 (30 m × i.d. 0.32 mm; Fisher Scientific GmbH, Vienna, Austria).

*(2E,4E)-5-(1,3-Benzodioxol-5-yl)-N,N-dibutyl-2,4-pentadienamide (**25**).* Piperic acid chloride (218 mg, 1 mmol) was dissolved in 2.5 mL of dry THF. Dibutylamine (595 μL, 3.5 mmol) was added and the reaction mixture was stirred overnight at rt. After evaporation of the solvent, the residue was taken up in ethyl acetate (EtOAc; 40 mL) and washed two times each with 5% $NaHCO_3$ and 2 N HCl. The organic layer was separated, dried with sodium sulfate, filtered, and evaporated. The pure product was obtained after recrystallization from ethanol.

Yield 76% (746 mg, 2.26 mmol), light brown crystals, mp 88−90 °C. ^{1}H NMR ($CDCl_3$, 200 MHz) δ 0.85−1.05 (m, 6H, CH_3), 1.22−1.45 (m, 4H, CH_2), 1.46−1.71 (m, 4H, CH_2), 3.25−3.47 (m, 2H, CH_2), 5.98 (s, 2H, O−CH_2−O), 6.35 (d, J = 14.6 Hz, 1H, H2), 6.70−6.85 (m, 3H), 6.86−6.95 (m, 1H), 7.00 (d, J = 7.9 Hz, 1H), 7.36−7.54 (m, 1H). ^{13}C NMR ($CDCl_3$, 50 MHz) δ 14.1 (q, CH_3), 14.1 (q, CH_3), 20.3 (t, CH_2), 20.5 (t, CH_2), 30.3 (t, CH_2), 32.2 (t, CH_2), 46.8 (t, N−CH_2), 48.1 (t, N−CH_2), 101.5 (t, O−CH_2−O), 105.9 (d), 108.7 (d), 120.5 (d), 122.7 (d), 125.6 (d), 131.2 (s), 138.6 (d), 142.6 (d), 148.3 (s, C−O), 148.4 (s, C−O), 166.3 (s, CO−N). Anal. Found, C 71.96, H 7.91, N 3.95; Calcd (·0.23H_2O), C 72.01, H 8.30, N 4.20.

*3-(Benzo[d][1,3]dioxol-5-yl)-N,N-dipropylbenzamide (**51**).* Benzodioxol-5-boronic acid (138 mg, 0.83 mmol, 1 equiv), **51a** (237 mg, 0.83 mmol, 1 equiv), $Pd(PPh_3)_4$ (19 mg, 2 mol %), and sodium carbonate (615 mg, 5.81 mmol, 7 equiv) were charged into a microwave vial. Then a mixture of dimethyl ether (DME)/EtOH 5:1 (6.4 mL) and water (1.8 mL) was added, and the resulting suspension was degassed by passing through argon for 5 min. The vial was sealed and heated to 140 °C for 1 h in the microwave. After cooling to rt, the reaction mixture was extracted with dichloromethane (DCM), the solvent was evaporated, and the crude product was directly subjected to column chromatography with light petroleum (LP)/EtOAc mixture as eluent.

Yield 60% (163 mg, 0.50 mmol), colorless oil. TLC 0.24 (LP/EtOAc 4:1). ^{1}H NMR ($CDCl_3$, 200 MHz) δ 0.76−0.98 (br m, 6H, CH_3), 1.57−1.67 (br m, 4H, CH_2), 3.20−3.47 (br m, 4H, N−CH_2−), 6.00 (s, 2H, O−CH_2−O), 6.86−6.90 (m, 1H, ArH), 7.03−7.08 (m, 2H, ArH), 7.25−7.30 (m, 1H, ArH), 7.42 (t, J = 7.4 Hz, 1H, ArH), 7.48−7.54 (m, 2H, ArH). ^{13}C NMR ($CDCl_3$, 50 MHz) δ 11.1 (q, CH_3), 11.4 (q, CH_3), 20.7 (t, CH_2), 22.0 (t, CH_2), 46.3 (t, CH_2), 50.7

dx.doi.org/10.1021/jm5002277 | J. Med. Chem. 2014, 57, 5602−5619

(t, CH_2), 101.2 (t, O−CH_2−O), 107.6 (d), 108.6 (d), 120.7 (d), 124.8 (d), 124.9 (d), 127.4 (d), 128.8 (d), 134.8 (s), 137.9 (s), 141.1 (s), 147.3 (s), 148.2 (s), 171.6 (s, −CO−N). HR-MS $[M + H]^+$ m/z (pred) = 326.1751, m/z (meas) = 326.1749, difference = −0.61 ppm.

*[5-(Benzo[d][1,3]dioxol-5-yl)naphthalen-1-yl](piperidin-1-yl)-methanone (**62**).* 1-Ethyl-3-(3-dimethylaminopropyl)carbodiimide hydrochloride (EDCI·HCl; 65 mg, 0.34 mmol, 2 equiv) was added to a suspension of **62a** (50 mg, 0.17 mmol, 1 equiv) and hydroxybenzotriazole (HOBt; 52 mg, 0.34 mmol, 2 equiv) in dry dichloromethane (2 mL) under argon at rt. After 2 h, the suspension was transformed into an opaque solution and TLC indicated full consumption of the starting material. Piperidine (0.5 mL) was added at rt and stirring was continued overnight. After full conversion was detected by TLC, the reaction mixture was diluted with EtOAc (30 mL); washed with 0.5 N HCl, saturated $NaHCO_3$, and brine (20 mL each); dried with sodium sulfate; and evaporated. The crude product was purified by column chromatography with LP/EtOAc mixture as eluent.

Yield 62% (0.11 mmol, 38 mg), colorless solid, mp 150−153 °C. TLC 0.09 (LP/EtOAc 4:1). ^{1}H NMR ($CDCl_3$, 200 MHz) δ 1.40−1.50 (m, 2H, CH_2), 1.66−1.80 (m, 4H, CH_2), 3.15−3.21 (m, 2H, N−CH_2), 3.87−3.93 (m, 2H, N−CH_2), 6.04 (s, 2H, O−CH_2−O), 6.93−6.95 (m, 3H, ArH), 7.39−7.56 (m, 4H, ArH), 7.84 (d, J = 8.3 Hz, 1H, ArH), 7.94 (dd, J^1 = 7.2 Hz, J^2 = 2.6 Hz, 1H, ArH). ^{13}C NMR ($CDCl_3$, 50 MHz) δ 24.6 (t, CH_2), 25.9 (t, CH_2), 26.7 (t, CH_2), 42.7 (t, N−CH_2), 48.3 (t, N−CH_2), 101.2 (t, O−CH_2−O), 108.2 (d), 110.6 (d), 123.3 (d), 123.4 (d), 124.4 (d), 125.3 (d), 126.2 (d), 126.9 (d), 127.4 (d), 120.9 (s), 131.9 (s), 134.3 (s), 135.2 (s), 140.3 (s), 147.0 (s), 147.5 (s), 169.4 (s, CO−N). HR-MS $[M + H]^+$ m/z (pred) = 360.1594, m/z (meas) = 360.1597, difference = 0.83 ppm.

*(E)-Methyl 3-(Naphtho[2,3-d][1,3]dioxol-5-yl)acrylate (**65a**).* For synthesis of **65a**, a modification of a previously published method[38] was employed. A 8-mL vial with magnetic stirrer, screw cap, and septum was charged with naphtho[2,3-*d*][1,3]dioxol-5-yl trifluoromethanesulfonate (synthesized according to ref 37) (480 mg, 1.5 mmol, 1 equiv), 1,10-phenanthroline monohydrate (16 mg, 0.083 mmol, 5.5 mol %), palladium(II) acetate (17 mg, 0.075 mmol, 5 mol %), and anhydrous *N*,*N*-dimethylformamide (DMF, 5 mL). Then triethylamine (250 μL, 1.8 mmol, 1.2 equiv) and methyl acrylate (680 μL, 7.5 mmol, 5 equiv) were added successively. The vial was flushed with argon and heated to 80 °C for 16 h. Reaction control by TLC showed full conversion. The solvent was evaporated, and the residue was taken up in DCM and adsorbed on silica. Column chromatography (45 g of SiO_2, eluent LP/EtOAc, 5% isocratic) yielded the pure product.

Yield 95% (364 mg, 1.425 mmol), colorless solid, mp 125−126 °C. TLC 0.44 (LP/EtOAc 4:1). ^{1}H NMR ($CDCl_3$, 200 MHz) δ 3.82 (s, 3H, CH_3), 5.99 (s, 2H, O−CH_2−O), 6.43 (d, J = 15.7 Hz, 1H, H3), 7.04 (s, 1H, ArH), 7.25 (t, J = 7.7 Hz, 1H, H7′), 7.38 (s, 1H, ArH), 7.52 (d, J = 7.1 Hz, 1H, ArH), 7.61 (d, J = 8.1 Hz, 1H, ArH), 8.29 (d, J = 15.7 Hz, 1H, H2). ^{13}C NMR ($CDCl_3$, 50 MHz) 51.7 (q, CH_3), 99.9 (d), 101.4 (t, O−CH_2−O), 104.4 (d), 119.9 (d), 123.5 (d), 124.0 (d), 128.7 (s), 129.5 (d), 130.7 (s), 130.9 (s), 142.1 (d), 147.6 (s), 148.6 (s), 167.3 (s, COOR). HR-MS $[M - MeOH]^+$ m/z (pred) = 225.0546, m/z (meas) = 225.0553, difference = 3.11 ppm.

*4,4,5,5-Tetramethyl-2-(naphtho[2,3-d][1,3]dioxol-6-yl)-1,3,2-dioxaborolane (**68a**).* For synthesis of **68a**, a modification of a procedure published by Ishyama et al.[39] was used. A three-necked flask with magnetic stirrer, septum, reflux condenser, and balloon was charged with naphtho[2,3-*d*][1,3]dioxole (1.72 g, 10 mmol, 1 equiv), bis(pinacolato)diboron (1.27 g, 5 mmol, 0.5 equiv), $[Ir(OMe)cod]_2$ (100 mg, 0.15 mmol, 1.5 mol %), and 4,4′-di-*tert*-butyl-2,2′-bipyridine (81 mg, 0.3 mmol, 3 mol %) and flushed with argon. Then cyclohexane (60 mL) was added and the reaction was heated to reflux and monitored with GC/MS. After 24 h the reaction did not proceed any further. After evaporation of the solvent, the residue was redissolved in DCM, adsorbed on silica, and directly subjected to column chromatography (45 g of SiO_2, eluent LP/EE 30:1), which yielded the pure product (683 mg of starting material could be reisolated in this step).

Yield 29% (48% based on recovered starting material, 874 mg, 2.9 mmol), colorless solid, mp 97−99 °C. TLC 0.18 (LP/EE 30:1). ^{1}H NMR ($CDCl_3$, 200 MHz) δ 1.38 (s, 12H, CH_3), 6.03 (s, 2H, O−CH_2−O), 7.10 (s, 1H), 7.64 (d, J = 8.2 Hz, 1H), 7.70 (d, J = 8.2 Hz, 1H), 8.16 (s, 1H, H5). ^{13}C NMR ($CDCl_3$, 50 MHz) 24.9 (q, 4C, CH_3), 83.8 (s, B−O−CR_3), 101.0 (t, O−CH_2−O), 103.8 (d), 104.4 (d), 126.2 (d), 129.3 (d), 129.8 (s), 132.5 (s), 134.9 (d), 147.4 (s), 148.4 (s); C6 signal could not be detected due to low signal intensity.

*6-Bromonaphtho[2,3-d][1,3]dioxole (**68b**).* For synthesis of **68b**, a modification of a published procedure[40] was used. In a three-necked flask with magnetic stirrer and reflux condenser, **68a** (700 mg, 2.35 mmol, 1 equiv) was dissolved in methanol. Copper(II) bromide (1.57 g, 7 mmol, 3 equiv) was dissolved in water (20 mL) and added. The reaction was heated to reflux for 18 h and checked with TLC. The reaction mixture was cooled, diluted with water (200 mL), and extracted with 3 × 50 mL of DCM. The combined organic extracts were washed with 50 mL each water and brine, dried with anhydrous sodium sulfate, and evaporated.

Yield 94% (555 mg, 2.21 mmol), colorless solid, mp 135−138 °C. TLC 0.40 (LP/EE 30:1). ^{1}H NMR ($CDCl_3$, 200 MHz) δ 6.04 (s, 2H, O−CH_2−O), 7.01 (s, 1H, ArH), 7.06 (s, 1H, ArH), 7.38 (dd, J^1 = 8.7 Hz, J^2 = 1.9 Hz, 1H, H7), 7.51 (d, J = 8.7 Hz, 1H, H8), 7.79 (d, J = 1.9 Hz, 1H, H5). ^{13}C NMR ($CDCl_3$, 50 MHz) 101.3 (t, O−CH_2−O), 103.0 (d), 103.8 (d), 118.1 (s), 127.5 (d), 128.5 (d), 128.9 (d), 131.8 (s), 148.0 (s), 148.3 (s). One signal could not be detected due to low signal intensity.

*(E)-Methyl 3-(Naphtho[2,3-d][1,3]dioxol-6-yl)acrylate (**68c**).* An 8-ml vial with magnetic stirrer, screw cap, and septum was charged with **68b** (300 mg, 1.2 mmol, 1 equiv), methyl acrylate (163 μL, 1.8 mmol, 1.5 equiv), palladium(II) acetate (8 mg, 0.036 mmol, 3 mol %), and tri-*o*-tolylphosphine (22 mg, 0.072 mmol, 6 mol %) and flushed with argon. Triethylamine (0.85 mL) was added via syringe and the reaction was heated to 80 °C. TLC monitoring (eluent LP/EE 30:1) showed full conversion after 8 h. The reaction mixture was diluted with diethyl ether (30 mL). Due to low solubility of the product in diethyl ether, it was necessary to add ethyl acetate (20 mL) and DCM (10 mL) to obtain a clear solution. The organic phase was washed with 3 × 10 mL of 0.5 N HCl and 30 mL of brine and dried with sodium sulfate. Evaporation of the solvent gave the pure product in quantitative yield.

Yield 100% (310 mg, 1.2 mmol), colorless solid, mp 151−152 °C. TLC 0.16 (LP/EE 30:1). ^{1}H NMR ($CDCl_3$, 200 MHz) δ 3.81 (s, 3H, CH_3), 6.06 (s, 2H, O−CH_2−O), 6.49 (d, J = 16.0 Hz, 1H, H3), 7.10 (s, 1H, ArH), 7.12 (s, 1H, ArH), 7.50 (dd, J^1 = 8.6 Hz, J^2 = 1.6 Hz, 1H, H7′), 7.64 (d, J = 8.6 Hz, 1H, H8′), 7.74−7.83 (m, 2H, H2, H5′). ^{13}C NMR ($CDCl_3$, 50 MHz) δ 51.7 (q, CH_3), 101.3 (t, O−CH_2−O), 103.9 (d), 104.4 (d), 116.9 (d), 127.6 (d), 128.7 (d), 130.3 (s), 130.4 (s), 131.7 (s), 145.1 (d), 148.2 (s), 148.7 (s), 167.6 (d, COOR). HR-MS $[M + H]^+$ m/z (pred) = 257.0808, m/z (meas) = 257.0807, difference = −0.39 ppm.

*Naphtho[2,3-d][1,3]dioxole-5-carboxylic acid (**71a**).* For synthesis of **71a**, a modification of a published procedure[41] was used. In a two-necked flask equipped with magnetic stirrer, septum, and balloon, naphtho[2,3-*d*][1,3]dioxol-5-yl trifluoromethanesulfonate[42] (96 mg, 0.3 mmol, 1 equiv), 1,3-bis(diphenylphosphino)propane (dppp; 7 mg, 0.018 mmol, 6 mol %), and palladium(II) acetate (2 mg, 0.009 mmol, 3 mol %) were suspended in DMF/water 3:1 (1 mL). A steel cannula reaching to the bottom of the flask was used to bubble carbon monoxide through the solution for 10 min; after that, the balloon was filled with CO gas in order to maintain its supply throughout the reaction time. Hünig's base (102 μL, 0.6 mmol, 2 equiv) was added via syringe and the reaction mixture was heated to 70 °C. After 3 h, reaction control with TLC indicated complete consumption of the starting material. The reaction mixture was diluted with ethyl acetate (10 mL) and extracted with 3 × 5 mL of saturated $NaHCO_3$. The combined aqueous extracts were acidified to pH = 2 with 2 N HCl and extracted with 3 × 10 mL of ethyl acetate. The combined organic extracts were washed with 10 mL each water and brine and dried with sodium sulfate. Evaporation of the solvent gave the pure product.

dx.doi.org/10.1021/jm5002277 | J. Med. Chem. 2014, 57, 5602−5619

Yield 67% (116 mg, 0.54 mmol), colorless solid, mp 259−263 °C. TLC 0.60 ($CHCl_3$/MeOH 10%). ^{1}H NMR (acetone-d_6, 400 MHz) δ 6.17 (s, 2H, O−CH_2−O), 7.33 (s, 1H, ArH), 7.41−7.45 (m, 1H, H7), 8.00 (d, J = 8.0 Hz, 1H, ArH), 8.18 (dd, J^1 = 7.4 Hz, J^2 = 1.1 Hz, 1H, ArH), 8.49 (s, 1H, ArH). ^{13}C NMR (acetone-d_6, 100 MHz) δ 101.7 (t, O−CH_2−O), 102.2 (d), 104.1 (d), 123.1 (d), 125.7 (s), 128.9 (d), 129.2 (s), 131.6 (s), 132.4 (d), 147.6 (s), 149.5 (s), 168.2 (s, COOH).

*Methyl 5,6,7,8-Tetrahydronaphtho[2,3-d][1,3]dioxole-6-carboxylate (**75a**).* For synthesis of **75a**, a modification of a published method[42] was used. A three-necked flask with magnetic stirrer, septum, reflux condenser, and balloon was charged with 5,6-bis(bromomethyl)benzo[*d*][1,3]dioxole (2.0 g, 6.5 mmol, 1 equiv), methyl acrylate (2.94 mL, 32.5 mmol, 5 equiv), and anhydrous DMF (50 mL) and was flushed with argon. Sodium iodide (3.9 g, 26 mmol, 4 equiv) was added and the reaction was heated to 90 °C overnight (in previous experiments on a smaller scale, full conversion had been reached after 2 h). Above 70 °C the reaction mixture began to turn red. The reaction was quenched with 200 mL of water, and then, sodium thiosulfate 5% was added until the mixture became colorless. The aqueous mixture was extracted with 5 × 50 mL of methyl *tert*-butyl ether (MTBE). The organic phase was washed with 50 mL each water and brine, dried with anhydrous sodium sulfate, and evaporated.

Yield 89% (1.35 g, 5.79 mmol), colorless solid, mp 71−72 °C. TLC 0.15 (LP/EE 30:1). ^{1}H NMR ($CDCl_3$, 200 MHz) δ 1.75−1.91 (m, 1H), 2.10−2.22 (m, 1H), 2.61−2.78 (m, 3H), 2.88−2.91 (m, 2H), 3.71 (s, 3H, CH_3), 5.87 (s, 2H, O−CH_2−O), 6.53 (s, 1H, ArH), 6.55 (s, 1H, ArH). ^{13}C NMR ($CDCl_3$, 50 MHz) δ 25.9 (t, CH_2), 28.6 (t, CH_2), 31.6 (t, CH_2), 39.9 (d, C6), 51.8 (q, CH_3), 100.6 (t, O−CH_2−O), 108.5 (d), 108.6 (d), 127.6 (s), 128.5 (s), 145.7 (s), 145.9 (s), 175.8 (d, COOR)

*Methyl Naphtho[2,3-d][1,3]dioxole-6-carboxylate (**75b**).* Compound **75a** (100 mg, 0.43 mmol, 1 equiv) was dissolved in benzene (3 mL, p.a.) under argon. DDQ (242 mg, 1.07 mmol, 2.5 equiv) was added and the reaction mixture was heated to 80 °C for 2 h. TLC analysis was inconclusive due to very similar R_f values of starting material and product. Staining with cerium molybdophosphoric acid dip reagent indicated full conversion (The starting material is readily stained; the product only weakly). The reaction was quenched with 20 mL of 2 N NaOH and changed color to brown. The reaction was extracted with 3 × 10 mL of EtOAc. The organic phase was washed with water until the washings were colorless (5 × 10 mL) and subsequently washed with brine, dried over sodium sulfate, and evaporated.

Yield 73% (72 g, 0.31 mmol), colorless solid, mp 130−132 °C, sublimation above 105 °C. TLC 0.15 (LP/EE 30:1). ^{1}H NMR ($CDCl_3$, 200 MHz) δ 3.95 (s, 3H, CH_3), 6.06 (s, 2H, O−CH_2−O), 7.11 (s, 1H, ArH), 7.17 (s, 1H, ArH), 7.66 (d, J = 8.6 Hz, 1H, H8), 7.90 (dd, J^1 = 8.6 Hz, J^2 = 1.6 Hz, 1H, H7), 8.38 (d, J = 1.6 Hz, 1H, H5). ^{13}C NMR ($CDCl_3$, 50 MHz) δ 52.1 (q, CH_3), 101.4 (t, O−CH_2−O), 103.8 (d), 104.9 (d), 124.1 (d), 125.9 (s), 127.0 (d), 129.6 (s), 129.7 (d), 133.3 (s), 148.2 (s), 149.5 (s), 167.4 (d, COOR). HR-MS $[M + H]^+$ m/z (pred) = 231.0652, m/z (meas) = 231.658, difference = 2.60 ppm.

■ ASSOCIATED CONTENT

Ⓢ Supporting Information

Synthetic procedures and characterization data for piperine analogues; shell script for evaluation of costs; Python script to divide MACCS fingerprints into bite strings; parameters obtained for model 3; full composition of 10 trees in model 4; and a table with the full list of descriptors calculated. This material is available free of charge via the Internet at http://pubs.acs.org.

■ AUTHOR INFORMATION

Corresponding Author

*Phone +43-1-4277-55310; fax +43-1-4277-9553; e-mail steffen.hering@univie.ac.at.

Present Address

▽(T.S.) Institute of Medical Genetics Medical University of Vienna, Waehringerstrasse 10, 1090 Vienna, Austria.

Author Contributions

⊥A.S., L.W., and D.G. contributed equally.

Notes

The authors declare no competing financial interest.

■ ACKNOWLEDGMENTS

This work was supported by the Austrian Science Fund (FWF doctoral program "Molecular drug targets" W1232 to S.H., G.F.E., and M.D.M.). We thank Mihaela Coner for technical assistance.

■ ABBREVIATIONS USED

DEPC, diethyl pyrocarbonate; EtOAc, ethyl acetate; $GABA_A$, γ-aminobutyric acid type A receptor; I_{GABA}, γ-aminobutyric acid-induced chloride current; $I_{GABA\text{-}max}$, maximum aminobutyric acid-induced chloride current potentiation; LP, light petroleum; rt, room temperature; TRPV1, transient receptor potential vanilloid type 1 receptor; VR1, vanilloid receptor 1

■ REFERENCES

(1) Macdonald, R. L.; Olsen, R. W. GABAA Receptor Channels. *Annu. Rev. Neurosci.* **1994**, *17*, 569−602.
(2) Sieghart, W. Structure and Pharmacology of Gamma-Aminobutyric Acid A Receptor Subtypes. *Pharmacol. Rev.* **1995**, *47*, 181−234.
(3) Sigel, E.; Steinmann, M. E. Structure, Function, and Modulation of GABA(A) Receptors. *J. Biol. Chem.* **2012**, *287*, 40224−40231.
(4) Connolly, C. N.; Wafford, K. A. The Cys-Loop Superfamily of Ligand-Gated Ion Channels: The Impact of Receptor Structure on Function. *Biochem. Soc. Trans.* **2004**, *32*, 529−534.
(5) Sigel, E.; Kaur, K. H.; Luscher, B. P.; Baur, R. Use of Concatamers to Study GABAA Receptor Architecture and Function: Application to Delta-Subunit-Containing Receptors and Possible Pitfalls. *Biochem. Soc. Trans.* **2009**, *37*, 1338−1342.
(6) Smart, T. G.; Paoletti, P. Synaptic Neurotransmitter-Gated Receptors. *Cold Spring Harbor Perspect. Biol.* **2012**, *4*, No. a009662, DOI: 10.1101/cshperspect.a009662.
(7) Barnard, E. A.; Skolnick, P.; Olsen, R. W.; Möhler, H.; Sieghart, W.; Biggio, G.; Braestrup, C.; Bateson, A. N.; Langer, S. Z. International Union of Pharmacology. XV. Subtypes of Gamma-Aminobutyric Acid A Receptors: Classification on the Basis of Subunit Structure and Receptor Function. *Pharmacol. Rev.* **1998**, *50*, 291−313.
(8) Simon, J.; Wakimoto, H.; Fujita, N.; Lalande, M.; Barnard, E. A. Analysis of the Set of GABA(A) Receptor Genes in the Human Genome. *J. Biol. Chem.* **2004**, *279*, 41422−41435.
(9) Olsen, R. W.; Sieghart, W. International Union of Pharmacology. LXX. Subtypes of Gamma-Aminobutyric Acid(A) Receptors: Classification on the Basis of Subunit Composition, Pharmacology, and Function. Update. *Pharmacol. Rev.* **2008**, *60*, 243−260.
(10) Chang, Y.; Wang, R.; Barot, S.; Weiss, D. S. Stoichiometry of a Recombinant GABA Receptor. *J. Neurosci.* **1996**, *16*, 5415−5424.
(11) Tretter, V.; Ehya, N.; Fuchs, K.; Sieghart, W. Stoichiometry and Assembly of a Recombinant GABAA Receptor Subtype. *J. Neurosci.* **1997**, *17*, 2728−2737.
(12) Baumann, S. W.; Baur, R.; Sigel, E. Individual Properties of the Two Functional Agonist Sites in GABA(A) Receptors. *J. Neurosci.* **2003**, *23*, 11158−11166.
(13) Möhler, H. GABAA Receptors in Central Nervous System Disease: Anxiety, Epilepsy, and Insomnia. *J. Recept. Signal Transduction Res.* **2006**, *26*, 731−740.
(14) Macdonald, R. L.; Kang, J. Q.; Gallagher, M. J. Mutations in GABA Receptor Subunits Associated with Genetic Epilepsies. *J. Physiol.* **2010**, *588*, 1861−1869.

(15) Rudolph, U.; Knoflach, F. Beyond Classical Benzodiazepines: Novel Therapeutic Potential of GABAA Receptor Subtypes. *Nat. Rev. Drug Discovery* **2011**, *10*, 685−697.
(16) Engin, E.; Liu, J.; Rudolph, U. Alpha2-Containing GABA(A) Receptors: A Target for the Development of Novel Treatment Strategies for CNS Disorders. *Pharmacol. Ther.* **2012**, *136*, 142−152.
(17) Trincavelli, M. L.; Da Pozzo, E.; Daniele, S.; Martini, C. The GABA-BZR Complex as Target for the Development of Anxiolytic Drugs. *Curr. Trends Med. Chem.* **2012**, *12*, 254−269.
(18) Whiting, P. J. GABA-A Receptors: A Viable Target for Novel Anxiolytics? *Curr. Opin. Pharmacol.* **2006**, *6*, 24−29.
(19) Atack, J. R. The Benzodiazepine Binding Site of GABA(A) Receptors as a Target for the Development of Novel Anxiolytics. *Expert Opin. Invest. Drugs* **2005**, *14*, 601−618.
(20) Atack, J. R. GABAA Receptor Subtype-Selective Modulators. I. Alpha2/Alpha3-Selective Agonists as Non-Sedating Anxiolytics. *Curr. Top. Med. Chem.* **2011**, *11*, 1176−1202.
(21) Hosie, A. M.; Wilkins, M. E.; da Silva, H. M.; Smart, T. G. Endogenous Neurosteroids Regulate GABAA Receptors through Two Discrete Transmembrane Sites. *Nature* **2006**, *444*, 486−489.
(22) Li, G. D.; Chiara, D. C.; Sawyer, G. W.; Husain, S. S.; Olsen, R. W.; Cohen, J. B. Identification of a GABAA Receptor Anesthetic Binding Site at Subunit Interfaces by Photolabeling with an Etomidate Analog. *J. Neurosci.* **2006**, *26*, 11599−11605.
(23) D'Hulst, C.; Atack, J. R.; Kooy, R. F. The Complexity of the GABAA Receptor Shapes Unique Pharmacological Profiles. *Drug Discovery Today* **2009**, *14*, 866−875.
(24) Forman, S. A.; Miller, K. W. Anesthetic Sites and Allosteric Mechanisms of Action on Cys-Loop Ligand-Gated Ion Channels. *Can. J. Anaesth.* **2011**, *58*, 191−205.
(25) Gunn, B. G.; Brown, A. R.; Lambert, J. J.; Belelli, D. Neurosteroids and GABA(A) Receptor Interactions: A Focus on Stress. *Front. Neurosci.* **2011**, *5*, 131 DOI: 10.3389/fnins.2011.00131.
(26) Chiara, D. C.; Dostalova, Z.; Jayakar, S. S.; Zhou, X.; Miller, K. W.; Cohen, J. B. Mapping General Anesthetic Binding Site(S) in Human Alpha1beta3 Gamma-Aminobutyric Acid Type A Receptors with [(3)H]Tdbzl-Etomidate, a Photoreactive Etomidate Analogue. *Biochemistry* **2012**, *51*, 836−847.
(27) Richter, L.; de Graaf, C.; Sieghart, W.; Varagic, Z.; Morzinger, M.; de Esch, I. J.; Ecker, G. F.; Ernst, M. Diazepam-Bound GABAA Receptor Models Identify New Benzodiazepine Binding-Site Ligands. *Nat. Chem. Biol.* **2012**, *8*, 455−464.
(28) Johnston, G. A.; Hanrahan, J. R.; Chebib, M.; Duke, R. K.; Mewett, K. N. Modulation of Ionotropic GABA Receptors by Natural Products of Plant Origin. *Adv. Pharmacol. (San Diego, CA, U. S.)* **2006**, *54*, 285−316.
(29) Hanrahan, J. R.; Chebib, M.; Johnston, G. A. Flavonoid Modulation of GABA(A) Receptors. *Br. J. Pharmacol.* **2011**, *163*, 234−245.
(30) Nilsson, J.; Sterner, O. Modulation of GABA(A) Receptors by Natural Products and the Development of Novel Synthetic Ligands for the Benzodiazepine Binding Site. *Curr. Drug Targets* **2011**, *12*, 1674−1688.
(31) Zaugg, J.; Baburin, I.; Strommer, B.; Kim, H. J.; Hering, S.; Hamburger, M. HPLC-Based Activity Profiling: Discovery of Piperine as a Positive GABA(A) Receptor Modulator Targeting a Benzodiazepine-Independent Binding Site. *J. Nat. Prod.* **2010**, *73*, 185−191.
(32) Pedersen, M. E.; Metzler, B.; Stafford, G. I.; van Staden, J.; Jager, A. K.; Rasmussen, H. B. Amides from Piper Capense with CNS Activity: A Preliminary SAR Analysis. *Molecules* **2009**, *14*, 3833−3843.
(33) McNamara, F. N.; Randall, A.; Gunthorpe, M. J. Effects of Piperine, the Pungent Component of Black Pepper, at the Human Vanilloid Receptor (TRPV1). *Br. J. Pharmacol.* **2005**, *144*, 781−790.
(34) Khom, S.; Strommer, B.; Schöffmann, A.; Hintersteiner, J.; Baburin, I.; Erker, T.; Schwarz, T.; Schwarzer, C.; Zaugg, J.; Hamburger, M.; Hering, S. GABAA Receptor Modulation by Piperine and a Non-TRPV1 Activating Derivative. *Biochem. Pharmacol.* **2013**, *85*, 1827−1836.
(35) Thomsen, I.; Clausen, K.; Scheibye, S.; Lawesson, S. O. Thiation with 2,4-Bis(4-methoxyphenyl)-1,3,2,4-dithiadiphosphetane 2,4-Disulfide: N-Methylthiopyrrolidone (2-pyrrolidinethione, 1-methyl-). *Org. Synth.* **1984**, *62*, 158−164.
(36) Hayashi, K.; Yamazoe, A.; Ishibashi, Y.; Kusaka, N.; Oono, Y.; Nozaki, H. Active Core Structure of Terfestatin A, a New Specific Inhibitor of Auxin Signaling. *Bioorg. Med. Chem.* **2008**, *16*, 5331−5344.
(37) Blanchot, M.; Candito, D. A.; Larnaud, F.; Lautens, M. Formal Synthesis of Nitidine and Nk109 via Palladium-Catalyzed Domino Direct Arylation/N-Arylation of Aryl Triflates. *Org. Lett.* **2011**, *13*, 1486−1489.
(38) Cabri, W.; Candiani, I.; Bedeschi, A.; Santi, R. 1,10-Phenanthroline Derivatives: A New Ligand Class in the Heck Reaction. Mechanistic Aspects. *J. Org. Chem.* **1993**, *58*, 7421−7426.
(39) Ishiyama, T.; Takagi, J.; Hartwig, J. F.; Miyaura, N. A Stoichiometric Aromatic C-H Borylation Catalyzed by Iridium(I)/2,2′-Bipyridine Complexes at Room Temperature. *Angew. Chem., Int. Ed.* **2002**, *41*, 3056−3058.
(40) Thompson, A. L. S.; Kabalka, G. W.; Akula, M. R.; Huffman, J. W. The Conversion of Phenols to the Corresponding Aryl Halides under Mild Conditions. *Synthesis* **2005**, *2005*, 547−550.
(41) Grimm, J. B.; Wilson, K. J.; Witter, D. J. Suppression of Racemization in the Carbonylation of Amino Acid-Derived Aryl Triflates. *Tetrahedron Lett.* **2007**, *48*, 4509−4513.
(42) Plunkett, K. N.; Godula, K.; Nuckolls, C.; Tremblay, N.; Whalley, A. C.; Xiao, S. Expeditious Synthesis of Contorted Hexabenzocoronenes. *Org. Lett.* **2009**, *11*, 2225−2228.
(43) Klopman, G.; Li, J. Y. Quantitative Structure-Agonist Activity Relationship of Capsaicin Analogues. *J. Comput.-Aided Mol. Des.* **1995**, *9*, 283−294.
(44) Hall, M.; Frank, E.; Holmes, G.; Pfahringer, B.; Reutemann, P.; Witten, I. H. The Weka Data Mining Software: An Update. *SIGKDD Explorations* **2009**, *11* (1), 10−18.
(45) Gunthorpe, M. J.; Chizh, B. A. Clinical Development of Trpv1 Antagonists: Targeting a Pivotal Point in the Pain Pathway. *Drug Discovery Today* **2009**, *14*, 56−67.
(46) Marsch, R.; Foeller, E.; Rammes, G.; Bunck, M.; Kossl, M.; Holsboer, F.; Zieglgansberger, W.; Landgraf, R.; Lutz, B.; Wotjak, C. T. Reduced Anxiety, Conditioned Fear, and Hippocampal Long-Term Potentiation in Transient Receptor Potential Vanilloid Type 1 Receptor-Deficient Mice. *J. Neurosci.* **2007**, *27*, 832−839.
(47) Kaneko, Y.; Szallasi, A. Transient Receptor Potential (Trp) Channels: A Clinical Perspective. *Br. J. Pharmacol.* **2013**, DOI: 10.1111/bph.12414.
(48) Goldin, A. L. In *Expression and Analysis of Recombinant Ion Channels: From Structural Studies to Pharmacological Screening*; Clare, J. J., Trezise, D. J., Eds.; Wiley−VCH Verlag: Weinheim, Germany, 2006; pp 1−25.
(49) Khom, S.; Baburin, I.; Timin, E. N.; Hohaus, A.; Sieghart, W.; Hering, S. Pharmacological Properties of GABAA Receptors Containing Gamma1 Subunits. *Mol. Pharmacol.* **2006**, *69*, 640−649.
(50) Baburin, I.; Beyl, S.; Hering, S. Automated Fast Perfusion of Xenopus Oocytes for Drug Screening. *Pfluegers Arch.* **2006**, *453*, 117−123.
(51) Demel, M. A.; Kraemer, O.; Ettmayer, P.; Haaksma, E.; Ecker, G. F. Ensemble Rule-Based Classification of Substrates of the Human ABC-Transporter ABCB1 Using Simple Physicochemical Descriptors. *Mol. Inf.* **2010**, *29*, 233−242.
(52) Kohavi, R.; Provost, F. Glossary of Terms. *Mach. Learn.* **1998**, *30*, 271−274.
(53) Oprea, T. I. Property Distribution of Drug-Related Chemical Databases. *J. Comput.-Aided Mol. Des.* **2000**, *14*, 251−264.
(54) Wildman, S. A.; Crippen, G. M. Prediction of Physicochemical Parameters by Atomic Contributions. *J. Chem. Inf. Model.* **1999**, *39*, 868−873.

4.4 Paper IV
Probing the Potential of Valerenic Acid and Derivatives as Scaffolds for the Development of Novel Anticonvulsants

Khom, S., **Hintersteiner, J.***, Luger, D.*, Haider, M., Pototschnig, G., Schwarzer, C., Mihovilovic, MD., Hering, S. *Probing the Potential of Valerenic Acid and Derivatives as Scaffolds for the Development of Novel Anticonvulsants.*

(*) Both authors contributed equally to the paper
Status: Paper draft in preparation, **version 2015 July 14**

Contribution

- Effects on explorative behavior by means of the EPM and LDT test
- Effects on locomotor activity by means of the OF test (Assistance)
- Effects on seizure threshold by means of PTZ-tail vein infusion (Assistance)

Probing the potential of valerenic acid and derivatives as scaffolds for the development of novel anticonvulsants

Khom, S. [1], Hintersteiner, J. [1]*, Luger, D. [1]*, Haider, M. [3], Pototschnig, G. [3], Schwarzer, C. [2], Mihovilovic, MD. [3], Hering, S[1].

[1]*Department of Pharmacology and Toxicology, University of Vienna, Althanstraße 14, A-1090 Vienna, Austria*
[2]*Department of Pharmacology, Medical University of Innsbruck, Peter-Mayr-Str. 1a, A-6020 Innsbruck*
[3]*Institute of Applied Synthetic Chemistry, Vienna University of Technology, Getreidemarkt 9, A-1060 Vienna, Austria*

Short running title
VA derivatives as novel anticonvulsants

Authors' contributions

S.K., C.S. and S.H. designed the research study; S.K., D.L., J.H and C.S performed research; S.K., D.L., J.H. and C.S. analyzed data; M.H, G.P. and M.D.M contributed novel research reagents. S.K. and S.H. wrote the manuscript. All authors read and approved the last version of the manuscript.

Abstract

Background and Purpose:

Valerenic acid (VA) is a β2/3-selective modulator of γ-aminobutyric acid (GABA) type A ($GABA_A$) receptors with anxiolytic and anticonvulsive effects in mice devoid of concomitant sedation making this compound an interesting drug candidate. In the present study, effects on seizure threshold and locomotor activity by a focused library of VA derivatives were studied to probe whether these compounds may represent structural scaffolds for the development of novel anticonvulsants.

Experimental approach:

Enhancement of GABA-induced chloride currents (I_{GABA}) by VA derivatives was determined in *Xenopus laevis* oocytes expressing α1β1γ2S, α1β2γ2S, or α1β3γ2S receptors. Effects on pentylenetetrazole-induced seizure threshold and locomotion were studied using male C57BL/6N mice and compared to saline-treated control animals.

Key results:

More potent and/or more efficacious I_{GABA} enhancement by β2/3-selective VA derivatives (VA-A, VA-MA and VA-TET) *in vitro* resulted in more pronounced elevation of PTZ-induced seizure threshold at low doses. In contrast, non-selective compounds were *in vivo* either inactive or displayed anticonvulsive effects only at high doses. Reduced locomotor activity at high doses was observed after application of VA-A, VA-MA and VA-TET.

Conclusions and implications:

Collectively, these data indicate that enhanced *in vitro* efficacy and potency of VA derivatives are associated with more pronounced anticonvulsive effects. Furthermore, efficacy of VA derivatives at β3-containing receptors is likely to correlate with seizure threshold elevation, while efficacy at β2-containing receptors is reflected in reduction of locomotor activity. Hence, VA derivatives preferentially targeting $GABA_A$ receptors containing β3-subunits might represent scaffolds for the development of novel anticonvulsants with limited side effects.

Introduction

Interaction of γ-aminobutyric acid (GABA) with GABA type A ($GABA_A$) receptors forms the basis of the majority of fast inhibitory neurotransmission in the mammalian brain (Olsen and Sieghart, 2008; Sigel and Steinmann, 2012). Like other members of the family of pentameric ligand-gated ion channels (pLGIC), $GABA_A$ receptors are constituted by pseudosymmetrical assembly of five identical or homologous subunits forming a chloride-conducting ion pore (Miller and Aricescu, 2014). The human genome comprises genes encoding for 19 different $GABA_A$ receptor subunits (α1-6, β1-3, γ1-3, δ, ε, ρ1-3, π and θ; Simon et al., 2004) theoretically allowing the formation of multiple $GABA_A$ receptor subtypes (Barnard et al., 1998; Olsen and Sieghart, 2008). Most notably, the receptor's subunit composition determines its pharmacological properties including agonist sensitivity as well as its sensitivity for drugs (Sieghart and Sperk, 2002). In addition, the highly specific cellular and subcellular distribution of $GABA_A$ receptor subunits/subtypes (Olsen and Sieghart, 2008; Pirker et al., 2000; Schwarzer et al., 2001) and in particular the assignment of therapeutic effects of commonly applied $GABA_A$ receptor modulators such as benzodiazepines (Möhler et al., 2001; Rudolph et al., 2001; Rudolph and Knoflach, 2011; Rudolph and Möhler, 2014) or anaesthetics (Jurd et al., 2003) to single $GABA_A$ receptor subunits raises the possibility to develop drugs selectively targeting specific brain circuits. Such subunit-selective $GABA_A$ receptor modulators are predicted to display the desired therapeutic effects devoid or at least with reduced side effects.

Valerenic acid (VA) – a sesquiterpenoid compound found in common *Valerian* – selectively modulates γ-aminobutyric acid (GABA) type A ($GABA_A$) receptors containing β_2- or β_3-subunits, while displaying only negligible effects on $GABA_A$ receptors comprising β_1-subunits (Khom et al., 2007). *In vivo*, VA induces anxiolytic (Benke et al., 2009; Khom et al., 2010) and anticonvulsive (Hintersteiner et al., 2014) effects. Most notably, VA does not significantly reduce locomotor activity even at high doses (Khom et al., 2010).

These findings combined with a promising pharmacokinetic profile (Sampath et al., 2012) make VA an interesting drug candidate. Previously, we have reported more pronounced anxiolytic and/or anticonvulsive effects by selected VA amide (Khom et al., 2010) and ester derivatives (Hintersteiner et al., 2014). In contrast to VA ester derivatives that are nearly inactive *in vitro* and thus might act as prodrugs releasing VA, VA amide derivatives displayed pronounced enhancement of $GABA_A$ receptors composed of α1β3 subunits expressed in *Xenopus* oocytes (Khom et al., 2010; Kopp et al., 2010).

Therefore, to evaluate the potential of VA amide derivatives as scaffold for the development of novel anticonvulsants, we analyzed β-subunit-dependent modulation of GABA-induced chloride currents (I_{GABA}) in *Xenopus laevis* oocytes expressing α1β1γ2S, α1β2γ2S or α1β3γ2S receptors by a small focused library of VA derivatives followed by a detailed *in vivo* investigation of their effects on pentylenetetrazole (PTZ)-induced seizure threshold and locomotor activity in male C57BL/6N mice.

Our study clearly shows that the amide (VA-A), methylamide (VA-MA) and tetrazole derivative (VA-TET) of VA derivatives modulating $GABA_A$ receptors more efficaciously and/or potently than VA also displayed significantly more pronounced elevation of PTZ-induced seizure threshold *in vivo*. These VA derivatives, however, also reduced locomotor activity at rather high doses. Correlating efficacy of I_{GABA} modulation and *in vivo* activity revealed a significant correlation of seizure threshold elevation and I_{GABA} modulation of β3-containing receptors, while impairment of locomotor activity is likely to correlate with efficacy at β2-containing receptors.

Hence, VA derivatives preferentially modulating $GABA_A$ receptors containing β3-subunits may represent structural scaffolds for the development of novel anticonvulsants with limited sedative side effects.

Materials and Methods

Animals

All procedures involving animals were approved by the Austrian Federal Ministry of Science and Research in compliance with the European convention for the protection of vertebrate animals used for experimental and other scientific purposes ETS no.: 123. Every effort was taken to minimize the number of animals used in this study.

Female *Xenopus laevis* frogs were purchased from NASCO (Fort Atkinson, USA) and kept in groups in temperature-controlled, continuous-flow water tanks (20±1°). Male mice (C57BL/6N) were obtained from Charles River Laboratories (Sulzfeld, Germany). Mice were group-housed (maximum 5 mice per type IIL cage) with free access to food and water. At least 24h before the commencement of experiments, they were transferred to the testing facility, continuing *ad libitum* access to food and water.

The temperature in the holding (for mice and frogs) and testing facilities was fixed to 22±2°C; the humidity ranged between 40-60%; a 12h light-dark cycle was in operation (lights on from 07.00 to 19.00).

Chemicals

All chemicals used in this study were obtained from Sigma Aldrich (Vienna, Austria) except were stated otherwise. Valerenic acid (VA) was purchased from HWI Pharma Solutions (Rülzheim, Germany). VA derivatives (structural formulae are depicted in Fig.1) were synthesized as previously described (Khom et al., 2010; Kopp et al., 2010). Stock solutions (100mM for *in vitro* experiments and 1mg/10µl for *in vivo* experiments, respectively) were prepared in 100% dimethylsulfoxide (DMSO). VA and its derivatives were used up to a concentration of 500µM in *in vitro* experiments. Equal amounts of DMSO were present in control and compound-containing solutions. The maximum DMSO concentration in the bath (0.5%) did not affect I_{GABA}. For *in vivo* experiments, working concentrations were adjusted by dilution with 0.9% sodium chloride; the final concentration of DMSO was fixed to 10% including control solutions. To enhance solubility of the compound Tween 80 (3% final concentration) was added to all solutions. pH was adjusted to 7.2-7.4 with 1M sodium hydroxide. All solutions were freshly prepared every day prior to experiments.

Expression and functional characterization of $GABA_A$ receptors

Preparation of stage V-VI oocytes from *Xenopus laevis* (NASCO, Fort Atkinson, USA), synthesis of capped off run-off poly(A^+) rat cRNA transcripts from linearized cDNA templates (pCMV vector) was performed as described elsewhere (Khom et al., 2006). Briefly, female *Xenopus laevis* were anaesthetized by exposing them for 15min to a 0.2% solution of MS-222 (methane sulfonate salt of 3-aminobenzoic acid ethyl ester) before surgically removing parts of the ovaries. Follicle membranes from isolated oocytes were enzymatically digested with 2mg/ml collagenase (Type 1A). Oocytes were stored at 18°C in ND96 solution (Methfessel et al., 1986). After isolation, oocytes were injected with about 10-50nl of nuclease-free water containing the different rat cRNAs (100-2000ng/µl/subunit). For expression of $\alpha_1\beta_3\gamma_{2S}$ receptors, cRNAs were mixed in a ratio of 1:1:10 (Boileau et al., 2002); to avoid formation of homooligomeric β_1-receptors in the case of $\alpha_1\beta_1\gamma_{2S}$ a ratio of 3:1:10 was used (Krishek et al., 1996). Electrophysiological experiments were done using the two-microelectrode-voltage-clamp-technique at a holding potential of -70 mV making use of a TURBO TEC 01C amplifier (npi electronic, Tamm, Germany) and an Axon Digidata 1322A interface (Molecular Devices, Sunnyvale, CA). Data acquisition was carried out using pCLAMP v.9.2 (Molecular Devices, Sunnyvale, CA). The bath solution contained 90mM NaCl, 1mM KCl, 1mM $MgCl_2 \cdot 6H_2O$, 1mM $CaCl_2$ and 5mM HEPES (pH 7.4). Microelectrodes were filled with 2M KCl and had resistances between 1 and 3 MΩ.

Perfusion system

GABA and drugs were applied by means of fast perfusion system; drug or control solutions were applied by means of a TECAN Miniprep 60 permitting automation of the experiments. To elicit I_{GABA} the chamber was perfused with 120 µl of GABA-containing solution at volume rate between 300 and 1000 µl/s. The I_{GABA} rise time ranged between 100 and 250ms (Khom et al., 2006). To account for possible slow recovery from increasing levels of desensitization in the presence of high compound concentrations, the duration of washout periods was extended stepwise, i.e. 1 min (GABA EC_{3-7}) to 1.5 min (co-application of GABA EC_{3-7} in the presence ≤ 1µM compound) to 2.5 min (co-application of GABA EC_{3-7} in the presence of ≤10 µM compound) to 5min (co-application of GABA EC_{3-7} and ≤ 100µM compound) to 15min (GABA EC_{3-7} in the presence of 300-500µM compound). Potential run-down or run-up effects were ruled out by application of GABA control at the end of each experiment. Oocytes with maximal current amplitudes >5µA were discarded to exclude voltage-clamp errors.

Analyzing concentration-response curves

Stimulation of chloride currents by modulators of the $GABA_A$ receptor was measured at a GABA concentration eliciting between 3 and 7% of the maximal current amplitude ($EC_{3–7}$). The EC_{3-7} was determined at the beginning of the experiment for each oocyte by application of 1mM GABA followed by submaximal GABA concentrations. Enhancement of the chloride current was defined as $(I_{(GABA+Comp)}/I_{GABA}) - 1$, where $I_{(GABA+Comp)}$ is the current response in the presence of compound and I_{GABA} is the control GABA current. Concentration-response curves were generated and the data were fitted by non-linear regression analysis using Origin software (OriginLab Corporation, USA). Data were fitted to the Hill equation:

$$y=A1+(A2-A1)*x^n/(k^n+x^{nH})$$

k corresponds to the EC_{50} value, x values are logs of concentration, and n_H is the Hill coefficient. Each data point represents the mean ± SEM from at least 5 oocytes and ≥ 2 oocyte batches.

In vivo characterization of VA derivatives

Only male C57BL/6N (age 3-6 months) were used in the tests described below. Intraperitoneal (i.p.) injection of control or compound-containing solutions was done 30min before the test. Application of the solvent alone did not influence animal behavior. All doses are indicated as mg/kg bodyweight of the animal.

Seizure threshold

Seizure threshold was determined by pentylenetetrazole (PTZ) tail-vein infusion on freely moving animals at a rate of 100µl/min (10 mg/ml PTZ in saline, pH=7.4). Infusion was stopped when animals displayed generalized clonic seizures. Animals were immediately killed by cervical displacement after onset of seizures. The seizure threshold dose was calculated from the infused dose in relation to body weight (mg/kg).

Open-field-test

Exploration of a novel environment was tested over 10min in a 50x50cm box build from gray PVC equipped with infra-red beams. Illumination intensity was set to 150 lux in the center. Animals' motor activity was analyzed using ActiMot-2 equipment and software (TSE-systems, Bad Homburg, Germany).

Correlation and statistical analysis

Statistical significance was calculated applying paired students t-test and one-way ANOVA followed by a post-hoc mean comparison with Bonferroni, respectively (OriginLab Corporation, USA or GraphPad, La Jolla, USA). *P*-values of <0.05 were accepted as statistically significant. All data are given as mean ± SEM. Efficacy at different $GABA_A$ receptor subtypes to effects on seizure threshold and locomotion was correlated by Spearman correlation (GraphPad, La Jolla, USA).

Results

Assessing β-subunit-dependency of I_{GABA} modulation by valerenic acid and VA derivatives

$GABA_A$ receptors composed of α1β1γ2S, α1β2γ2S or α1β3γ2S subunits were expressed in *Xenopus laevis* oocytes and modulation of GABA-induced chloride currents (I_{GABA}, GABA EC_{3-7}) by valerenic acid and seven carboxyl-group modified derivatives was analyzed by means of the 2-microelectrode voltage clamp technique (for structural formulae of investigated VA derivatives, see Fig. 1). Amidation of VA (VA-amide, VA-A, $E_{max(α1β2γ2S)}$: 1119±72%, n=6) and subsequent mono-methylation of VA-A (VA-mono-methylamide, VA-MA, $E_{max(α1β2γ2S)}$: 917±36%, n=3) resulted in significantly stronger enhancement of I_{GABA} through β2- and β3-subunit-containing receptors, while modulation of I_{GABA} trough β1-containing receptors by VA-A was comparably to VA. VA-A yielded efficacies of $E_{max(α1β1γ2S)}$: 218±78%, n=6 vs. $E_{max(α1β2γ2S)}$: 1119±72%, n=6 and $E_{max(α1β3γ2S)}$: 972±69%, n=6, respectively ($p<0.05$; Fig.2C and D) and VA-MA ($E_{max(α1β1γ2S)}$: 387±56%, n=5 vs. $E_{max(α1β2γ2S)}$: 917±36%, n=3 and $E_{max(α1β3γ2S)}$: 1043±57%, n=5, respectively ($p<0.05$; Fig. 2E and F).

Replacement of the carboxyl-moiety by the bioisosteric tetrazole group (VA-TET) significantly increased efficacy on α1β2γ2S ($E_{max(α1β2γ2S)}$: 1091±87%, n=5) receptors though with a slightly reduced potency compared to VA, while efficacy of I_{GABA} enhancement on α1β1γ2S ($E_{max(α1β1γ2S)}$: 176±43%, n=7) and α1β3γ2S ($E_{max(α1β2γ2S)}$: 668±57%, n=8; Fig.2G) receptors did not differ from that of the parent compound (see Fig. 2 for representative current traces for β-subunit-dependent I_{GABA} enhancement by (B) VA, (D) VA-A (F) VA-MA and (H) for VA-TET; data for I_{GABA} enhancement of $GABA_A$ channels composed of α1β3γ2S subunits, data from *Luger et al. submitted;* for data with VA-TET compare Kopp et al., 2010). Similarly, substituting VA's carboxyl group by a nitrile (VA nitrile, VA-CN) did not affect β2/3-subunit-selective I_{GABA} potentiation: I_{GABA} enhancement by VA-CN through α1β1γ2S ($E_{max(α1β1γ2S)}$: 55±14%, n=7), α1β2γ2S ($E_{max(α1β2γ2S)}$:765±117%, n=4) and α1β3γ2S ($E_{max(α1β3γ2S)}$: 522±114%, n=7) channels, respectively, was similar to that of VA; however, a trend towards slightly decreased potency on β2- and β3-subunit containing receptors was observed (see Fig.3A).

Most notably, introducing bulkier residues such as mono-ethylamide (VA-EA), di-methylamide (VA-DMA) or di-ethylamide (VA-DEA) significantly elevated efficacy on $β_1$-containing receptors (VA-DMA $E_{max(α1β1γ2S)}$: 305±67%, n=6: VA-EA: $E_{max(α1β1γ2S)}$: 458±124%, n=5; and VA-DEA $E_{max(α1β1γ2S)}$: 318±84%, n=7) comparable to the estimated

efficacies on β2- and β3-containing receptors, respectively indicating a loss of subunit-selectivity (Fig.3B-D). Data for maximal I_{GABA} enhancement (E_{max}), EC_{50}, Hill-coefficients (n_H) and number of experiments for all receptor subunit compositions tested are summarized in Table 1.

β-subunit-selectivity of VA derivatives determines pentylenetetrazole (PTZ)-induced seizure threshold

Hintersteiner et al. (2014) reported that the elevation of PTZ-induced seizure threshold by VA (3mg/kg bodyweight) is most pronounced 30min after application. In the present study, dose-dependent effects of VA on seizure threshold were determined. As depicted in Fig.4A, VA did not alter seizure threshold at doses <3mg/kg bodyweight; in contrast, pronounced seizure threshold elevation was observed after application of VA at a dose of 3 or 10 mg/ kg bodyweight (control: 40.4±1.4 mg/kg PTZ, n=6 vs. VA 3 mg/kg: 47.7±1.4 mg/kg PTZ, n=4, $p<0.01$ and VA 10 mg/kg: 49.0±1.8 mg/kg PTZ, n=4; $p<0.05$, respectively; data for seizure threshold elevation by VA at a dose of 3 mg/kg bodyweight are taken from Hintersteiner et al., 2014). Notably, seizure threshold of animals treated with VA at a dose of 30 mg/kg bodyweight did not differ significantly from diluent-treated control animals (30 mg/kg VA: 43.4±1.8 mg/kg PTZ, n=3, $p>0.05$; Fig. 4A). Compared to VA, VA-A exerted significantly more pronounced anticonvulsive activity at doses ≥3mg/kg (see Fig. 4B, VA-A 3 mg/kg: 57.9±1.9 mg/kg PTZ, n=4; VA-A 10 mg/kg: 55.4±0.7 mg/kg PTZ, n=4, $p<0.001$). Like the parent compound also VA-A displayed a trend towards dropping anticonvulsive activity at higher doses (Fig.4B, VA-A 30 mg/kg: 50.6±2.2 mg/kg PTZ, n=3, $p<0.01$).

A similar bell-shaped dose-response curve on PTZ-induced seizure threshold was observed for VA-TET: at a dose of 0.3 mg/kg bodyweight (Fig.4C: VA-TET 0.3 mg/kg: 47.3±0.5 mg/kg PTZ, n=5, $p<0.05$) VA-TET's anticonvulsive activity was comparable to that of VA at 10-fold higher doses indicating a significantly increased potency, however also VA-TET at doses ≥1mg/kg lost its anticonvulsive properties.

The methylated VA-A derivative (VA-MA) induced the most pronounced increase in seizure threshold of all tested compounds; first significant effects were observed at a dose of 10 mg/kg (Fig. 4D: VA-MA 10 mg/kg: 50.4±1.4 mg/kg PTZ, n=4, $p<0.001$). In contrast to VA, VA-A and VA-TET, application of higher doses (i.e. 30 mg/kg) VA-MA resulted in an even further elevated seizure threshold (VA-MA 30 mg/kg: 63.6±2.5 mg/kg PTZ, n=3, $p<0.001$).

As shown in Fig. 4F, G and H, higher doses of VA-EA, VA-DEA and VA-CN were required for seizure threshold elevation similar to that of VA (compare VA 3mg/kg: 47.7±1.4 PTZ,

n=4 vs. Fig. 4H: VA-CN 10 mg/kg: 51.1±0. 6mg/kg PTZ, n=3 vs. Fig. 4F: VA-EA 30 mg/kg: 55.6±0.4 mg/kg PTZ, n=4 vs. Fig.4G: VA-DEA: 48.7±1.7 mg/kg PTZ, n=3).

Seizure threshold of mice treated with VA-DMA (Fig. 4E) did not significantly differ at any tested dose from diluent-treated control littermates.

Effect of VA derivatives on locomotion in the open field test

As illustrated in Fig. 5A, locomotor activity of VA-treated mice did not differ significantly from control animals at any tested dose in the open field test (control: 38.3±1.5m, n=25 vs. VA 3mg/kg: 34.9±1.3m, n=12 vs. VA 3 mg/kg: 38.7±2.1m, n=16 vs. VA 10 mg/kg: 38.0±1.4 m, n=16 vs. VA 30mg/kg: 37.6±2.5m, n=16).

Application of VA derivative VA-A at doses of 1 mg/kg and 3 mg/kg bodyweight, respectively, did also not affect total distance covered compared to control littermates; however, reduced locomotor activity in the open field test was measured after application of VA-A at doses ≥10 mg/kg (control: 38.3±1.5m, n=25 vs. VA-A 10 mg: 29.9±2.6%, n=11, $p<0.05$ vs. VA-A 30mg/kg: 23.5±2.2m, n=18, $p<0.001$; see Fig. 5B).

Like VA-A, derivatives VA-TET (Fig. 5C), VA-MA (Fig. 5D) and VA-CN (Fig. 5E) did not affect locomotor activity at low doses (≤10 mg/kg), however, at high doses reduced ambulation was observed for these compounds (control: 38.3±1.5m, n=25 vs. VA-TET 30 mg/kg: 19.2±2.1m, n=13, $p<0.001$ vs. VA-MA 30 mg/kg: 29.7±2.0, n=12, $p<0.01$ vs. VA-CN 30mg/kg: 31.5±1.5m, n=14 $p<0.05$).

Finally, analysis of total distance did not reveal any significantly different behavior of animals treated with any dose of the β-subunit-unselective VA derivatives VA-DMA (Fig. 5F), VA-EA (Fig. 5G) and VA-DEA (Fig. 5H) or diluent-treated control animals.

Discussion

Subunit-selective $GABA_A$ receptor modulators are expected to exhibit a therapeutic profile with fewer side effects and thus represent interesting lead structures for drug development. The natural compound valerenic acid (VA) selectively modulates $GABA_A$ receptors comprising either β2- or β3-subunits with only residual modulatory activity on $GABA_A$ receptors comprising β1-subunits at high concentrations (Benke et al., 2009; Khom et al., 2007). This selectivity profile combined with pronounced anticonvulsive effects (Hintersteiner et al., 2014) accompanied by anxiolytic activity (Benke et al., 2009; Khom et

al., 2010) and devoid of significant impairment of locomotor activity makes VA and potentially also its derivatives promising drug candidates.

Previously, we and others have reported more efficacious and/or potent modulation of $GABA_A$ receptors expressed in *Xenopus* oocytes by carboxyl-modified VA derivatives (Khom et al., 2010; Kopp et al., 2010). Furthermore, more pronounced anxiolytic effects by the amide derivative of VA (VA-A) (Khom et al., 2010) as well as stronger anxiolytic and anticonvulsive effects of VA ester derivatives compared to VA were observed (Hintersteiner et al., 2014).

To further evaluate the potential of VA and selected derivatives as structural scaffolds for the development of novel anticonvulsants with limited impairment of locomotor activity, we determined β-subunit-dependency of I_{GABA} modulation by seven selected carboxyl-modified VA derivatives (for structural formulae, see Fig.1) and subsequently analyzed the compounds' effects on PTZ-induced seizure threshold and on locomotion.

Anticonvulsive effects by VA derivatives correlate with positive modulation of β3-containing receptors

Our study shows that both amidation and subsequent methylation of the amide, respectively, yielding compounds VA-A and VA-MA, significantly increased efficacy and potency of I_{GABA} enhancement of β2- and β3-containing receptors compared to VA (compare Fig.2A, 2C and 2E). In line with the more pronounced I_{GABA} enhancement *in vitro*, seizure threshold elevation was also more pronounced compared to VA (compare Fig. 4A, 4B and 4D). However in contrast to VA, reduced locomotor activity – even though significantly weaker than after diazepam-treatment (3mg/kg bodyweight; data not shown) - was observed suggesting concomitant sedative effects of VA-A and VA-MA (compare Fig. 5A, 5B and 5D). Like VA-A, derivative VA-TET modulated I_{GABA} through β3-containing receptors more potently than VA, while efficacy of I_{GABA} enhancement was comparable with that of VA; most notably, I_{GABA} modulation through β2-containing receptors was significantly more pronounced (Fig. 2G). In line with these findings, VA-TET was also significantly more potent than VA *in vivo* while the extent of seizure threshold elevation was comparable to that of VA (compare Fig. 4A and Fig. 4C). VA-TET, however, also induced the most marked reduction of locomotor activity of all tested VA derivatives (Fig. 5C).

Efficacy and potency of I_{GABA} enhancement (α1β1-3γ2S) by the nitrile derivative (VA-CN) did not differ significantly from that of VA. A trend towards – although not reaching statistical significance- reduced potency for β1- and β3-containing receptors compared to VA

was observed (Fig. 3A). Similarly, higher doses of VA-CN were required for seizure threshold elevation (Fig. 4H) and additionally, VA-CN also slightly reduced locomotion at high doses (Fig. 5E).

A loss of β-subunit-selectivity (i.e. significantly increased modulatory activity at β1-containing receptors, while efficacy and potency of I_{GABA} enhancement through β2- and β3-containing receptors was comparable to VA) was observed for the three remaining VA derivatives in this study (Fig. 3B-C): Residual anticonvulsive effects – even though pronounced, but occurring at rather high doses- were observed for VA-EA (Fig. 4F) and VA-DEA (Fig. 4G), no effects on locomotion as well as no significant behavioral effects by VA-DMA were measured at any tested dose.

Correlating maximal seizure threshold elevation versus efficacy of I_{GABA} enhancement at different subunit compositions revealed a significant correlation between the compounds' efficacy at β3-containing receptors and anticonvulsive effects. Derivatives enhancing I_{GABA} at β3-containing receptors more efficaciously than VA also displayed stronger protection against PTZ-induced seizures (*Pearson's r*=0.84397; see Fig. 6A). Conversely, efficacy at neither β2- nor β1-containing receptors correlated with the extent of seizure threshold elevation. However, VA derivatives modulating β2-containing receptors more efficaciously also induced more pronounced impairment of locomotor activity (*Pearson's r*=-0.92782; Fig. 6B), while neither efficacy nor potency of VA and its derivatives on β1- or β3-containing receptors apparently correlated with occurring sedation.

These data suggest that the motor-impairing effects (probably sedation) of VA derivatives are mostly dependent on β2-containing receptors, while their anticonvulsive effects are predominantly mediated by receptors containing β3-subunits. Indeed, there is compelling evidence for the role of β2-containing receptors in mediating sedative effects of $GABA_A$ receptor modulators such as loreclezole (Groves et al., 2006), etomidate (Reynolds et al., 2003; Zeller et al., 2005) or even benzodiazepines (Antkowiak, 2015). In contrast, anticonvulsive effects of $GABA_A$ receptor ligands apparently result from a broader, less selective modulation of GABAergic neurotransmission including more than a single $GABA_A$ receptor subtype: Rudolph et al. have shown that anticonvulsive effects of diazepam are only partially blunted in α1His101R mice indicating that also α2, α3 and/or α5-containing $GABA_A$ receptors mediate anticonvulsive effects *in vivo* (Crestani et al., 2002; Fradley et al., 2007; Löw et al., 2000; Rudolph et al., 1999). In line with our data, the β2/3-selective $GABA_A$ receptor ligand loreclezole retained – even though reduced - seizure-protecting activity in β2N265S mice suggesting a role for β3-containing receptors in mediating anticonvulsive

effects (Groves et al., 2006). Most notably, the expression of β3-subunits is particularly high in dendritic regions of the hippocampus and dentate gyrus (Hörtnagl et al., 2013; Miralles et al., 1999; Sperk et al., 1997). Assuming the fundamental role of the hippocampus in the pathophysiology of seizures and epilepsy (Coulter et al., 2011; Schwartzkroin, 1994; Sendrowski and Sobaniec, 2013; Sperk et al., 1997), it is thus likely that selectively enhancing GABAergic neurotransmission in the hippocampus via β3-containing receptors might represent an alternative approach to develop anticonvulsants with reduced side effects including sedation. Whether it is possible to synthesize $GABA_A$ receptor modulators based on the VA scaffold discriminating between β2- and β3-subunits will be in the scope of future studies. Even though this chemical approach might be challenging, it is apparently not impossible to achieve such a subunit-selectivity. In a recent study, the isothiazol GABA analogue thio-THIP (4,5,6,7-tetrahydroisothiazolo[5,4-*c*]pyridin-3-ol) was reported to be the first $GABA_A$ ligand displaying different potencies and efficacies for β2- and β3-containing receptors *in vivo* (Hoestgaard-Jensen et al., 2014).

Conclusion

Taken together, our study provides further evidence that anticonvulsive and sedative effects of $GABA_A$ modulators might not be inevitably linked. Thus, the development of positive allosteric modulators selectively or preferentially interacting with β3-containing receptors might represent interesting structural scaffold for the development of novel anticonvulsants lacking sedative side effects.

Acknowledgments

The authors wish to thank the Austrian Science Fund (FWF) for financial support (P-22395, TRP-107; D. Luger, J. Hintersteiner and Gerit Pototschnig are fellows of the FWF-funded doctoral program "Ion channels and transporters as drug targets" W-1232). Technical assistance by Lisa Holler, Helga Dobernig, Daniela Hrabak, Maria Magdalena Müllner and Erwin Kirnbauer is greatly acknowledged.

References

Antkowiak, B., 2015. Closing the gap between the molecular and systemic actions of anesthetic agents. Adv. Pharmacol. San Diego Calif 72, 229–262. doi:10.1016/bs.apha.2014.10.009

Barnard, E.A., Skolnick, P., Olsen, R.W., Mohler, H., Sieghart, W., Biggio, G., Braestrup, C., Bateson, A.N., Langer, S.Z., 1998. International Union of Pharmacology. XV. Subtypes of gamma-aminobutyric acidA receptors: classification on the basis of subunit structure and receptor function. Pharmacol. Rev. 50, 291–313.

Benke, D., Barberis, A., Kopp, S., Altmann, K.-H., Schubiger, M., Vogt, K.E., Rudolph, U., Möhler, H., 2009. GABA A receptors as in vivo substrate for the anxiolytic action of valerenic acid, a major constituent of valerian root extracts. Neuropharmacology 56, 174–181. doi:10.1016/j.neuropharm.2008.06.013

Coulter, D.A., Yue, C., Ang, C.W., Weissinger, F., Goldberg, E., Hsu, F.-C., Carlson, G.C., Takano, H., 2011. Hippocampal microcircuit dynamics probed using optical imaging approaches. J. Physiol. 589, 1893–1903. doi:10.1113/jphysiol.2010.202184

Crestani, F., Keist, R., Fritschy, J.-M., Benke, D., Vogt, K., Prut, L., Blüthmann, H., Möhler, H., Rudolph, U., 2002. Trace fear conditioning involves hippocampal alpha5 GABA(A) receptors. Proc. Natl. Acad. Sci. U. S. A. 99, 8980–8985. doi:10.1073/pnas.142288699

Fradley, R.L., Guscott, M.R., Bull, S., Hallett, D.J., Goodacre, S.C., Wafford, K.A., Garrett, E.M., Newman, R.J., O'Meara, G.F., Whiting, P.J., Rosahl, T.W., Dawson, G.R., Reynolds, D.S., Atack, J.R., 2007. Differential contribution of GABA(A) receptor subtypes to the anticonvulsant efficacy of benzodiazepine site ligands. J. Psychopharmacol. Oxf. Engl. 21, 384–391. doi:10.1177/0269881106067255

Groves, J.O., Guscott, M.R., Hallett, D.J., Rosahl, T.W., Pike, A., Davies, A., Wafford, K.A., Reynolds, D.S., 2006. The role of GABAbeta2 subunit-containing receptors in mediating the anticonvulsant and sedative effects of loreclezole. Eur. J. Neurosci. 24, 167–174. doi:10.1111/j.1460-9568.2006.04890.x

Hintersteiner, J., Haider, M., Luger, D., Schwarzer, C., Reznicek, G., Jäger, W., Khom, S., Mihovilovic, M.D., Hering, S., 2014. Esters of valerenic acid as potential prodrugs. Eur. J. Pharmacol. 735, 123–131. doi:10.1016/j.ejphar.2014.03.019

Hoestgaard-Jensen, K., Dalby, N.O., Krall, J., Hammer, H., Krogsgaard-Larsen, P., Frølund, B., Jensen, A.A., 2014. Probing α4βδ GABAA receptor heterogeneity: differential regional effects of a functionally selective α4β1δ/α4β3δ receptor agonist on tonic and phasic inhibition in rat brain. J. Neurosci. Off. J. Soc. Neurosci. 34, 16256–16272. doi:10.1523/JNEUROSCI.1495-14.2014

Hörtnagl, H., Tasan, R.O., Wieselthaler, A., Kirchmair, E., Sieghart, W., Sperk, G., 2013. Patterns of mRNA and protein expression for 12 GABAA receptor subunits in the mouse brain. Neuroscience 236, 345–372. doi:10.1016/j.neuroscience.2013.01.008

Jurd, R., Arras, M., Lambert, S., Drexler, B., Siegwart, R., Crestani, F., Zaugg, M., Vogt, K.E., Ledermann, B., Antkowiak, B., Rudolph, U., 2003. General anesthetic actions in vivo strongly attenuated by a point mutation in the GABA(A) receptor beta3 subunit. FASEB J. Off. Publ. Fed. Am. Soc. Exp. Biol. 17, 250–252. doi:10.1096/fj.02-0611fje

Khom, S., Baburin, I., Timin, E., Hohaus, A., Trauner, G., Kopp, B., Hering, S., 2007. Valerenic acid potentiates and inhibits GABA(A) receptors: molecular mechanism and subunit specificity. Neuropharmacology 53, 178–187. doi:10.1016/j.neuropharm.2007.04.018

Khom, S., Strommer, B., Ramharter, J., Schwarz, T., Schwarzer, C., Erker, T., Ecker, G.F., Mulzer, J., Hering, S., 2010. Valerenic acid derivatives as novel subunit-selective GABAA receptor ligands - in vitro and in vivo characterization. Br. J. Pharmacol. 161, 65–78. doi:10.1111/j.1476-5381.2010.00865.x

Kopp, S., Baur, R., Sigel, E., Möhler, H., Altmann, K.-H., 2010. Highly potent modulation of GABA(A) receptors by valerenic acid derivatives. ChemMedChem 5, 678–681. doi:10.1002/cmdc.201000062

Löw, K., Crestani, F., Keist, R., Benke, D., Brünig, I., Benson, J.A., Fritschy, J.M., Rülicke, T., Bluethmann, H., Möhler, H., Rudolph, U., 2000. Molecular and neuronal substrate for the selective attenuation of anxiety. Science 290, 131–134.

Miller, P.S., Aricescu, A.R., 2014. Crystal structure of a human GABAA receptor. Nature 512, 270–275. doi:10.1038/nature13293

Miralles, C.P., Li, M., Mehta, A.K., Khan, Z.U., De Blas, A.L., 1999. Immunocytochemical localization of the beta(3) subunit of the gamma-aminobutyric acid(A) receptor in the rat brain. J. Comp. Neurol. 413, 535–548.

Möhler, H., Crestani, F., Rudolph, U., 2001. GABA(A)-receptor subtypes: a new pharmacology. Curr. Opin. Pharmacol. 1, 22–25.

Olsen, R.W., Sieghart, W., 2008. International Union of Pharmacology. LXX. Subtypes of gamma-aminobutyric acid(A) receptors: classification on the basis of subunit composition, pharmacology, and function. Update. Pharmacol. Rev. 60, 243–260. doi:10.1124/pr.108.00505

Pirker, S., Schwarzer, C., Wieselthaler, A., Sieghart, W., Sperk, G., 2000. GABA(A) receptors: immunocytochemical distribution of 13 subunits in the adult rat brain. Neuroscience 101, 815–850.

Reynolds, D.S., Rosahl, T.W., Cirone, J., O'Meara, G.F., Haythornthwaite, A., Newman, R.J., Myers, J., Sur, C., Howell, O., Rutter, A.R., Atack, J., Macaulay, A.J., Hadingham, K.L., Hutson, P.H., Belelli, D., Lambert, J.J., Dawson, G.R., McKernan, R., Whiting, P.J., Wafford, K.A., 2003. Sedation and anesthesia mediated by distinct GABA(A) receptor isoforms. J. Neurosci. Off. J. Soc. Neurosci. 23, 8608–8617.

Rudolph, U., Crestani, F., Benke, D., Brünig, I., Benson, J.A., Fritschy, J.M., Martin, J.R., Bluethmann, H., Möhler, H., 1999. Benzodiazepine actions mediated by specific gamma-aminobutyric acid(A) receptor subtypes. Nature 401, 796–800. doi:10.1038/44579

Rudolph, U., Crestani, F., Möhler, H., 2001. GABA(A) receptor subtypes: dissecting their pharmacological functions. Trends Pharmacol. Sci. 22, 188–194.

Rudolph, U., Knoflach, F., 2011. Beyond classical benzodiazepines: novel therapeutic potential of GABAA receptor subtypes. Nat. Rev. Drug Discov. 10, 685–697. doi:10.1038/nrd3502

Rudolph, U., Möhler, H., 2014. GABAA receptor subtypes: Therapeutic potential in Down syndrome, affective disorders, schizophrenia, and autism. Annu. Rev. Pharmacol. Toxicol. 54, 483–507. doi:10.1146/annurev-pharmtox-011613-135947

Sampath, C., Haug, K., Thanei, S., Hamburger, M., Derendorf, H., Frye, R., Butterweck, V., 2012. Pharmacokinetics of valerenic acid in rats after intravenous and oral administrations. Planta Med. 78, 575–581. doi:10.1055/s-0031-1298301

Schwartzkroin, P.A., 1994. Role of the hippocampus in epilepsy. Hippocampus 4, 239–242. doi:10.1002/hipo.450040302

Schwarzer, C., Berresheim, U., Pirker, S., Wieselthaler, A., Fuchs, K., Sieghart, W., Sperk, G., 2001. Distribution of the major gamma-aminobutyric acid(A) receptor subunits in the basal ganglia and associated limbic brain areas of the adult rat. J. Comp. Neurol. 433, 526–549.

Sendrowski, K., Sobaniec, W., 2013. Hippocampus, hippocampal sclerosis and epilepsy. Pharmacol. Rep. PR 65, 555–565.

Sieghart, W., Sperk, G., 2002. Subunit composition, distribution and function of GABA(A) receptor subtypes. Curr. Top. Med. Chem. 2, 795–816.

Sigel, E., Steinmann, M.E., 2012. Structure, function, and modulation of GABA(A) receptors. J. Biol. Chem. 287, 40224–40231. doi:10.1074/jbc.R112.386664

Simon, J., Wakimoto, H., Fujita, N., Lalande, M., Barnard, E.A., 2004. Analysis of the set of GABA(A) receptor genes in the human genome. J. Biol. Chem. 279, 41422–41435. doi:10.1074/jbc.M401354200

Sperk, G., Schwarzer, C., Tsunashima, K., Fuchs, K., Sieghart, W., 1997. GABA(A) receptor subunits in the rat hippocampus I: immunocytochemical distribution of 13 subunits. Neuroscience 80, 987–1000.

Zeller, A., Arras, M., Lazaris, A., Jurd, R., Rudolph, U., 2005. Distinct molecular targets for the central respiratory and cardiac actions of the general anesthetics etomidate and propofol. FASEB J. Off. Publ. Fed. Am. Soc. Exp. Biol. 19, 1677–1679. doi:10.1096/fj.04-3443fje

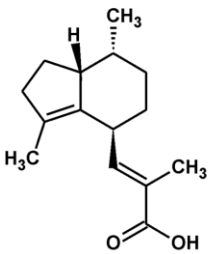

VA

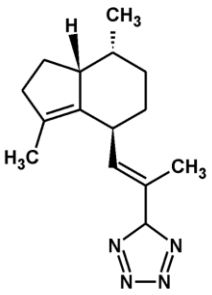

VA-TET

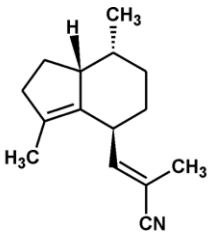

VA-CN

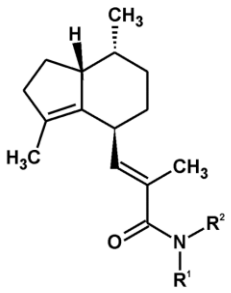

Code	R^1	R^2
VA-A	H	H
VA-MA	CH_3	H
VA-DMA	CH_3	CH_3
VA-EA	CH_2-CH_3	H
VA-DEA	CH_2-CH_3	CH_2-CH_3

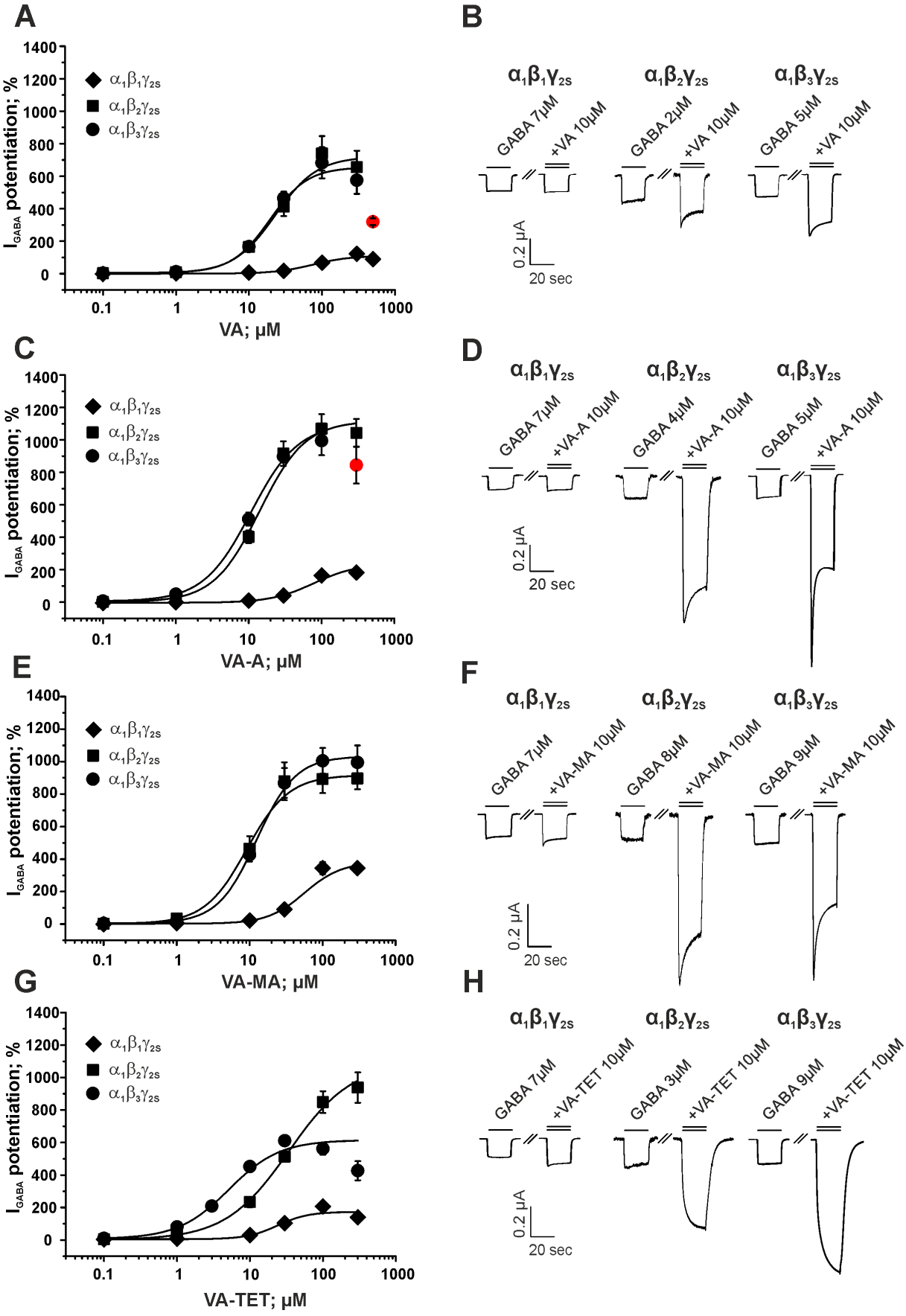
A
B
C
D
E
F
G
H
I_{GABA} potentiation; %
VA; μM
VA-A; μM
VA-MA; μM
VA-TET; μM
$\alpha_1\beta_1\gamma_{2s}$
$\alpha_1\beta_2\gamma_{2s}$
$\alpha_1\beta_3\gamma_{2s}$
GABA 7μM
+VA 10μM
GABA 2μM
GABA 5μM
+VA-A 10μM
GABA 4μM
+VA-MA 10μM
GABA 8μM
GABA 9μM
+VA-TET 10μM
GABA 3μM
0.2 μA
20 sec

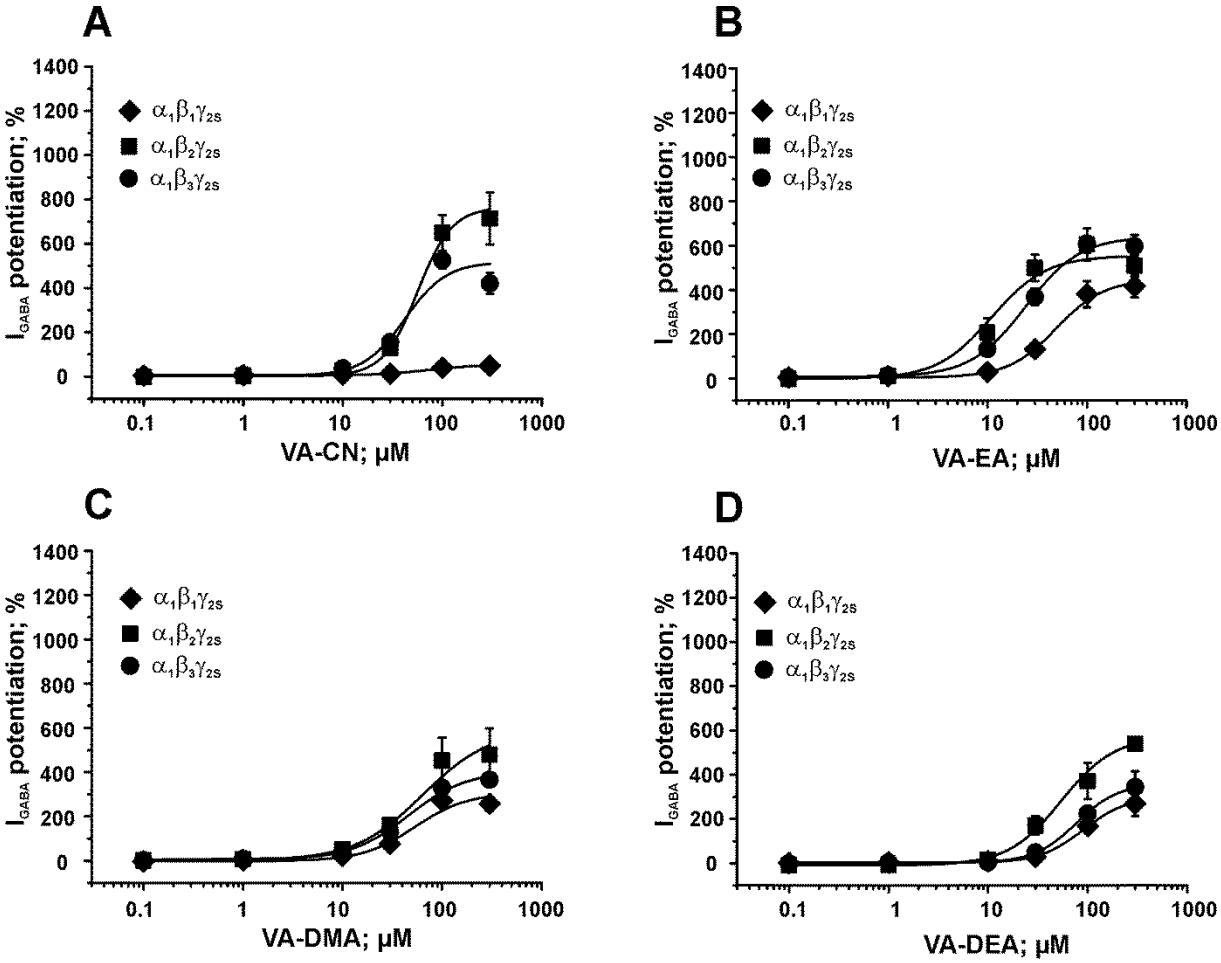
A
B
C
D
I_{GABA} potentiation; %
$\alpha_1\beta_1\gamma_{2S}$
$\alpha_1\beta_2\gamma_{2S}$
$\alpha_1\beta_3\gamma_{2S}$
VA-CN; μM
VA-EA; μM
VA-DMA; μM
VA-DEA; μM

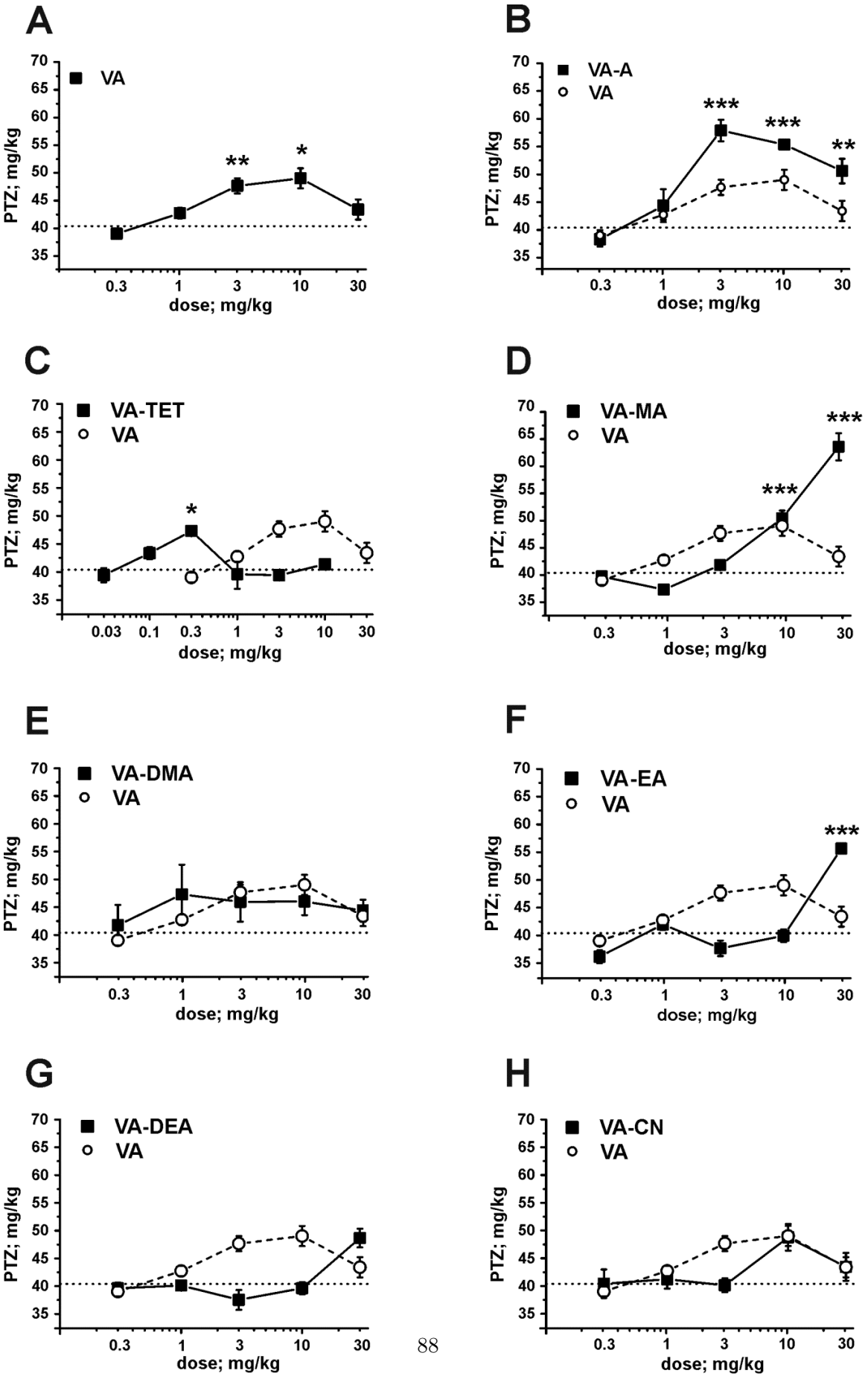
A
VA
PTZ; mg/kg
dose; mg/kg
B
VA-A
VA
C
VA-TET
VA
D
VA-MA
VA
E
VA-DMA
VA
F
VA-EA
VA
G
VA-DEA
VA
H
VA-CN
VA

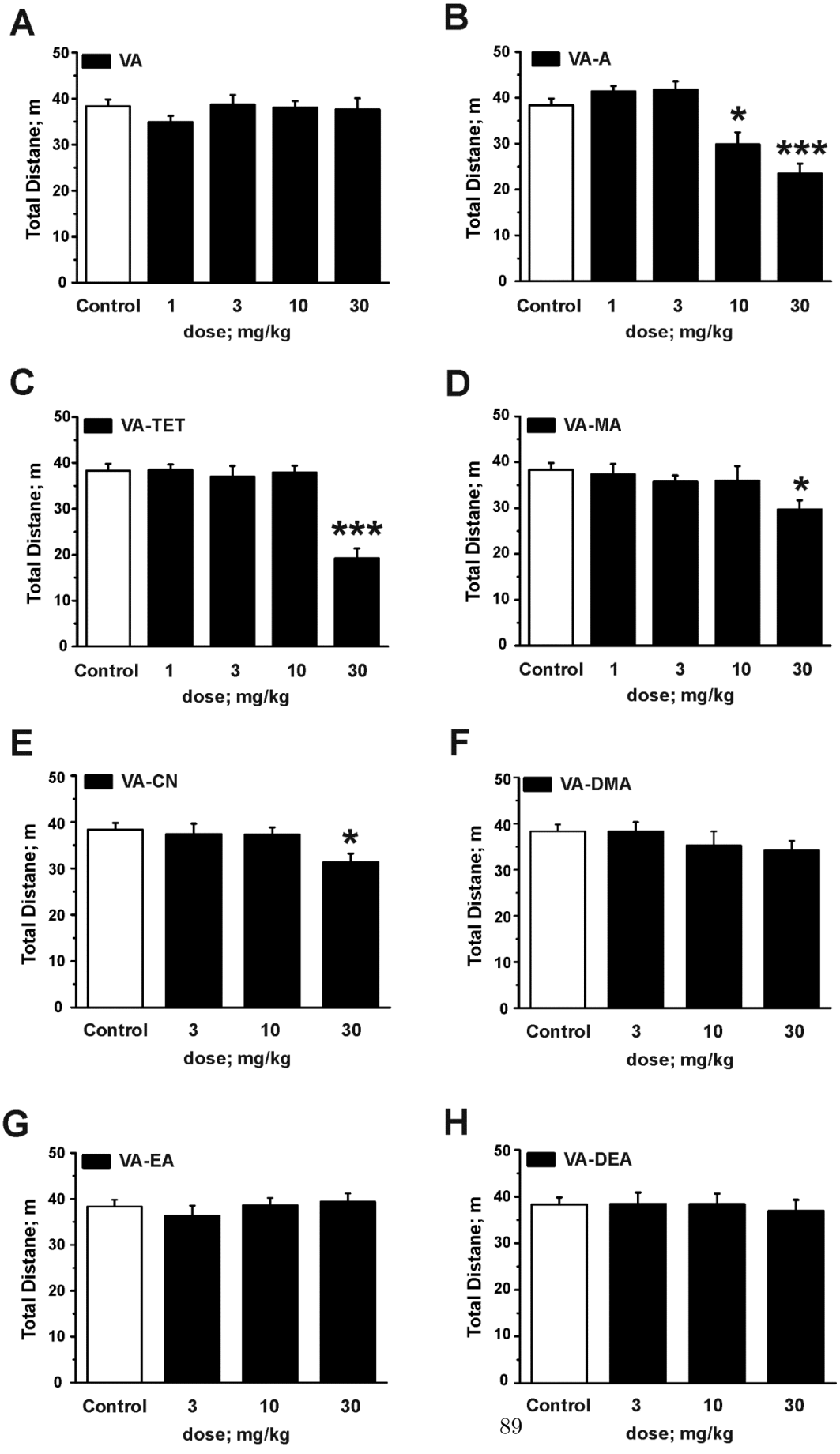
A
VA
Total Distane; m
50
40
30
20
10
0
Control
1
3
10
30
dose; mg/kg
B
VA-A
*
***
C
VA-TET
***
D
VA-MA
*
E
VA-CN
*
F
VA-DMA
G
VA-EA
H
VA-DEA

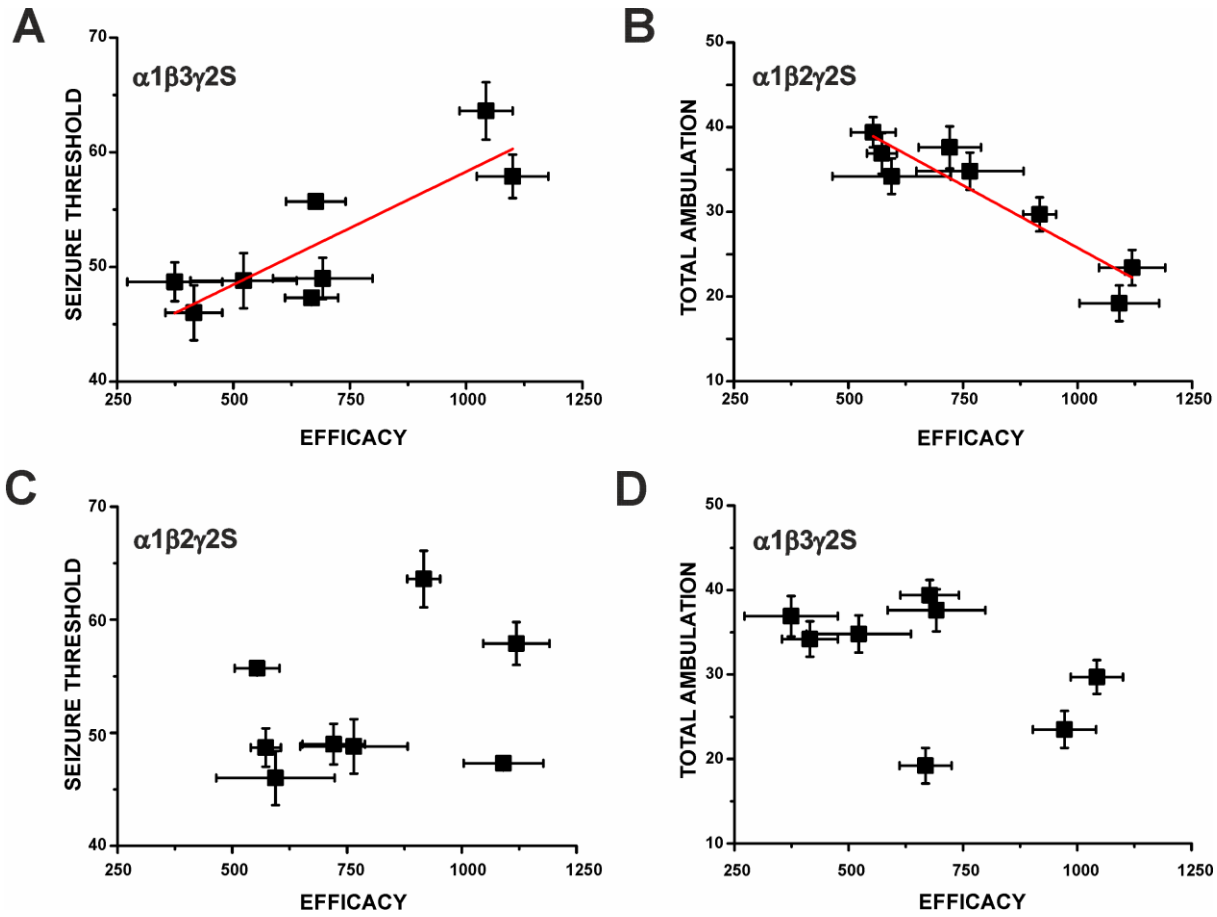
A
α1β3γ2S
SEIZURE THRESHOLD
EFFICACY
B
α1β2γ2S
TOTAL AMBULATION
EFFICACY
C
α1β2γ2S
SEIZURE THRESHOLD
EFFICACY
D
α1β3γ2S
TOTAL AMBULATION
EFFICACY

Legends to Figures and Tables

Figure 1

Structural formulae of studied valerenic acid (VA) and VA derivatives

Figure 2

Structural modifications result in more potent and efficacious I_{GABA} modulation

Concentration-dependent modulation of $GABA_A$ receptors composed of (●) α1β3γ2S, (■) α1β2γ2S and (♦) α1β1γ2S subunits by **(A)** VA, **(C)** VA-A, **(E)** VA-MA, and **(G)** VA-TET**.** Data were fitted by non-linear regression, as described in Materials and Methods. Maximal potentiation of I_{GABA} (E_{max}), EC_{50} values, Hill-coefficients (n_H) and number of experiments for each compound on α1β1γ2S, α1β2γ2S and α1β3γ2S receptors are summarized in Table 1. Each data point represents a mean±S.E.M from at least 4 different oocytes from 2 different frog batches. I_{GABA} potentiation at 300µM (α1β3γ2S receptors, red symbols) for VA and VA-A, respectively, were excluded from the fit. Typical traces for the enhancement of GABA-induced chloride currents (I_{GABA}, EC_{3-7}, single bar) by 10 µM of VA **(B)**, VA-A **(D)**, VA-MA **(F)** and VA-TET **(H)** (double bar; indicating co-application of GABA and compound) at the indicated $GABA_A$ receptor subtype are illustrated.

Figure 3

β-subunit-selective I_{GABA} modulation by VA derivatives

Concentration-response curves for the I_{GABA} enhancement through (●) α1β3γ2S, (♦) α1β2γ2S and (■) α1β1γ2S channels by VA derivatives **(A)** VA-CN, **(B)** VA-EA, **(C)** VA-DMA, and **(D)** VA-DEA. Data were fitted by non-linear regression, as described in Materials and Methods. Maximal potentiation of I_{GABA} (E_{max}), EC_{50} values, Hill-coefficients (n_H) and number of experiments for each compound on α1β1γ2S, α1β2γ2S and α1β3γ2S receptors are summarized in Table 1. Each data point represents a mean±S.E.M from at least 5 different oocytes from 2 different frog batches.

Figure 4

Anticonvulsive effects of VA and VA derivatives

Elevation of seizure threshold upon tail-vain infusion of PTZ 30 min after i.p. application of **(A)** VA is illustrated. The dotted line represents the seizure threshold of saline-treated control

animals. Effect on PTZ-induced seizure threshold 30 min. after i.p. application by the VA derivatives **(B)** VA-A, **(C)** VA-TET, **(D)** VA-MA, **(E)** VA-DMA, **(F)** VA-EA, **(G)** VA-DEA and **(H)** VA-CN is compared to VA (dashed line, white circles) and control animals (dotted line). Each data point represents a mean ± S.E.M from at least 3 mice. Statistical significance (p-values <0.05 were accepted as significant; *=p<0.05, **=p<0.01 and ***=p<0.001) against control was calculated by one-way ANOVA followed by Bonferroni post-hoc mean comparison.

Figure 5

Effect on locomotion by VA and VA derivatives in the open field test (OF) test

Black bars indicate changes in total ambulation (expressed in % of control) measured in the OF test 30 min after i.p. application of **(A)** VA compared to diazepam (grey bars), **(B)** VA-A, **(C)** VA-TET, **(D)** VA-MA, **(E)** VA-CN, **(F)** VA-DMA, **(G)** VA-EA and **(H)** VA-DEA at the indicated doses compared to saline-treated control animals (white bars in all panels). Each bar represents a mean ± S.E.M from at least 10 different mice. Statistical significance (p-values <0.05 were accepted as significant; *=p<0.05 and ***=p<0.001) against control was calculated by one-way ANOVA followed by a Bonferroni post-hoc mean comparison.

Figure 6

Correlating in vitro efficacies with behavioral effects

Efficacies of I_{GABA} enhancement (%) by VA derivatives at the indicated $GABA_A$ receptor subtype were plotted against the maximal seizure threshold elevations (indicated as required dose of pentylenetetrazole in mg/kg bodyweight; (**A))** and the maximal effects on total ambulation in the open field test **(C**) (indicated as total distance covered in m; **(B)** and **(D)**) at the highest tested dose of the respective derivative. Estimated correlation coefficients were 0.84397 (A, p<0.01) and -0.92782 (B, p<0.01).

Table 1

Summary of pharmacological properties of I_{GABA} enhancement through $\alpha_1\beta_1\gamma_{2S}$, $\alpha_1\beta_2\gamma_{2S}$ and $\alpha_1\beta_3\gamma_{2S}$ receptors including maximal I_{GABA} enhancement (E_{max}), half-maximal effective concentrations (EC_{50}), Hill-coefficients (n_H) and number of experiments for each compound at the tested subunit combinations. Asteriks (*=*p<0.05*; **=*p<0.01*, ***=*p<0.001*) indicate statistical significance against control (=VA) calculated for each derivative by unpaired student's test.

	VA	VA-A	VA-TET	VA-CN	VA-MA	VA-DMA	VA-EA	VA-DEA
$\alpha_1\beta_1\gamma_{2S}$								
E_{max} (%)	111±16	218±78	176±43	55±14	387±56	305±67	458±124	318±84
EC_{50} (µM)	74.4±19.3	66.6±34.6	23.5±10.9	73.0±38.7	58.1±16.5	52.5±20.1	51.4±19.8	97.2±33.8
n_H	1.6±0.5	1.8±0.6	1.8±0.9	1.7±0.7	1.6±0.3	1.7±0.5	1.6±0.3	1.8±0.3
n	8	6	7	7	5	6	5	7
$\alpha_1\beta_2\gamma_{2S}$								
E_{max} (%)	721±68	1119±72	1091±87	765±117	917±36	594±129	554±49	573±33
EC_{50} (µM)	23.1±4.2	14.0±2.2	34.1±6.3	56.5±13.3	9.1±1.4	63.9±23.7	11.0±3.6	54.4±11.1
n_H	1.4±0.2	1.4±0.2	1.0±0.1	2.5±0.7	1.5±0.1	1.3±0.2	1.6±0.3	1.6±0.3
n	5	6	5	4	3	5	3	5
$\alpha_1\beta_3\gamma_{2S}$								
E_{max} (%)	692±107	972±69	668±57	522±114	1043±57	415±61	677±64	374±102
EC_{50} (µM)	22.1±5.7	7.5±1.8	6.0±1.0	42.4±15.8	12.7±0.9	48.0±16.0	27.2±6.7	80.8±31.3
n_H	1.4±0.2	1.5±0.2	1.1±0.1	2.1±0.8	1.5±0.1	1.4±0.2	1.3±0.2	1.9±0.5
n	7	6	8	7	6	6	12	5

4.4.1 Supplemental Data

In addition to Paper IV, effects on anxiety-related behavior of selected VA derivatives and DZP were studied in the EPM and LDT. Mice were tested after 30 minutes of i.p. application of either solvent or drug containing solution for 5 min (EPM) or 10 min (LDT) at indicated doses in mg/kg bodyweight. Controls were set as 100 % to compare each compound with control animals from the respective experiment. Structural formulae of VA and derivatives see Paper IV. Anticonvulsive effects of VA-A and VA-AA were observed upon PTZ-infusion after i.p. application drug containing solution at 3 mg/kg bodyweight.

4.4.1.1 Anxiolytic Effects of VA and VA Amide Derivatives in the EPM Test

As illustrated in Figure 4.1, animals treated with DZP at doses of 0.3 and 1 mg/kg bodyweight spent significantly more time in the open arms than saline-treated controls (control 100 % ± 0.3 % for n = 12; DZP at 0.3 mg/kg, 140.6 % ± 14.4 %; n= 9; $p<0.01$; DZP at 1 mg/kg, 200.7 % ± 14.4 % for n = 13; $p<0.01$). However, at a dose of 3 mg/kg mice treated with DZP spent approximately 25 % less time in the open arms than controls.

Mice treated with VA at 0.3 mg/kg spent a comparable amount of time in the open arms to control littermates. At higher doses of 1 and 3 mg/kg VA, mice spent significantly more time in the open arms than saline-treated control littermates (control 100 % ± 3.9 % for n = 13; VA at 1 mg/kg, 162.4 % ± 23.8 % for n = 9; $p<0.01$; VA at 3 mg/kg, 136.2 % ± 13.1 % for n = 14; $p<0.01$, Figure 4.1 A).

Animals treated with 0.3 mg/kg VA-A spent significantly more time in the open arms than controls (control 100 % ± 2.3 % for n = 11; VA-A at 0.3 mg/kg, 141.1 % ± 19.2 % for n = 14; $p<0.05$, Figure 4.1 B); this effect was even more pronounced at a dose of 1 mg/kg VA-A (control 100 % ± 2.3 % for n = 11; VA-A at 1 mg/kg, 214.3 ± 23.8 % for n = 8; $p<0.01$, Figure 4.1 B).

At a dose of 3 mg/kg VA-A, only a slight increase in time spent in the open arms was observed compared to saline-treated controls (control 100 % ± 2.3 % for n = 11; VA-A at 3 mg/kg, 120.0 ± 11.5 % for n = 8; $p<0.05$, Figure 4.1 B).

VA-TET significantly increased the open arm time at 0.3 and 1 mg/kg, with its maximum effect at 1 mg/kg compared to saline-treated controls (control 100 % ± 2.6 % for n = 11; VA-TET at 0.3 mg/kg, 136.8 % ± 14.8 % for n = 15; $p<0.05$; VA-TET at 1 mg/kg, 180.5 % ± 28.5 % for n = 10; $p<0.01$, Figure 4.1 C).

For animals treated with 0.3 mg/kg VA-CN, the time in the open arms was not significantly different from control littermates (Figure 4.1 D). Most notably, VA-CN significantly increased the time in the open arms at a dose of 1 mg/kg compared to controls (control 100 % ± 4.9 % for

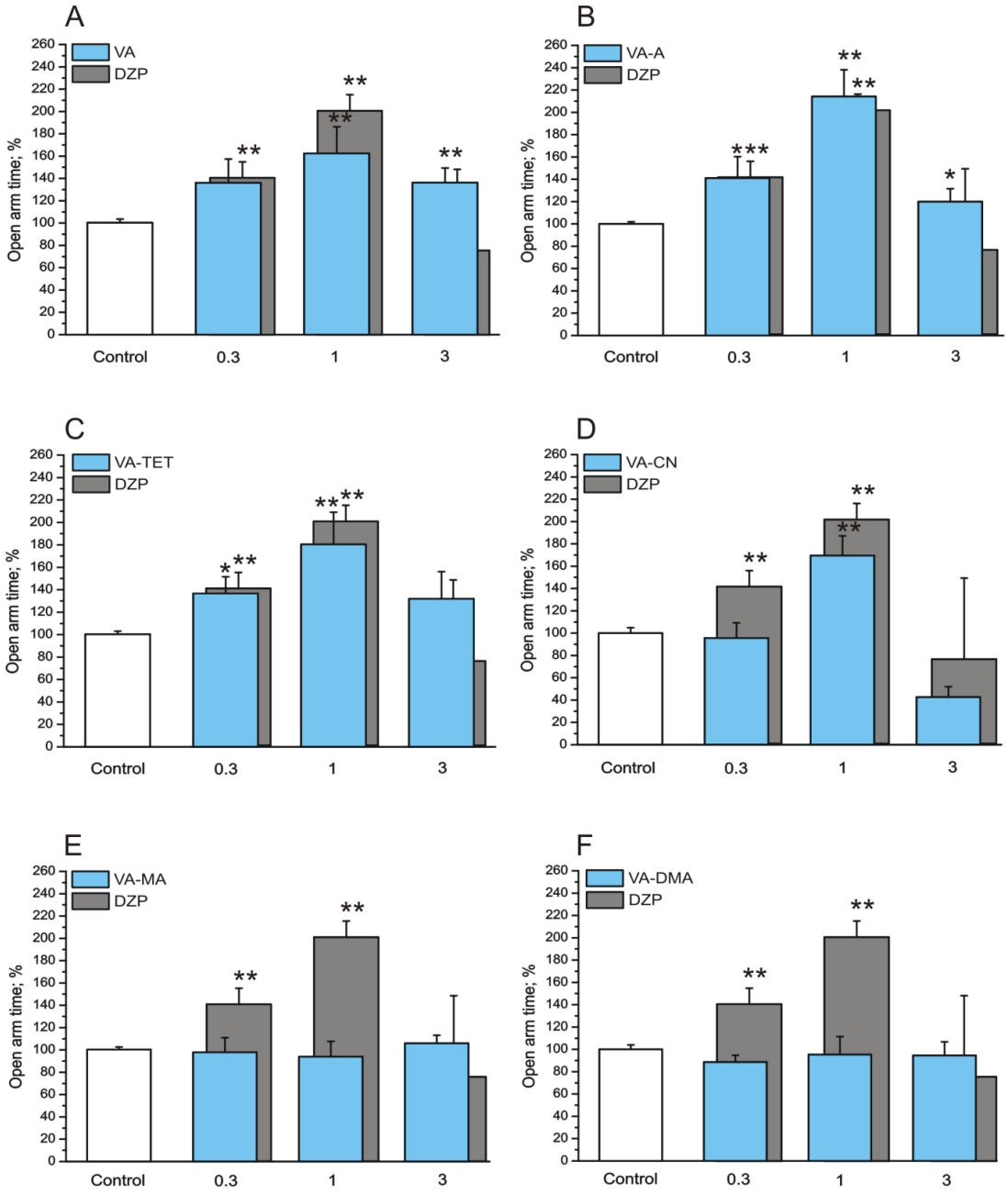

Figure 4.1: Effects on explorative behavior of VA and derivatives in EPM test are compared at indicated doses (mg/kg bodyweight) to saline-treated control mice (white bars) and DZP (diazepam; gray bars). Bars represent the time spent (in % of control) on the open arms, 30 min after i.p. application of the indicated compounds. Each bar represents a mean ± SEM from at least eight different mice. (*) indicates statistically significant differences with $p < 0.05$, (**) with $p < 0.01$ to control [analysis of variance (ANOVA) with Bonferroni].

n = 17; VA-CN at 1 mg/kg, 169.5 % ± 17.7 % for n = 9; p<0.01, Figure 4.1 D). However, at a higher dose of 3 mg/kg VA-CN, the time by mice spent in the open arms returned to control levels (Figure 4.1 D).

Neither VA-MA nor VA-DMA increased the time in the open arms compared to control animals at any of the doses tested (Figure 4.1 E and Figure 4.1 F).

As shown in Figure 4.2, application of DZP at doses of 0.3 and 1 mg/kg significantly increased the distance that mice covered in the open arms compared to controls (control 100 % ± 0.6 % for n = 12; DZP at 0.3 mg/kg, 141.9 % ± 11.3 %; n= 9; p<0.01; DZP at 1 mg/kg, 187.9 % ± 19.3 % for n = 13; p<0.01).

Application of VA did not affect the distance travelled by the animals in the open arms compared to control littermates at any of the doses tested (Figure 4.2 A).

The distance in the open arms was slightly but not significantly increased upon application of VA-A at a dose of 0.3 mg/kg (Figure 4.2 B). The distance the mice covered in the open arms increased further at 1 mg/kg VA-A (control 100 % ± 2.2 % for n = 11; VA-A at 1 mg/kg, 181.9 ± 22.2 % for n = 8; p<0.01, Figure 4.2 B). However, application of a higher dose of 3 mg/kg VA-A did not affect the distance the mice covered in the open arms compared to saline-treated controls (Figure 4.2 B).

VA-TET significantly increased the distance the mice travelled in the open arms already at doses of 0.3 mg/kg and 1 mg/kg compared to control animals (control 100 % ± 3.6 % for n = 11; VA-TET at 0.3 mg/kg, 136.8 % ± 14.8 % for n = 15; p<0.05; VA-TET at 1 mg/kg, 144.9 % ± 17.5 % for n = 10; p<0.05, Figure 4.2 C). However, application of a higher dose of 3 mg/kg VA-TET did not affect the distance the mice covered in the open arms compared to saline-treated controls (Figure 4.2 C).

With VA-CN no change in the distance travelled by mice in the open arms was observed at 0.3 mg/kg, but at the higher dose of 1 mg/kg VA-CN an increase in distance travelled was observed compared to saline-treated controls (control 100 % ± 5.8 % for n = 17; VA-CN at 1 mg/kg, 170.3 % ± 26.9 % for n = 9; p<0.01, Figure 4.2 D). However, at the still higher dose of 3 mg/kg VA-CN the distance the mice travelled in the open arms was actually lower than controls (Figure 4.2 D). Finally, analysis of the open arm distance did not reveal any significant effects of any dose of VA-MA and VA-DMA compared to saline-treated controls (Figure 4.2 E and Figure 4.2 F).

Figure 4.3 shows the total ambulation of animals in the EPM test.

The ambulation of mice was not affected after treatment of DZP at doses of 0.3 and 1 mg/kg compared to control littermates. However, 3 mg/kg DZP reduced ambulation to 63 % compared to control littermates (control 100 % ± 0.9 % for n = 12; DZP at 1 mg/kg, 36.8 % ± 20.9 %; n= 8; p<0.01, Figure 4.3).

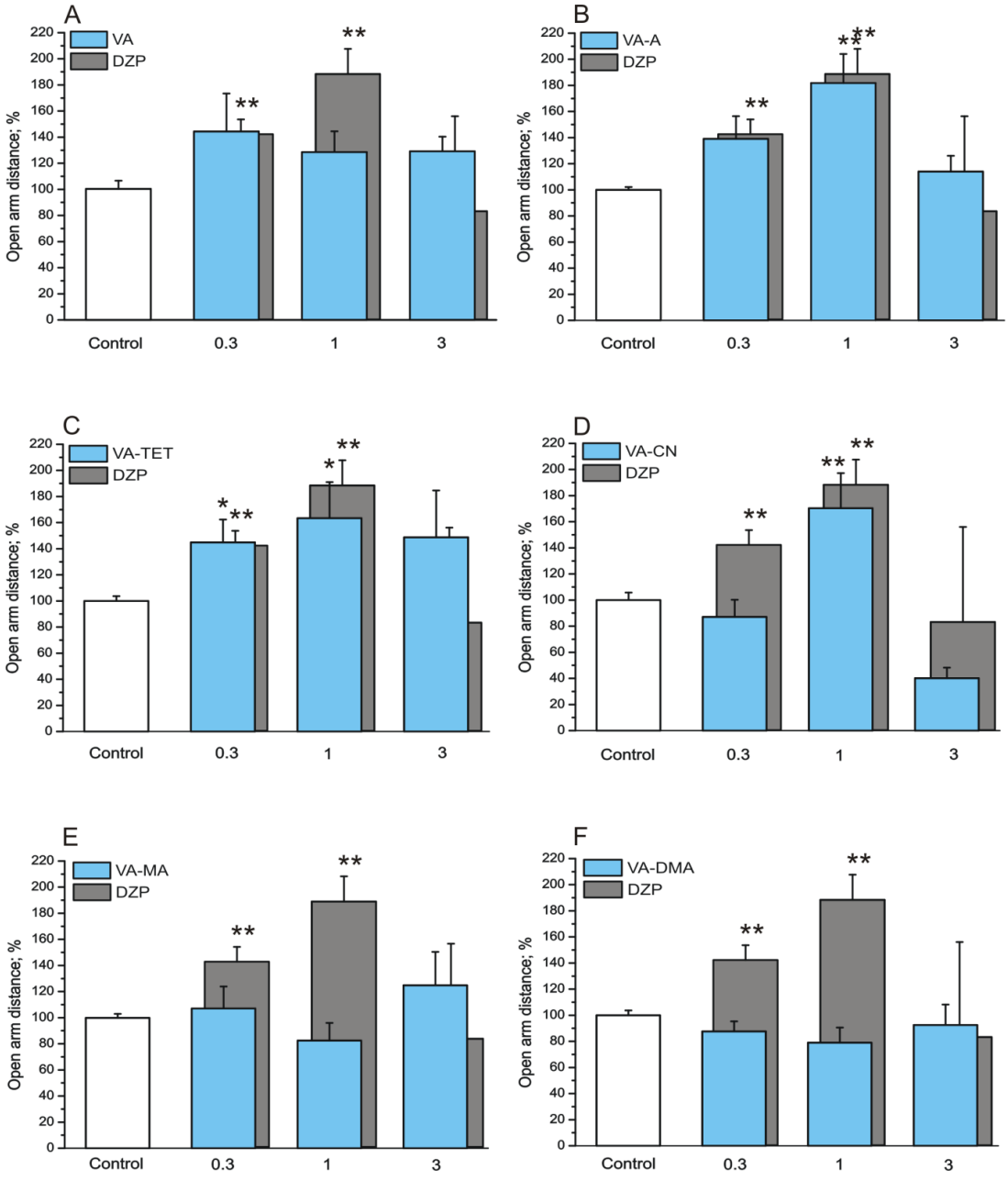

Figure 4.2: Effects on explorative behavior of VA and derivatives in EPM test are compared at indicated doses (mg/kg bodyweight) to saline-treated control mice (white bars) and DZP (diazepam; gray bars). Bars represent the distance spent (in % of control) on the open arms, 30 min after i.p. application of the indicated compounds. Each bar represents a mean ± SEM from at least eight different mice. (*) indicates statistically significant differences with $p < 0.05$, (**) with $p < 0.01$ to control [analysis of variance (ANOVA) with Bonferroni].

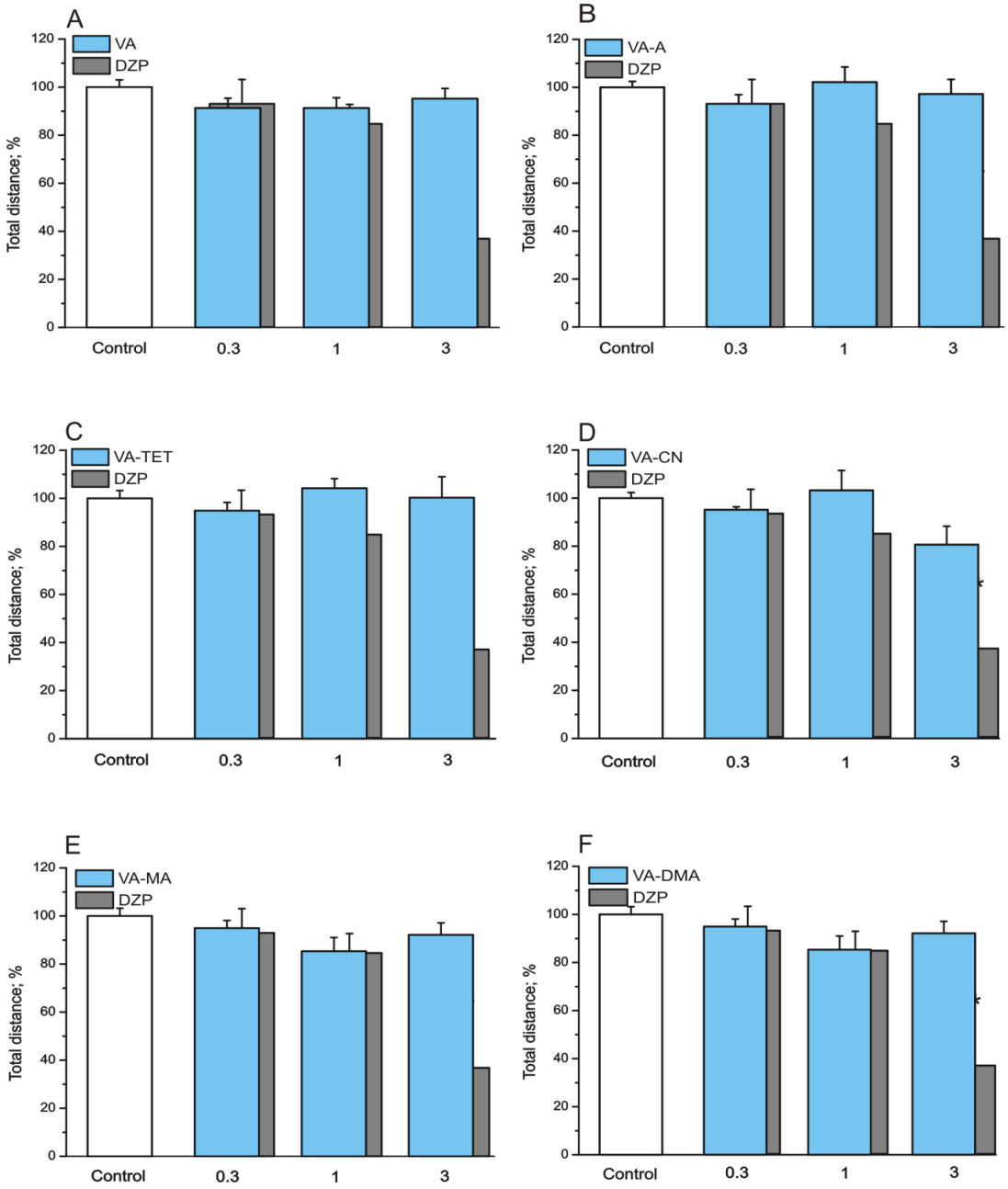

Figure 4.3: Effects on explorative behavior of VA and derivatives in EPM test are compared at indicated doses (mg/kg bodyweight) to saline-treated control mice (white bars) and DZP (diazepam; gray bars). Bars represent the total distance (in % of control) 30 min after i.p. application of the indicated compounds. Each bar represents a mean ± SEM from at least eight different mice. (*) indicates statistically significant differences with $p < 0.05$, (**) with $p < 0.01$ to control [analysis of variance (ANOVA) with Bonferroni].

Analysis of the total distance did not reveal any significant differences of mice treated with VA or its derivatives (VA-A, VA-TET, VA-CN, VA-MA, and VA-DMA) compared to saline-treated controls (Figure 4.3 A-F).

4.4.1.2 Anxiolytic Effects of VA and VA Amide Derivatives in the LDT

Animals treated with DZP at doses of 0.1 and 0.3 mg/kg spent significantly more time in the lit area than controls (control 100 % ± 5.2 % for n = 24; DZP at 0.1 mg/kg, 131.1 % ± 10.1 % for n = 16; $p<0.01$; DZP at 0.3 mg/kg, 152.7 % ± 20.3 % for n = 14; $p<0.01$, Figure 4.4).

Application of 0.1 mg/kg VA did not increase the time mice spent in the lit area compared to control littermates (Figure 4.4 A). Most notably, mice treated with higher doses of 0.3, 1, and 3 mg/kg VA spent significantly more time in the lit area than saline-treated controls (control 100 % ± 2.3 % for n = 20; VA at 0.3 mg/kg, 116.9 % ± 3.6 % for n = 16; $p < 0.01$; VA at 1 mg/kg, 125.7 % ± 4.2 % for n = 18; $p<0.01$; VA at 3 mg/kg, 134.2 % ± 4.1 % for n = 16; $p<0.01$, Figure 4.4 A).

Similar to VA, 0.1 mg/kg VA-A did not increase the time in the lit area compared to control littermates (Figure 4.4 B), whereas higher doses of 0.3, 1, and 3 mg/kg VA-A significantly increased the time the mice spent in the lit area (control 100 % ± 3.1 % for n = 18; VA-A at 0.3 mg/kg, 139.3 % ± 8.3 % for n = 13; $p<0.01$; VA-A at 1 mg/kg, 136.2 % ± 6.1 % for n = 20; $p<0.01$; VA-A at 3 mg/kg, 131.1 % ± 6.2 % for n = 19; $p<0.01$, Figure 4.4 B).

Animals treated with VA-TET at doses of 0.1, 0.3, and 1 mg/kg spent significantly more time in the lit area than control littermates (control 100 % ± 3.1 % for n = 20; VA-TET at 0.1 mg/kg, 123.5 % ± 7.6 % for n = 15; $p<0.01$; VA-TET at 0.3 mg/kg, 130.2 % ± 5.9 % for n = 21; $p<0.01$; VA-TET at 1 mg/kg, 119.0 % ± 3.0 % for n = 21; $p<0.01$, Figure 4.4 C). However, at 3 mg/kg VA-TET the time spent by the mice in the lit area did not differ from saline-treated controls (Figure 4.4 C).

With VA-CN at doses of 0.1 mg/kg and 0.3 mg/kg no increase was observed in the time animals spent in the lit area compared to control littermates (Figure 4.4 D). At a higher dose of 1 mg/kg VA-CN, mice spent significantly more time in the lit area than controls (control 100 % ± 3.0 % for n = 21; VA-CN at 1 mg/kg, 132.3 % ± 5.2 % for n = 14; $p<0.01$, Figure 4.4 D). But once again, the even higher dose of 3 mg/kg VA-CN the time spent by the mice in the lit area did not differ from control littermates (Figure 4.4 D).

The time mice spent in the lit area upon application of VA-MA did not differ from controls at any of the doses tested (Figure 4.4 E).

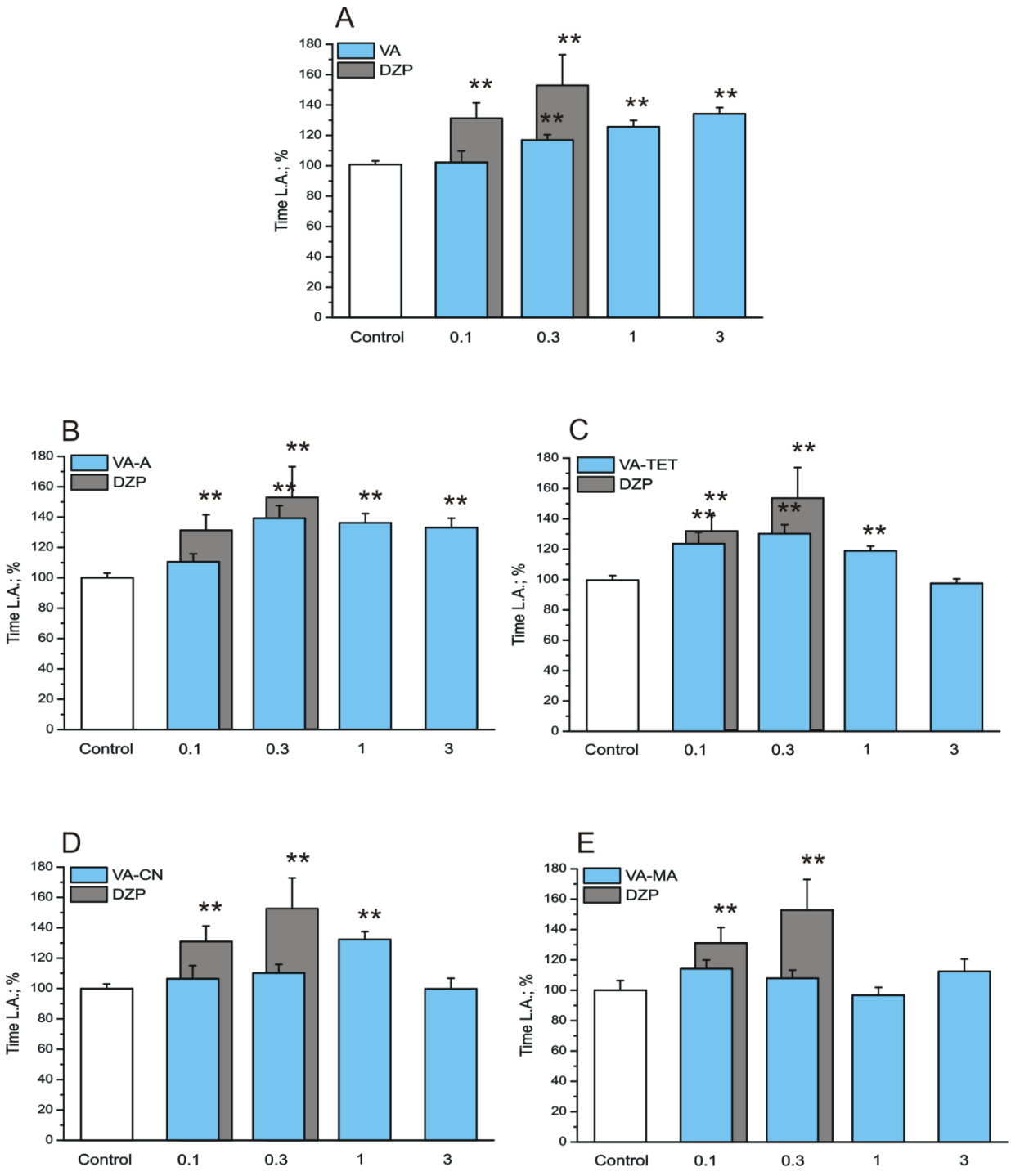

Figure 4.4: Effects on explorative behavior of VA and derivatives in the LDT are compared at indicated doses (mg/kg bodyweight) to saline-treated control mice (white bars) and DZP (diazepam; gray bars).Bars represent the time spent (in % of control) in the lit area, 30 min after i.p. application of the indicated compounds. Each bar represents a mean ± SEM from at least eight different mice. (*) indicates statistically significant differences with $p < 0.05$, (**) with $p < 0.01$ to control [analysis of variance (ANOVA) with Bonferroni].

4.4.1.3 Time-dependent Anticonvulsive Effects of Selected VA Amide Derivatives in the PTZ Test

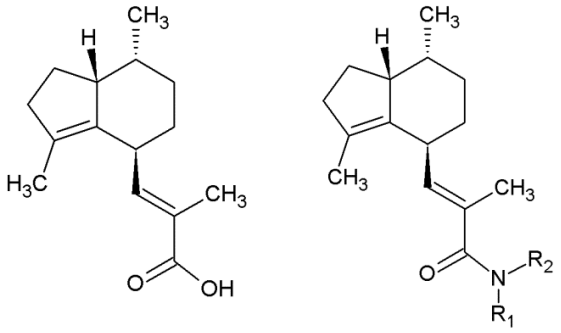

Code	R1	R2
VA-A	H	H
VA-AA	CH-CH_2	H

Figure 4.5: Structural formulae of VA and selected derivatives

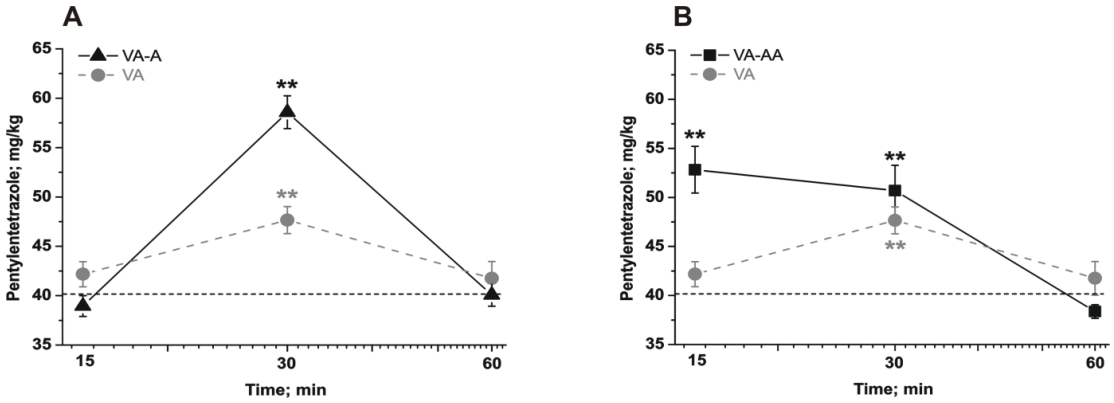

Figure 4.6: Changes in seizure threshold upon PTZ-infusion after 15, 30 and 60 minutes of i.p. application of VA (dotted gray), VA-A (black), and VA-AA (black) are compared to control mice treated with saline solution (dotted line) at a dose of 3 mg/kg bodyweight. Each data point represents the mean ± S.E.M. from at least three different mice; (**) indicates statistically significant differences with $p<0.01$ to controls [analysis of variance (ANOVA) with Bonferroni].

As illustrated in Figure 4.6, VA-A did not elevate the seizure threshold upon PTZ infusion 15 min after application compared to controls (Figure 4.6 A). However, after 30 minutes, a significantly increased seizure threshold was observed for VA-A (Control 40.2 mg/kg ± 1.1 mg/kg for n = 8; VA-A 30 min after application at 3 mg/kg, 58.6 mg/kg ± 1.7 mg/kg for n = 5; $p<0.01$, Figure 4.6 A). This effect was even more pronounced than that observed with VA (VA 30 min after application at 3 mg/kg, 47.7 mg/kg ± 1.4 mg/kg for n = 4; VA-A 30 min after application at 3 mg/kg, 58.6 mg/kg ± 1.7 mg/kg for n = 5; $p<0.01$, Figure 4.6 A). However, 60 min after application of VA-A, no protective effect against PTZ-induced seizures was observed (Figure 4.6 A).

In contrast to VA and VA-A, VA-AA induced a higher seizure threshold than VA, and this effect

was already apparent 15 min after application (VA after 15 min at 3 mg/kg, 42.2 mg/kg ± 1.3 mg/kg for n = 4; VA-AA after 15 min at 3 mg/kg, 52.8 mg/kg ± 2.4 mg/kg for n = 4; $p<0.01$, Figure 4.6 B). This effect of VA-AA declined slightly after 30 min (to a level similar to that of VA, see Figure 4.6 B), and was no longer observable after 60 min (control 40.2 mg/kg ± 1.1 mg/kg for n = 8; VA-AA 30 min after application at 3 mg/kg, 50.7 mg/kg ± 2.6 mg/kg for n = 3; $p<0.01$, Figure 4.6 B).

Discussion of Supplemental Data

The anxiolytic activity of VA (Benke et al., 2009; Khom et al., 2010) and VA-A (Khom et al., 2010) has been described previously. To study applicability of VA, VA-A and four derivatives (VA-MA, VA-TET, VA-CN, and VA-DMA) as scaffolds for the development of novel anxiolytics, effects on anxiety-related behavior were characterized. To check for concomitant sedative effects, we also investigated whether VA and derivatives would change locomotor activity.

Since mice naturally avoid open spaces and heights, if they spend more time in the open arms of the EPM, it can be seen as indicative of reduced anxiety (Lister, 1987). The distances they cover in the open arms give information about their locomotor activity. A decrease in locomotor activity may reflect sedation.

Anxiolytic effects and effects on locomotor activity of VA and selected VA amide derivatives in the EPM test

VA-A and VA-TET induced significant anxiolytic effects comparable to DZP at a dose of 0.3 mg/kg (Figure 4.1 and Figure 4.2). The most marked anxiolytic effects for VA and all selected derivatives were observed at a dose of 1 mg/kg (Figure 4.1 and Figure 4.2). A trend - although not reaching statistical significance - towards an even more pronounced anxiolytic effect of VA-A compared to DZP at this dose was observed (Figure 4.1 B). Remarkably, the anxiolytic effect of VA-TET was comparable to DZP at 1 mg/kg. In contrast, the anxiolytic effects of VA-CN and VA at 1 mg/kg were weaker than that of DZP (Figure 4.1).

The anxiolytic effects of VA and VA-TET were slightly less pronounced at 3 mg/kg than at 1 mg/kg, suggesting saturation of effects. Surprisingly, the anxiolytic effects of VA-A and VA-CN were at 3 mg/kg significantly lower than controls, implicating a drop in anxiolytic activity of VA-A and VA-CN (Figure 4.1).

VA-MA and VA-DMA did not induce anxiolytic effects at any dose tested in the EPM (Figure 4.1 and Figure 4.2).

Sedative effects may be side effects of anxiolytic drugs. DZP reduced locomotor activity compared to control animals at a dose of 3 mg/kg (Figure 4.3). Most notably, VA and none of the derivatives

tested reduced locomotor activity in the EPM , suggesting that there was no concomitant sedation (Figure 4.3).

Anxiolytic effects of VA and selected VA amide derivatives in the LDT

In the LDT, more time spent by the mice in the lit area of the test equipment can be interpreted as reduced anxiety (Crawley and Goodwin, 1980).

VA had its maximum anxiolytic effect at 3 mg/kg (Figure 4.4 A). Remarkably, VA-A and VA-TET exerted their maximum of effects at a tenfold lower dose (Figure 4.4 B), comparable to the effect of DZP at this dose.

VA-MA did not induce anxiolytic effects at any of the doses tested, which is consistent with the effects observed in the EPM test (Figure 4.1 E). The effect of VA-DMA was not measured, due to its lack of anxiolytic effect in the EPM test (Figure 4.1 F).

VA-CN induced a more pronounced anxiolytic effect than control only at 1 mg/kg, being ineffective at all other doses tested in the LDT (Figure 4.4 D), which agrees with the observations from the EPM test (Figure 4.1 D).

Effects on seizure threshold upon PTZ-induced seizures of selected derivatives at different time points

The elevation of seizure threshold by VA is strongest after 30 min of application at a dose of 3 mg/kg bodyweight (Figure 4.6). The results of Paper I show that the methylester of VA elevates seizure threshold with faster onset (at a dose of 3 mg/kg), whereas the anticonvulsive effect of the ethylester of VA occurred with later onset and was longer lasting (at a dose of 3 mg/kg) (Hintersteiner et al., 2014). The results of Paper IV show, that the amid derivative VA-A induced significantly greater elevation of the seizure threshold at a dose of 3 mg/kg compared to VA (see Paper IV). In the present study, time-dependent effects of seizure threshold of VA-A and the allylamide of VA (VA-AA) are investigated.

VA-A and VA-AA were tested at different application times at a dose of 3 mg/kg upon PTZ-infusion to observe their effects on seizure threshold over a period of 60 min. The anticonvulsive action of VA-A may be short-lived, since no seizure protecting effects after 15 or 60 min were observed (Figure 4.6 A). Most notably, application of VA-AA induced anticonvulsive effects after 15 min (Figure 4.6 B). In analogy to the effect of VA-ME (Hintersteiner et al., 2014), it may be concluded that the faster onset of anticonvulsive effect may result from VA-AA acting as a prodrug with faster release of VA.

5 Conclusion

Derivatization of VA and piperine may lead to interesting drug candidates. The esters of VA were identified as prodrugs; they release VA and moreover, they display anxiolytic and anticonvulsive effects that are even more pronounced and have faster onset (VA-ME) or longer duration (VA-EE) of effects than VA (Figure 3 and 5 in Paper I (Hintersteiner et al., 2014)). VA-allylamide (VA-AA) was also suggested as potential prodrug of VA. Its anticonvulsive activity has an earlier onset than VA (Figure 4.6 B), further studies on plasma levels of released VA could provide an explanation for this effect.

Three other VA amide derivatives VA-amide (VA-A), VA-methylamide (VA-MA), and VA-tetrazole (VA-TET) also represent interesting scaffolds. VA-A and VA-MA induced a more pronounced positive modulation of β2/3-containing $GABA_A$ receptors than VA, and moreover, a remarkable enhancement of the seizure threshold *in vivo* (Figure 2 and Figure 4 in Paper IV). VA-A also had stronger anxiolytic effects in the EPM and the LDT than VA (Figure 4.1 B and Figure 4.4 B).

VA-TET had a more potent effect on β3-containing receptors *in vitro* and *in vivo*, it showed not only a potent anxiolytic effect (Figure 4.1 C and Figure 4.4 C), but also stronger anticonvulsive effects than VA (Figure 4 in Paper IV).

However, these effects were accompanied by reductions in locomotor activity at higher doses of VA-A ($\geq$ 10 mg/kg), VA-MA ($\geq$ 30 mg/kg), and VA-TET ($\geq$ 30 mg/kg) (Figure 5 in Paper IV).

While the efficacy of these derivatives at β3-containing receptors is reflected in seizure threshold elevation, efficacy at β2-containing receptors correlates with a reduction in locomotor activity (Figure 6 in Paper IV). VA amide derivatives that did not distinguish between β subunits *in vitro* were found to be inactive *in vivo* (VA-dimethylamide) (Figure 4.1 F) or induced anticonvulsive effects only at high doses (VA-ethylamide, VA-diethylamide) (Figure 4 in Paper IV). Consequently, VA derivatives with a preference for β3 over β2-containing $GABA_A$ receptors represent more promising scaffolds for the development of novel anticonvulsants.

The non-TRPV1 activating piperine derivative SCT-66 (compound 24 in Paper III) displayed a more pronounced anxiolytic effect (Figure 6 in Paper II (Khom et al., 2013)) than piperine and did not reduce body temperature of mice like piperine (Figure 4 in Paper II (Khom et al., 2013)). At higher doses, SCT-66 elevated seizure threshold (Figure 7B in Paper II (Khom et al., 2013)), but also induced impairment of motor activity (Figure 5A in Paper II (Khom et al., 2013)).

These potentially sedative effects may be a consequence of the relatively unselective but strong modulation of $GABA_A$ receptors containing $\alpha 1$, $\alpha 2$, or $\alpha 3$ subunits by SCT-66. Another non-TRPV1 activating piperine derivative compound 23 displayed more pronounced anxiolytic effects in the EPM test than piperine (Figure 8A in Paper III (Schöffmann et al., 2014)), but additionally induced motor impairment at higher doses in the OF test (Figure 8C in Paper III (Schöffmann et al., 2014)).

The anxiolytic and anticonvulsive VA (VA-A, VA-TET) and piperine (SCT-66, compound 23) derivatives reduced locomotor activity of mice. However, these possible sedative effects occur at doses 10-100fold higher than their anxiolytic (Figure 4.1 B and C, Figure 6 in Paper II (Khom et al., 2013), Figure 8A in Paper III (Schöffmann et al., 2014)) and/or anticonvulsive effects (Figure 4 in Paper IV, Figure 7B in Paper II (Khom et al., 2013)). For some uses, though, sedative effects at higher doses could be an advantage for potent anxiolytics/anticonvulsants with desired additional sedative properties.

Taken together, this work characterized the *in vivo* effects of VA and piperine derivatives modulating $GABA_A$ receptors. Their interesting pharmacological profile with more pronounced anxiolytic and/or anticonvulsive effects than their parent scaffolds makes them candidates for lead optimization and drug development.

List of Figures

References on Scientific Publications

Adams, J. M., Thomas, P., and Smart, T. G. (2015). Modulation of neurosteroid potentiation by protein kinases at synaptic- and extrasynaptic-type GABAA receptors. *Neuropharmacology*, 88:63–73.

Alam, S., Laughton, D. L., Walding, A., and Wolstenholme, A. J. (2006). Human peripheral blood mononuclear cells express GABAA receptor subunits. *Molecular Immunology*, 43(9):1432–1442.

Bateson, A. N. (2004). The benzodiazepine site of the GABAA receptor: an old target with new potential? *Sleep Medicine*, 5 Suppl 1:S9–15.

Baur, R., Tan, K. R., Lüscher, B. P., Gonthier, A., Goeldner, M., and Sigel, E. (2008). Covalent modification of GABAA receptor isoforms by a diazepam analogue provides evidence for a novel benzodiazepine binding site that prevents modulation by these drugs. *Journal of Neurochemistry*, 106(6):2353–2363.

Belelli, D. and Lambert, J. J. (2005). Neurosteroids: endogenous regulators of the GABA(A) receptor. *Nature Reviews. Neuroscience*, 6(7):565–575.

Belelli, D., Lambert, J. J., Peters, J. A., Wafford, K., and Whiting, P. J. (1997). The interaction of the general anesthetic etomidate with the gamma-aminobutyric acid type A receptor is influenced by a single amino acid. *Proceedings of the National Academy of Sciences of the United States of America*, 94(20):11031–11036.

Benke, D., Barberis, A., Kopp, S., Altmann, K.-H., Schubiger, M., Vogt, K. E., Rudolph, U., and Möhler, H. (2009). GABA A receptors as in vivo substrate for the anxiolytic action of valerenic acid, a major constituent of valerian root extracts. *Neuropharmacology*, 56(1):174–181.

Berezhnoy, D., Nyfeler, Y., Gonthier, A., Schwob, H., Goeldner, M., and Sigel, E. (2004). On the benzodiazepine binding pocket in GABAA receptors. *The Journal of Biological Chemistry*, 279(5):3160–3168.

Bjurstöm, H., Wang, J., Wang, J., Ericsson, I., Bengtsson, M., Liu, Y., Kumar-Mendu, S., Issazadeh-Navikas, S., and Birnir, B. (2008). GABA, a natural immunomodulator of T lymphocytes. *Journal of Neuroimmunology*, 205(1-2):44–50.

Bocquet, N., Nury, H., Baaden, M., Le Poupon, C., Changeux, J.-P., Delarue, M., and Corringer,

P.-J. (2009). X-ray structure of a pentameric ligand-gated ion channel in an apparently open conformation. *Nature*, 457(7225):111–114.

Boileau, A. J., Newell, J. G., and Czajkowski, C. (2002). GABA(A) receptor beta 2 Tyr97 and Leu99 line the GABA-binding site. Insights into mechanisms of agonist and antagonist actions. *The Journal of Biological Chemistry*, 277(4):2931–2937.

Boue-Grabot, E., Roudbaraki, M., Bascles, L., Tramu, G., Bloch, B., and Garret, M. (1998). Expression of GABA receptor rho subunits in rat brain. *Journal of Neurochemistry*, 70(3):899–907.

Bradley, C. A., Taghibiglou, C., Collingridge, G. L., and Wang, Y. T. (2008). Mechanisms involved in the reduction of GABAA receptor alpha1-subunit expression caused by the epilepsy mutation A322d in the trafficking-competent receptor. *The Journal of Biological Chemistry*, 283(32):22043–22050.

Busti, D., Geracitano, R., Whittle, N., Dalezios, Y., Mańko, M., Kaufmann, W., Sätzler, K., Singewald, N., Capogna, M., and Ferraguti, F. (2011). Different fear states engage distinct networks within the intercalated cell clusters of the amygdala. *The Journal of Neuroscience: The Official Journal of the Society for Neuroscience*, 31(13):5131–5144.

Chang, C.-s. S., Olcese, R., and Olsen, R. W. (2003). A single M1 residue in the beta2 subunit alters channel gating of GABAA receptor in anesthetic modulation and direct activation. *The Journal of Biological Chemistry*, 278(44):42821–42828.

Cherubini, E. and Conti, F. (2001). Generating diversity at GABAergic synapses. *Trends in Neurosciences*, 24(3):155–162.

Chiara, D. C., Dostalova, Z., Jayakar, S. S., Zhou, X., Miller, K. W., and Cohen, J. B. (2012). Mapping general anesthetic binding site(s) in human alpha1beta3 gamma-aminobutyric acid type A receptors with [^{3}H]TDBzl-etomidate, a photoreactive etomidate analogue. *Biochemistry*, 51(4):836–847.

Chouinard, G. (2004). Issues in the clinical use of benzodiazepines: potency, withdrawal, and rebound. *The Journal of Clinical Psychiatry*, 65 Suppl 5:7–12.

Cohen, C. and Sanger, D. J. (1994). Tolerance, cross-tolerance and dependence measured by operant responding in rats treated with triazolam via osmotic pumps. *Psychopharmacology*, 115(1-2):86–94.

Connolly, C. N., Krishek, B. J., McDonald, B. J., Smart, T. G., and Moss, S. J. (1996). Assembly and cell surface expression of heteromeric and homomeric gamma-aminobutyric acid type A receptors. *The Journal of Biological Chemistry*, 271(1):89–96.

Cossette, P., Lachance-Touchette, P., and Rouleau, G. A. (2012). Mutated GABAA receptor subunits in idiopathic generalized epilepsy.

Crawley, J. and Goodwin, F. K. (1980). Preliminary report of a simple animal behavior model for the anxiolytic effects of benzodiazepines. *Pharmacology, Biochemistry, and Behavior*, 13(2):167–170.

Crestani, F., Lorez, M., Baer, K., Essrich, C., Benke, D., Laurent, J. P., Belzung, C., Fritschy, J. M., Lüscher, B., and Mohler, H. (1999). Decreased GABAA-receptor clustering results in enhanced anxiety and a bias for threat cues. *Nature Neuroscience*, 2(9):833–839.

Crestani, F., Löw, K., Keist, R., Mandelli, M., Möhler, H., and Rudolph, U. (2001). Molecular targets for the myorelaxant action of diazepam. *Molecular Pharmacology*, 59(3):442–445.

Crestani, F., Martin, J. R., Möhler, H., and Rudolph, U. (2000). Mechanism of action of the hypnotic zolpidem in vivo. *British Journal of Pharmacology*, 131(7):1251–1254.

Cromer, B. A., Morton, C. J., and Parker, M. W. (2002). Anxiety over GABA(A) receptor structure relieved by AChBP. *Trends in Biochemical Sciences*, 27(6):280–287.

Depoortere, H., Zivkovic, B., Lloyd, K. G., Sanger, D. J., Perrault, G., Langer, S. Z., and Bartholini, G. (1986). Zolpidem, a novel nonbenzodiazepine hypnotic. I. Neuropharmacological and behavioral effects. *The Journal of Pharmacology and Experimental Therapeutics*, 237(2):649–658.

Devaud, L. L., Fritschy, J. M., Sieghart, W., and Morrow, A. L. (1997). Bidirectional alterations of GABA(A) receptor subunit peptide levels in rat cortex during chronic ethanol consumption and withdrawal. *Journal of Neurochemistry*, 69(1):126–130.

Dias, R., Sheppard, W. F. A., Fradley, R. L., Garrett, E. M., Stanley, J. L., Tye, S. J., Goodacre, S., Lincoln, R. J., Cook, S. M., Conley, R., Hallett, D., Humphries, A. C., Thompson, S. A., Wafford, K. A., Street, L. J., Castro, J. L., Whiting, P. J., Rosahl, T. W., Atack, J. R., McKernan, R. M., Dawson, G. R., and Reynolds, D. S. (2005). Evidence for a significant role of alpha 3-containing GABAA receptors in mediating the anxiolytic effects of benzodiazepines. *The Journal of Neuroscience: The Official Journal of the Society for Neuroscience*, 25(46):10682–10688.

Diaz, M. R., Christian, D. T., Anderson, N. J., and McCool, B. A. (2011). Chronic ethanol and withdrawal differentially modulate lateral/basolateral amygdala paracapsular and local GABAergic synapses. *The Journal of Pharmacology and Experimental Therapeutics*, 337(1):162–170.

Drafts, B. C. and Fisher, J. L. (2006). Identification of structures within GABAA receptor alpha subunits that regulate the agonist action of pentobarbital. *The Journal of Pharmacology and Experimental Therapeutics*, 318(3):1094–1101.

Ebert, B., Anderson, N. J., Cremers, T. I., Rasmussen, S., Vogel, V., Fahey, J. M., and Sánchez, C. (2008). Gaboxadol – a different hypnotic profile with no tolerance to sleep EEG and sedative effects after repeated daily dosing. *Pharmacology, Biochemistry, and Behavior*, 90(1):113–122.

Ehlers, C. L. and Slawecki, C. J. (2000). Effects of chronic ethanol exposure on sleep in rats. *Alcohol (Fayetteville, N.Y.)*, 20(2):173–179.

Ehrlich, I., Humeau, Y., Grenier, F., Ciocchi, S., Herry, C., and Lüthi, A. (2009). Amygdala inhibitory circuits and the control of fear memory. *Neuron*, 62(6):757–771.

Elliot, E. E. and White, J. M. (2000). Precipitated and spontaneous withdrawal following adminis-

tration of lorazepam but not zolpidem. *Pharmacology, Biochemistry, and Behavior*, 66(2):361–369.

Engin, E., Liu, J., and Rudolph, U. (2012). alpha2-containing GABA(A) receptors: a target for the development of novel treatment strategies for CNS disorders. *Pharmacology & Therapeutics*, 136(2):142–152.

Epi4K Consortium, Epilepsy Phenome/Genome Project, Allen, A. S., Berkovic, S. F., Cossette, P., Delanty, N., Dlugos, D., Eichler, E. E., Epstein, M. P., Glauser, T., Goldstein, D. B., Han, Y., Heinzen, E. L., Hitomi, Y., Howell, K. B., Johnson, M. R., Kuzniecky, R., Lowenstein, D. H., Lu, Y.-F., Madou, M. R. Z., Marson, A. G., Mefford, H. C., Esmaeeli Nieh, S., O'Brien, T. J., Ottman, R., Petrovski, S., Poduri, A., Ruzzo, E. K., Scheffer, I. E., Sherr, E. H., Yuskaitis, C. J., Abou-Khalil, B., Alldredge, B. K., Bautista, J. F., Berkovic, S. F., Boro, A., Cascino, G. D., Consalvo, D., Crumrine, P., Devinsky, O., Dlugos, D., Epstein, M. P., Fiol, M., Fountain, N. B., French, J., Friedman, D., Geller, E. B., Glauser, T., Glynn, S., Haut, S. R., Hayward, J., Helmers, S. L., Joshi, S., Kanner, A., Kirsch, H. E., Knowlton, R. C., Kossoff, E. H., Kuperman, R., Kuzniecky, R., Lowenstein, D. H., McGuire, S. M., Motika, P. V., Novotny, E. J., Ottman, R., Paolicchi, J. M., Parent, J. M., Park, K., Poduri, A., Scheffer, I. E., Shellhaas, R. A., Sherr, E. H., Shih, J. J., Singh, R., Sirven, J., Smith, M. C., Sullivan, J., Lin Thio, L., Venkat, A., Vining, E. P. G., Von Allmen, G. K., Weisenberg, J. L., Widdess-Walsh, P., and Winawer, M. R. (2013). De novo mutations in epileptic encephalopathies. *Nature*, 501(7466):217–221.

Erlander, M. G., Tillakaratne, N. J., Feldblum, S., Patel, N., and Tobin, A. J. (1991). Two genes encode distinct glutamate decarboxylases. *Neuron*, 7(1):91–100.

Farrant, M. and Nusser, Z. (2005). Variations on an inhibitory theme: phasic and tonic activation of GABA(A) receptors. *Nature Reviews. Neuroscience*, 6(3):215–229.

ffrench Mullen, J. M., Barker, J. L., and Rogawski, M. A. (1993). Calcium current block by (-)-pentobarbital, phenobarbital, and CHEB but not (+)-pentobarbital in acutely isolated hippocampal CA1 neurons: comparison with effects on GABA-activated Cl- current. *The Journal of Neuroscience: The Official Journal of the Society for Neuroscience*, 13(8):3211–3221.

File, S. E. (1981). Rapid development of tolerance to the sedative effects of lorazepam and triazolam in rats. *Psychopharmacology*, 73(3):240–245.

Fisher, R. S., van Emde Boas, W., Blume, W., Elger, C., Genton, P., Lee, P., and Engel, J. (2005). Epileptic seizures and epilepsy: definitions proposed by the International League Against Epilepsy (ILAE) and the International Bureau for Epilepsy (IBE). *Epilepsia*, 46(4):470–472.

Fitzgerald, A. C., Wright, B. T., and Heldt, S. A. (2014). The behavioral pharmacology of zolpidem: evidence for the functional significance of alpha1-containing GABA(A) receptors. *Psychopharmacology*, 231(9):1865–1896.

Fradley, R. L., Guscott, M. R., Bull, S., Hallett, D. J., Goodacre, S. C., Wafford, K. A., Garrett, E. M., Newman, R. J., O'Meara, G. F., Whiting, P. J., Rosahl, T. W., Dawson, G. R., Reynolds, D. S., and Atack, J. R. (2007). Differential contribution of GABA(A) receptor subtypes to the

anticonvulsant efficacy of benzodiazepine site ligands. *Journal of Psychopharmacology (Oxford, England)*, 21(4):384–391.

Fritschy, J.-M. (2008). Epilepsy, E/I Balance and GABA(A) Receptor Plasticity. *Frontiers in Molecular Neuroscience*, 1:5.

Galpern, W. R., Lumpkin, M., Greenblatt, D. J., Shader, R. I., and Miller, L. G. (1991). Chronic benzodiazepine administration. VII. Behavioral tolerance and withdrawal and receptor alterations associated with clonazepam administration. *Psychopharmacology*, 104(2):225–230.

Glykys, J., Peng, Z., Chandra, D., Homanics, G. E., Houser, C. R., and Mody, I. (2007). A new naturally occurring GABA(A) receptor subunit partnership with high sensitivity to ethanol. *Nature Neuroscience*, 10(1):40–48.

Goa, K. L. and Heel, R. C. (1986). Zopiclone. A review of its pharmacodynamic and pharmacokinetic properties and therapeutic efficacy as an hypnotic. *Drugs*, 32(1):48–65.

Goddard, A. W., Mason, G. F., Almai, A., Rothman, D. L., Behar, K. L., Petroff, O. A., Charney, D. S., and Krystal, J. H. (2001). Reductions in occipital cortex GABA levels in panic disorder detected with 1h-magnetic resonance spectroscopy. *Archives of General Psychiatry*, 58(6):556–561.

Grenningloh, G., Gundelfinger, E., Schmitt, B., Betz, H., Darlison, M. G., Barnard, E. A., Schofield, P. R., and Seeburg, P. H. (1987). Glycine vs GABA receptors. *Nature*, 330(6143):25–26.

Griffiths, R. R., Sannerud, C. A., Ator, N. A., and Brady, J. V. (1992). Zolpidem behavioral pharmacology in baboons: self-injection, discrimination, tolerance and withdrawal. *The Journal of Pharmacology and Experimental Therapeutics*, 260(3):1199–1208.

Hancili, S., Önal, Z. E., Ata, P., Karatoprak, E. Y., Gürbüz, T., Bostancı, M., Paçal, Y., Nuhoğlu, a., and Ceran, m. (2014). The GABAA receptor gamma2 subunit (R43q) mutation in febrile seizures. *Pediatric Neurology*, 50(4):353–356.

Hedblom, E. and Kirkness, E. F. (1997). A novel class of GABAA receptor subunit in tissues of the reproductive system. *The Journal of Biological Chemistry*, 272(24):15346–15350.

Hevers, W. and Lüddens, H. (1998). The diversity of GABAA receptors. Pharmacological and electrophysiological properties of GABAA channel subtypes. *Molecular Neurobiology*, 18(1):35–86.

Hibbs, R. E. and Gouaux, E. (2011). Principles of activation and permeation in an anion-selective Cys-loop receptor. *Nature*, 474(7349):54–60.

Hilf, R. J. C. and Dutzler, R. (2008). X-ray structure of a prokaryotic pentameric ligand-gated ion channel. *Nature*, 452(7185):375–379.

Hill-Venning, C., Belelli, D., Peters, J. A., and Lambert, J. J. (1997). Subunit-dependent interaction of the general anaesthetic etomidate with the gamma-aminobutyric acid type A receptor. *British Journal of Pharmacology*, 120(5):749–756.

Hintersteiner, J., Haider, M., Luger, D., Schwarzer, C., Reznicek, G., Jäger, W., Khom, S.,

Mihovilovic, M. D., and Hering, S. (2014). Esters of valerenic acid as potential prodrugs. *European Journal of Pharmacology*, 735:123–131.

Hosie, A. M., Wilkins, M. E., da Silva, H. M. A., and Smart, T. G. (2006). Endogenous neurosteroids regulate GABAA receptors through two discrete transmembrane sites. *Nature*, 444(7118):486–489.

Jacob, T. C., Moss, S. J., and Jurd, R. (2008). GABA(A) receptor trafficking and its role in the dynamic modulation of neuronal inhibition. *Nature Reviews. Neuroscience*, 9(5):331–343.

Jurd, R., Arras, M., Lambert, S., Drexler, B., Siegwart, R., Crestani, F., Zaugg, M., Vogt, K. E., Ledermann, B., Antkowiak, B., and Rudolph, U. (2003). General anesthetic actions in vivo strongly attenuated by a point mutation in the GABA(A) receptor beta3 subunit. *FASEB journal: official publication of the Federation of American Societies for Experimental Biology*, 17(2):250–252.

Khom, S., Baburin, I., Timin, E. N., Hohaus, A., Sieghart, W., and Hering, S. (2006). Pharmacological properties of GABAA receptors containing gamma1 subunits. *Molecular pharmacology*, 69(2):640–649.

Khom, S., Strommer, B., Ramharter, J., Schwarz, T., Schwarzer, C., Erker, T., Ecker, G. F., Mulzer, J., and Hering, S. (2010). Valerenic acid derivatives as novel subunit-selective GABAA receptor ligands - in vitro and in vivo characterization. *British journal of pharmacology*, 161(1):65–78.

Khom, S., Strommer, B., Schöffmann, A., Hintersteiner, J., Baburin, I., Erker, T., Schwarz, T., Schwarzer, C., Zaugg, J., Hamburger, M., and Hering, S. (2013). GABAA receptor modulation by piperine and a non-TRPV1 activating derivative. *Biochemical Pharmacology*, 85(12):1827–1836.

Kittler, J. T., Chen, G., Honing, S., Bogdanov, Y., McAinsh, K., Arancibia-Carcamo, I. L., Jovanovic, J. N., Pangalos, M. N., Haucke, V., Yan, Z., and Moss, S. J. (2005). Phospho-dependent binding of the clathrin AP2 adaptor complex to GABAA receptors regulates the efficacy of inhibitory synaptic transmission. *Proceedings of the National Academy of Sciences of the United States of America*, 102(41):14871–14876.

Kittler, J. T., Chen, G., Kukhtina, V., Vahedi-Faridi, A., Gu, Z., Tretter, V., Smith, K. R., McAinsh, K., Arancibia-Carcamo, I. L., Saenger, W., Haucke, V., Yan, Z., and Moss, S. J. (2008). Regulation of synaptic inhibition by phospho-dependent binding of the AP2 complex to a YECL motif in the GABAA receptor gamma2 subunit. *Proceedings of the National Academy of Sciences of the United States of America*, 105(9):3616–3621.

Kittler, J. T., Delmas, P., Jovanovic, J. N., Brown, D. A., Smart, T. G., and Moss, S. J. (2000). Constitutive endocytosis of GABAA receptors by an association with the adaptin AP2 complex modulates inhibitory synaptic currents in hippocampal neurons. *The Journal of Neuroscience: The Official Journal of the Society for Neuroscience*, 20(21):7972–7977.

Kittler, J. T., Rostaing, P., Schiavo, G., Fritschy, J. M., Olsen, R., Triller, A., and Moss, S. J.

(2001). The subcellular distribution of GABARAP and its ability to interact with NSF suggest a role for this protein in the intracellular transport of GABA(A) receptors. *Molecular and Cellular Neurosciences*, 18(1):13–25.

Kloda, J. H. and Czajkowski, C. (2007). Agonist-, antagonist-, and benzodiazepine-induced structural changes in the alpha1 Met113-Leu132 region of the GABAA receptor. *Molecular Pharmacology*, 71(2):483–493.

Kokka, N., Sapp, D. W., Taylor, A. M., and Olsen, R. W. (1993). The kindling model of alcohol dependence: similar persistent reduction in seizure threshold to pentylenetetrazol in animals receiving chronic ethanol or chronic pentylenetetrazol. *Alcoholism, Clinical and Experimental Research*, 17(3):525–531.

Kopp, C., Rudolph, U., and Tobler, I. (2004). Sleep EEG changes after zolpidem in mice. *Neuroreport*, 15(14):2299–2302.

Krishek, B. J., Moss, S. J., and Smart, T. G. (1996). Homomeric beta 1 gamma-aminobutyric acid A receptor-ion channels: evaluation of pharmacological and physiological properties. *Molecular Pharmacology*, 49(3):494–504.

Kucken, A. M., Teissére, J. A., Seffinga-Clark, J., Wagner, D. A., and Czajkowski, C. (2003). Structural requirements for imidazobenzodiazepine binding to GABA(A) receptors. *Molecular Pharmacology*, 63(2):289–296.

Kumar, S., Porcu, P., Werner, D. F., Matthews, D. B., Diaz-Granados, J. L., Helfand, R. S., and Morrow, A. L. (2009). The role of GABA(A) receptors in the acute and chronic effects of ethanol: a decade of progress. *Psychopharmacology*, 205(4):529–564.

Lachance-Touchette, P., Brown, P., Meloche, C., Kinirons, P., Lapointe, L., Lacasse, H., Lortie, A., Carmant, L., Bedford, F., Bowie, D., and Cossette, P. (2011). Novel alpha1 and gamma2 GABAA receptor subunit mutations in families with idiopathic generalized epilepsy. *The European Journal of Neuroscience*, 34(2):237–249.

Langer, S. Z., Arbilla, S., Benavides, J., and Scatton, B. (1990). Zolpidem and alpidem: two imidazopyridines with selectivity for omega 1- and omega 3-receptor subtypes. *Advances in Biochemical Psychopharmacology*, 46:61–72.

Laurie, D. J., Wisden, W., and Seeburg, P. H. (1992). The distribution of thirteen GABAA receptor subunit mRNAs in the rat brain. III. Embryonic and postnatal development. *The Journal of Neuroscience: The Official Journal of the Society for Neuroscience*, 12(11):4151–4172.

Lüddens, H., Seeburg, P. H., and Korpi, E. R. (1994). Impact of beta and gamma variants on ligand-binding properties of gamma-aminobutyric acid type A receptors. *Molecular Pharmacology*, 45(5):810–814.

Leeb-Lundberg, F., Snowman, A., and Olsen, R. W. (1980). Barbiturate receptor sites are coupled to benzodiazepine receptors. *Proceedings of the National Academy of Sciences of the United States of America*, 77(12):7468–7472.

Leil, T. A., Chen, Z.-W., Chang, C.-S. S., and Olsen, R. W. (2004). GABAA receptor-associated protein traffics GABAA receptors to the plasma membrane in neurons. *The Journal of Neuroscience: The Official Journal of the Society for Neuroscience*, 24(50):11429–11438.

Li, G.-D., Chiara, D. C., Sawyer, G. W., Husain, S. S., Olsen, R. W., and Cohen, J. B. (2006). Identification of a GABAA receptor anesthetic binding site at subunit interfaces by photolabeling with an etomidate analog. *The Journal of Neuroscience: The Official Journal of the Society for Neuroscience*, 26(45):11599–11605.

Liang, J., Suryanarayanan, A., Abriam, A., Snyder, B., Olsen, R. W., and Spigelman, I. (2007). Mechanisms of reversible GABAA receptor plasticity after ethanol intoxication. *The Journal of Neuroscience: The Official Journal of the Society for Neuroscience*, 27(45):12367–12377.

Lindemeyer, A. K., Liang, J., Marty, V. N., Meyer, E. M., Suryanarayanan, A., Olsen, R. W., and Spigelman, I. (2014). Ethanol-induced plasticity of GABAA receptors in the basolateral amygdala. *Neurochemical Research*, 39(6):1162–1170.

Lister, R. G. (1987). The use of a plus-maze to measure anxiety in the mouse. *Psychopharmacology*, 92(2):180–185.

Löscher, W. and Rogawski, M. A. (2012). How theories evolved concerning the mechanism of action of barbiturates. *Epilepsia*, 53 Suppl 8:12–25.

Luscher, B., Fuchs, T., and Kilpatrick, C. L. (2011). GABAA receptor trafficking-mediated plasticity of inhibitory synapses. *Neuron*, 70(3):385–409.

Löw, K., Crestani, F., Keist, R., Benke, D., Brünig, I., Benson, J. A., Fritschy, J. M., Rülicke, T., Bluethmann, H., Möhler, H., and Rudolph, U. (2000). Molecular and neuronal substrate for the selective attenuation of anxiety. *Science (New York, N.Y.)*, 290(5489):131–134.

Macdonald, R. L., Kang, J.-Q., and Gallagher, M. J. (2010). Mutations in GABAA receptor subunits associated with genetic epilepsies. *The Journal of Physiology*, 588(Pt 11):1861–1869.

Macdonald, R. L. and Olsen, R. W. (1994). GABAA receptor channels. *Annual Review of Neuroscience*, 17:569–602.

MacDonald, R. L., Rogers, C. J., and Twyman, R. E. (1989). Barbiturate regulation of kinetic properties of the GABAA receptor channel of mouse spinal neurones in culture. *The Journal of Physiology*, 417:483–500.

Malizia, A. L. (1999). What do brain imaging studies tell us about anxiety disorders? *Journal of Psychopharmacology (Oxford, England)*, 13(4):372–378.

Malizia, A. L., Cunningham, V. J., Bell, C. J., Liddle, P. F., Jones, T., and Nutt, D. J. (1998). Decreased brain GABA(A)-benzodiazepine receptor binding in panic disorder: preliminary results from a quantitative PET study. *Archives of General Psychiatry*, 55(8):715–720.

Mathers, D. A. and Barker, J. L. (1980). (-)Pentobarbital opens ion channels of long duration in cultured mouse spinal neurons. *Science (New York, N.Y.)*, 209(4455):507–509.

May, A. C., Fleischer, W., Kletke, O., Haas, H. L., and Sergeeva, O. A. (2013). Benzodiazepine-site pharmacology on GABAA receptors in histaminergic neurons. *British Journal of Pharma-*

cology, 170(1):222–232.

McKernan, R. M., Rosahl, T. W., Reynolds, D. S., Sur, C., Wafford, K. A., Atack, J. R., Farrar, S., Myers, J., Cook, G., Ferris, P., Garrett, L., Bristow, L., Marshall, G., Macaulay, A., Brown, N., Howell, O., Moore, K. W., Carling, R. W., Street, L. J., Castro, J. L., Ragan, C. I., Dawson, G. R., and Whiting, P. J. (2000). Sedative but not anxiolytic properties of benzodiazepines are mediated by the GABA(A) receptor alpha1 subtype. *Nature Neuroscience*, 3(6):587–592.

Methfessel, C., Witzemann, V., Takahashi, T., Mishina, M., Numa, S., and Sakmann, B. (1986). Patch clamp measurements on Xenopus laevis oocytes: currents through endogenous channels and implanted acetylcholine receptor and sodium channels. *Pflügers Archiv: European journal of physiology*, 407(6):577–588.

Möhler, H. (2006). GABAA receptors in central nervous system disease: anxiety, epilepsy, and insomnia. *Journal of receptor and signal transduction research*, 26(5-6):731–740.

Möhler, H., Fritschy, J. M., and Rudolph, U. (2002). A new benzodiazepine pharmacology. *The Journal of Pharmacology and Experimental Therapeutics*, 300(1):2–8.

Middendorp, S. J., Maldifassi, M. C., Baur, R., and Sigel, E. (2015). Positive modulation of synaptic and extrasynaptic GABAA receptors by an antagonist of the high affinity benzodiazepine binding site. *Neuropharmacology*, 95:459–467.

Miller, P. S. and Aricescu, A. R. (2014). Crystal structure of a human GABAA receptor. *Nature*, 512(7514):270–275.

Minuk, G. Y., Zhang, M., Gong, Y., Minuk, L., Dienes, H., Pettigrew, N., Kew, M., Lipschitz, J., and Sun, D. (2007). Decreased hepatocyte membrane potential differences and GABAA-beta3 expression in human hepatocellular carcinoma. *Hepatology (Baltimore, Md.)*, 45(3):735–745.

Mizuta, K., Xu, D., Pan, Y., Comas, G., Sonett, J. R., Zhang, Y., Panettieri, R. A., Yang, J., and Emala, C. W. (2008). GABAA receptors are expressed and facilitate relaxation in airway smooth muscle. *American Journal of Physiology. Lung Cellular and Molecular Physiology*, 294(6):L1206–1216.

Moraga-Cid, G., Yevenes, G. E., Schmalzing, G., Peoples, R. W., and Aguayo, L. G. (2011). A Single phenylalanine residue in the main intracellular loop of alpha1 gamma-aminobutyric acid type A and glycine receptors influences their sensitivity to propofol. *Anesthesiology*, 115(3):464–473.

Moragues, N., Ciofi, P., Tramu, G., and Garret, M. (2002). Localisation of GABA(A) receptor epsilon-subunit in cholinergic and aminergic neurones and evidence for co-distribution with the theta-subunit in rat brain. *Neuroscience*, 111(3):657–669.

Morris, H. V., Dawson, G. R., Reynolds, D. S., Atack, J. R., and Stephens, D. N. (2006). Both alpha2 and alpha3 GABAA receptor subtypes mediate the anxiolytic properties of benzodiazepine site ligands in the conditioned emotional response paradigm. *The European Journal of Neuroscience*, 23(9):2495–2504.

Neelands, T. R. and Macdonald, R. L. (1999). Incorporation of the pi subunit into functional

gamma-aminobutyric Acid(A) receptors. *Molecular Pharmacology*, 56(3):598–610.

Nelson, L. E., Guo, T. Z., Lu, J., Saper, C. B., Franks, N. P., and Maze, M. (2002). The sedative component of anesthesia is mediated by GABA(A) receptors in an endogenous sleep pathway. *Nature Neuroscience*, 5(10):979–984.

Newell, J. G. and Czajkowski, C. (2003). The GABAA receptor alpha 1 subunit Pro174-Asp191 segment is involved in GABA binding and channel gating. *The Journal of Biological Chemistry*, 278(15):13166–13172.

Newell, J. G., McDevitt, R. A., and Czajkowski, C. (2004). Mutation of glutamate 155 of the GABAA receptor beta2 subunit produces a spontaneously open channel: a trigger for channel activation. *The Journal of Neuroscience: The Official Journal of the Society for Neuroscience*, 24(50):11226–11235.

Nuss, P. (2015). Anxiety disorders and GABA neurotransmission: a disturbance of modulation. *Neuropsychiatric Disease and Treatment*, 11:165–175.

Nutt, D. J., Glue, P., Lawson, C., and Wilson, S. (1990). Flumazenil provocation of panic attacks. Evidence for altered benzodiazepine receptor sensitivity in panic disorder. *Archives of General Psychiatry*, 47(10):917–925.

Olsen, R. W. (1981). GABA-benzodiazepine-barbiturate receptor interactions. *Journal of Neurochemistry*, 37(1):1–13.

Olsen, R. W., Hanchar, H. J., Meera, P., and Wallner, M. (2007). GABAA receptor subtypes: the "one glass of wine" receptors. *Alcohol (Fayetteville, N.Y.)*, 41(3):201–209.

Olsen, R. W. and Sieghart, W. (2008). International Union of Pharmacology. LXX. Subtypes of gamma-aminobutyric acid(A) receptors: classification on the basis of subunit composition, pharmacology, and function. Update. *Pharmacological reviews*, 60(3):243–260.

Olsen, R. W. and Sieghart, W. (2009). GABAA Receptors: Subtypes Provide Diversity of Function and Pharmacology. *Neuropharmacology*, 56(1):141–148.

Olsen, R. W. and Tobin, A. J. (1990). Molecular biology of GABAA receptors. *FASEB journal: official publication of the Federation of American Societies for Experimental Biology*, 4(5):1469–1480.

Owens, D. F. and Kriegstein, A. R. (2002). Is there more to GABA than synaptic inhibition? *Nature Reviews. Neuroscience*, 3(9):715–727.

Perrault, G., Morel, E., Sanger, D. J., and Zivkovic, B. (1992). Lack of tolerance and physical dependence upon repeated treatment with the novel hypnotic zolpidem. *The Journal of Pharmacology and Experimental Therapeutics*, 263(1):298–303.

Pritchett, D. B. and Seeburg, P. H. (1991). gamma-Aminobutyric acid type A receptor point mutation increases the affinity of compounds for the benzodiazepine site. *Proceedings of the National Academy of Sciences of the United States of America*, 88(4):1421–1425.

Ramerstorfer, J., Furtmüller, R., Sarto-Jackson, I., Varagic, Z., Sieghart, W., and Ernst, M. (2011). The GABAA receptor alpha+beta- interface: a novel target for subtype selective

drugs. *The Journal of Neuroscience: The Official Journal of the Society for Neuroscience*, 31(3):870–877.

Reynolds, D. S., Rosahl, T. W., Cirone, J., O'Meara, G. F., Haythornthwaite, A., Newman, R. J., Myers, J., Sur, C., Howell, O., Rutter, A. R., Atack, J., Macaulay, A. J., Hadingham, K. L., Hutson, P. H., Belelli, D., Lambert, J. J., Dawson, G. R., McKernan, R., Whiting, P. J., and Wafford, K. A. (2003). Sedation and anesthesia mediated by distinct GABA(A) receptor isoforms. *The Journal of Neuroscience: The Official Journal of the Society for Neuroscience*, 23(24):8608–8617.

Reynolds, L. M., Engin, E., Tantillo, G., Lau, H. M., Muschamp, J. W., Carlezon, W. A., and Rudolph, U. (2012). Differential roles of GABA(A) receptor subtypes in benzodiazepine-induced enhancement of brain-stimulation reward. *Neuropsychopharmacology: Official Publication of the American College of Neuropsychopharmacology*, 37(11):2531–2540.

Richardson, J. E., Garcia, P. S., O'Toole, K. K., Derry, J. M. C., Bell, S. V., and Jenkins, A. (2007). A conserved tyrosine in the beta2 subunit M4 segment is a determinant of gamma-aminobutyric acid type A receptor sensitivity to propofol. *Anesthesiology*, 107(3):412–418.

Roy-Byrne, P. P., Cowley, D. S., Greenblatt, D. J., Shader, R. I., and Hommer, D. (1990). Reduced benzodiazepine sensitivity in panic disorder. *Archives of General Psychiatry*, 47(6):534–538.

Rudolph, U. and Antkowiak, B. (2004). Molecular and neuronal substrates for general anaesthetics. *Nature Reviews. Neuroscience*, 5(9):709–720.

Rudolph, U., Crestani, F., Benke, D., Brünig, I., Benson, J. A., Fritschy, J. M., Martin, J. R., Bluethmann, H., and Möhler, H. (1999). Benzodiazepine actions mediated by specific gamma-aminobutyric acid(A) receptor subtypes. *Nature*, 401(6755):796–800.

Rudolph, U. and Möhler, H. (2014). GABAA receptor subtypes: Therapeutic potential in Down syndrome, affective disorders, schizophrenia, and autism. *Annual Review of Pharmacology and Toxicology*, 54:483–507.

Sampath, C., Haug, K., Thanei, S., Hamburger, M., Derendorf, H., Frye, R., and Butterweck, V. (2012). Pharmacokinetics of valerenic acid in rats after intravenous and oral administrations. *Planta medica*, 78(6):575–581.

Sancar, F. and Czajkowski, C. (2004). A GABAA receptor mutation linked to human epilepsy (gamma2r43q) impairs cell surface expression of alphabetagamma receptors. *The Journal of Biological Chemistry*, 279(45):47034–47039.

Sanger, D. J. and Zivkovic, B. (1992). Differential development of tolerance to the depressant effects of benzodiazepine and non-benzodiazepine agonists at the omega (BZ) modulatory sites of GABAA receptors. *Neuropharmacology*, 31(7):693–700.

Schöffmann, A., Wimmer, L., Goldmann, D., Khom, S., Hintersteiner, J., Baburin, I., Schwarz, T., Hintersteininger, M., Pakfeifer, P., Oufir, M., Hamburger, M., Erker, T., Ecker, G. F., Mihovilovic, M. D., and Hering, S. (2014). Efficient modulation of gamma-aminobutyric acid type A receptors by piperine derivatives. *Journal of Medicinal Chemistry*, 57(13):5602–5619.

Serafini, R., Bracamontes, J., and Steinbach, J. H. (2000). Structural domains of the human GABAA receptor 3 subunit involved in the actions of pentobarbital. *The Journal of Physiology*, 524 Pt 3:649–676.

Sherin, J. E., Elmquist, J. K., Torrealba, F., and Saper, C. B. (1998). Innervation of histaminergic tuberomammillary neurons by GABAergic and galaninergic neurons in the ventrolateral preoptic nucleus of the rat. *The Journal of Neuroscience: The Official Journal of the Society for Neuroscience*, 18(12):4705–4721.

Shin, H.-W., Morinaga, N., Noda, M., and Nakayama, K. (2004). BIG2, a guanine nucleotide exchange factor for ADP-ribosylation factors: its localization to recycling endosomes and implication in the endosome integrity. *Molecular Biology of the Cell*, 15(12):5283–5294.

Sieghart, W. (2015). Allosteric Modulation of GABAA Receptors via Multiple Drug-Binding Sites. *Advances in Pharmacology (San Diego, Calif.)*, 72:53–96.

Siegwart, R., Jurd, R., and Rudolph, U. (2002). Molecular determinants for the action of general anesthetics at recombinant alpha(2)beta(3)gamma(2)gamma-aminobutyric acid(A) receptors. *Journal of Neurochemistry*, 80(1):140–148.

Sigel, E., Baur, R., Trube, G., Möhler, H., and Malherbe, P. (1990). The effect of subunit composition of rat brain GABAA receptors on channel function. *Neuron*, 5(5):703–711.

Sigel, E. and Buhr, A. (1997). The benzodiazepine binding site of GABAA receptors. *Trends in Pharmacological Sciences*, 18(11):425–429.

Sigel, E. and Lüscher, B. P. (2011). A closer look at the high affinity benzodiazepine binding site on GABAA receptors. *Current Topics in Medicinal Chemistry*, 11(2):241–246.

Sigel, E. and Steinmann, M. E. (2012). Structure, function, and modulation of GABA(A) receptors. *The Journal of biological chemistry*, 287(48):40224–40231.

Simon, J., Wakimoto, H., Fujita, N., Lalande, M., and Barnard, E. A. (2004). Analysis of the set of GABA(A) receptor genes in the human genome. *The Journal of Biological Chemistry*, 279(40):41422–41435.

Sinkkonen, S. T., Hanna, M. C., Kirkness, E. F., and Korpi, E. R. (2000). GABA(A) receptor epsilon and theta subunits display unusual structural variation between species and are enriched in the rat locus ceruleus. *The Journal of Neuroscience: The Official Journal of the Society for Neuroscience*, 20(10):3588–3595.

Srivastava, S., Cohen, J., Pevsner, J., Aradhya, S., McKnight, D., Butler, E., Johnston, M., and Fatemi, A. (2014). A novel variant in GABRB2 associated with intellectual disability and epilepsy. *American Journal of Medical Genetics. Part A*, 164A(11):2914–2921.

Steinlein, O. K. (2001). Genes and mutations in idiopathic epilepsy. *American Journal of Medical Genetics*, 106(2):139–145.

Stewart, D. S., Pierce, D. W., Hotta, M., Stern, A. T., and Forman, S. A. (2014). Mutations at beta N265 in gamma-aminobutyric acid type A receptors alter both binding affinity and efficacy of potent anesthetics. *PloS One*, 9(10):e111470.

Study, R. E. and Barker, J. L. (1981). Diazepam and (–)-pentobarbital: fluctuation analysis reveals different mechanisms for potentiation of gamma-aminobutyric acid responses in cultured central neurons. *Proceedings of the National Academy of Sciences of the United States of America*, 78(11):7180–7184.

Sundstrom-Poromaa, I., Smith, D. H., Gong, Q. H., Sabado, T. N., Li, X., Light, A., Wiedmann, M., Williams, K., and Smith, S. S. (2002). Hormonally regulated alpha(4)beta(2)delta GABA(A) receptors are a target for alcohol. *Nature Neuroscience*, 5(8):721–722.

Tan, K. R., Brown, M., Labouèbe, G., Yvon, C., Creton, C., Fritschy, J.-M., Rudolph, U., and Lüscher, C. (2010). Neural bases for addictive properties of benzodiazepines. *Nature*, 463(7282):769–774.

Tanida, I., Ueno, T., and Kominami, E. (2004). LC3 conjugation system in mammalian autophagy. *The International Journal of Biochemistry & Cell Biology*, 36(12):2503–2518.

Teissére, J. A. and Czajkowski, C. (2001). A (beta)-strand in the (gamma)2 subunit lines the benzodiazepine binding site of the GABA A receptor: structural rearrangements detected during channel gating. *The Journal of Neuroscience: The Official Journal of the Society for Neuroscience*, 21(14):4977–4986.

Thompson, S. A., Whiting, P. J., and Wafford, K. A. (1996). Barbiturate interactions at the human GABAA receptor: dependence on receptor subunit combination. *British Journal of Pharmacology*, 117(3):521–527.

Treiman, D. M. (2001). GABAergic mechanisms in epilepsy. *Epilepsia*, 42 Suppl 3:8–12.

Uusi-Oukari, M. and Korpi, E. R. (2010). Regulation of GABA(A) receptor subunit expression by pharmacological agents. *Pharmacological Reviews*, 62(1):97–135.

Venkatachalan, S. P. and Czajkowski, C. (2008). A conserved salt bridge critical for GABA(A) receptor function and loop C dynamics. *Proceedings of the National Academy of Sciences of the United States of America*, 105(36):13604–13609.

Vlainić, J. and Pericić, D. (2009). Effects of acute and repeated zolpidem treatment on pentylenetetrazole-induced seizure threshold and on locomotor activity: comparison with diazepam. *Neuropharmacology*, 56(8):1124–1130.

Voss, J., Sanchez, C., Michelsen, S., and Ebert, B. (2003). Rotarod studies in the rat of the GABAA receptor agonist gaboxadol: lack of ethanol potentiation and benzodiazepine cross-tolerance. *European Journal of Pharmacology*, 482(1-3):215–222.

Wagner, D. A. and Czajkowski, C. (2001). Structure and dynamics of the GABA binding pocket: A narrowing cleft that constricts during activation. *The Journal of Neuroscience: The Official Journal of the Society for Neuroscience*, 21(1):67–74.

Wagner, D. A., Czajkowski, C., and Jones, M. V. (2004). An arginine involved in GABA binding and unbinding but not gating of the GABA(A) receptor. *The Journal of Neuroscience: The Official Journal of the Society for Neuroscience*, 24(11):2733–2741.

Wallner, M., Hanchar, H. J., and Olsen, R. W. (2003). Ethanol enhances alpha 4 beta 3 delta

and alpha 6 beta 3 delta gamma-aminobutyric acid type A receptors at low concentrations known to affect humans. *Proceedings of the National Academy of Sciences of the United States of America*, 100(25):15218–15223.

Wallner, M., Hanchar, H. J., and Olsen, R. W. (2014). Alcohol selectivity of beta3-containing GABAA receptors: evidence for a unique extracellular alcohol/imidazobenzodiazepine Ro15-4513 binding site at the alpha+beta- subunit interface in alphabeta3delta GABAA receptors. *Neurochemical Research*, 39(6):1118–1126.

Walters, R. J., Hadley, S. H., Morris, K. D., and Amin, J. (2000). Benzodiazepines act on GABAA receptors via two distinct and separable mechanisms. *Nature Neuroscience*, 3(12):1274–1281.

Wegelius, K., Pasternack, M., Hiltunen, J. O., Rivera, C., Kaila, K., Saarma, M., and Reeben, M. (1998). Distribution of GABA receptor rho subunit transcripts in the rat brain. *The European Journal of Neuroscience*, 10(1):350–357.

Whiting, P., McKernan, R. M., and Iversen, L. L. (1990). Another mechanism for creating diversity in gamma-aminobutyrate type A receptors: RNA splicing directs expression of two forms of gamma 2 phosphorylation site. *Proceedings of the National Academy of Sciences of the United States of America*, 87(24):9966–9970.

Wieland, H. A., Lüddens, H., and Seeburg, P. H. (1992). A single histidine in GABAA receptors is essential for benzodiazepine agonist binding. *The Journal of Biological Chemistry*, 267(3):1426–1429.

Wisden, W., Laurie, D. J., Monyer, H., and Seeburg, P. H. (1992). The distribution of 13 GABAA receptor subunit mRNAs in the rat brain. I. Telencephalon, diencephalon, mesencephalon. *The Journal of Neuroscience: The Official Journal of the Society for Neuroscience*, 12(3):1040–1062.

Yaffe, R. B., Borger, P., Megevand, P., Groppe, D. M., Kramer, M. A., Chu, C. J., Santaniello, S., Meisel, C., Mehta, A. D., and Sarma, S. V. (2014). Physiology of functional and effective networks in epilepsy. *Clinical Neurophysiology: Official Journal of the International Federation of Clinical Neurophysiology*.

Yanovsky, Y., Schubring, S., Fleischer, W., Gisselmann, G., Zhu, X.-R., Lübbert, H., Hatt, H., Rudolph, U., Haas, H. L., and Sergeeva, O. A. (2012). GABAA receptors involved in sleep and anaesthesia: beta1- versus beta3-containing assemblies. *Pflügers Archiv: European Journal of Physiology*, 463(1):187–199.

Yip, G. M. S., Chen, Z.-W., Edge, C. J., Smith, E. H., Dickinson, R., Hohenester, E., Townsend, R. R., Fuchs, K., Sieghart, W., Evers, A. S., and Franks, N. P. (2013). A propofol binding site on mammalian GABAA receptors identified by photolabeling. *Nature Chemical Biology*, 9(11):715–720.

Zhang, J. H., Sato, M., and Tohyama, M. (1991). Different postnatal development profiles of neurons containing distinct GABAA receptor beta subunit mRNAs (beta 1, beta 2, and beta 3) in the rat forebrain. *The Journal of Comparative Neurology*, 308(4):586–613.

Curriculum Vitae

Personal Information

Mag. pharm. Juliane Hintersteiner

E-mail julianehintersteiner@gmx.at

Born June 24, 1986 in Melk

Nationality Austria

Education

11/2010-01/2015
Doctoral studies
Department of Pharmacology and Toxicology, University of Vienna under supervision of Prof. Dr. Steffen Hering
"In vivo Characterization of Natural Product $GABA_A$ Modulators and their Derivatives"

09/2012
Introductory course into Laboratory Animal Science (FELASA B criteria)
Institute of Laboratory Animal Science, University of Veterinary Medicine, Vienna

02/2012
EMA/DIA Training Course Excellence in Pharmacovigilance: Clinical trials and Post-Marketing
European Medicines Agency, London, UK

01/2011, 03/2011
Internship Medical University of Innsbruck Host: Prof. Dr. Christoph Schwarzer Training in behavioral pharmacology (PTZ tain-vein infusion, Open field test)

11/2009-11/2010
Practical year in pharmacy
Approbation as registered pharmacist with honors (Austrian's pharmacist diploma)

10/2004-07/2009
Diploma studies pharmacy, University of Vienna
Graduation with distinction
"Evaluierung geschlechtsspezifischer Unterschiede im Rahmen der Spätfolgen des Diabetes mellitus Typ 1"

2004 High School Certificate (Wieselburg, Austria)

1996-2004 High School Bundesgymnasium/Bundesrealgymnasium, Wieselburg, Austria

Academic Positions

10/2011-01/2015
Associate PhD student in FWF funded doctoral program *"Ion channels and transporters as molecular drug targets"*

02/2011-01/2015
University assistant "praedoc" at Department of Pharmacology and Toxicology, University of Vienna

11/2010-01/2011
Project assistant at Department of Pharmacology and Toxicology, University of Vienna

Teaching activities

2011-2015 Instructor of practical courses

PR Pharmacology, Pharmacotherapy and Toxicology I + II
PR First Aid for Pharmacists
PR Laboratory Course in Microbiology

Professional Experience

since 2015 Pharmacist in local pharmacy, Vienna

Scientific Scills

Electrophysiology
Two-microelectrode voltage clamp technique

Behavioral Pharmacology
Elevated plus maze (EPM) test paradigm
Light/dark choice test (LDT) paradigm
Open field (OF) test paradigm
Determination of seizure threshold via pentylenetetrazlole (PTZ) tail-vein infusion
Stress induced hyperthermia (SIH) test paradigm

Publications and Posters

Publications in Peer Reviewed Journals

Hintersteiner, J., Haider, M., Luger, D., Schwarzer, C., Reznicek, G., Jäger, W., Khom, S., Mihovilovic, M.D., Hering, S., 2014. *Esters of valerenic acid as potential prodrugs.* Eur. J. Pharmacol. 735, 123–131. doi:10.1016/j.ejphar.2014.03.019

Kautzky-Willer, A., Stich, K., **Hintersteiner, J.**, Kautzky, A., Kamyar, M.R., Saukel, J., Johnson, J., Lemmens-Gruber, R., 2013. *Sex-specific-differences in cardiometabolic risk in type 1 diabetes: a cross-sectional study.* Cardiovasc. Diabetol. 12, 78. doi:10.1186/1475-2840-12-78

Khom, S., Strommer, B., Schöffmann, A., **Hintersteiner, J.**, Baburin, I., Erker, T., Schwarz, T., Schwarzer, C., Zaugg, J., Hamburger, M., Hering, S., 2013. *GABAA receptor modulation by piperine and a non-TRPV1 activating derivative.* Biochem. Pharmacol. 85, 1827–1836. doi:10.1016/j.bcp.2013.04.017

Schöffmann, A., Wimmer, L., Goldmann, D., Khom, S., **Hintersteiner, J.**, Baburin, I., Schwarz, T., Hintersteininger, M., Pakfeifer, P., Oufir, M., Hamburger, M., Erker, T., Ecker, G.F., Mihovilovic, M.D., Hering, S., 2014. *Efficient modulation of γ-aminobutyric acid type A receptors by piperine derivatives.* J. Med. Chem. 57, 5602–5619. doi:10.1021/jm5002277

Publication in Preparation

Khom, S., **Hintersteiner, J.***, Luger, D.*, Haider, M., Pototschnig, G., Schwarzer, C., Mihovilovic, MD., Hering, S. *Probing the Potential of Valerenic Acid and Derivatives as Scaffolds for the Development of Novel Anticonvulsants.*

(*) Both authors contributed equally to the paper

Conference Posters

Khom, S., Luger, D., **Hintersteiner, J.**, Haider, M., Schwarzer, C., Mihovilovic, M.D., Hering, S.
On the role of β2/3-subunit-selective $GABA_A$ receptor Modulation in Mediating Anxiolytic and Anticonvulsive Effects of Valerenic Acid Derivatives.
44th Annual Meeting of the Society for Neuroscience, 2014 Nov 15-19, Washington, DC

Hintersteiner, J., Haider, M., Luger, D., Schwarzer, C., Reznicek, G., Jäger, W., Khom, S., Mihovilovic, M.D., Hering, S.
Effect of Esterification on Onset and Duration of Anxiolytic and Anticonvulsive Activity of Valerenic Acid Derivatives.
43th Annual Meeting of the Society for Neuroscience, 2013 Nov 9-13, San Diego, California

Hintersteiner, J., Khom, S., Haider, M., Mihovilovic, MD., Luger, D., Schwarzer, C., Hering, S.
In vivo Characterization of Natural Product $GABA_A$ Modulators and their Derivatives.
SAB Retreat Molecular Drug Targets, 2013 Oct 17-18, Bad Aussee, Austria

Hintersteiner, J., Haider, M., Luger, D., Schwarzer, C., Reznicek, G., Jäger, W., Khom, S., Mihovilovic, M.D., Hering, S.
In vivo Characterization of Natural Product $GABA_A$ Modulators and their Derivatives.
Molecular Drug Targets Science Day, 2013 Feb 22, Pharmacy Centre, Vienna

Selected Presentations

In vivo Characterization of Natural Product $GABA_A$ Modulators and their Derivatives.
SAB Retreat Molecular Drug Targets, 2012 December 12, Pharmacy Centre, Vienna

The anxiolytic Potential of Valerenic Acid Derivatives.
Internal Retreat Molecular Drug Targets, 2012 October 2, Pharmacy Centre, Vienna